Secretory and synaptic proteins in brain and cerebrospinal fluid in normal and Alzheimer's disease animal models

Irene Sánchez Domínguez

Secretory and synaptic proteins in brain and cerebrospinal fluid in normal and Alzheimer's disease animal model

Irene Sánchez Domínguez

Tesis Doctoral

UNIVERSITAT DE BARCELONA

Institut de Neurociències
UNIVERSITAT DE BARCELONA

Departamento de Biología Celular, Fisiología e Inmunología

Facultad de Biología

Programa de Doctorado en Biomedicina

SECRETORY AND SYNAPTIC PROTEINS IN BRAIN AND CEREBROSPINAL FLUID IN NORMAL AND ALZHEIMER'S DISEASE ANIMAL MODEL

Memoria presentada por

Irene Sánchez Domínguez

para optar al grado de

Doctora

por la Universidad de Barcelona

Irene Sánchez Domínguez

Doctoranda

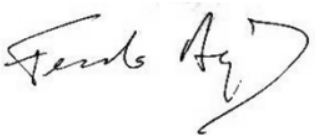

Dr. Fernando Aguado Tomás

Director de Tesis

Septiembre 2017 – Septiembre 2022

"Estoy convencido de que en este día
somos dueños de nuestro destino,
que la tarea que se nos ha impuesto
no es superior a nuestras fuerzas,
que sus acometidas no están
por encima de lo que puedo soportar.
Mientras tengamos fe en nuestras causas
y una indeclinable voluntad de vencer,
la victoria estará a nuestro alcance".

Winston Churchill

"Un viaje de mil millas comienza con un primer paso"

Lao Tse

AGRADECIMIENTOS

Después de varios años de intenso trabajo y sacrificio, pero también de grandes alegrías, ha llegado el momento de poder plasmar en esta memoria los resultados de este gran en el que me embarqué: realizar una tesis doctoral. Una tesis en la que he entregado mi alma y pasión desde el primer día hasta el último. Ahora bien, sin duda, llegar hasta aquí no hubiese sido posible sin el apoyo de varias personas.

En primer lugar, no puedo estar más agradecida a la oportunidad que me dio el Dr. Fernando Aguado de realizar mi tesis doctoral en su laboratorio. Desde que fui alumna en tus clases de Neurobiología sentí tu pasión por la ciencia, por aquello que nos mueve por dentro que nos hace ser quien somos. Desde que el primer día que entré en tu despacho para ver si podía realizar las prácticas del trabajo final de carrera, sentí tu gran generosidad y ganas por trabajar que no disminuyeron hasta este momento. Si hoy mismo puedo estar terminando de escribir este tesis, ha sido gracias a que confiaste en mí desde des de un inicio ofreciéndome sin dudar la oportunidad de solicitar una beca predoctoral asociada a tu proyecto de investigación. Esos proyectos que, gracias a tu sabiduría, intuición y competencia, has logrado obtener año tras año. A día de hoy, soy quien soy personalmente y, sobre todo, profesionalmente gracias a ti. Juntos hemos abordado una gran cantidad de retos que nos han permitido descifrar ciertos mecanismos del funcionamiento del cerebro. Yo me he entregado fielmente a la ciencia, pero sin tu ayuda y apoyo, no habría podido llegar hasta aquí.

Durante estos años he tenido la oportunidad que cruzarme en el camino con mucha gente, tanto estudiantes de grado, máster y doctorado, como postdoc, profesores, personal administrativo, personal de limpieza, de seguridad… De todos y cada uno de ellos me llevo experiencias de aprendizaje. Vosotros habéis podido ver mi evolución pero, sin duda, tampoco hubiese sido posible sin vuestra colaboración. Me llevo varios amigos que estoy segura que, en el futuro, serán compañeros de viaje para muchas experiencias.

Sin duda, agradezco enormemente el apoyo incondicional recibido por mi familia. Siempre habéis estado ahí en cada una de las decisiones que he tomado en la vida. En las etapas de incertidumbre dónde se generan tantas dudas de hacia dónde dirigir tu vida y tu carrera, vosotros me habéis apoyado siempre, ofreciéndome todo lo que estaba en vuestra mano, confiando plenamente en mí y traspasándome vuestras energías para afrontar el camino de mi vida. Un camino en el que también he tenido la suerte de crear otra familia. He sentido vuestra admiración desde el primer día y vuestro indudable apoyo también me ha llevado a conseguir esta tesis. El camino que construye cada uno viene determinado por las piedrecitas que vas alineando día a día y, gracias a vosotros, hace que ese camino no tenga fin.

Gracias. Termino esta etapa siendo plenamente feliz de haber logrado llevar a cabo diferentes retos de este gran mundo de la ciencia por la que tanta pasión siento. Como dice una chapa que conseguí en un congreso: "me siento orgullosa de ser neurocientífica". Durante este camino, he crecido profesional y personalmente hasta el punto de que, los siguientes retos que me deparen en el futuro, los abordo con gran valentía, seguridad y entusiasmo.

ABSTRACT

The central nervous system represents a huge network architecture where intercellular communication governs and coordinates the proper function of the brain. Regulated secretion of neuropeptides and growth factors from dense-core vesicles (DCV) exert key roles in neural circuit development, function, and plasticity. However, these organelles have received significantly less attention than synaptic vesicles. Here, we investigated different aspects of DCV in the healthy and pathological brain by analyzing their molecular components. First, we studied the developmental acquisition of peptidergic regulated secretion in cortical neurons *in situ* and *in vitro*. We found that the competence for regulated secretion is determined sequentially for different DCV subsets. Importantly, the association between acquisition of regulated competence and levels and location of synaptotagmin-IV pointed out this vesicular component as a key mechanism in the developmental maturation of DCV secretion. Second, due to the significance of astrocytes in the neural circuitry physiology, we developed new adeno-associated vectors to express neuropeptides tagged with fluorescent proteins specifically in neurons, but also in astrocytes to evaluate glial peptidergic secretion into neuronal networks. Neuronal stimulation triggered a robust astrocyte DCV secretion in a calcium-dependent manner, presumably by NMDA glutamate receptors, although in a lesser extent than classical neuronal secretion. Last, alterations in synaptic function underlie early pathogenic events in Alzheimer's disease (AD) which precedes symptoms onset but initiate a remarkably impairment of cognitive function. In line with recent research directed toward the identification of early biomarkers of synaptic degeneration, we studied age- and sex- dependent protein changes in the brain and cerebrospinal fluid (CSF) of TgF344-AD rats, evidencing alterations in DCV and other synaptic components even prior to Aβ deposition, markedly in males. The CSF proteome revealed that this transgenic model undergoes alterations in biological pathways involved in glia-neuron communication, neuronal assembly, memory or neuroinflammation. Hence, we consider TgF344-AD rats as a suitable model for the search of early fluid biomarkers that sustain the development of new therapeutic strategies for pre-clinical AD trials. Altogether, this dissertation shows new evidence of neuronal and glial communication in the physiology and neuropathology of the cerebral cortex.

RESUMEN

El sistema nervioso central está formado por una enorme red altamente organizada en la que una adecuada comunicación intercelular es responsable del procesamiento de información y del correcto funcionamiento del cerebro. La secreción regulada de neuropéptidos y factores de crecimiento, almacenados en vesículas de núcleo denso (VCD), desempeña un papel crucial en el desarrollo, la función y la plasticidad de los circuitos neuronales. Sin embargo, estos orgánulos han sido menos estudiados que las vesículas sinápticas. En este estudio hemos investigado el papel de las VCD en el cerebro sano y patológico analizando sus componentes moleculares. En primer lugar, hemos estudiado la adquisición de la secreción regulada peptidérgica durante el desarrollo de neuronas corticales tanto *in situ* como *in vitro*. Hemos encontrado que la competencia para la secreción regulada se determina secuencialmente para diferentes subpoblaciones de VCD. Es importante destacar que la asociación entre la adquisición de la capacidad de secretarse de forma regulada y los niveles y la localización de la sinaptotagmina-IV señaló a este componente vesicular como un mecanismo clave en el proceso de maduración de las VCD. En segundo lugar, por la funciones tan relevantes que desempeñan los astrocitos en la fisiología de los circuitos neuronales, hemos desarrollado nuevos vectores adeno-asociados para expresar neuropéptidos marcados con proteínas fluorescentes específicamente en neuronas, pero también en astrocitos, para así evaluar la secreción peptídica glial en las redes neuronales. Como consecuencia de la estimulación neuronal, se observó una robusta secreción de VCD por parte de los astrocitos de forma dependiente de calcio, presumiblemente a partir de los receptores de glutamato NMDA, aunque en un grado menor que la secreción regulada clásica de neuronas. Por último, las alteraciones de la función sináptica son la base de los primeros acontecimientos patogénicos desencadenados en la enfermedad de Alzheimer (EA), precediendo a la aparición de los síntomas, pero que acaba desencadenando un notable deterioro de la función cognitiva. En línea con las recientes investigaciones dirigidas a la identificación de biomarcadores tempranos de la degeneración sináptica, hemos estudiado los cambios proteicos dependientes de la edad y del sexo en el cerebro y el líquido cefalorraquídeo (LCR) de ratas TgF344-AD, evidenciando alteraciones en las VCD y otros componentes sinápticos incluso antes de la aparición de placas de Aβ, particularmente en los machos. Además, el proteoma del LCR reveló que este modelo transgénico sufre alteraciones en vías biológicas implicadas en la comunicación glía-neurona, el ensamblaje neuronal, la memoria o la neuroinflamación. Por lo tanto, consideramos a las ratas TgF344-AD como un modelo adecuado para la búsqueda de biomarcadores tempranos en fluidos que respalden el desarrollo de nuevas estrategias terapéuticas para ensayos preclínicos de la EA. En conjunto, esta tesis muestra diferentes evidencias nuevas sobre la comunicación neuronal y glial en la fisiología y neuropatología de la corteza cerebral.

TABLE OF CONTENTS

LIST OF FIGURES

LIST OF TABLES

LIST OF ABBREVIATIONS

ACSF	Artificial cerebrospinal fluid
AD	Alzheimer's disease
AMPA	A-amino-3-hydroxy-5-methyl-4-isoxazolepropionic acid
ANP	Atrial natriuretic peptide
ApoE	Apolipoprotein E
APP	Amyloid precursor protein
ATP	Adenosine triphosphate
Aβ	Amyloid beta
Basp1	Brain acid soluble protein 1
ChR2	Channelrhodopsin-2
Cg	Chromogranin
CPE	Carboxypeptidase E
CSF	Cerebrospinal fluid
DCV	Dense-core vesicle
DIV	Days in vitro
EGTA	Ethylene-bis(oxyethylenenitrilo)tetraacetic acid
ER	Endoplasmic reticulum
FDR	False discovery rate
GABA	Gamma-aminobutyric acid
GAP-43	Growth-associated protein-43
GFAP	Glial fibrillary acidic protein
GSK3	Glycogen synthase kinase- 3
hSyn	Human Synapsin
IL	Interleukin
IP_3	Inositol (1,4,5)-triphosphate
iPSC	Induced pluripotent stem cells
ISG	Immature secretory granule
Lamp	Lysosome-associated membrane glycoprotein
LPS	Lipopolysaccharide
LTD	Long-term depression
LTP	Long-term potentiation
mGluR	Metabotropic glutamate receptors

MRI	Magnetic resonance imaging
MSGs	Mature secretory granules
Nf-L	Neurofilament light polypeptide
NMDA	N-methyl-D-aspartate
NPR	Natriuretic peptide receptor
NPY	Neuropeptide Y
Nrgn	Neurogranin
PBS	Phosphate-buffered saline
PC	Prohormone convertase
PCR	Polymerase chain reaction
PET	Positron emission tomography
POMC	Proopiomelanocortin
PS	Presenilin
PSD	Postsynaptic density
p-tau	Phosphorylated tau
SEM	Standard error of the mean
Sg	Secretogranin
SLMV	Synaptic-like microvesicle
SNAP	Synaptosomal-Associated Protein
SNARE	Soluble N-ethylmaleimide-sensitive factor attachment protein receptor
SV	Synaptic vesicle
TBOA	Threo-b-benzyloxyaspartic acid
TG	Transgenic
TGN	Trans-Golgi network
Tpm	Tropomyosin
TREM2	Triggering receptor expressed on myeloid cells
t-tau	Total tau
TTX	Tetradotoxin
VAMP4	Vesicle-associated membrane protein 4
WT	Wild-type

INTRODUCTION

INTRODUCTION

Nervous system entirely sense, organize, and react to information in the environment. Brain function essentially requires neurons to communicate with each other in a highly precise and organized manner that ensures the correct information processing. Understanding how synaptic connections are accurately formed and maintained remains essential to comprehend the hardwired neuronal networks.

Chemical and electrical synapses are the two main modalities of synaptic transmission (Pereda, 2014). The vast majority of the studies in chemical signals have been focused on synaptic vesicles (SVs), the most characteristic component of the nerve ending. Classical neurotransmitters including acetylcholine, catecholamines, glutamate and gamma-aminobutyric acid (GABA) are stored in these small vesicles, representing the biochemical interface between neurons (Curtis & Johnston,1974; Maycox et al., 1990; Jahn & Südhof, 1994) and playing a central role in a large number of brain functions, including learning and memory processes (Kopelman, 1986).

Coexisting in neurons with classical amino acid transmitters, another key component participates in the modulation of chemical transmission: peptide neurotransmitters (Hökfelt, 1991; Merighi, 2002). Peptide hormones, neuropeptides and neurotrophins are sorted and packaged into dense-core vesicles (DCVs), also named secretory granules. The peptidergic system has received considerably less attention than classical neurotransmitters, but they participate in a wide-ranging functions in the brain. These modulators exert key roles regulating the neuronal circuit development and function. In particular, they contribute to cell proliferation, axon and dendrite growth, synaptogenesis and synaptic plasticity, which finally impact on the neuronal activity (Huang & Reichardt, 2001; H. Park & Poo, 2013; Zaben & Gray, 2013).

Communication within the nervous system relies primarily on the stimulus-dependent release of classical and peptidergic neurotransmitters from SVs and DCVs, respectively (de Camilli & Navone, 1987). To further understand how secretory vesicles contribute to neurotransmission, neuronal secretory pathways are detailed herein.

Neuronal secretory pathways

In a neuronal communication system, chemical compounds are delivered to the extracellular milieu in a spatially and temporarily regulated fashion. Adjacent cells adapted to specifically trigger downstream cascade signals will be capable of generating precise responses.

Proteins are first translocated into the endoplasmic reticulum (ER) where they are folded, assembled and N-glycosylated (Braakman & Bulleid, 2011; Burgess & Kelly, 1987). Subsequently, they pass through the cis-, medial- and trans-cisternae of the Golgi apparatus. In the meanwhile, they undergo further post-translational modifications including O-glycosylation, phosphorylation and proteolytic cleavage. Afterwards, proteins destined for secretion are sorted, packaged and segregated in the trans-Golgi network (TGN), a specialized organelle responsible for routing proteins (Griffiths & Simons, 1986; Vázquez-Martínez et al., 2012) (Figure 1).

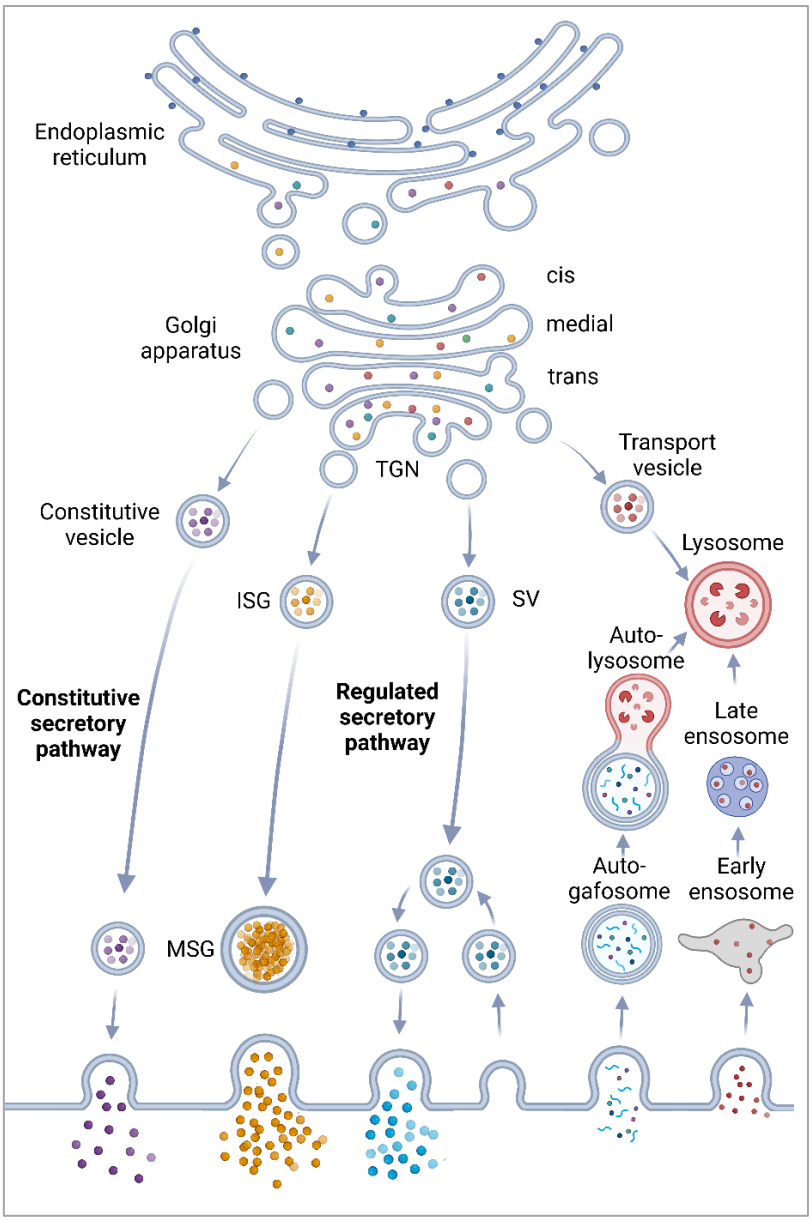

Figure 1. Constitutive and regulated neuronal secretory pathways.
Created with BioRender

Constitutive vesicles

Plasma membrane proteins, extracellular matrix proteins or metalloproteases are stored in constitutive vesicles, which fuse to the plasma membrane in a stimulus-independent fashion. Aside from neurons, constitutive secretory pathway is a default itinerary common to all cells (Burgess & Kelly, 1987).

Lysosomes

Hydrolytic enzymes and specific membrane proteins are mainly recognized by receptors for mannose 6-phosphate and subsequently destined to lysosomes (Kornfeld & Mellman, 1989). This acidic organelle is capable of digestion and protein degradation processes (de Duve & Wattiaux, 1966). Apart from newly vacuoles segregated from the TGN, lysosomes are also formed by an indirect route via the plasma membrane or by a direct intracellular route, as they can be made up of

endocytic, autophagic and phagocytic processes. In any case, lysosomes finally act as a dynamic degradative compartment (Blott & Griffiths, 2002; Luzio et al., 2007).

Apart from receiving and degrading biological macromolecules, lysosomes have been observed to fuse with the plasma membrane for the purpose of membrane repair (Luzio et al., 2007). Lysosome exocytosis would be controlled by the Ca^{2+} sensor synaptotagmin-VII and soluble NSF-attachment protein receptors (SNAREs) as a consequence of an increase in the concentration of cytosolic Ca^{2+} (Rao et al., 2004) .

In addition to conventional lysosomes, some cell types, most of them derived from the haematopoietic lineage, also contain secretory lysosomes, specialized organelles that stored newly synthesized secretory proteins. Particularly, they undergo regulated secretion as a result of the action of synaptotagmins, SNAREs and Rabs (Blott & Griffiths, 2002).

Regulated vesicles

The regulated secretory pathway is a hallmark of endocrine, exocrine, and neuronal cells, although it also exists in mast cells, platelets, large granular lymphocytes and neurotrophils (Vázquez-Martínez et al., 2012). In neurons, regulated secretion involves SVs and DCVs that contain classical neurotransmitters and peptidergic neurotransmitters, respectively, as mentioned before. Even though both compartments fuse in a stimulus calcium-dependent fashion, vesicular mechanisms referred to biogenesis, maturation and secretion differ considerably and remain strictly regulated.

Despite newly secretory proteins coming from the ER-Golgi-TGN system, classical neurotransmitters are predominantly synthesized locally at nerve endings (Südhof, 2004). At that point, SVs cluster in front of the active zone, a specialized area composed of an insoluble protein complex anchored to the presynaptic plasma membrane and opposed to the postsynaptic density (Südhof, 2012). This domain contains multiple individual sites for vesicle docking and release (Emperador-Melero & Kaeser, 2020). Fusion of SVs will take place in response to the arrival of an action potential, giving rise to synaptic transmission (Katz B, 1969). Thereafter, SV undergo endocytosis, recycle, and refill with neurotransmitters, going through trafficking cycles (Südhof, 2004) (Figure 2A).

In order to maintain an effective transmission, different pools of SV are positioned in a resting terminal following different capabilities of exocytosis. Population of vesicles are defined as readily releasable pool (consisting of 1%, primed and docked for a rapid mobilization and depletion at high frequencies of stimulation), the recycling pool (10-15%, for moderate stimulation) and the reserve pool (80-90%, released only during intense stimulation) (Rizzoli & Betz, 2005).

In contrast to SVs, DCVs undergo a different biosynthetic process. Rather than exhibit a local synthesis and recycling at the nerve terminal, granules are formed from budding of the TGN and mature into competent vesicles as long as they are transported toward the plasma membrane in a cytoskeleton-dependent fashion where exocytosis occur (Vazquez-Martinez & Gasman, 2014) (Figure 2B).

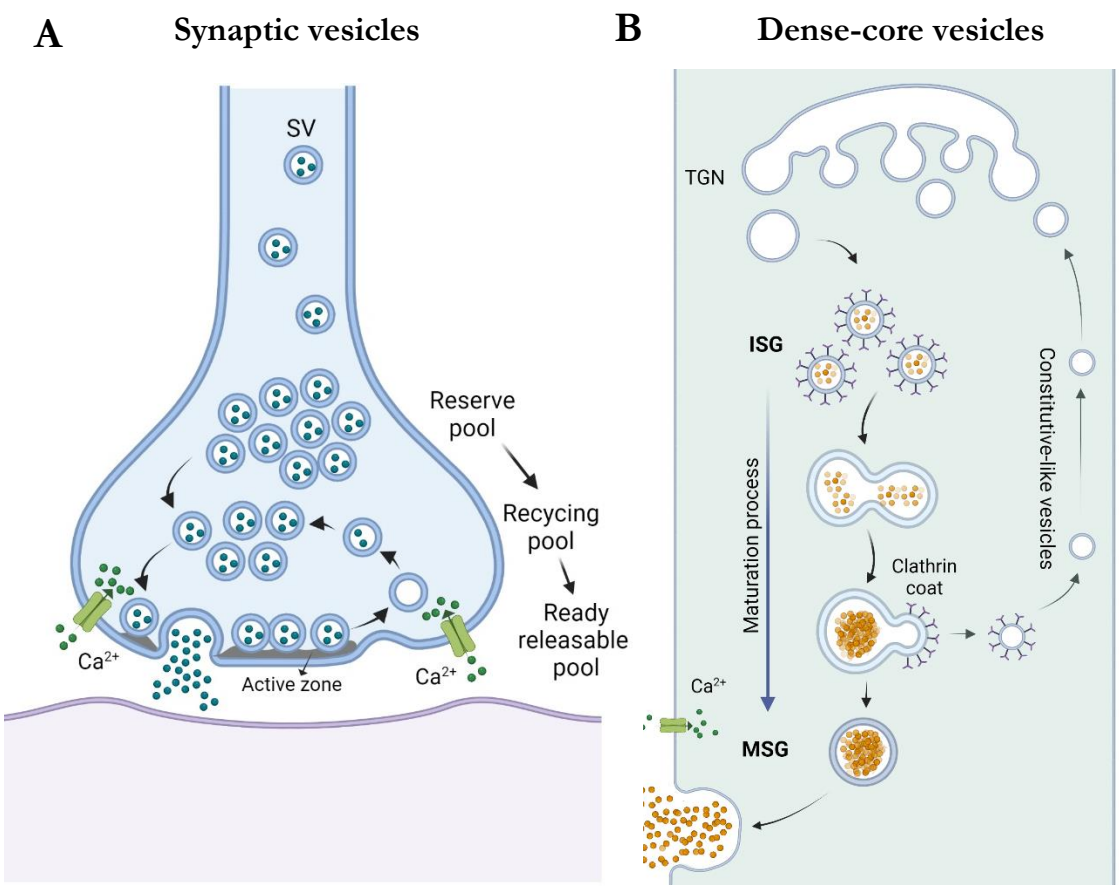

Figure 2. Biogenesis of synaptic vesicles (A) and dense-core vesicles (B).
Created with BioRender

At the TGN, peptidergic transmitters are firstly sorted into immature secretory granules (ISGs). These vesicles go through sequential maturation steps including the removal of constitutive secretory proteins, lysosomal enzymes, and some membrane proteins inaccurately packaged (Arvan et al., 1991; Kim et al., 2006; Kögel & Gerdes, 2009; Kuliawat et al., 1997). Moreover, maturation of ISGs involves homotypic fusion that enable their increase in size (Urbé et al., 1998). This event has been described to be dependent on syntaxin 6 and synaptotagmin-IV (Ahras et al., 2006; Wendler et al., 2001). As long as mature secretory granules (MSGs) are established, lumen become increasingly acidic (from pH 6.3-5.7 in ISG to pH 5.5-5.0 in MSG) (Urbé et al., 1997). Increases in H^+ pump density and decreases in H^+ permeability are responsible for the acidification process. Consequently, processing proteins become active, and hormones and neuropeptides mature into bioactive peptides that undergo condensation (Kim et al., 2006). This aggregation is evidenced as electro-dense material, a hallmark of DCVs (Palade, 1956). Furthermore, during ISG maturation, granules get rid of the clathrin coat and SNARE proteins such as synaptotagmin-IV and vesicle-associated membrane protein 4 (VAMP4) (Eaton et al., 2000). Resulting MSGs are stored and prepared to be exocytosed in response to specific secretagogues.

According to the existence of SV subpopulations, mature DCV are also segregated into different pools for specific fusion probabilities. Two main pools have been described: a ready releasable pool for immediate release, and a reserve pool for slower exocytosis under sustained stimulation (Kögel & Gerdes, 2009; Neher & Zuckert, 1993). However, for many cells most DCV are contained into the reserve pool (Rorsman et al., 2000).

SVs and DCVs not only exhibit a differential biogenesis process, but they also differ in size. Whereas SV is defined as a uniformly small vesicle that measures 40-55 nm in diameter, DCV is a larger vacuole that reaches more than 70 nm, fluctuating from neuron to neuron (de Camilli & Navone, 1987; Südhof, 2004; Thureson-Klein & Klein, 1990).

Moreover, in terms of content, SVs has been typically described to store only classical neurotransmitters with an amount of 1,000-5,000 molecules for each vesicle. However, much larger cargo is included in DCV, coming to 85,000 for each one (Leng, 2018). This evidence is supported by ultrastructural correlates, where SVs exhibit a clear core by electron microscopy in contrast to DCVs that manifest an electron-dense core (Burgess & Kelly, 1987) (Figure 3). In this core, other signalling molecules as catecholamines and monoamines are included (de Camilli & Navone, 1987; Kögel & Gerdes, 2009).

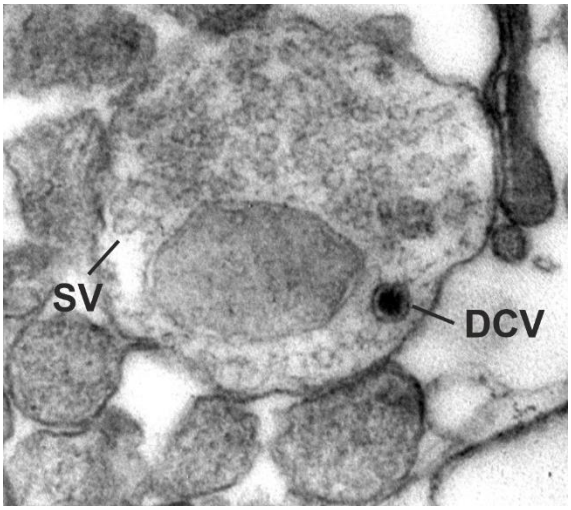

Figure 3. Transmission electron micrograph of cortical synaptosomes containing SV and DCV.

Maturation steps mentioned above allow vesicles turn into competent organelles capable of proceed exocytosis in a Ca^{2+}-dependent manner. However, where, when and how this occur differ in several important aspects from both SVs and DCVs.

Biosynthesis of SV ends once these vesicles are primed and docked at the presynaptic active zone (Südhof, 2004). Hence, classical neurotransmitters are basically released at the synapses, triggering the activation of postsynaptic receptors with a half-life of 5 ms, approximately (Ludwig & Leng, 2006).

Conversely, secretory granules fuse mainly at nonsynaptic sites (Figure 4). Exocytosis of neuropeptides has been observed in the cell body, dendrites, the perisynaptic membrane of axonal boutons, and axon shafts (Ludwig & Leng, 2006; Thureson-Klein & Klein, 1990; van den Pol, 2012). Peptides reach the extracellular milieu acting in close targets, but they can also diffuse long distances resulting in a volume transmission (Jansson et al., 2002). In contrast to fast amino acid transmitters, effects of peptidergic transmission on neuronal physiology are observed within seconds to minutes (van den Pol, 2012).

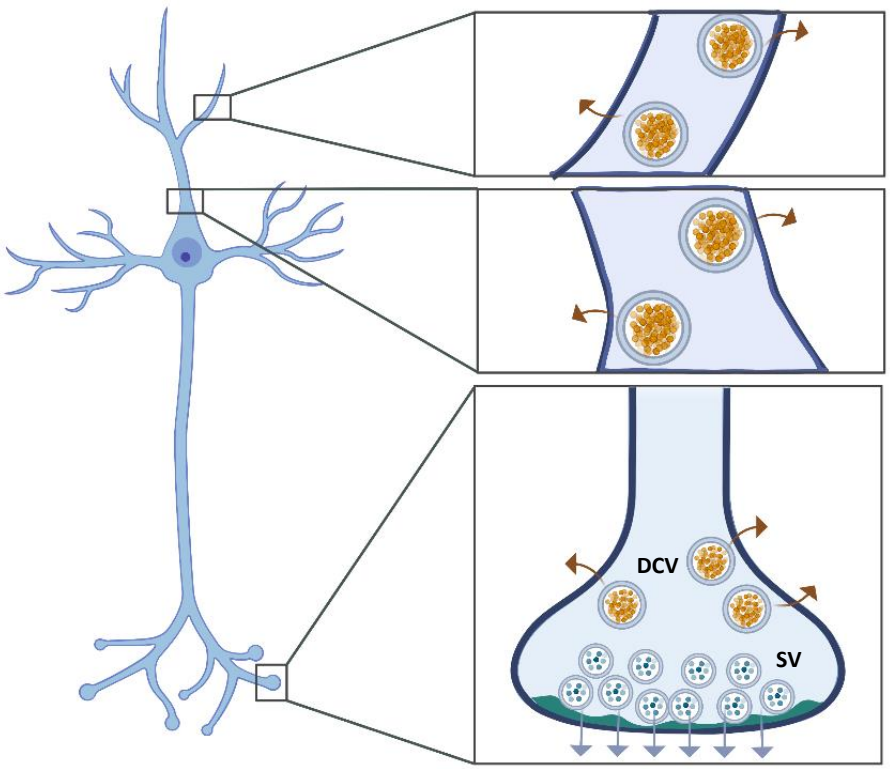

Figure 4. Schematic representation of synaptic vesicles fusing at presynaptic active zone and dense-core vesicles at nonsynaptic sites. Created with BioRender

In general terms, vesicle fusion occurs as a consequence of the Ca^{2+} influx through the plasma membrane. This event takes place as a result of the arrival of an action potential that depolarize the membrane potential, triggering the activation of voltage-gated calcium channels. Ca^{2+} is responsible for both SV and DCV release. However, peptide secretion requires a greater increase in cytoplasmic calcium compared to amino acid transmitters. This variation has a connection with the subcellular localization of these vesicles (Tallent, 2007).

Synaptic distribution of SV let them be positioned in close proximity to calcium channels. Therefore, they detect high concentrations of Ca^{2+}, being enough to activate their low affinity calcium sensors (Ludwig et al., 2017). In contrast, DCV are located in nonsynaptic sites, thus not being exposed to such high concentrations of calcium. This way, granules might be released by intense activation, considering that the machinery of DCV exocytosis has a high affinity for calcium. Moreover, dendritic release of secretory granules depends not only on extracellular sources but also on intracellular founts. Release of Ca^{2+} sequestered in the ER is regulated by second messengers pathways (Ludwig & Leng, 2006). Dendrite and axonal secretion of peptidergic neurons involve different exocytosis-related proteins and different calcium channels (Tobin et al., 2012; van den Pol, 2012).

Taken all this concepts into account, the regulated secretory pathway in neurons involves SV and DCV release in a calcium-dependent manner. However, not only different transmitters are contained in both vesicles, but they also vary in terms of localization, release mechanisms and the molecular machinery involved in exocytosis.

Molecular machinery of DCV

Peptide hormones and neuropeptides, such as brain-derived neurotrophic factor, neuropeptide Y (NPY), proopiomelanocortin (POMC) or somatostatin, are first synthetised at the rough ER as larger precursors. Then, they undergo several posttranslational processing steps to finally conform a mature bioactive peptide that will be stored in secretory granules until their stimulus-dependent release (Bonnemaison et al., 2013).

Sorting and processing of peptidergic transmitters are spatially and temporally regulated by the molecular machinery involving DCV. This essentially includes members of the granin family, the prohormone convertase (PC) family and a carboxypeptidase (Figure 5), analyzed in detail below.

Chromogranins (Cgs) A and B (CgA and CgB), secretogranins (Sgs) II and III (SgII and SgIII) and additional related proteins such as 7B2 (SgIV), neuroendocrine secretory protein of Mr 55,000 (NESP55) (SgVI), VGF (SgVII) and proSAAS (SgVIII) together comprise the granin family (Bartolomucci et al., 2011; Burgess & Kelly, 1987).

Granins constitute the major soluble proteins packaged in secretory granules (Bartolomucci et al., 2011). These acidic components bind to calcium and then aggregate (sorting by retention) in the presence of low pH, conditions established within the TGN (Chanat & Huttner, 1991; Gerdes et al., 1989). Moreover, they contain specific sorting signals that interact with concrete binding proteins or lipids that enable their movement to the regulated secretory pathway (sorting by entry (Arvan & Castle, 1998; Taupenot et al., 2003). In some way, aggregation would play an essential role for protein concentration before binding to sorting receptors (Bartolomucci et al., 2011).

CgA, CgB and SgIII act as granulogenic proteins driving budding at the TGN to constitute secretory granules (Kim et al., 2006). Certain domains contained in CgA and CgB have been observed to be associated with TGN membrane (Glombik et al., 1999; Taupenot et al., 2002). In fact, CgA specifically interact with SgIII, a lipid raft-associated protein that bind to cholesterol-rich membranes (Hosaka et al., 2002). All at once facilitates aggregation and curvature formation for granule biogenesis.

Precursor forms of peptidergic transmitters, packaged into immature secretory granules, are recognized and processed by endo- and exoproteases to ultimately generate active peptides. However, the catalytic activity of the endoproteases prohormone convertase 1 and 2 (PC1 and PC2) is modulated by the granin proteins proSAAS and 7B2, respectively (Braks & Martens, 1994; Fricker et al., 2000). Both granins exhibit structural homology and act as endogenous inhibitors (Cameron et al., 2000).

PCs are initially synthesized as inactive zymogens that must be proteolytically activated. First at the ER and later within immature granules, PC1/3 is activated by autocatalytic intramolecular cleavages. However, a further regulation step involves the C-terminal domain of proSAAS that play an inhibitor role of PC1/3 catalytic activity (Lee et al., 2004). In the case of PC2, proPC2 binds to 7B2 and this interaction enable the zymogen to be transported from the ER to the TGN, where PC2 catalytic activity is inhibited by the C-terminal domain of 7B2 (Muller et al., 1997). Nevertheless, 7B2

is internally cleaved allowing PC2 to be autocatalytically processed. In this way, active PC2 is finally reached in maturating secretory granules (Mbikay et al., 2001; Steiner, 1998).

Once prohormone convertases are functionally actives, they execute the proteolytic processing of many precursor proteins. PC1/3 and PC2 are calcium-dependent subtilisin-like endoproteases. This category also includes furin, PC4, PACE4, PC5/6, PC7/LPC/PC8, and SKI-1/S1P but they exhibit a distinctive tissue distribution (Seidah & Chretien, 1999; Steiner, 1998). In neuronal and endocrine cells, Furin, PC1/3 and PC2 play an essential role in the secretory system. Furin is localized ubiquitously and has a major role in processing enzymes of the constitutive secretory pathway, whereas PC1/3 and PC2 are serine endoproteases restrictedly localized in neuroendocrine tissues and responsible for the processing of precursor proteins within the regulated secretory pathway (Day et al., 1992).

Aside from differences in prohormones distribution, all members contain a N-terminal signal peptide, a proregion, a catalytic domain, a P or Homo B domain, and a C-terminal domain (Steiner, 1998). Most conserved regions include the catalytic domain followed by the P domain, required for processing activity, and described as essential for modulating enzymatic function and substrate specificity, as well as calcium and pH dependence (Zhou et al., 1998). In contrast, C-terminal domain is specific for each PC and contain structural regions essential for membrane attachment and sorting (Creemers et al., 1996; Muller et al., 2000). Trafficking to regulated secretory pathway has been supported by evidence in PC1/3 and PC2 association with lipid rafts in granule membranes (Arnaoutova et al., 2003; Blázquez et al., 2000).

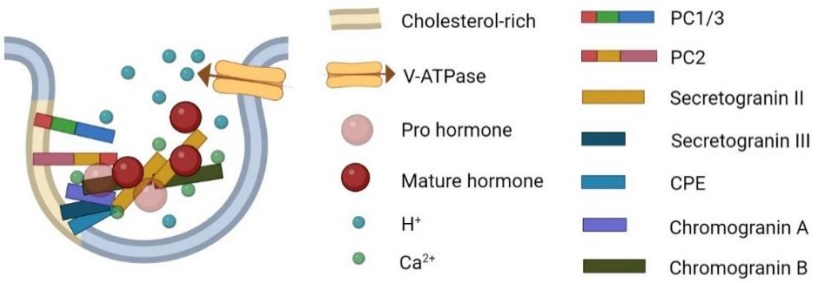

Figure 5. Molecular machinery of dense-core vesicles. Created with BioRender

Carboxypeptidase E (CPE) is a zinc-binding carboxypeptidase that hydrolyze the C-terminal arginine or lysine basic residues of peptide intermediates previously exposed by PCs. In this sense, CPE is similarly distributed in peptidergic neurons and endocrine cells (Fricker, 2004; Fricker & Snyder, 1982; Hook & Loh, 1984). This metallocarboxypeptidase protein structure consist of a signal peptide, a pro-domain, a catalytic domain and a highly acidic C-terminal region. Once CPE reaches the TGN, pro-region is removed facilitating the mature enzyme to take part in distinct roles (Cawley et al., 2012; Ji et al., 2017).

The acidic pH existing at the TGN is optimal for CPE to aggregate and for the carboxy-terminal domain to bind to cellular membranes (Frickersg et al., 1990; Song & Fricker, 1995). In consequence, CPE result in a lipid raft-associated protein sorted to secretory granules (Dhanvantari & Loh, 2000). In this trafficking, CPE play an essential role as a sorting receptor for prohormones such as POMC (Cool & Loh, 1998). Moreover, CPE facilitate the transport of DCV to the cell periphery considering that an additional CPE transmembrane form exhibits a cytoplasmatic tail that interact with microtubule motors and cytoskeletal proteins (Cawley et al., 2012; Park et al., 2008).

Taken together, the basis for synaptic transmission in neuronal networks includes regulated secretion of SVs and DCVs. In this respect, most investigations focused on how these vesicles are formed and secreted in the adult system. However, characterization of secretory pathways in developing neurons remains limited. To date, only one study evaluated SV and DCV secretion capacity during maturation of human induced pluripotent stem cells (iPSC)-derived neuronal cultures (Emperador Melero et al., 2017). Considering that neurotransmitters also regulate neuronal circuit development and function, more efforts are needed to better understand regulated secretory pathways during development of the mammalian nervous system.

Astrocyte contribution to brain function

In brain networks, neurons have been conceived as basic components orchestrating cellular communication. In this classical paradigm, information flow involves primarily synaptic contacts between pre- and postsynaptic neurons. However, accumulated evidence from the past twenty years referred a third element particularly modulating these connections: astrocytes.

Astrocytes are specialized glial cells exerting essential roles in the development, homeostasis and protection of the central nervous system. Hence, they are intimately associated with neurons. Referring to cellular communication, astrocytes actively regulate synaptic transmission giving rise to the concept of "tripartite synapse" (Araque et al., 1999) (Figure 6). In this sense, they enwrap nerve terminals and are capable of sensing neuronal activity, triggering an internal Ca^{2+} increase and, consequently, release chemical transmitters (called gliotransmitters) (Bezzi & Volterra, 2001; Cornell-Bell et al., 1990). This, in turn, causes feedback regulating neuronal activity and synaptic strength (Araque et al., 1999; Cornell-Bell et al., 1990; Halassa & Haydon, 2009; Perea et al., 2009).

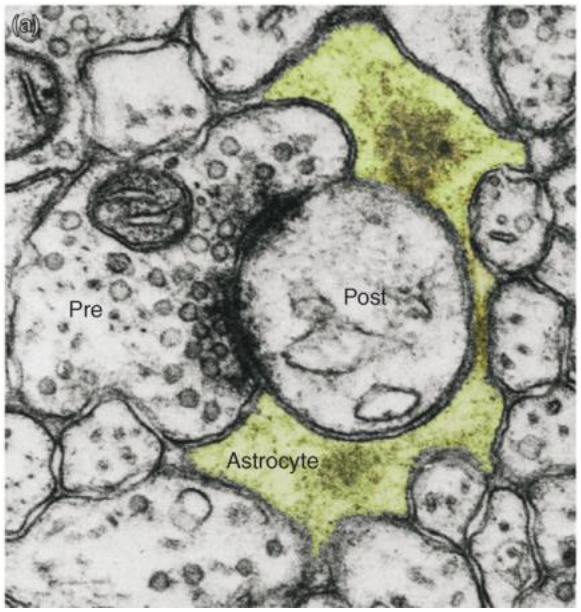

Figure 6. Electron micrograph of a trypartite synapse (Halassa et al., 2007)

Decoding neuronal information

In the tripartite synaptic context, astrocytes are optimally positioned encompassing neuronal membranes. In fact, the distance between terminal structures of astrocytes and neuronal membrane is often about few nanometres (Khakh, 2019; Octeau et al., 2018). In this way, they lie in close proximity to secreted neuronal transmitters, empowering astrocytes to sense, integrate and process synaptic information.

Astrocytes receive neuronal information through the expression of a wide array of membrane receptors, including ionotropic and metabotropic receptors. Actually, nearly any type of receptor in the central nervous system is found in astrocytic membranes (Verkhratsky & Nedergaard, 2018). However, they are variably distributed depending on the brain region. Some of the most important receptors are highlighted below.

Purinergic receptors

Purinergic transmission is a widespread pathway in cellular communications that play a special role in neuroglia networks (Abbracchio et al., 2009). Adenosine triphosphate (ATP) acts as a co-transmitter in neuronal secretory vesicles exerting specific intracellular signalling in astrocytes. After being released, ATP undergo rapid degradation by extracellular ectonucleotidases, generating different metabolites (ADP, AMP and adenosine) that mediate diverse physiological functions.

Adenosine activates P1 purinergic receptors, a metabotropic receptor family that is divided in four subtypes (A_1, A_2A, A_2B, and A_3). Interestingly, all of them have been identified in astrocytes *in vitro* and *in situ* (Biber et al., 2001; Chen et al., 2001; Doengi et al., 2008; Nez et al., 1999; Porter & McCarthy, 1995; Verkhratsky & Nedergaard, 2018). In this way, astrocytes adenosine receptors modulate glycogen metabolism, glutamate transporters, astrogliosis and astrocyte swelling (Daré et al., 2007; Nishizaki et al., 2002).

P2 receptors are divided into P2X (ionotropic receptors) and P2Y (metabotropic receptors) and are recognized by ATP. In particular, astrocytic P2X7 receptors have been implicated in pathological processes, including apoptosis, astrogliosis or regulation of cytokines release (Franke et al., 2012; Sperlágh et al., 2006). In the case of P2Y receptors, they are widely distributed in astrocytes and their activation is linked to several functions (Verkhrasky et al., 2009). They are linked to the IP_3-mediated Ca^{2+}-signalling, playing a particular role in the maintenance of propagating Ca^{2+} waves (Verkhratsky, 2005; Verkhratsky et al., 1998). In fact, they actively regulate gliotransmitters release (Anderson et al., 2004). Moreover, P2Y receptors are linked to neuropathological aspects (Brambilla et al., 1999).

However, purines and pyrimidines are not only secreted by neurons. Astrocytes are also capable of releasing both adenosine and ATP through vesicle exocytosis and via membrane channels (Bowser & Khakh, 2007; Luisa Cotrina et al., 2000). Therefore, ATP acts as a widespread gliotransmitter involving a reciprocal neuron-glia communication (Butt, 2011).

Glutamate receptors

Glutamate is the major excitatory neurotransmitter in the brain exerting a wide range of neuronal functions. Specifically, glutamate act as a key neuromodulator in synaptic transmission, playing an essential role in neuron-glia interactions.

Glutamate signalling activates a family of receptors that consist of ionotropic receptors and metabotropic receptors. Most characterized ionotropic glutamate receptors in astrocytes include a-amino-3-hydroxy-5-methyl-4-isoxazolepropionic acid (AMPA) and N-methyl-D-aspartate (NMDA) receptors. All four main subunits of AMPA receptors have been described in this cell type (Conti et al., 1994). Referring to NMDA receptors, those predominantly found in rodents are GluN1 and GluN2A/B/C (Conti et al., 1999; Paco et al., 2016; Schipke et al., 2001), whereas transcripts for all seven NMDA subunits were identified in human astrocytes (Lee et al., 2010).

Regarding metabotropic glutamate receptors (mGluR), mGluR3 and mGluR5 have been functionally identified in astrocytes. Nevertheless, during life span, their protein profile remains somewhat altered (Sun et al., 2013). mGluR3 was abundantly detected in astrocytes at all developmental stages; in contrast, mGluR5 appeared enriched at early postnatal development (Cai et al., 2000). This observation has a functional impact considering that mGluR5 mediate Ca^{2+} astroglial signals and intracellular Ca^{2+} oscillations (D'Ascenzo et al., 2007; Porter & Mccarthy, 1996). Being glutamatergic signalling the most frequent neuronal input, mGluR5 could represent a key element in gliotransmission. However, the downregulation of mGluR5 expression questions regulated release of gliotransmitters at later developmental stages (Fiacco & McCarthy, 2018). Nevertheless, other receptors participate in adulthood gliotransmission, including purinergic receptors (Santello et al., 2011) or cholinergic receptors (Navarrete et al., 2012).

In connection with glutamatergic transmission, astrocytes exert another key role in synaptic modulation. When extracellular glutamate levels are maintained for long-time, astrocytes are capable of removing this excess by excitatory amino acid transporters and convert it intracellularly to glutamine (Danbolt, 2001). This clearance contributes to reducing glutamate-mediated excitotoxicity (Andersen et al., 2021; Parpura et al., 2012). At this time, glutamine can be safely transported to presynaptic terminals where it is enzymatically transformed into glutamate. In this way, astroglial glutamate-glutamine shuttle remain essential in the glutamatergic transmission.

Neuropeptide receptors

Astrocytes react to neuromodulators from the neuropil due to the expression of neuropeptide receptors, providing another example of the extended neuron-glia interaction (Krisch & Mentlein, 1994; van den Pol, 2012). Different neuropeptides and hormones activate astroglial surface receptors. For instance, astrocytes exhibit vasopressin and oxytocin receptors (di Scala-Guenot et al., 1994; Jurzak et al., 1995).

Another example relies on natriuretic peptide signalling. These compounds regulate extracellular fluid volume and blood pressure but play specific roles in modulating brain function acting as neurotransmitters or neuromodulators (Hodes & Lichtstein, 2014). Particularly, several members of this family have an effect through interaction with concrete astrocytic receptors. In general, atrial natriuretic peptide (ANP) binds preferentially to natriuretic peptide receptor (NPR)-A, while brain natriuretic peptide and C-type natriuretic peptides bind to NPR-B. Moreover, all

natriuretic peptides bind with equal affinity to NPR-C. Hence, all three types of receptors have been identified in astrocytes (Sumners et al., 1994).

Furthermore, other neuropeptide elements such as somatostatin, substance P, endothelins, Pituitary adenylyl cyclase activating polypeptide, vasoactive intestinal peptide act through specific receptors in astrocytes (Hösli & Hösli, 1991; Joo et al., 2004; Krisch et al., 1991; Torrens et al., 1986). Therefore, astrocytes are actively involved in a wide range of peptidergic circuitries being considered as a target cell of different neuropeptides.

Ca^{2+} signalling in response to neuronal activity

In synaptic transmission, neurons receive a wide variety of input signals that efficiently process to finally elicit concrete responses. Generation of an action potential play a central role in the transmission of these signals, ensuring neuron-to-neuron communication. The origin of an action potential in neurons is basically achieved due to the unique membrane properties and the presence of active channel conductance.

In synaptic networks, astrocytes respond to neuronal activity and actively participate in the regulation of synaptic neurotransmission (Perea et al., 2009). As previously described, they are capable of receiving neuronal inputs via a wide range of membrane receptors. However, in contrast to neurons, astrocytes are electrically nonexcitable cells. Nevertheless, they translate these signals into a complex intracellular Ca^{2+} code (Araque et al., 2001; Cornell-Bell et al., 1990). Of note, Ca^{2+} excitability in astrocytes might also appear spontaneously, reflected as intrinsic oscillations (Aguado et al., 2002; Nett et al., 2002).

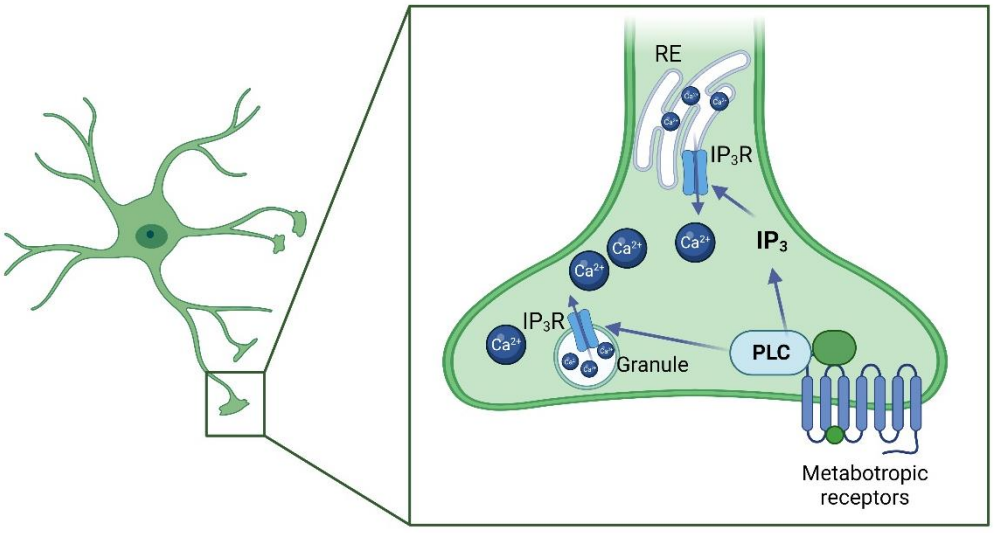

Figure 7. Schematic representation of IP_3-induced Ca^{2+} mobilization from intracellular stores in astrocytes. Created with BioRender

Apart from other molecular cascades involved in intracellular calcium signalling, the major mechanism for Ca^{2+} release in astrocytic internal stores involve the formation of inositol (1,4,5)-triphosphate (IP_3) (Verkhratsky et al., 1998). For instance, metabotropic receptors distributed in astrocytic membranes are associated with G proteins that, upon activation, stimulate phospholipase

C. This, in turn, elevates IP_3 levels that, consequently, increases intracellular Ca^{2+} concentration through the release of Ca^{2+} from intracellular IP_3-sensitive Ca^{2+} stores (Hua et al., 2004). In particular, Ca^{2+} stores in astrocytes involve predominantly the ER (Verkhratsky et al., 1998), although isoforms from IP_3 receptors have also been identified in astrocytic granules (Hur et al., 2010) (Figure 7).

Interestingly, variations in intracellular Ca^{2+} levels can be propagated to neighbouring astrocytes as intercellular waves (Scemes & Giaume, 2006). This intercellular communication is mediated by two specific pathways. On one side, gap junctions facilitate the transfer of Ca^{2+}-mobilizing second messengers between the cytosols of two adjacent cells (Finkbeiner, 1992) while, on the other side, such secondary messengers are generated through the activation of membrane receptors. As mentioned before, secretion of gliotransmitters activates membrane receptors on neighbouring cells triggering the production of IP_3, which follow in Ca^{2+} release from intracellular stores. In this manner, fluctuations in intracellular Ca^{2+} can generate a global intercellular reaction (Hirase et al., 2004).

During wave propagation, several cellular and molecular targets can be activated inducing changes in astrocytes. Astroglia express Ca^{2+}-dependent ion channels, mostly potassium channels, that contribute to wave transmission (Armstrong et al., 2005; Gebremedhin et al., 2003). Furthermore, the Na^+/Ca^{2+} exchanger distributed in astrocytic plasma and ER membranes eventually become more active contributing to ionic content regulation within the cytoplasm and the extracellular space (Reyes et al., 2012). Other effective target could involve calcium-sensitive protein kinases such as protein kinase C or calmoculin leading to the production of second messengers (Scemes & Giaume, 2006).

Additionally, another key Ca^{2+}- dependent mechanism affected during elevation of intracellular Ca^{2+} concentration concern the molecular machinery involved in vesicle exocytosis. The evolutionary conserved family of SNARE proteins play a key role in vesicle release (Söllner et al., 1993; Weber et al., 1998). SNARE components are not identical in astrocytes and neurons (Montana et al., 2006; Parpura et al., 1995). In general terms, suprathreshold cytosolic Ca^{2+} concentrations in neurons activate VAMP2, synaptosomal-associated protein 25 (SNAP25) and syntaxins that form a protein complex facilitating vesicle fusion with the plasma membrane. Instead, astrocytes express VAMP2/3, SNAP23 and syntaxins (Bezzi et al., 2004; Paco et al., 2009; Wilhelm et al., 2004). Although SNARE complex in astrocytes has been characterized to a lesser extent, this mechanism enables gliotransmitter release.

Gliotransmitters

Astrocytes respond to neuronal activity with an increase of intracellular Ca^{2+} levels, which trigger in vesicle fusion. They participate in the neuron-glia network releasing classic neurotransmitters, neuropeptides, hormones, and trophic, metabolic and plastic factors. In fact, similar to neurons, the astroglial exocytic compartment includes synaptic-like microvesicles (SLMVs), dense-core-like vesicles (DCV-like), lysosomes, exosomes and ectosomes (Verkhratsky et al., 2016; Verkhratsky & Nedergaard, 2018) (Figure 8).

Lysosomes, exosomes and ectosomes

Lysosomes represent an intracellular organelle, whereas exo- and ectosomes correspond to extracellular compartments released into the surrounding environment. Besides differences in the origin, these vesicles are defined as a heterogenous population that differs in size and function. However, some similarities are observed regarding cargo content.

Lysosomes are vesicles of 300-500 nm in diameter that primarily contribute to membrane repair. Exosomes are smaller in size, between 40 and 100 nm, originated in the endosomal compartment and included in multivesicular bodies. This extracellular vesicle participates in homeostasis and regulate intercellular communication, playing a role in pathological conditions. In the case of ectosomes, it includes microvesicles, microparticles and large vesicle displaying a wide range size, from 100 to more than 1.000 nm in diameter that are formed via outward budding (Verkhratsky et al., 2016; Verkhratsky & Nedergaard, 2018).

In terms of content, astrocytic lysosomes abundantly contain ATP (Zhang et al., 2007), apart from proteolytic enzymes. In the case of exosomes and ectosomes, both are typically loaded with cytokines, signalling proteins and nucleic acids. In particular, astrocytic ectosomes include activity-regulated factors such as fibroblast growth factor 2 and vascular endothelial growth factor, and matrix metalloproteases (Proia et al., 2008; Sbai et al., 2010). Of note, exosomes also carry mitochondrial DNA (Guescini et al., 2010).

Synaptic-like microvesicles

In astrocytes, SLMVs are 30-100 nm-diameter vesicles typically localized in somata and perisynaptic processes. It conforms a small group of a few tens of vesicles, in contrast to the hundreds to thousands that typically exhibit a neuronal presynaptic terminal (Bergersen et al., 2012; Bezzi et al., 2004). Specifically, classical amino acid transmitters D-serine and glutamate have been observed to be contained in astroglial SLMVs (Araque et al., 1998; Martineau et al., 2008). This accumulation is particularly accomplished as a result of the expression of vesicular neurotransmitter transporters: vesicular D-serine transporter for the storage of D-serine, and vesicular glutamate transporters 1-3 for glutamate package (Bezzi et al., 2004; Martineau et al., 2013; Ormel et al., 2012).

Glutamate in astrocytes can be secreted following different routes (Malarkey & Parpura, 2008). It can also be released by plasma membrane transporters (Szatkowski et al., 1990), anion channels (Kimelberg et al., 1990) or hemichannels on the cell surface (Ye et al., 2003). However, glutamate was the first gliotransmitter identified to follow a Ca^{2+}-dependent release, suggesting an astrocytic regulated secretory pathway (Araque et al., 2000; Bezzi et al., 1998; Montana et al., 2004; Parpura et al., 1994). Of note, D-serine also evidenced a vesicular storage competent to Ca^{2+}-regulated secretion (Martineau et al., 2008; Mothet et al., 2005).

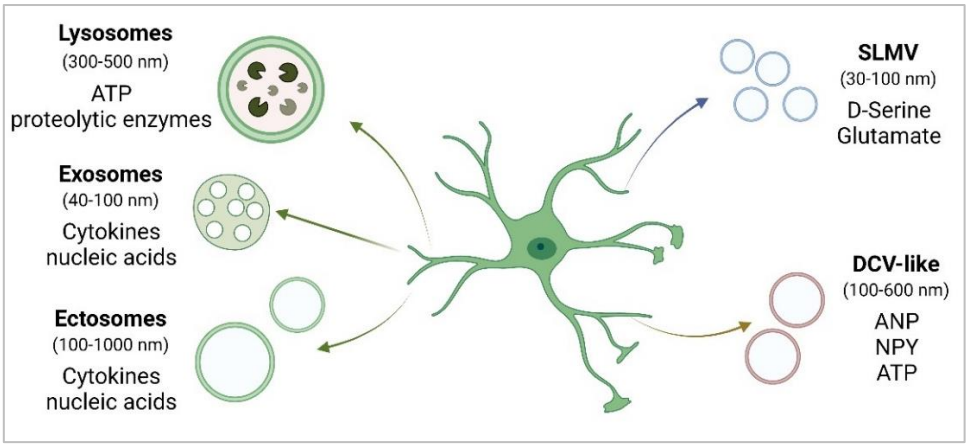

Figure 8. Astrocytic secretory compartment. Created with BioRender

Dense-core-like vesicles

Astrocytes express some neuropeptides and store them in vesicles similar to neuronal DCV. These astrocytic vesicles are larger compared to SLMVs, reaching a diameter of 100-600 nm (Hur et al., 2010; Verkhratsky et al., 2016). However, the ultrastructural morphology evidence a vesicle core not as electron-dense as neuronal secretory granules (Potokar et al., 2008).

In cultured astrocytes, DCV-like carry NPY (Ramamoorthy & Whim, 2008; Zafra et al., 1992), ANP (Kreft et al., 2004; Paco et al., 2009), proenkephalin (Klein & Fricker, 1992; Spruce et al., 1990), but also ATP (Coco et al., 2003). Interestingly, they also express neuropeptide processing enzymes such as SgII and SgIII (Calegari et al., 1999; Paco et al., 2010), chromogranins (Hur et al., 2010) and CPE (Klein & Fricker, 1992; Vilijn et al., 1989). Some studies have demonstrated reactivity of ANP and secretogranins in astrocytes *in situ* (Hur et al., 2010; McKenzie, 1992; Paco et al., 2009). However, expression of DCV proteins *in situ* is largely unknown.

Similar to SLMVs containing glutamate, peptidergic vesicles have been described to follow a regulated secretion controlled by Ca^{2+}-dependent mechanisms (Calegari et al., 1999). ANP, NPY, and ATP have been defined to be secreted by Ca^{2+}-regulated exocytosis (Coco et al., 2003; Krzan et al., 2003; Paco et al., 2009; Pangršič et al., 2007; Ramamoorthy & Whim, 2008). However, most results come from studies performed in astroglial primary cultures and little is known about the secretory profile *in vivo*.

Taken together, astrocytes produce a wide variety of secretory organelles that differ in size, origin, cargo and function, being released into the surrounding environment by multiple secretory pathways (Verkhratsky et al., 2016). Astrocytes respond to neuronal activity with an increase of intracellular Ca^{2+} levels, which trigger in vesicle fusion. This secretory pattern has been classically demonstrated in pure astrocytes cultures. However, whether astrocytes can secrete gliotransmitter in a calcium-regulated manner under physiological conditions having a functional outcome remain under debate (Fiacco & McCarthy, 2018; Savtchouk & Volterra, 2018). Considering that astrocyte activity directly regulates synaptic transmission, relevant for the physiology of the central nervous system, it remains essential to further investigate the coordinated activity of a network involving neuron-glia communication.

Synaptic function in Alzheimer's disease

Brain network act in a coordinated dynamic fashion that enable us to sense the world, communicate these sensations to other cells and, finally, execute precise responses. In this way, regulation of the synaptic activity allows us to generate concrete thoughts, decisions, memories and emotions.

To guarantee efficient information flow between neurons, the synapse must be maintained anatomically and functionally intact. However, the neural network is dramatically exposed to insults affecting the central nervous system (Henstridge et al., 2016). In particular, synaptic dysfunction underlie many neurodegenerative diseases, such as Parkinson's disease, Lewy body diseases or Alzheimer's disease (AD) (Selkoe, 2002).

Alzheimer's disease

AD is the most common cause of dementia in the elderly (60% to 80% of cases), which affects around 55 millions of people across the world, and it is characterized by a progressive memory impairment and other cognitive disabilities such as disorientation, apathy or depression.

AD is a multifactorial disease; therefore, several factors contribute to AD pathogenesis. The vast majority of people develop late-onset Alzheimer, being age the greatest risk factor (Guerreiro & Bras, 2015). Additionally, several genes increase the risk of AD. Apolipoprotein E (apoE), in particular the isoform ε4, has the strongest impact in humans (Tsai et al., 1994). However, a small percentage of AD cases develop early-onset familial AD, which involves genetic mutations in amyloid precursor protein (APP) genes or in proteins associated with APP processing, such as presenilin-1 (PS1) and PS2 (Lanoiselée et al., 2017).

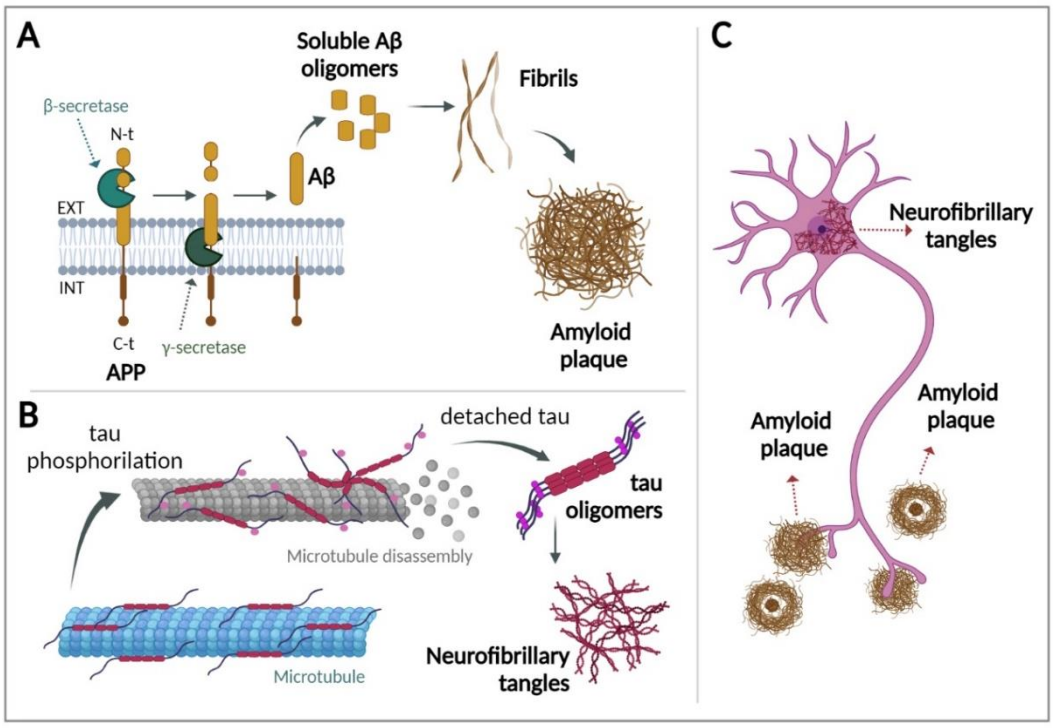

Figure 9. Neuropathological hallmarks of AD. Created with BioRender

The neuropathological hallmarks of AD consist of an extracellular deposition of aggregated amyloid beta (Aβ) peptides that conforms the senile plaques, followed by intracellular accumulation of hyperphosphorylated tau producing neurofibrillary tangles (Hyman, 1997; Serrano-Pozo et al., 2011). Additionally, these changes are accompanied by damage and death of neurons, causing neurodegeneration (Figure 9).

The progression of AD from brain changes result in three clinical stages: a preclinical phase where people have not yet developed symptoms, but they have measurable brain changes indicating early signs of the disease; a mild-cognitive impairment phase where patients undergo evident brain changes plus new symptoms; and the AD dementia phase, which implies clear brain changes accompanied by noticeable symptoms (Albert et al., 2013; McKhann et al., 2011; Sperling et al., 2011) (Figure 10). In spite of all scientific advances to identify initial brain changes, early clinical diagnosis is still challenging. To achieve this objective, greater efforts to understand the neuropathology of AD remains essential to further detect molecular targets of the disease.

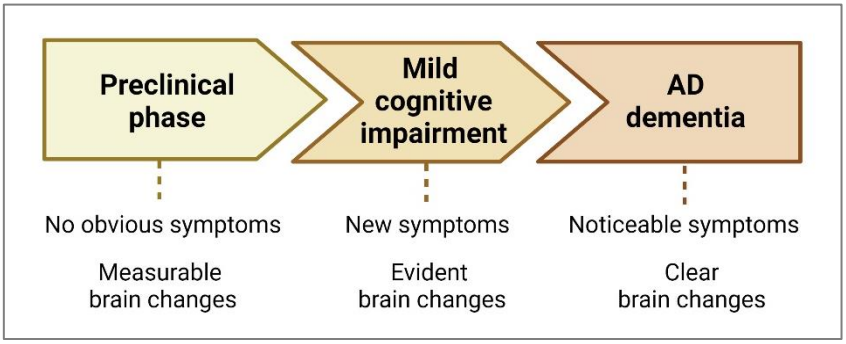

Figure 10. The progression of Alzheimer's disease. Created with BioRender

Role of Aβ in AD pathogenesis

Aβ peptides result from the proteolytic cleavage of the transmembrane APP, mediated by integral membrane proteases called secretases. APP can be initially cleaved by α-secretase or β-secretase at single sites in the extracellular domain and then, sequentially cleaved by γ-secretase, generating diverse intracellular fragments and Aβ40 and Aβ42 peptides (Citron et al., 1996; Klafki et al., 1996), both having pathogenic effects. However, Aβ42 is more prone to aggregation and believed to be more neurotoxic than Aβ40 (Figure 9).

Traditionally, the "amyloid cascade hypothesis" focused on amyloid plaques as the key upstream factor for AD-related pathology (Hardy & Allsop, 1991; Selkoe, 1991), which commonly precedes the development of clinical symptoms by at least ten years. Senile plaques caused by Aβ overproduction or reduced clearance was considered essential causing synaptic and neuronal toxicity, cell death and cognitive decline.

This hypothesis is strongly supported by the genetics of familial AD, where mutations in PS1 and PS2, the catalytic subunits of γ-secretase, cause familial AD implicating Aβ overproduction (Bettens et al., 2010; Scheuner et al., 1996; Tanzi, 2012). Moreover, development of dystrophic neurites in the vicinity of the plaque has been reported in human patients and in transgenic mice (Knowles et al., 1999; Meyer-Luehmann et al., 2008).

However, drugs developed on the basis of the amyloid cascade hypothesis did not fully rescue normal function (Selkoe & Hardy, 2016). Several approaches that include aggregation inhibitors, secretase inhibitors and immunotherapies failed both in animal models and human patients (Holmes et al., 2008). Furthermore, mouse models of AD that express mutant human APP, sometimes together with mutant presenilins, reported high concentrations of Aβ in the brain followed by plaque depositions with aging. Nevertheless, they undergo a minimal neuronal loss and not necessarily correlated with plaque deposition (Boncristiano et al., 2005; Hsia et al., 1999). Therefore, several evidence indicates that plaques alone are not responsible for pathological features of AD.

In fact, the exact meaning of the amyloid hypothesis varied throughout the years. Instead of being senile plaques the major focus of AD pathology, soluble microaggregates of Aβ peptides (called Aβ oligomers) attracted more attention (Lesné et al., 2006). Aβ oligomers in APP transgenic mouse brain and in human AD brain exert several synaptotoxic effects.

Taken together, Aβ oligomers are involved in several toxic events affecting synaptic function. However, the specific sizes and types of Aβ oligomers promoting synaptic impairment remain under debate. Moreover, another aspect to consider involve amyloid plaques acting as a potential reservoir that can release soluble Aβ oligomers. Therefore, we do not have to ignore senile plaques contribution to neuropathology in AD.

Role of tau in AD pathogenesis

Tau is a binding protein associated with neuronal microtubules that stabilizes them and regulate the transport of vesicles or organelles along them (Mandelkow et al., 1995). Tau receives post-translational modifications including phosphorylation, but an altered phosphorylation pattern is involved in AD pathogenesis. In AD, hyperphosphorylated tau loss stability and undergo aggregates inside neurons, establishing paired neurofilaments (Grundke-Iqbal et al., 1986; Mandelkow & Mandelkow, 1998; Morris et al., 2015) (Figure 9).

In the amyloid cascade hypothesis, tau hyperphosphorylation is considered a key step downstream of Aβ aggregation. In fact, Aβ oligomers can induce tau phosphorylation (de Felice et al., 2008). However, aggregated forms of tau can also be generated in the absence of Aβ. Therefore, whether Aβ causes tau pathology remains under discussion.

To point out, neurofilament deposition is more closely correlated with neurodegeneration and cognitive dysfunction than plaque pathology (Bancher et al., 1993; Braak & Braak, 1991a). Hence, generation of tau transgenic mice also result in synaptic impairment and neuronal death in an age-dependent fashion (Tanemura et al., 2001; Tatebayashi et al., 2002). In this sense, tau-targeting therapies show potential results in animal models (Iqbal et al., 2018).

In AD pathology, neurofibrillary tangles exhibit a characteristic spatiotemporal distribution in the brain. Tau accumulation occurs in a hierarchical manner beginning in the entorhinal cortex, progressing through hippocampal formation, and spreading to isocortical areas, as defined in the traditional Braak staging system used for postmortem AD diagnosis (Arnold et al., 1991; Braak & Braak, 1991b).

The characteristic distribution pattern of neurofibrillary tangles contributed to generation of "tau propagation hypothesis". In this context, pathological tau is transmitted from neuron to neuron similarly to prion proteins (Holmes & Diamond, 2014; Hyman, 2014; Sanders et al., 2014). However, the exact mechanism by which tau accumulation is released by one cell and uptake by the next one is yet unknown. In fact, accumulated evidence indicates now that soluble tau oligomers, rather than neurofilament tangles, play more toxic roles in the pathology (Guerrero-Muñoz et al., 2015; Kopeikina et al., 2012; Lasagna-Reeves et al., 2012).

In essence, early manifestation of AD pathology involves memory impairment, which can be closely related to neurofibrillary degeneration. Moreover, neurofilament tangles is associated with impair cognitive progression. Nevertheless, the role of tau in synapse loss is less established. More research is needed to understand this process and to potentially target new therapeutic strategies.

Neuropathology of AD impacting synaptic function

As described before, the neuropathological hallmarks of AD are the extracellular deposition of Aβ and the accumulation of twisted strands of tau within neurons in the brain. Both markers coexist intimately in relation with memory loss, cognitive decline and neurodegeneration. However, none of the currently available treatments targeted to these pathological features are capable of stopping the disease process and cognitive decline. Therefore, it remains essential to further investigate the molecular mechanisms underlying AD pathology to develop more specific interventions.

In this sense, apart from the "positive" lesions described in AD (amyloid plaques and neurofibrillary tangles), the disease is accompanied by "negative" lesions that play a central role in this pathology: the neuronal and synaptic loss. Indeed, the loss of synapses is the strongest neuropathological correlate of cognitive impartment in patients with AD (Terry et al., 1991). It occurs early in the disease and continues to parallel cognitive decline throughout disease progression (Akram et al., 2008; Dekosky & Scheff, 1990; Scheff et al., 1990), being a better predictor than the amyloid plaque load.

Synapse loss is a morphological reflection of the synaptic dysfunction. In this way, disruptions in synaptic composition impact in synaptic function, leading to altered network activity and finally to clinical manifestation of the disease. Of note, it is clear that Aβ peptides and tau exert toxic effects on synapse integrity. However, the exact pathogenic pathways underlying synapse loss and synapse-based neurodegeneration are yet to be fully elucidated.

Role of Aβ in synaptic dysfunction

Several mechanisms link Aβ peptides to synaptic dysfunction (Forner et al., 2017; Sheng et al., 2012). For instance, oligomeric synaptotoxicity involve binding to ionotropic and metabotropic postsynaptic receptors. Aβ receptors at synapses may include NMDA receptors (de Felice et al., 2007; Decker et al., 2010), mGluR5 (Renner et al., 2010) and a7-nicotinic acetylcholine receptors (Dineley

et al., 2001; Wang et al., 2000). These interactions together with Aβ binding to L-type voltage-gated Ca^{2+} channels, alter Ca^{2+} concentration in dendrites having an effect on multiple synaptic functions (Ueda et al., 1997).

Ca^{2+} influx influence long-term potentiation (LTP) and long-term depression (LTD). Hence, Aβ oligomers impairs LTP *in vivo* (Shankar et al., 2008; Walsh et al., 2002). Moreover, changes in Ca^{2+} concentration activates calcineurin which facilitates internalization of AMPA and NMDA receptors. Consequently, Aβ species enhance LTD, correlating it with the reduction and the loss of dendritic spines (Hsieh et al., 2006; Snyder et al., 2005). Furthermore, Aβ peptides also stimulates protein kinase glycogen synthase kinase- 3 (GSK3) activity. This, in turn promotes LTD and inhibit LTP via NMDA-receptor. Interestingly, GSK3 have been related to APP processing, increasing Aβ production (Ryder et al., 2003), evolving in a loop of synaptic dysfunction.

Another pathway activated directly or indirectly by Aβ species is the mitochondrial pathway of apoptosis. Increased activity of caspase-3, the main caspase mediator in apoptosis, has been detected in the dendritic spines of hippocampal neurons of transgenic mice (D'Amelio et al., 2011). Moreover caspase-3 immunoreactivity was observed in granulovacuolar degeneration, a neuropathological feature of AD (Stadelmann et al., 1999). Of note, LTD and AMPA receptor internalization requires activation of caspase-3. Therefore, the mitochondrial pathway of apoptosis is involved in synaptic depression and cell death (Li et al., 2010). Taken together, Aβ may induce synaptic failure via a combination of synaptic pathways.

Role of tau in synaptic dysfunction

The mechanisms of synapse dysfunction associated with pathological changes in tau are less well identified. In fact, the function of tau in the basic biology of neurons is less stablished, but it is known that tau is implicated in several mechanisms of synaptic function (Forner et al., 2017).

Tau has been primarily observed at the axonal level (Dixit et al. 2008). Nevertheless, hyperphosphorylated tau also accumulates in the somatodendritic compartment (Ballatore et al., 2007; Li et al., 2011; Stoothoff & Johnson, 2005). Especially, recent studies have revealed an important role for tau in the postsynaptic density (PSD) (Mondragón-Rodríguez et al., 2012). Being tau a microtubule binding protein that mediate protein trafficking, disruption of microtubule stability in dendritic spines result in failed trafficking of critical proteins required for synaptic function. For instance, hyperphosphorylated tau disturbs the trafficking of glutamate receptor subunits (Crimins et al., 2013; Ittner et al., 2010), also affecting the stability of the PSD-95/NMDA receptor complex.

In the postsynaptic compartment, tau is a substrate for GSK3 and p38 mitogen-activated protein kinase (p38MAPK) (Feijoo et al., 2005; Hanger et al., 1992), enzymes involved in the regulation of synaptic function, specially LTP. But tau has also been observed to play a role in LTD (Kimura et al., 2014). Therefore, pathological tau may alter the normal function of synapses.

Additionally, hyperphosphorylated tau mediate presynaptic dysfunction. Tau regulates the transport of axonal mitochondria to the presynaptic terminal (Reddy, 2011), which impacts synaptic vesicle release. Moreover, tau may play a critical role modulating calcium signalling (Moreno et al., 2016), which affects the neurotransmitter release. Hence, pathological tau is involved in the failure of synaptic transmission.

The neuroinflammatory context in AD

Processes mentioned above impact on synaptic function. However, neurons do not work alone. In the AD pathological context, interactions between neurons, astrocytes, microglia and vascular cells are perturbed (Henstridge et al., 2019).

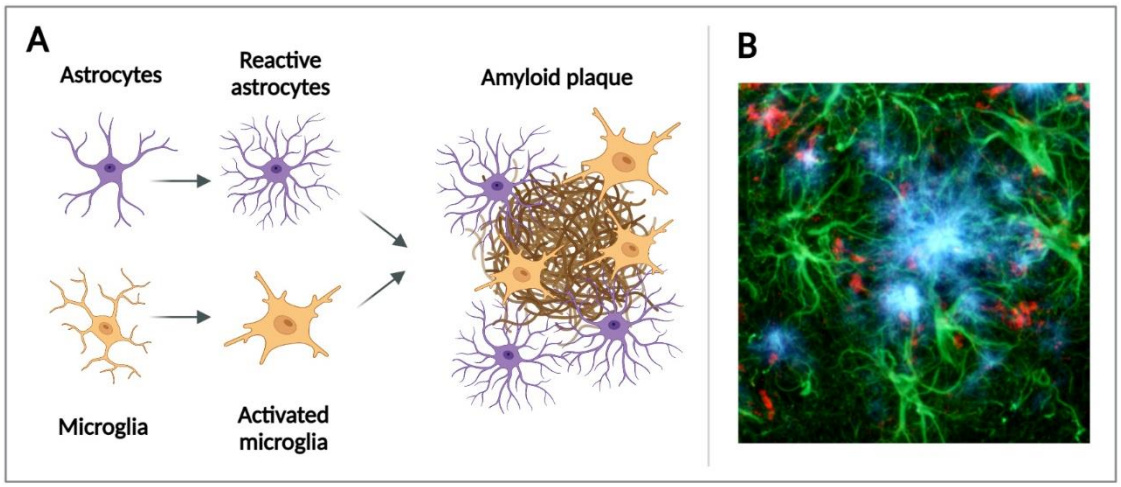

Figure 11. Astrocyte and microglia activation in AD pathology (A). Created with BioRender. Fluorescent images showing a simultaneous localization of amyloid plaques (blue), hypertrophied astrocytes (green) and activated microglia (red) in the hippocampus of a transgenic mouse (B). Source: tebu-bio.com

In addition to the "positive" lesions of AD pathology (amyloid plaques and neurofibrillary tangles), the disease is accompanied by an inflammatory response that directly involve astrocyte and microglia (Akiyama et al., 2000). Likewise, inflammation could implicate beneficial or devastating effects depending on the severity of the disease, which can converge on synapse degeneration.

During initial AD pathology, astrocytes and microglia are activated early in the disease, even before the formation of Aβ plaques (Ahmad et al., 2019). Then, they accumulate around plaques exerting key roles in Aβ degradation and clearance (Wyss-Coray et al., 2003; Yu & Ye, 2015) (Figure 11). In fact, Aβ binding to microglia promote phagocytosis, also in its soluble form (Czirr et al., 2017).

Astrocytes and microglia react to toxic stimuli modifying their gene expression. ApoE, a strong risk factor for AD, is highly expressed in both cell types and its expression becomes altered in the AD pathology (Krasemann et al., 2017; Tulloch et al., 2018). In astrocytes, apoE contribute to amyloid clearance, being the isoform apoE ε4 more associated to defective clearance (Mulder et al., 2012; Prasad & Rao, 2018). In addition, genes encoding triggering receptor expressed on myeloid cells 2 (TREM2), which bind to apoE, have also been linked to microglial function in AD (Krasemann et al., 2017; Yeh et al., 2016).

Gene regulation also impact on genes associated with Ca^{2+} signalling. Aβ and tau induce Ca^{2+} dysregulation in astrocytes (Kuchibhotla et al., 2009; Lim et al., 2013; Piacentini et al., 2017), which contribute to impaired astrocyte synaptic function. In fact, astrocytes also regulate synaptic dysfunction through modulation of excitotoxicity (Matos et al., 2013).

During the progression of the disease, the inflammatory profile of astrocytes and microglia is also impaired. Activated microglia overexpress pro-inflammatory cytokines such as interleukin (IL) IL-1β, IL-6 and tumor necrosis factor-α. Astrocytes also release cytokines and proinflammatory mediators. Of note, it occurs in a destructive loop. Microglia can secrete cytokines that, in turn, activates astrocytes (Liddelow et al., 2017). Furthermore, pro-inflammatory signalling cascade affect APP processing, resulting in an increased activity of β- and γ-secretases which, in turn, lead to increased Aβ production and burden (Liaoi et al., 2004; Sastre et al., 2003). As a result, chronic glial activation becomes toxic to neurons, resulting in neurodegenerative processes such as cognitive dysfunction (Hoozemans et al., 2006).

In conclusion, pathological species of Aβ and tau are involved in presynaptic and postsynaptic dysfunction, together activated glia contributing to synaptic changes. Altogether, multiple cell types and interactions directly affect synaptic function in AD. The identification of potential synaptic pathways may provide clinical targets to the underlying symptoms of AD. In this sense, if we can early detect synaptic dysfunction and prevent synaptic loss, we may be able to reduce or reverse neurodegenerative processes in AD. For this reason, it would be appropriate to identify biomarkers for synapse pathology that led us act early in the disease.

Synaptic biomarkers in Alzheimer's disease

Biomarkers are defined as objective indications of medical state observed from outside the patient which can be measured accurately and reproducibly (Strimbu & Tavel, 2010). This makes biomarker discovery essential for accurate diagnosis, monitoring the disease progression, monitoring therapeutic interventions, but also for detecting early onset of the disease.

Identifying preclinical AD patients remains critical to facilitate an early efficient treatment of the disease. This concept involves a shift from the traditional approach of identifying and diagnosing specific types of late-life neurodegenerative dementia based on clinical phenotype of cognitive failure. In this respect, actual strategies focus on imaging and biochemical methods (Maji et al., 2010; Perrin et al., 2009).

Up-to-date, neuroimaging techniques used for AD monitoring include basically the positron emission tomography (PET) and the magnetic resonance imaging (MRI). PET images can reveal where β-amyloid and tau have been accumulated (Klunk et al., 2004) and can also track glucose metabolism, being low glucose levels associated with reduced synaptic activity (Foster et al., 2007). MRI can reveal structural alterations such as atrophy, which correlate with cognitive impairment (Frisoni et al., 2010). In fact, AD generates regionally specific neurodegeneration, starting in the hippocampus and the entorhinal cortex (Dickerson et al., 2001; Guo et al., 2020; van Hoesen et al., 1991). However, imaging approaches are confounded and their use alone in clinical routines is limited.

Biochemical methods involve sampling of cerebrospinal fluid and plasma. Plasma can be easily isolated from whole blood by non-invasive methodology, which make it ideal for biomarker research. Nevertheless, plasma biomarkers have provided little success, principally because of the discrepancy observed between studies. Instead, cerebrospinal fluid (CSF) biomarkers have gained increased attention. CSF is a biofluid that can be easily extracted by lumbar puncture in humans and has more physical contact with brain than other fluids. In this way, altered protein levels in the brain directly affect CSF composition. Moreover, CSF biomarkers are very sensitive to small changes in the brain. Therefore, CSF is probably the most informative fluid sample available for preclinical and presymptomatic AD diagnosis (Maji et al., 2010).

In AD patients, the most intensively studied CSF biomarkers include tau and Aβ species (Blennow & Hampel, 2003; Formichi et al., 2006; Lleó et al., 2015). $A\beta_{1–42}$ peptide, and more pronounced $A\beta_{1–42}$:$A\beta_{1–40}$ ratio, are reduced in the CSF of AD patients (Hansson et al., 2007; Motter et al., 1995). This is consistent with the fact that aggregation and, consequently, retention of the peptides into plaques, reduce their availability to diffuse into the CSF.

In the case of tau, total tau (t-tau) levels in CSF are increased in patients with autosomal dominant AD and sporadic AD, which correlate with neuronal tissue damage, reflecting overall cytoskeletal derangement. However, this pathological change is observed in other brain disorders. Instead, phosphorylated tau (p-tau) peptides are more specific to AD, particularly p-tau_{181}. In this case, phosphorylated peptides are also increased in the CSF of AD patients and probably reflect neurofibrillary tangle pathology. Of note, the combination of the core AD biomarkers $A\beta_{1–42}$, t-tau and p-tau perform high diagnostic accuracy (Hansson et al., 2006; Johansson et al., 2011).

Regarding plasma analysis, Aβ peptides and tau have also been detected in plasma but findings from these studies comparing AD dementia with control have revealed contradictory results (Irizarry, 2004; Mehta et al., 2000; Mielke et al., 2018; Tamaoka et al., 1996). Therefore, CSF biomarkers, together with images from PET and MRI, conform an accurate picture used in actual clinical diagnosis (Jack et al., 2016, 2018).

Taken together, biomarkers mentioned above are focused on detecting classical hallmarks of AD. However, as mentioned in previous sections, synaptic changes could play an early and central role of the disease. In this respect, CSF research have a particular interest because synaptic proteins can be released into the CSF, which may display a reflection of synaptic dysfunction. Hence, substantial efforts have been stepped up to tackle synaptic pathology detection in CSF samples for improving diagnosis and for monitoring the pathological process (Figure 12).

Emerging CSF biomarkers for synapse dysfunction include proteins concerning the pre- and postsynaptic compartment (Camporesi et al., 2020; Nilsson et al., 2021). Growth-associated protein-43 (GAP-43), SNAP-25 and synaptotagmin-1, presynaptic proteins involved in synaptic fusion and recycling, are increased in CSF of AD patients compared with controls (Galasko et al., 2019; Sandelius et al., 2019; Sjögren et al., 2001; Tible et al., 2020; Zhang et al., 2018). In fact, SNAP-25 levels are increased in patients with AD even in the very early stages (Brinkmalm et al., 2014). Moreover, higher levels of GAP-43 are positively correlated with t-tau (Sjögren et al., 2001).

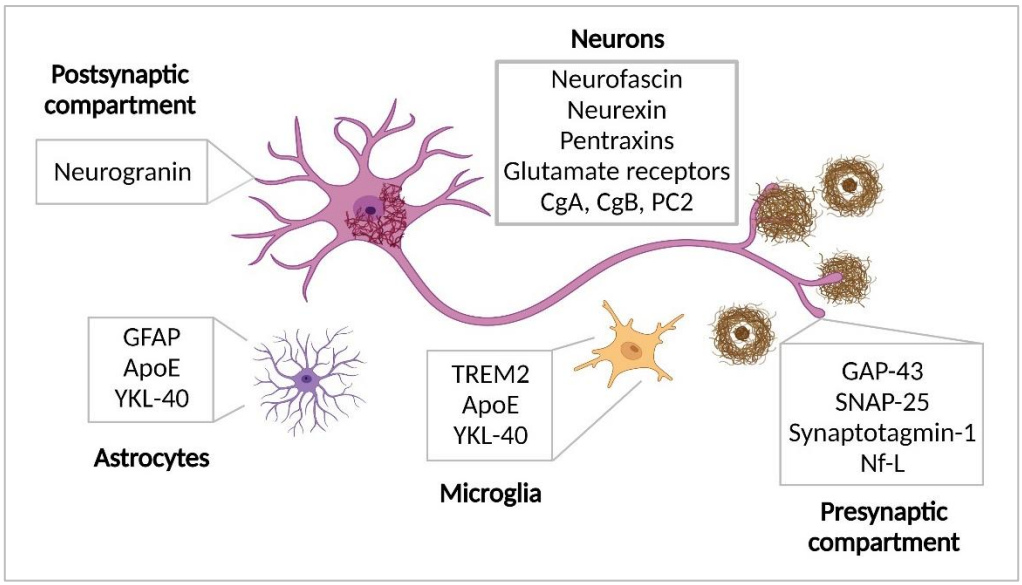

Figure 12. Most relevant fluid biomarkers for AD synaptic pathology in neural cells. Created with BioRender.

Regarding the postsynaptic compartment, neurogranin, a dendritic protein involved in synaptic plasticity, show increased levels in CSF of AD dementia and this increase is seemingly specific for AD (Kester et al., 2015; Thorsell et al., 2010). Also, increased CSF levels of the neurofilament light polypeptide (Nf-L), a cytoskeletal protein abundantly expressed in neuronal axons, have been reported in neurodegenerative diseases (Mattsson et al., 2016).

Proteome-wide analysis have recently detected synaptic proteins associated with AD, including neurofascin, neurexin, neuronal pentraxins, glutamate receptors (Brinkmalm et al., 2018; Lleó et al., 2019; Wesenhagen et al., 2020). Additionally, variations in CSF levels of released DCV-cargos such as CgA, CgB and PC2, which belongs to the regulated secretory pathway, have also been related to AD pathology (Bai et al., 2020; Barranco et al., 2021; Park et al., 2020).

Moreover, apart from the pathophysiologic alterations at the neuronal level, inflammation also represent a hallmark in AD pathology. In this sense, detection of glial biomarkers in CSF are also increasing attention, as it represents a broadly applicable approach for neurotoxicity safety assessment (O'Callaghan & Sriram, 2005). For instance, chitinase-3 like-1, human cartilage glycoprotein39, and chondrex (YKL-40), a glycoprotein expressed in both microglia and astrocytes, is increased in CSF samples of AD patients (Bonneh-Barkay et al., 2008; Craig-Schapiro et al., 2010). Furthermore, markers of reactive astrocytes and microglia, glial fibrillary acidic protein (GFAP) and TREM2, respectively, are also elevated in CSF of AD patients (Fukuyama et al., 2001; Suárez-Calvet et al., 2016).

In essence, substantial progress has been made to identify fluid biomarkers that precedes neuronal death and symptom onset, as it can offer valuable opportunities for determining a preventive therapy. However, more effort is needed to reach a complete scenario/picture in AD pathology.

Rodent models for Alzheimer's disease

Investigating AD in animal models is key to ensure a better understanding of the physiopathology and, consequently, to allow testing of therapeutic strategies. In this sense, animal models must reproduce, as accurately as possible, human pathophysiology and should enable the study of cognitive functions as learning and memory, as well as the application of imaging techniques and biochemical techniques.

Among vertebrates, mice are by far the most important species for transgenic modelling. This is based on the fact that mice have a short life span, which entails cheaper maintenance costs, besides the well-developed techniques involving genetic modifications.

Since familial AD mutations were defined, many transgenic mouse models developing several characteristics of AD physiopathology have emerged (Esquerda-Canals et al., 2017; Kitazawa et al., 2012). It must be noted that, unlike humans, rodents do not develop AD. Therefore, the introduction of human FAD-associated mutations in mice is required to model the pathology, although phenotypes will be modulated by mouse genetic background.

The first transgenic mouse model for Alzheimer's disease overexpressed a human mutated form of APP (Games et al., 1995). PDAPP mice display increased human $A\beta_{1-40}$ and $A\beta_{1-42}$ levels, develop amyloid plaques starting at 6–9 months of age, and exhibit age-dependent spatial learning impairment (Chen et al., 2000). After that, new models came out: Tg2576 (Hsiao et al., 1996) exhibiting Aβ at 10-12 months, and APP23 (Sturchler-Pierrat et al., 1997) at 6 months. The age of the onset of Aβ plaques formation depend on the type of mutations, the promoters used for the transgene expression, and the resulting transgene levels in the brain. Similar to PDAPP mice, APP23 show neural loss, but Tg2576 do not have significance loss.

In addition, double transgenic mouse emerged by crossing APP and presenilin transgenic lines. In this case, APP+PSEN1 transgenic mice, such as APP/PS1 model (Borchelt et al., 1996), PSAPP model (Holcomb et al., 1998) or 5xFAD model (Oakley et al., 2006), display an earlier onset and more rapid amyloid accumulation and cognitive impairment.

Mouse models mentioned above only reflect the amyloidosis dimension of the disease. However, another major hallmark of AD encompasses tau pathology. In contrast to APP or PSEN genes, no genetic mutations related to AD pathology has been found in MAPT gene, which encodes tau. Therefore, generating a relevant transgenic model for tau pathology has become a fundamental challenge.

Crossing Tg2576 and JNPL3 mice, a tau transgenic line which exhibit neurofibrillary tangles in an age-dependent manner (Lewis et al., 2000), generated a new model developing Aβ and tau pathologies (Lewis et al., 2001). Another mouse model, 3xTg-AD line (Oddo et al., 2003), which possesses mutations in APP, PSEN and tau genes, also develop an age-dependent Aβ and tau pathologies in relevant regions and a cognitive decline (Billings et al., 2005).

Taken together, mouse models have offered invaluable data in respect of the AD pathology. Although mice do not fully recapitulate the human disease process of AD, they have significantly contributed to understanding the disease mechanisms and provide valuable tools for evaluating therapeutic strategies.

However, fundamental inconsistencies between human AD and mouse models are considered (Kitazawa et al., 2012). Mouse models require higher levels of APP expression to develop Aβ pathology and, indeed, Aβ plaques may be physically different (Duff & Suleman, 2004; Maeda et al., 2007). In addition, mouse genetic background may also influence neuropathological and behavioural outcomes, which directly implies poor predictive power of mouse models for drug efficacy in human beings. Therefore, data obtained from transgenic mouse model need to be used prudently.

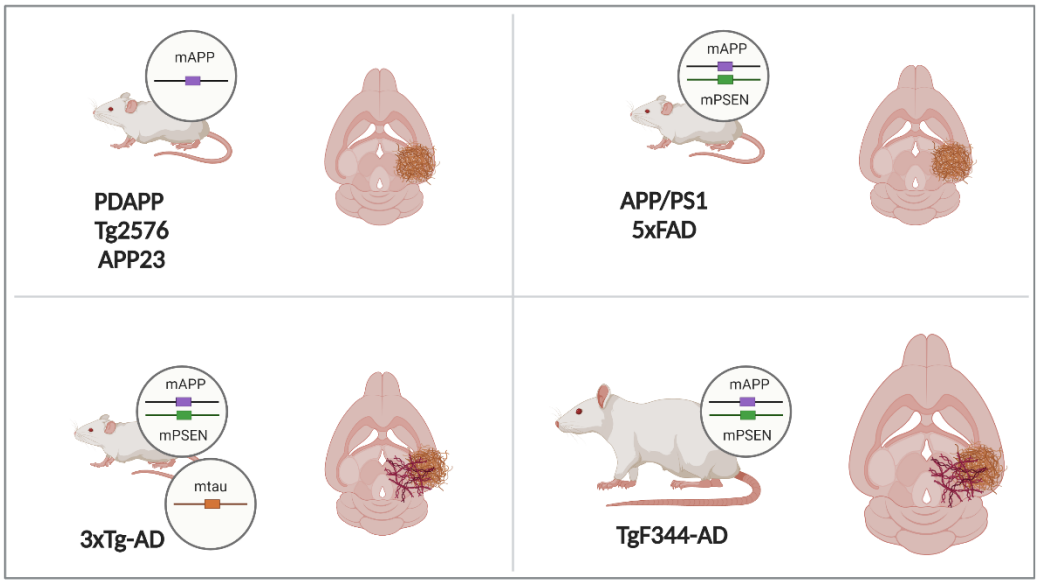

Figure 13. Key rodent models for AD and their major pathological hallmarks. Created with BioRender.

In this context, the development of transgenic technology has allowed the generation of transgenic rat models more easily (Leon et al., 2010). Rat models offer some advantages compared to mouse models. Rats are 4–5 million years closer to humans and have similar physiological processes compared to human being (Yang et al., 2004). In research, they constitute a suitable model for neurosurgical manipulations, neuroimaging, histopathology and CSF serial sampling (Benedikz et al., 2009). In fact, higher volume of CSF can be collected from rats compared to mice. Therefore, rats also become an appropriate model for biomarker discovery in biofluids.

In this regard, a recent transgenic rat model (TgF344-AD) was generated bearing mutant human APP and PS1 (Cohen et al., 2013). These rats manifest the full spectrum of age-dependent AD pathologies in conjunction with cognitive disturbance. They suffer age-dependent cerebral amyloidosis, gliosis and neuronal loss parallel to human pathology. NFT-like structures were frequently observed, although whether these rats perform a consistent tau pathology remain under debate. Anyhow, TgF344-AD deserves a lot of attention for basic and translational AD research.

OBJECTIVES

OBJECTIVES

The general objective of this dissertation is to study the neuronal and astrocytic peptidergic secretory pathway in the physiology of the central nervous system and synaptic alterations in Alzheimer's disease neuropathology.

It is the object of this work to accomplish the following specific objectives in rodent models:

1. To investigate the developing acquisition of peptidergic regulated secretion in cortical neurons *in situ* and *in vitro*.

2. To evaluate peptidergic secretory profile of astrocytes into cortical neural networks *in vitro* and *in situ*.

3. To analyze age- and sex-dependent protein changes in the brain and CSF of TgF344-AD rats, an Alzheimer's disease animal model.

MATERIALS AND METHODS

MATERIALS AND METHODS

Animals

CD1 mice and transgenic TgF344-AD (Cohen et al., 2013) and non-transgenic littermate rats (males and females) were acquired from the Laboratory Animal Service of the University of Barcelona. Animals were housed under controlled temperature (22 ± 2ºC), humidity (40-60%), and light (12-h light/dark cycles) and handled in accordance with the guidelines for animal research (European Community Directive 2010/63/EU). All procedures were approved by the Ethics Committee for Animal Experimentation, University of Barcelona (Barcelona, Spain). Maximum efforts were taken to minimize the number used and animal suffering.

DNA extraction and PCR amplification

TgF344-AD rats genotype was determined by polymerase chain reaction (PCR) amplification of APP KM670/671NL (Swedish) and PSEN1:ΔE9 mutations on DNA samples extracted from ear tissues. 500 µL of NaOH 50 mM were added to each microtube containing the ear tissue, and heated two times at 100 ºC for 5 min, homogenizing with a pipette tip between both steps. 60 µL of Tris-HCl 1M (pH 6.8) were added to previous solution and heated again at 100 ºC for 5 min. Microtubes were centrifugated at 4ºC, 16,000 g for 15 min. Supernatant-contained DNA was used for PCR amplification. The PCR (25 µL) was composed of 0.25 µM of each primer (for APP and/or PSEN mutations), 200 µM deoxy-ribonucleoside triphosphate, 5xGoTaq® reaction buffer in a 1x reaction (Mg^{2+} free), 1 U of Taq DNA polymerase (Promega Biotech Ibérica, Madrid, Spain), 1.5 mM $MgCl_2$, and 0.3 µl of DNA solution. The cycling conditions for all primers were denaturation at 94 °C for 3 min; 35 cycles of 30 s at 90 °C, 1 min at 64 °C, and 1 min at 72 °C; followed by 72 °C for 2 min.

Brain homogenates

Dissected cerebral cortices, hippocampi and diencephalons from P1 to adult CD1 mice, and hippocampi from 4, 10'5 and 16'5-month-old TgF344-AD and WT littermate rats (n=5-8/group) were sonicated twice during 30s using an ultrasonic probe in pH 7.4 ice-cold lysis buffer (50mM Tris/HCl, 150mM NaCl, 5mM $MgCl_2$, 1mM Ethylene-bis(oxyethylenenitrilo)tetraacetic acid (EGTA) and protease inhibitor cocktail from Roche Diagnostics, Indianapolis, IN, USA). Protein concentrations were determined using the Pierce BCA Protein Assay Kit (Thermo Fisher Scientific, Waltham, MA, USA) and samples were analyzed by SDS–PAGE and immunoblotting.

Astrocytic primary cultures

Cerebral cortices from 2-day-old CD1 mice were dissected in Hank's balanced salt solution and treated with 0.25% trypsin and 0.01% DNase in a water bath at 37ºC. Dissociated cells were seeded in flasks and grown in high-glucose Dulbecco's Modified Eagle's Medium and F-12 (1:1) (Gibco), supplemented with 10% fetal bovine serum, 10 mM HEPES and 1/100 penicillin/streptomycin at 37ºC in a 5% CO_2 atmosphere. At confluence (10-12 days), flasks were shaken overnight and cells were rinsed. Detached cells were sub-cultured on poly-D-lysine coated culture plates and coverslips. As previously described (Paco et al., 2009), our cultures were principally composed by astrocytes (92.2 ± 1.3%), virtually devoid of neuronal cells (0.2 ± 0.2%) and containing a minor percentage of microglia (5.2 ± 1%) and immature oligodendrocytes (2.6 ± 1.2%). Secretory

experiments were performed at 9 days *in vitro* (DIV). Before release experiments, astrocytes were rinsed twice with serum-free medium and deprivated for 2 h. Cells were rinsed again and incubated in serum free-medium containing 1 μM ionomycin for 15 min. Cell media was collected and centrifuged at 600 g for 15 min to remove dislodged cells. Proteins in the supernatant were precipitated with 5% trichloroacetic acid using sodium deoxycholate as a carrier. Cultured cells were homogenized in ice-cold lysis buffer (50 mM Tris/HCl, pH 7.4, 150 mM NaCl, 5 mM MgCl2, 1 mM EGTA, 1% Triton X-100, protease inhibitor cocktail from Roche Diagnostics, Indianapolis, IN, USA). Secretory proteins were analyzed by SDS–PAGE and immunoblotting.

Neuronal primary cultures

Hippocampi of E18 mouse embryos were dissected in phosphate-buffered saline (PBS) supplemented with glucose and bovine serum albumin, and treated with 0.25% trypsin and 0.01% DNase. Dissociated cells were seeded onto poly-D-lysine-coated culture plates and grown in Neurobasal™-A medium containing 1% fetal bovine serum (Gibco), 1/50 B27 supplement (Invitrogen), 1/200 L-glutamine (Gibco) and 1/100 penicillin/streptomycin (Gibco) at 37ªC in a 5% CO2 incubator. Media was supplemented with 20 μg/mL 5-Fluoro-2'-deoxyuridine and 50 μg/mL uridine (Sigma-Aldrich) at 4 DIV to inhibit mitotic activity of glial cells. Under these conditions, neurons were grown with a small percentage of astrocytes (25 ± 4.3 %). For secretion experiments, neurons were rinsed and maintained with serum- and B27-free medium for 30 min. Release pattern was evaluated in 15-minute basal and stimulated secretion in standard media containing the appropriate secretagogue (55 mM KCl, 1μM ionomycin or 2 μM tetradotoxin, TTX). Secretion in absence of extracellular calcium was achieved in a nominally Ca^{2+}-free media containing 2 mM EGTA. Cell media was collected and centrifuged at 600 g for 15 min and proteins were precipitated with 5% trichloroacetic acid and sodium deoxycholate. Cultured cells were homogenized in ice-cold lysis buffer (see above). Secretory proteins were analyzed by western blot. Glutamate levels were measured using Amplex Red Glutamic Acid/Glutamate Oxidase Assay kit (Molecular Probes, Eugene, OR, USA) following the manufacturer's protocol.

Optogenetic stimulation

Channelrhodopsin-2 expression (ChR2) was induced by transduction of 4-DIV neuronal cultures with AAV-hSyn-hChR2(H134R)-mCherry (viral titer $2.2x10^{13}$ vg/mL, final dilution $1x10^{9}$ gc/mL) (UNC Vector Core, North Carolina, USA). Adenovirus vectors were maintained in culture plates for 9 days (13 DIV) at 37ºC in a 5% CO_2 atmosphere. The expression of ChR2 was confirmed by visualizing the red fluorescent protein. For optogenetic stimulation, neuronal culture media was removed and substituted with Neurobasal™-A medium minus phenol red (Gibco). After 30 min of stabilization, culture plates were moved to a home-made dark chamber settled in a room temperature area. Basal and stimulated secretion was evaluated in 15-min periods. Photostimulation was achieved with 10-ms blue-light (455 nm) pulses at frequencies between 5 and 40Hz, controlled by a TTL Train Generator adapted to a UHP-T-LED Controller (Prizmatix). The power intensity of light emitted from the laser was calibrated to about 8 mW. Cell media and lysates were evaluated by SDS-PAGE and immunoblotting.

Immunocytochemistry

Cells grown on glass coverslips were washed with ice-cold PBS and fixed with 4% paraformaldehyde in phosphate buffer 0.1M for 15 min. Cells were incubated in blocking solution (PBS, 10% serum, 0.02% Triton X-100, 0.2% glycine, 0.2% gelatin) for 1 hour at room temperature. Primary antibodies were diluted in PBS-gelatin containing 1% serum and 0.02% Triton X-100 and incubated overnight at 4°C. After washing, cells were incubated with Alexa fluorochrome-conjugated secondary antibodies (Thermo Fisher Scientific, Waltham, MA, USA) for 1 h at room temperature in dark. Double immunofluorescences were performed by using primary antibodies raised in different species. Cells were mounted with Mowiol. Fluorescent images were obtained with the Olympus fluorescent BX-61 (Olympus Corp., Tokyo, Japan) and ZEISS LSM 880 Confocal Laser Scanning Microscope (Carl Zeiss Microscopy GmbH, Jena, Germany). Colocalization analyses were performed using ImageJ® software. Images were smoothed and filtered using a Gaussian blur radius of 0.5% of the image size. Red and green images were background-subtracted with a rolling ball radius of 50 pixels and contrast-enhanced. The degree of colocalization between red and green channels from a region of interest (n=9-11 images/group) was determined using Manders' correlation coefficient (Manders et al., 1993).

Viral vectors *in vitro*

ANP expression in neurons was achieved infecting neuronal cultures with AAV-EF1a-DIO-ANP-eGFP (viral titer 2.9 x 10^{13} vg/mL) or AAV-EF1a-DIO-ANP-pHluorin (viral titer 3.81 x 10^{13} vg/mL) at 4 DIV, in combination with AAV1-hSyn-Cre-WPRE-hGH (Addgene #105553, viral titer 3.1 x 10^{13} vg/mL) at 7 DIV. Secretory experiments were performed at 11 DIV. For astrocytic expression, neuronal cultures (grown with a small percentage of astrocytes) at 4 DIV and astrocytic primary cultures at 2 DIV were transduced with AAV-GFAP-ANP-eGFP (viral titer 1.28 x 10^{13} vg/mL) or AAV-GFAP-ANP-pHluorin (viral titer 2,3 x 10^{13} vg/mL). In these cases, release experiments were carried out at 10 DIV. All adenovirus reached a final dilution of 1x10^{10} gc/mL. Except for the Cre recombinase, constructs were generated in collaboration with Luis de Lecea's lab (Stanford, California). Constructs were sequence-verified and subcloned into pAdenoassociated vectors and the adeno-associated virus (AAV) particles were used for cell culture infection.

Stereotaxic surgery for virus delivery *in vivo*

Adult CD1 mice were anesthetized with ketamine-xylazine (100mg/kg:6mg/kg) and fixed on a stereotaxic frame. Anesthetic depth was assessed by monitoring pinch withdrawal and respiration rate. A 2 cm incision was made in the skin overlying the skull and a small cavity was created in lateromedial 2.2 mm, anteroposterior -2 mm and dorsoventral 2 mm to get access to hippocampus. AAV (see above) were injected with a Hamilton microsyringe. The needle was slowly lowered to the hippocampus and remained for 5 min before injection. 1 µL virus was delivered at a rate of 0.1 µL/min and, after injection, the needle was left in place for 5 min to minimize the upward flow of viral solution. The skin was sutured after the needle was retracted. Mice were placed on a heating pad until fully recovered from anaesthesia and received appropriate postoperative care. PBS

injection served as a control. Three weeks after injection, mouse brains were prepared for immunohistochemistry and for obtaining acute brain slices. Mice receiving astrocyte-targeted AAV were injected intraperitoneally with lipopolysaccharide (LPS) at a dose of 5 mg/Kg of body weight before perfusion to induce neuroinflammation and enhance viral expression.

Acute brain slices

Acute brain slices from postnatal and adult mice were obtained as previously described (Aguado et al., 2002; Plá et al., 2017) with minor modifications. Animals were decapitated and brains were rapidly removed and placed in cold artificial cerebrospinal fluid (ACSF) (in mM: 120 NaCl, 3 KCl, 10 D-glucose, 26 $NaHCO_3$, 2.25 NaH_2PO_4 and 8 $MgSO_4$) bubbled with 95% O_2 and 5% CO_2. Postnatal and adult brains were cut into 400µm- and 300µm-thickness horizontal slices, respectively, with a vibratome (Pelco Vibratome Sectioning System™, Ted Pella, Redding, CA, USA). After 1 hour of stabilization in ACSF supplemented with 2mM $CaCl_2$, slices were transferred to a release chamber. Secretion experiments were performed in ACSF bubbled continuously with 95% O_2 and 5% CO_2 at room temperature (22–25ºC).

Immunohistochemistry

Rats were anesthetized with ketamine-xylazine (90mg/kg:10mg/kg) and perfused with PBS, followed by perfusion with 4 % paraformaldehyde in 0.1 M phosphate buffer (pH 7.4). Mice were anesthetized with ketamine-xylazine (100mg/kg:6mg/kg) and directly perfused with 4% paraformaldehyde. Brains were dissected, post-fixed and cryoprotected in a 30% sucrose solution. Brains were frozen and histological sections of 40µm were obtained using a Leica CM 3050 S cryostat (Leica Biosystems, Wetzlar, Germany). For immunofluorescent analyses, brain sections were incubated in blocking solution (PBS, 10%, 0.02% Triton X-100, 0.2% gelatin) for 1 hour at room temperature. Incubations with the primary antibodies were carried out overnight at 4°C. Sections were incubated with Alexa fluorochrome-conjugated secondary antibodies (Thermo Fisher Scientific, Waltham, MA, USA) for 1 h at room temperature in dark. Preparations were mounted with Mowiol. Immunofluorescences were visualized in a ZEISS LSM 880 Confocal Laser Scanning Microscope (Carl Zeiss Microscopy GmbH, Jena, Germany). For peroxidase staining, crioprotected brain sections were incubated with blocking solution (PBS, 10 % methanol, 3% H_2O_2) for 30 minutes followed by a general blockage (PBS, 10% serum, 0.2% Triton X-100, 0.2% gelatin) for 1 h at room temperature. Primary antibodies were incubated overnight at 4ºC and biotinylated secondary antibodies for 1 hour at room temperature in dark. Conjugation of horseradish peroxidase to secondary antibody was done using the Vectastain ABC kit (Vector Laboratories, Burlingame, CA, USA). Chromogenic reaction was obtained adding 0'05% diaminobenzidine and 0'01% H_2O_2 in PBS. Sections were mounted, dehydrated and coverslipped in Eukitt® (Sigma-Aldrich, Diesenhofen, Germany).

Live imaging

Levels of exogenous ANP targeted to neurons or astrocytes in primary cultures were evaluated visualizing the tag pHluorin in a ZEISS LSM 880 confocal laser scanning microscope (Carl Zeiss Microscopy GmbH, Jena, Germany) with a 63x oil-immersion objective at 37ºC. Culture media was removed and substituted with Neurobasal™-A medium for neuronal cultures and with Dulbecco's Modified Eagle Medium for astrocytic cultures (Gibco), both without phenol red and supplemented with 10 mM HEPES (Gibco). A 50 µL drop of KCl or ionomycin to achieve a final dilution of 55 mM and 1 µM, respectively, was gently introduced in culture media to elicit stimulated secretion. Images were taken at a single excitation wavelength of 488 nm. Time lapse image acquisitions were performed using a 4-s sampling interval during periods of 15 min. pHluorin image processing was performed using ImageJ® software.

For Ca^{2+} imaging, neuronal cultures were transduced with AAV1-CAG-Flex.NEX-jRGECO1b.WPRE.SV40 (Addgene #100855, viral titer 2.4 x 10^{13} vg/mL, final dilution 1x10^{10} gc/mL) and with AAV1-hSyn-Cre-WPRE-hGH (Addgene #105553, viral titer 3.1 x 10^{13} vg/mL, final dilution: 1x10^{10} gc/mL) at 4 DIV and maintained for five days. Images were collected at a wavelength of 568 nm at 3s intervals during 10 min. Image processing was performed using Matlab functions previously described (Sun & Südhof, 2021). Briefly, time-lapse image files were converted to .tif format using ImageJ. Circular ROIs were chosen by hand at the center of the soma (10 µm diameter). Datasheets containing raw Ca^{2+} traces were used to obtain fluorescent change over time, defined as $\Delta F/F = (F-F_0)/F_0$.

CSF Collection

Before perfusion, CSF was carefully extracted from the cisterna magna compartment of anesthetized CD1 mice (for monitorization of AAV injection) and from 4, 10'5 and 16'5-month-old TgF344-AD and non-transgenic littermate rats (n=8-12/group). CSF collection was performed in the morning as previously described in DeMattos et al., 2002, with slight modification. Animals were immobilized in a stereotaxic frame under a dissecting microscope. An incision was preformed from the skull to the thorax and skin and musculature were removed until meninges covering the cisterna magna were visible. Tissue above the cisterna magna was removed and the adjacent area was cleaned of any blood residue using a cotton swab. CSF was collected with a borosilicate narrow capillary puncturing the arachnoid membrane covering the cistern. CSF resulting volumes (3-12µL in mice, 50-100 µL in rats) were then transferred into Eppendorf tubes and inspected for blood contamination. CSF samples were immediately centrifuged at 4ºC, 16,000 g for 1.5min to remove any possible blood or cellular residue. Only visible clear CSF samples were considered for analysis.

Proteomics

Proteomic analyses were performed in the CRG/UPF Proteomics Unit (Barcelona, Spain). CSF samples (35 µl) were precipitated with 6 volumes of cold acetone and the pellet was dissolve in 28 µl of 6M Urea / 200mM ammonium bicarbonate. Samples were reduced with dithiothreitol (42 nmol, 37 ºC, 60 min) and alkylated in the dark with iodoacetamide (84 nmol, 25 ºC, 30 min). The

resulting protein extracts were first diluted to 2M urea with 200 mM ammonium bicarbonate for digestion with endoproteinase LysC (1:10 w:w, 37ºC, overnight, Wako), and then diluted 2-fold with 200 mM ammonium bicarbonate for trypsin digestion (1:10 w:w, 37ºC, 8h, Promega). After digestion, peptide mixes were acidified with formic acid and desalted with a MicroSpin C18 column (The Nest Group, Inc) prior to LC-MS/MS analysis.

Samples were analyzed using a Orbitrap Eclipse mass spectrometer (Thermo Fisher Scientific, San Jose, CA, USA) coupled to an EASY-nLC 1200 (Thermo Fisher Scientific (Proxeon), Odense, Denmark). Peptides were loaded directly onto the analytical column and were separated by reversed-phase chromatography using a 50-cm column with an inner diameter of 75 μm, packed with 2 μm C18 particles spectrometer (Thermo Scientific, San Jose, CA, USA).

The mass spectrometer was operated in positive ionization mode with nanospray voltage set at 2.4 kV and source temperature at 305°C. Ultramark 1621 for the was used for external calibration of the FT mass analyzer prior the analyses, and an internal calibration was performed using the background polysiloxane ion signal at m/z 445.1200. The acquisition was performed in data-dependent adquisition (DDA) mode and full MS scans with 1 micro scans at resolution of 120,000 were used over a mass range of m/z 350-1400 with detection in the Orbitrap mass analyzer. Auto gain control (AGC) was set to Auto and charge state filtering disqualifying singly charged peptides was activated. In each cycle of data-dependent acquisition analysis, following each survey scan, the most intense ions above a threshold ion count of 10,000 were selected for fragmentation. The number of selected precursor ions for fragmentation was determined by the "Top Speed" acquisition algorithm and a dynamic exclusion of 60 seconds. Fragment ion spectra were produced via high-energy collision dissociation (HCD) at normalized collision energy of 28% and they were acquired in the ion trap mass analyzer. AGC was set to 2E4, and an isolation window of 0.7 m/z and a maximum injection time of 12 ms were used. All data were acquired with Xcalibur software v4.1.31.9. Digested bovine serum albumin (New england biolabs) was analyzed between each sample to avoid sample carryover and to assure stability of the instrument and QCloud has been used to control instrument longitudinal performance during the project.

Acquired spectra were analyzed using the Proteome Discoverer software suite (v2.4, Thermo Fisher Scientific) and the Mascot search engine (v2.6, Matrix Science). The data were searched against the reference proteome from Uniprot, UP_Rat, database (as in January 2021, 29943 entries) plus a list of common contaminants and all the corresponding decoy entries. False discovery rate (FDR) in peptide identification was set to a maximum of 5%. Peptide quantification data were retrieved from the "Precursor ion quantifier" node from Proteome Discoverer (v2.4).

Peptide data was analyzed by MSqRob Shiny App v0.7.7 (Goeminne et al., 2018), executed in RStudio, using Variance Stabilizing Normalization for the normalization and variance stabilization. Protein fold-changes and their corresponding adjusted p-values were obtained performing the Standard statistical analysis. PANTHER (Protein Analysis Through Evolutionary Relationships, v17.0) (Mi et al., 2009; Thomas et al., 2003) was used to perform a Statistical enrichment test providing log2 protein fold-changes. PathfindR (v.1.6.3) (Ulgen et al., 2019) was used for enrichment analysis and protein interactions of significant protein changes of the proteomic analysis.

SDS-PAGE and Western blotting

Brain homogenates, cell media and lysates from cultures and media from acute brain slices, as well as CSF samples from mice and rats were electrophoresed in 10% sodium dodecyl sulfate-polyacrylamide gels. Proteins were transferred to polyvinylidene difluoride immobilization membranes (Bio-Rad Laboratories, Hercules, CA, USA), stained with Ponceau-S for total protein staining as loading control. Membranes were blocked with 5% skimmed milk in Tris-buffered saline and Tween-20 (100 mM Tris/HCl, 140 mM NaCl, pH 7.4, 1% v/v Tween-20) for at least 1 hour at room temperature and then incubated with primary antibodies overnight at 4°C. After washing with Tris-buffered saline and Tween-20, membranes were reacted with horseradish peroxidase-conjugated anti-rabbit or anti-goat secondary antibodies (1:2,000; Dako, Agilent Technologies Inc, Santa Clara, CA, USA) or anti-mouse secondary antibody (1:1,000; Bio-Rad Laboratories, Hercules, CA, USA) for 1 hour at room temperature. Bound antibodies were visualized with Clarity Western ECL Substrate (Bio-Rad Laboratories, Hercules, CA, USA) and blot images were captured with a scanner. Densitometric values were obtained using ImageJ® software.

Statistical analysis

Except for proteomic analysis (see above), quantitative data were statistically analyzed using GraphPad Prism 8® software (GraphPad Software, CA, USA). For two-group categorical variables, non-parametric analysis was performed using a two-tailed Mann-Whitney test and one-sample Wilcoxon test when the reference media was zero. For more than two categorical variables, analysis of data was performed using a Kruskal-Wallis test followed by Dunn's multiple comparisons test. Data are presented as mean ± standard error of the mean (SEM) $p < 0.05$ was considered significant.

Primary antibodies

Antibodies used in the dissertation are listed below.

Name	Manufacturer	Identifier
ANP (Goat)	R&D Systems	AF3366
ApoE (Goat)	Calbiochem	178479
APP (Rabbit)	Abcam	ab2072
CgA (Rabbit)	Abcam	ab15160
CPE (Goat)	R&D Systems	AF3587
CPE (Mouse)	BD Transduction Laboratories	610758
Cys C (Rabbit)	EMD Millipore	ABC20
EEA1 (Rabbit)	R&D Systems	MAB8047
GADPH (Mouse)	EMD Millipore	MAB374
GFAP (Mouse)	Sigma-Aldrich	MAB360

GFP (Rabbit)	GeneTex	GTX113617
Iba1 (Rabbit)	GeneTex	GTX100042
LAMP1 (Mouse)	Developmental Studies Hybridoma Bank	AB_2296838
LCN2 (Mouse)	R&D Systems	AF1857
MAP2 (Mouse)	EMD Millipore	MAB3418
NF-L (Mouse)	Cell Signalling Technology	2835S
PC1/3 (Rabbit)	Abcam	ab3532
PC2 (Rabbit)	Dr. Iris Lindberg	-
SgII (Rabbit)	Dr. Fischer-Colbrie	-
SgIII (Rabbit)	Sigma-Aldrich	HPA006880
SV2 (Mouse)	Developmental Studies Hybridoma Bank	AB_2315387
SytIV (Mouse)	EMD Millipore	MABN109
SytVI (Mouse)	Biolegend	853902
β-actin (mouse)	Sigma-Aldrich	A3854

Table 1. List of used primary antibodies

RESULTS

RESULTS

1. Acquisition of peptidergic regulated secretion during forebrain development

Brain network is defined as a complex and highly organized communication system that requires one neuron to efficiently communicate with each other to generate precise responses transmitted through the brain. Neurons primarily communicate chemical signals by regulated secretion of SV and DCV. In last decades, major emphasis was placed on the characterization of SV, as classical neurotransmitters participate in relevant processes such as development, learning and memory. However, DCV-stored peptidergic transmitters also play essential roles in neuronal circuit development and function, but they have been studied in a lesser extent. Indeed, most efforts on DCV characterization have been focused on the endocrine system.

Currently, very few studies have attempted to investigate the peptidergic regulated secretory pathway in the central nervous system and neither to examine how it is constituted during development. One of the few studies conducted on this topic focused on SV and DCV secretion capacity during maturation of human iPSC-derived neuronal cultures (Emperador Melero et al., 2017). However, more efforts are needed to further comprehend the acquisition of peptidergic transmission in the mammalian nervous system.

Therefore, the current section of the present dissertation aims to investigate how peptidergic regulated secretory pathway is established in the developing brain. For this purpose, we evaluated the distribution and secretion of DCV markers in mice during neuronal development *in situ* (from brain sections and slices) and *in vitro* (from primary hippocampal cultures).

Distribution of DCV components in developing cortical neurons *in situ*

To examine the peptidergic secretory pathway, we labelled members of the granin family, the prohormone convertase family and the carboxypeptidase E, which together comprise the molecular machinery of DCV, responsible for the sorting and processing of peptidergic transmitters (Bonnemaison et al., 2013). In detail, we evaluated levels of DCV components by western blotting procedures in whole forebrain homogenates at different developmental stages and, particularly, in the cerebral cortex, the hippocampus and the diencephalon at early and late stages (**Figure 14A**).

DCV markers CPE, PC1/3, SgIII, PC2 and CgA were abundantly detected during brain development, even in the first postnatal day. Distinctly, mature forms of CPE (~ 53 KDa), PC1/3 (~ 66 KDa), PC2 (~ 66 KDa), and mature and precursor forms of SgIII (~ 48 KDa and 63 KDa, respectively) were highly expressed at early stages, exhibiting a peak at the first postnatal

week (P7). Oppositely, expression of PC1/3 precursor form (~ 87 KDa) were absent at first stages and progressively increased during maturation, in a similar manner to CgA (~ 36 KDa). Levels of Cystatin C (Cys C), a secretory component mainly contained in constitutive-like vesicles (Warfel et al., 1987), were decreased throughout the developmental forebrain. Focusing on specific brain areas, mature forms of PC1/3 and PC2 were enriched in the cerebral cortex of a P5 mouse, whereas the diencephalon exhibited higher levels of CPE and SgIII. In contrast, the most abundant DCV markers in adult diencephalon were the mature forms of PC1/3 and SgIII. At later stages, CPE was particularly enriched in the hippocampus. In the case of CgA and CysC, they displayed similar levels in the three brain areas.

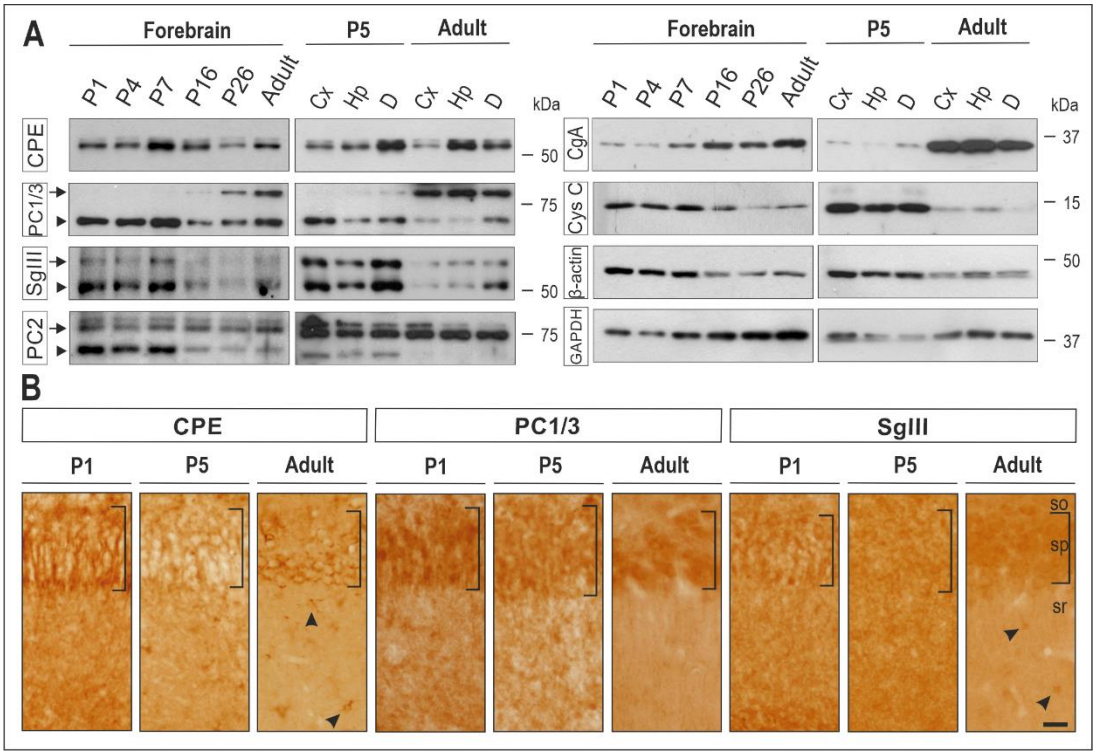

Figure 14. DCV proteins are widely distributed throughout the developing brain. **(A)** Immunoblots illustrate levels of DCV markers CPE, PC1/3, SgIII, PC2 and CgA in whole forebrain homogenates and in the cerebral cortex (Cx), hippocampus (Hp) and diencephalon (D) during development. DCV components were early expressed in the forebrain exhibiting a general widespread peak at P7. Precursor forms of PC1/3 and CgA increased during maturation, whereas SgIII and mature forms of PC1/3 and PC2 progressively decreased. In P5, PC1/3 and PC2 were enriched in the cerebral cortex, while CPE and SgIII showed higher levels in the diencephalon. At later stages CPE was particularly enriched in the hippocampus. The mobility of molecular mass markers (in KDa) is indicated. Arrows and arrowheads indicate precursor and mature protein forms, respectively. **(B)** Immunoperoxidase staining for CPE, PC1/3 and SgIII is found in pyramidal neurons of the CA1 region of the hippocampus. Additionally, immunolabeling for SgIII and CPE is detected in astroglial cells in the adult tissue (arrowheads). Scale bar: 20 μm. Abbreviations: so, stratum oriens; sp, stratum pyramidale; sr, stratum radiatum.

To determine the cellular location of DCV components in the mouse developing cerebral cortex *in situ*, we performed immunohistochemistry analyses at P1, P5 and adult stages (**Figure 14B**). High levels of CPE, PC1/3 and SgIII were found in pyramidal neurons of the hippocampal CA1 region. In particular, immunoreactive puncta was observed throughout the neuropil, resembling axon terminals, and in neuronal processes and perikarya, prominently labelled in the adult. Additionally, at these later stages, CPE and SgIII were also found in astrocyte-like glial cells, as previously reported in our laboratory (Paco et al., 2010; Plá et al., 2013).

Next, to further determine the subcellular distribution of some DCV markers, we performed immunofluorescence analyses in P1, P5 and adult CA3 sections. By double immunofluorescence staining with SV2, an integral membrane protein of synaptic vesicles (Volknandt, 1995) which is predominantly found in presynaptic terminals, we observed that CPE and PC1/3 only colocalized with SV2 at later stages **(Figure 15A)**. Similarly, both DCV markers displayed a marked colocalization only in adult CA3 region, mainly resembling axosomatic contacts **(Figure 15B)**.

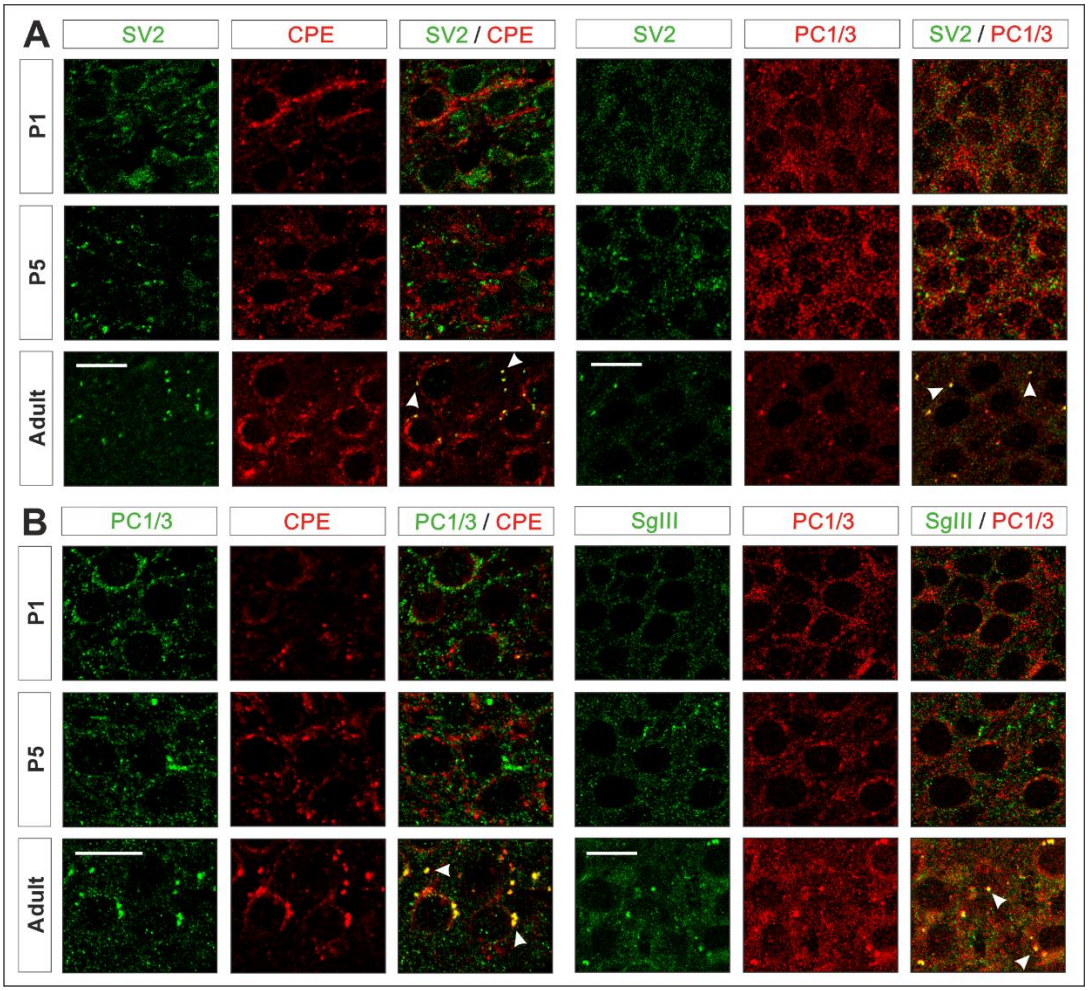

Figure 15. DCV markers CPE and PC1/3 are associated with SV2-stained presynaptic terminals at adult stages. **(A)** Double immunofluorescence in CA3 region of the hippocampus reveals that CPE and PC1/3 location in presynaptic terminals, labelled with SV2, is only reached in the adult. **(B)** DCV markers colocalization is observed only in adult CA3 sections, predominantly displaying a synaptic distribution. Scale bars: 20 µm.

Overall, DCV markers that conform the molecular machinery of these vesicles were widely distributed throughout cortical areas from a very early developing stage. However, subcellular localization was regulated during development. Although neuronal somata and processes were prominently labelled with CPE, PC1/3 and SgIII, DCV markers only colocalized in the adult, reaching SV2-containing presynaptic terminals in the mature brain.

Acquisition of DCV regulated secretion in the developing cerebral cortex

DCVs are destined for the regulated secretory pathway. In response to stimulation, cargo molecules are released to the extracellular compartment in a calcium-dependent manner (de Camilli & Navone, 1987). This secretory pattern is broadly established in the mature brain. However, little is known about how peptidergic regulated secretion is constituted during development.

To gain further insight into the acquisition of DCV regulated secretion, we next performed secretory experiments on acute forebrain slices from neonatal to adult stages **(Figure 16)**. We evaluated levels of DCV proteins in a K^+-evoked condition compared to the basal situation. Extracellular media was collected and concentrated, and secretory proteins were evaluated by western blotting procedures **(Figure 16A)**. In all developmental stages, CPE release increased in response to depolarization by KCl 55 mM for 15 min (P0-P1: 0.64, $p=0.0098$; P2-P5: 0.74, $p=0.0001$; P7: 0.63, $p=0.001$; adult: 0.65, $p=0.0001$). However, PC1/3 exhibited a transient unconventional release. At very early postnatal stages, PC1/3 evoked release diminished comparing to the basal levels, in a non-expected manner (P0-P1: -0.43, $p=0.0273$). Progressively, the release pattern switched over to the mature phenotype (adult: 1.62, $p<0.0001$).

We carried out additional secretory experiments on acute forebrain slices analyzing other DCV-stored components by immunoblotting **(Figure 16B)**. Whereas in the adult brain all DCV proteins (CPE, PC1/3, SgIII, PC2 and CgA) displayed a robust evoked secretion, in the early postnatal forebrain some stimulated responses were absent. Similar to the release pattern previously described for PC1/3, K^+-evoked secretion of PC2 and CgA was not completely achieved. Additionally, CysC exhibited similar levels in both basal and stimulated condition at early and late stages, as expected for a constitutive-secreted protein.

With the aim to determine whether acquisition of the peptidergic regulated secretory pathway could specifically vary from brain areas, we next dissected the cerebral cortex and the diencephalon from acute brain slices at different stages and, subsequently, examined the secretion of DCV markers in response to KCl-depolarization **(Figure 16C)**.

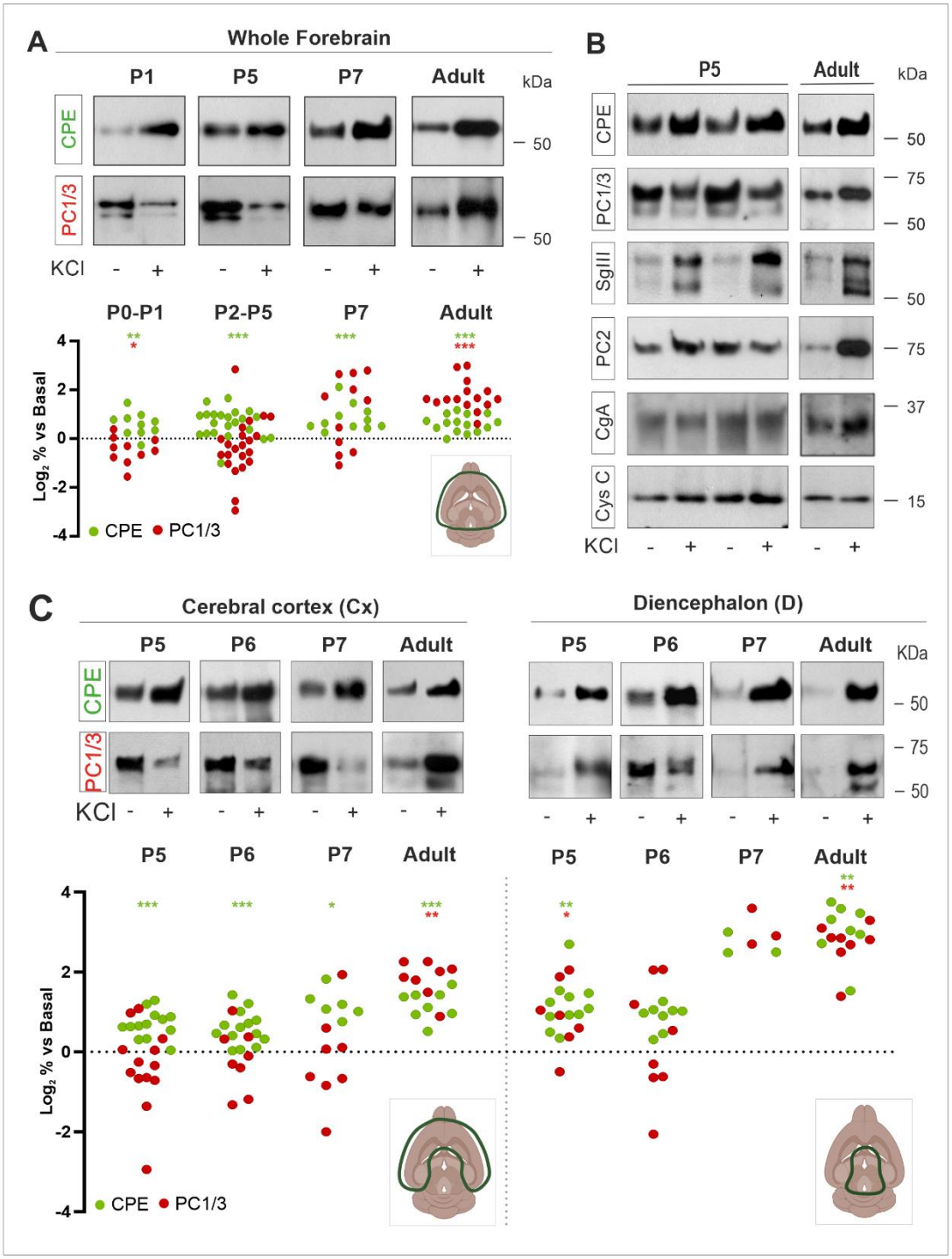

Figure 16. Regulated secretion of DCV markers in acute slices from developing and mature forebrain. **(A)** Representative immunoblots of CPE and PC1/3 in the same samples after 15 min of basal (-) and 55 mM KCl (+) conditions. From very early stages, CPE was secreted in a typical regulated manner, whereas PC1/3 exhibited a transient unconventional release. The mobility of molecular mass markers (in KDa) is indicated. Scatter dot plot summarize variations of released CPE, pSgIII and mSgIII after KCl stimulation represented as the Log_2 of the percentage of variation compared to basal levels. **(B)** Western Blot analysis show a heterogeneous early regulated response for DCV proteins CPE, PC1/3, PC2, SgIII, PC2 and CgA. Constitutive secretion was contrasted with levels of CysC. **(C)** Immunoblots and scatter dot plots summarize K^+-evoked secretion for CPE and PC1/3 in acute brain slices dissecting the cerebral cortex and the diencephalon. Similar developmental secretory pattern was observed for both proteins, although PC1/3 non-conventional release was more noticeable in the cerebral cortex. *$p < 0.05$; **$p < 0.01$; ***$p < 0.001$, One-sample Wilcoxon test.

Evaluating CPE levels, both brain areas displayed the classical regulated secretory pattern in both developing and mature system (Cx, P5: 0.65, p=0.002; Cx, P6: 0.54, p=0.0001; Cx, P7: 1.13, p=0.0313; Cx, adult: 1.25, p=0.0078; D, P5: 1.08, p=0.0010; D, P6: 0.99, p=0.0078; D, P7: 2.50, p=0.2500; D, adult: 3.17, p=0.0078). By contrast, PC1/3 again presented a transient non-conventional release in the cerebral cortex. Although at early stages levels of PC1/3 did not achieve a significant reduction, the decrease clearly followed a tendency. However, PC1/3 regulated secretion in the diencephalon reproduced a mature phenotype earlier, from a P5 stage (D, P5: 0.92, p=0.0469).

Therefore, acquisition of peptidergic regulated secretion *in situ* could differ depending on DCV subpopulations. Whereas CPE followed the classical regulated secretory pathway from neonatal stages, PC1/3 displayed a non-expected calcium-evoked reduction at early stages. Isolating specific brain regions, this unconventional secretory pattern appeared more pronounced in the cerebral cortex than in the diencephalon.

DCV components in cultured cortical neurons

Regulated secretion of DCV in brain slices could follow an area-specific maturation process that particularly modulate release of DCV subpopulations in a heterogenous manner. Thus, we next explored peptidergic secretion specifically in hippocampal neurons *in vitro*. We prepared primary hippocampal cultures from E18 mouse embryos and evaluated the distribution and secretion of DCV components at different developmental stages.

First, we characterized the cellular composition of hippocampal cultures **(Figure 17A)**, where neurons (labelled with MAP2) were accompanied by a fraction of astrocytes (around 25%, labelled with GFAP), which improve neuronal survival. To confirm the expression of key DCV proteins in developing neurons, we performed western blotting analysis in cell lysates at early stages (4 DIV), at an intermediate development (8 DIV) and in a mature culture (12 DIV) **(Figure 17B)**. DCV markers and CysC were noticeably detected from early stages. Specifically, CPE and CysC increased at later stages, whilst mature form of PC2 and, more robustly, PC1/3 decreased in differentiated neurons. Next, we evaluated the neuronal subcellular distribution of CPE, PC1/3 and SgIII **(Figure 17C)**. MAP2 co-labeling was used to validate dendritic location, whereas Nf-L co-labeling mainly revealed an axonal distribution. All DCV markers were strongly detected throughout the dendritic and the axonal compartment, in accordance with existing literature (van den Pol, 2012).

In conclusion, hippocampal neuronal cultures widely expressed DCV markers throughout the expected compartments, which made an appropriate *in vitro* approach to study the cortical peptidergic secretory pathway.

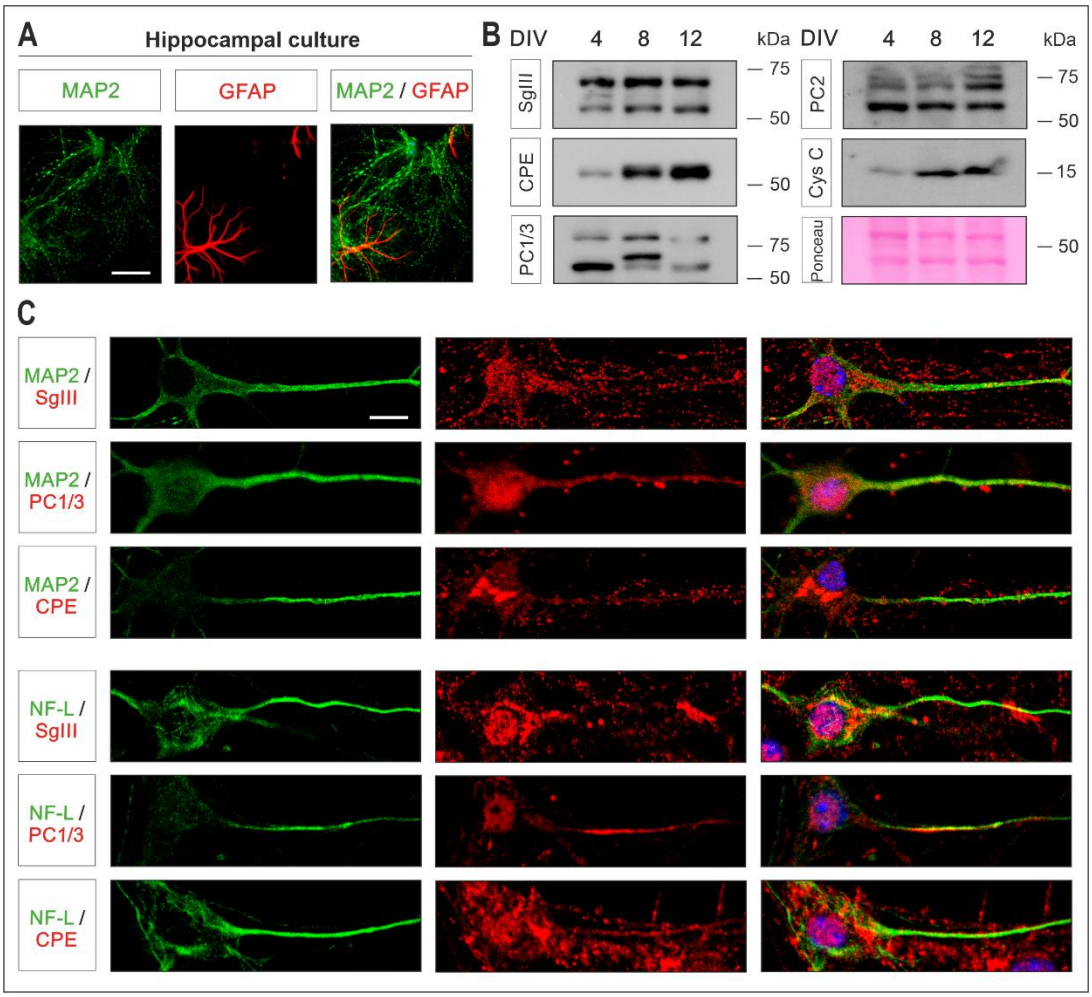

Figure 17. DCV protein profile in hippocampal primary cultures. **(A)** Double immunofluorescences of *in vitro* cultures show a hippocampal neuronal subpopulation accompanied by a fraction of astroglia. **(B)** Immunoblots illustrate cellular content of DCV markers, where levels of CPE and CysC increased during development and mature forms of PC2 and PC1/3 decreased at intermediate and later stages. Ponceau S staining was used as loading control. **(C)** Confocal immunofluorescent images show a dendritic and axonal location of the DCV markers CPE, PC1/3 and SgIII. Scale bars in μm: A, 50; C, 10.

Regulated secretion of DCV subpopulations is heterogeneously acquired in cultured neurons

In previous experiments, we observed that calcium-dependent secretion of CPE and PC1/3 was achieved in distinct developmental phases *in situ*. To further examine the acquisition of peptidergic regulated secretion in hippocampal cultured neurons, we next performed secretory experiments at different stages **(Figure 18)**. For all experiments, we evaluated basal and stimulating secretion in neurons from the same well. Although similar secretory pattern was observed evaluating both conditions in different culture wells, in this way we were able to accomplish a larger number of experiments from the same culture and we could ensure that levels of secreted DCV markers came from the same neuronal population **(Figure 18A)**.

To determine the secretory dynamics of DCV during development, we carried out release experiments in cultured neurons from 3 DIV to 15 DIV. Extracellular media was collected, concentrated and, secreted DCV markers were subsequently analyzed by immunoblotting procedures **(Figure 18B)**. At later stages, K^+-evoked release of CPE, PC1/3 and SgIII showed the mature phenotype. However, it was acquired in a different developmental period: at 8-9 DIV for SgIII (1.59, p=0.023), at 10-11 DIV for CPE (1.51, p<0.001) and at 12-15 DIV for PC1/3 (0.46, p=0.0313). Moreover, similarly to the *in situ* approach, PC1/3 levels under stimulating conditions decreased at early stages (3-5 DIV; -2.73, p=0.0313; 6-7 DIV: -1.74, p=0.002; 8-9 DIV: -2.48; p=0.0098). However, in cultured neurons, evoked secretion of CPE at 3-5 DIV also diminished compared to the basal situation (-2.16, p=0.0156). Therefore, in comparison to neurons *in situ*, hippocampal cultures could achieve more immature stages where unconventional release could be detected for more DCV markers.

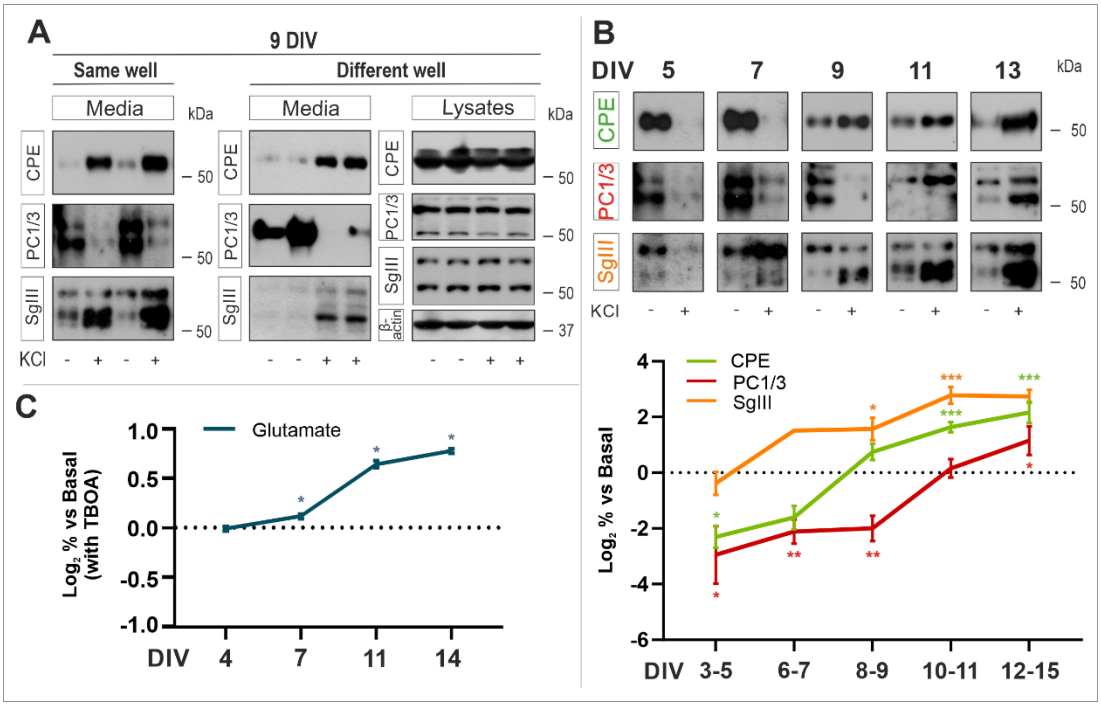

Figure 18. Regulated secretion of DCV markers in developing hippocampal cultures in comparison with glutamate dynamics. **(A)** Immunoblots illustrate basal (-) and 55 mM KCl (+) secretion analysing extracellular media from the same well and in different wells. **(B)** Representative immunoblots of CPE, PC1/3 and SgIII after basal and depolarizing conditions. DCV markers acquired a competent regulated secretion in a heterogeneous manner, exhibiting an early unconventional release for CPE and PC1/3. The graph below summarize K^+-evoked release represented as the Log_2 of the percentage of variation compared to basal levels. The mobility of molecular mass markers (in KDa) is indicated. **(C)** Glutamate release in the presence of TBOA, evaluated by a colorimetric assay, exhibited high levels under depolarizing conditions at later stages. Data are presented as the mean ± SEM. *p < 0.05; **p < 0.01; ***p < 0.001, One-sample Wilcoxon test.

Next, to examine SV regulated secretion in comparison to DCV dynamics, we evaluated glutamate exocytosis during developing neurons (**Figure 18C**). To ensure the detection of total secreted levels, glutamate re-uptake was blocked by addition of the excitatory amino acid transporter inhibitor threo-b-benzyloxyaspartic acid (TBOA, 75 μM). The extracellular content was determined by a colorimetric assay. Similar to DCV markers, glutamate levels in response to KCl-depolarization for 15 min increased at later stages (7 DIV: 0.1, 11 DIV: 0.59, 14 DIV: 0.70, all p=0.0313). However, when evoked response was not completely acquired (4 DIV), secreted glutamate during depolarization did not diminish compared to the basal situation, in accordance to previous results (Andreae et al., 2012).

In conclusion, regulated exocytosis of DCV subpopulations was acquired heterogeneously in hippocampal cultured neurons. Additionally, the early calcium-evoked reduction of some DCV components could be specific for peptidergic vesicles, as this secretory profile was not observed in SV.

To study whether unconventional release of some DCV markers at early stages was specifically dependent on Ca^{2+}-influx, we next evaluated K^+-induced release of CPE and PC1/3 in hippocampal cultures using a media devoid of Ca^{2+}. To achieve this, Ca^{2+}-free experimental media was supplemented with 2 mM EGTA. Once secretory experiments were completed, extracellular media were collected, concentrated and, secreted DCV markers were evaluated by western blotting procedures **(Figure 19A)**. As expected in differentiated neurons (12-13 DIV), enhancement of CPE and PC1/3 release under depolarizing conditions (CPE 0.8, PC1/3 0.79, p=0.0313) was completely abolished in a Ca^{2+}-free medium (CPE -1.54, PC1/3 -1.02, p=0.0313). In contrast, calcium-evoked reduction observed for CPE at 6-7 DIV (-1.36, p=0.0078) and for PC1/3 at 6-7 DIV (-1.6, p=0.0078) and at 9 DIV (-1.18, p=0.0078) was maintained even in absence of calcium (6-7 DIV: CPE -3.12, p=0.0078; PC1/3 -1.595, p=0.0078; 9 DIV: PC1/3 -1.64, p=0.0156), suggesting that extracellular calcium did not have a major effect on reducing the release of DCV components.

To further investigate the role of Ca^{2+} in DCV-evoked release from developing neurons, we next examined CPE and PC1/3 secretion triggering $[Ca^{2+}]_i$ elevation by ionophores **(Figure 19B)**. Remarkably, exposure to 1 μM ionomycin over 15 min at 10 DIV caused a robust decrease of PC1/3 levels (-3.15, p=0.078) and an increase in CPE (1.03, p=0.078), similar to depolarization effects induced by K^+. Ca^{2+} influx mediated by both secretagogues was confirmed with Ca^{2+} imaging analysis **(Figure 19C)**. In this way, these results clearly highlighted a calcium contribution.

Overall, both *in situ* and *in vitro* approaches revealed that DCV subpopulations acquired the classical regulated secretion at different developmental stages. Moreover, our results suggest that a transient unconventional release for some DCV markers could be calcium-dependent. However, more experiments are needed to understand its contribution.

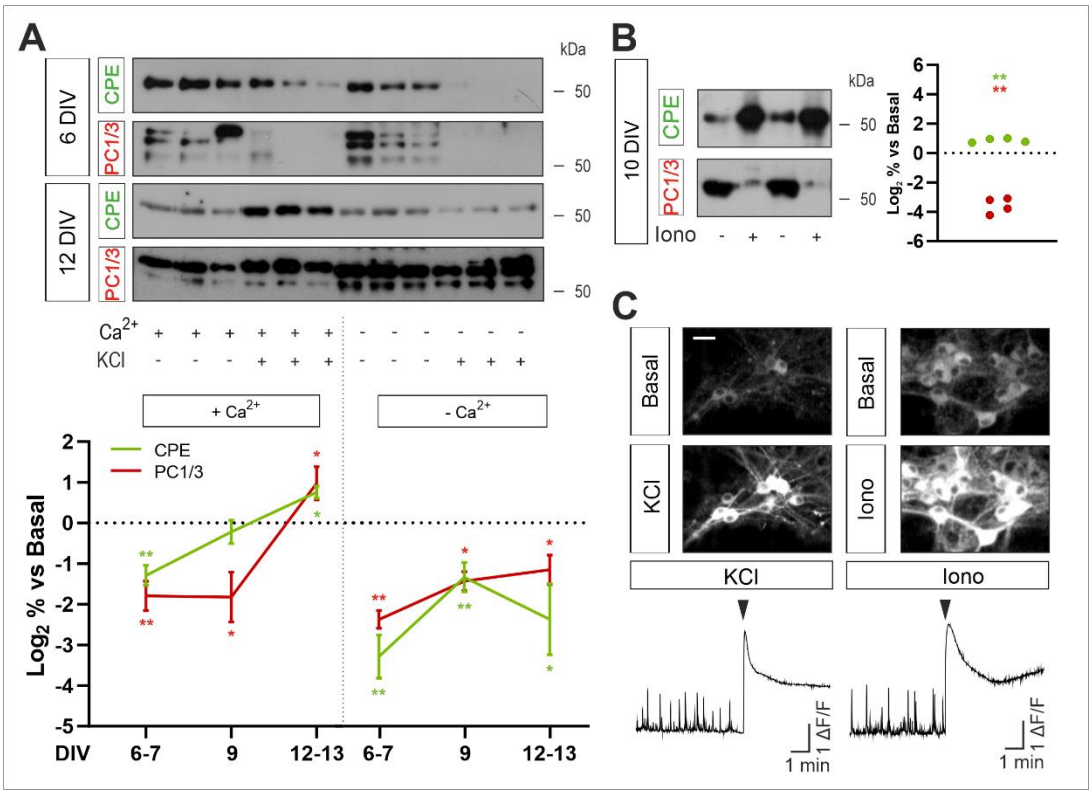

Figure 19. Role of extracellular calcium in DCV exocytosis during neuronal development. **(A)** Representative immunoblots of CPE and PC1/3 after 15 min of basal (-) and 55 mM KCl (+) conditions in standard media containing Ca^{2+} (+) and in a nominally Ca^{2+}-free (-) media (0 mM $[Ca^{2+}]_o$, 2 mM EGTA). The mobility of molecular mass markers (in KDa) is indicated. Graph below summarizes CPE and PC1/3 evoked release represented as the Log_2 of the percentage of variation compared to basal levels. Increased levels of CPE and PC1/3 at later stages during depolarization were abolished in absence of extracellular Ca^{2+}. However, the reduction for both markers observed at early stages and for PC1/3 in an intermediate phase were preserved in both experimental conditions. Data are presented as the mean ± SEM. *p < 0.05; **p < 0.01, One-sample Wilcoxon test. **(B)** Immunoblots and histogram illustrate secretion of CPE and PC1/3 induced by the exposure of 1 μM ionomycin over 15 min at 10 DIV. Comparing to basal conditions, CPE levels were increased by the ionophore, whereas PC1/3 robustly decreased. **(C)** Representative images and profiles of $[Ca^{2+}]_i$ in neurons encoding calcium indicators (detailed in Materials and Methods) which receive high $[K^+]_o$ or ionomycin during 5 min. Ca^{2+} imaging performed at 10 DIV revealed a noteworthy calcium influx with both secretagogues in comparison to the basal situation. Scale bar: 20 μm.

DCV subpopulations in developing and differentiated cortical neurons

The variable secretory profile for some DCV markers during developing neurons suggested the existence of DCV subpopulations. Hence, to further investigate the distribution of DCV subpopulations in hippocampal neurons, we performed colocalization analyses in confocal immunofluorescence images at different developmental stages **(Figure 20)**.

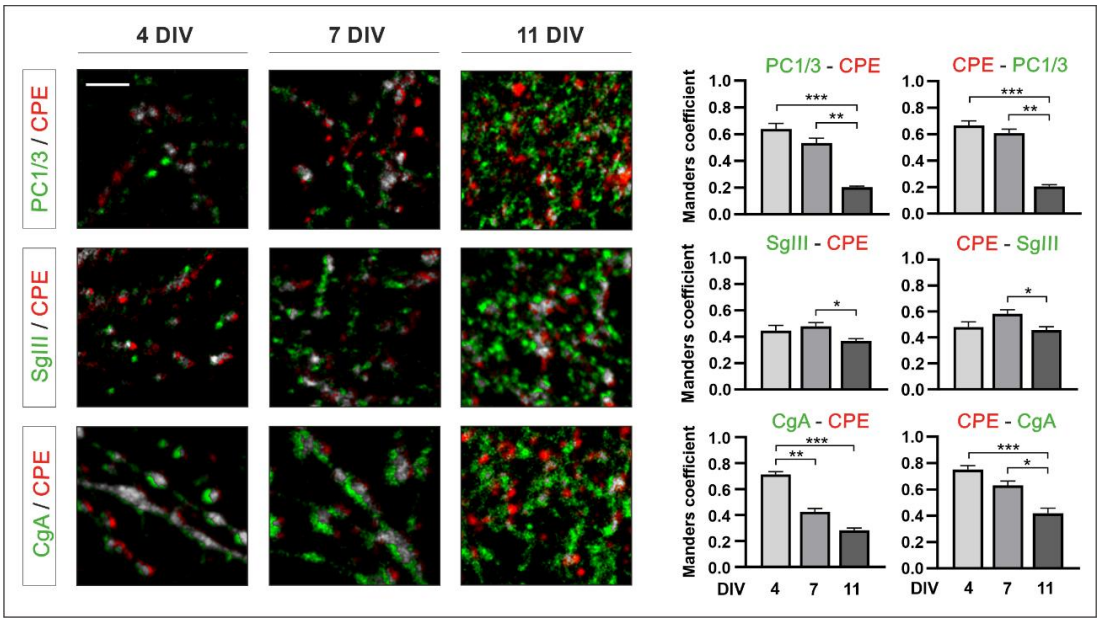

Figure 20. Composition of DCV subpopulations is developmentally regulated. *Left* Representative confocal immunofluorescence images showing colocalization of PC1/3 and CPE, of SgIII and CPE, and of CgA and CPE. Decreased colocalization in all cases was apparent at later stages. Scale bar: 5 µm. *Right* Graphs illustrate Manders' coefficient of some DCV markers at 4, 7 and 11 DIV (0 reflecting no-colocalization and 1 a total overlap). Graphs in the right column indicate colocalization between green channel (PC1/3, SgIII or CgA) and red channel (CPE), and graphs in the left show red channel overlap with green channel. At later stages (11 DIV), CPE containing PC1/3, SgIII or CgA decreased in comparison with intermediate stages (7 DIV). Additionally, CPE containing PC1/3 decreased from 4 DIV to 11 DIV and CPE containing CgA also decreased from 4 DIV to 7 DIV. Data are presented as the mean ± SEM. *p < 0.05; **p < 0.01; ***p < 0.001, Kruskal-Wallis test followed by Dunn's multiple comparisons test.

Referring to PC1/3 and CPE colocalization, at early stages (4 DIV), both markers displayed a relatively high colocalization rate (Manders' coefficient of 0.63 for PC1/3 containing CPE). This ratio robustly decreased at later stages (11 DIV: PC1/3-CPE 0.20, $p<0.0001$) and also comparing this mature stage with an intermediate phase (7 DIV: PC1/3-CPE 0.53, $p=0.006$). In addition, vesicles containing both SgIII and CPE did not vary from 4 DIV to 11 DIV, but colocalization significantly decreased from 7 DIV to 11 DIV (SgIII-CPE $p=0.013$). Similar results were obtained analysing the overlap between the red channel with the green channel. In relation to CgA, another DCV component, colocalization with CPE was again reduced from 4 to 7 DIV ($p=0.007$) and from 4 to 11 DIV ($p<0.0001$). In the case of CPE containing CgA, Manders' coefficient did not diminish from 4 to 7 DIV ($p=0.213$), but it did from 7 to 11 DIV ($p=0.015$).

In summary, composition of peptidergic vesicles in hippocampal neurons were regulated during development. In general, high colocalization rates were observed at early stages. However, in differentiated neurons, peptidergic vesicles containing PC1/3, CPE, SgIII or CgA very little overlapped.

Levels of synaptotagmin-IV content in DCV subpopulations is regulated during neuronal development

In order to study the molecular mechanisms that could be contributing to the acquisition of a mature peptidergic secretory pathway, we next examined the potential role of synaptotagmins (Syts). These are membrane-trafficking proteins widely expressed throughout the endocrine and nervous system that modulate regulated exocytosis (Moghadam & Jackson, 2013). SytI, SytIV, SytVII and SytIX have been found in distinct DCV, whose specific composition determine the vesicle release mode (reviewed in Zhang et al., 2011). Synaptotagmins differ in their Ca^{2+} sensitivities and SytIV has been linked to specifically inhibit regulated exocytosis (Dean et al., 2009; Wang et al., 2001).

To correlate levels of SytIV with the secretory dynamics of DCV components in developing neurons, we analyzed the protein profile of SytIV *in situ* (mouse forebrain homogenates) and *in vitro* (hippocampal lysates) by western blot. Cellular and subcellular distribution was determined by immunochemical approaches **(Figure 21A)**. SytIV was abundantly detected during the first postnatal week. However, protein levels decreased in the adult. Similarly, another member of the synaptotagmin family, SytVI, which is associated with the ER and the plasma membrane (Fukuda & Mikoshiba, 1999) but also found in DCV (Wong et al., 2015), exhibited a similar protein downregulation, although it displayed a maximum peak at P7. In contrast, analysing protein levels of both SytIV and SytVI during neuronal development from hippocampal cultures, we observed that SytIV robustly decreased from 4 to 12 DIV, whereas levels of SytVI were constantly maintained. Noteworthy, the reduction of SytIV levels during cultured neurons occurred in parallel with the switch to a mature evoked secretion phenotype. In detail, immunohistochemical analyses performed in mouse hippocampal sections revealed that somata of pyramidal neurons from CA1 region at P5 copiously displayed SytIV, which evolve in a somatodendritic and neuropil distribution in the mature brain. Furthermore, immunocytochemical analyses performed hippocampal cultures labelling MAP2, to identify dendrites, and Nf-L, to visualize axons, showed a SytIV subcellular distribution along both processes.

To further investigate the association of SytIV with DCV subpopulations during neuronal development, we performed colocalization analyses with some DCV markers in hippocampal cultures at different stages **(Figure 21B)**. Double immunofluorescence analyses revealed that association of CPE, PC1/3 and SgIII with SytIV decreased from 4 DIV to 11 DIV (CPE: $p=0.0007$; PC1/3: $p<0.0001$; SgIII: $p=0.0008$). In addition, SgIII containing SytIV also diminished from 4 DIV to 7 DIV ($p=0.002$). Similar results were obtained examining SytIV overlap with DCV markers. In this case, SytIV puncta containing CPE additionally decreased from 4 DIV to 7 DIV ($p=0.0296$) and vesicles containing PC1/3 was reduced from 7 to 11 DIV ($p=0.0067$). Comparing the overlap of SytIV with the DCV markers at each developmental stage, we observed that SytIV containing CPE or PC1/3 showed a similar colocalization ratio at 4 and 7 DIV, but significantly diminished in comparison with SgIII (at 4 DIV, CPE: $p=0.0189$; PC1/3: $p= 0.0345$; at 7 DIV, CPE: $p=0.0011$; PC1/3: $p= 0.0076$). At 11 DIV, Manders' correlation

showed low colocalization levels. Particularly, SytIV containing SgIII was reduced in comparison with SytIV containing CPE (p=0.0405).

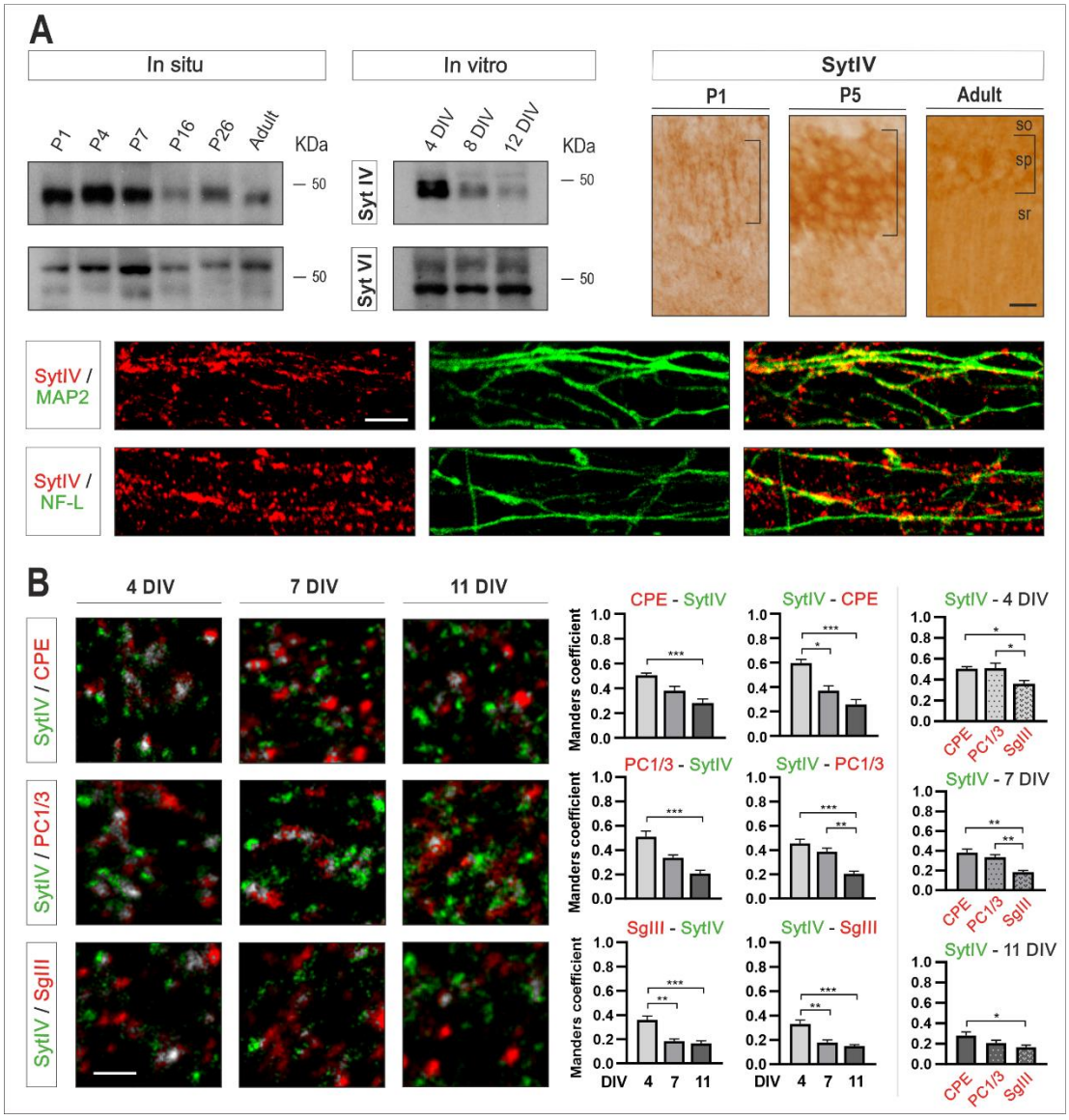

Figure 21. SytIV association with DCV markers during neuronal development. **(A)** Western blots show developmental levels of SytIV and SytVI *in situ* (mouse forebrain homogenates) and *in vitro* (hippocampal cultures). *In situ* analyses revealed a marked reduction in levels of SytIV and SytIV during development, whereas the decrease was more notably for SytIV *in vitro*. The mobility of molecular mass markers (in KDa) is indicated. Immunoperoxidase staining for *in situ* sections and confocal immunofluorescences performed in hippocampal cultures show cellular and subcellular distribution of SytIV. SytIV was broadly distributed throughout pyramidal hippocampal layers, specifically in somatodendritic and axonal processes. **(B)** Representative confocal immunofluorescence images and histograms illustrate colocalization of SytIV with CPE, PC1/3 and SgIII. Manders' coefficient (0 reflecting no-colocalization and 1 a total overlap) show that association of vesicular membrane protein with DCV markers decreased during development and, at early stages, colocalization of SytIV was more prominent with CPE and PC1/3. Data are presented as the mean ± SEM. *p < 0.05; **p < 0.01; ***p < 0.001, Kruskal-Wallis test followed by Dunn's multiple comparisons test. Scale bars in μm: A right, 20; A bottom, 10; B, 5.

These results illustrated that distinct DCV subpopulations contained SytIV, although its association was downregulated during development. CPE and PC1/3 colocalization with SytIV was particularly higher at early stages, when these DCV markers displayed a calcium-evoked reduction. By contrast, in differentiated neurons, when the release of DCV subpopulations switch over the mature phenotype, the overlap with SytIV was very low

In conclusion, maturation of the peptidergic secretory pathway in developing cortical neurons was achieved heterogeneously depending on DCV subpopulations. DCV markers in cortical neurons *in situ* and *in vitro*, which are located in neuronal somata and processes and mainly distributed at presynaptic terminals in the mature brain, exhibited a developmentally regulated secretory profile which resulted in a progressive acquisition of regulated secretion in peptidergic subpopulations containing SgIII, later CPE and last PC1/3, somehow mediated by extracellular calcium. Interestingly, the switch over the mature phenotype occurred in parallel with SytIV downregulation. Moreover, DCV markers CPE and PC1/3 which were the last to show the classical regulated profile, where those that presented higher colocalization rates with SytIV at early stages. Nevertheless, further experiments are required to confirm the molecular mechanisms implicated the maturation of peptidergic regulated secretion.

2. Astrocyte peptidergic secretion into cortical neural networks

The classical picture of brain circuitries uniquely implies neuron-to-neuron communication responsible for information flow, providing inferior roles to astrocytes. However, accumulated evidence suggests a more active role of astroglial cells in the physiology of the central nervous system. They interact closely with neurons and control synaptic neurotransmission, contributing to the concept of tripartite synapses (Araque et al., 1999).

As addressed in the previous section, peptidergic vesicles are targeted to a regulated secretory pathway in neurons, which involves the secretion of DCV in a stimulus-dependent manner in the mature brain. Similar to neurons, the astroglial exocytic compartment includes SLMVs and DCV-like. In contrast, astrocytes are electrically nonexcitable cells. However, they respond to neuronal activity converting the signals into a complex intracellular Ca^{2+} code (Araque et al., 2001; Bezzi & Volterra, 2001; Verkhratsky & Nedergaard, 2018). Whether astrocytes release gliotransmitters in a Ca^{2+}-dependent manner is still under debate. Glutamate secretion, contained in SLMVs, has been demonstrated to follow a Ca^{2+}-dependent process that involves functional vesicle-associated proteins, evidencing a regulated secretory pathway (Araque et al., 2000; Montana et al., 2004). However, little is known about astrocytic peptidergic exocytosis. Of note, main studies come from pure astrocyte cultures, whose morphology, molecular composition and physiology differs to a large extent from that exhibited *in vivo*.

Thus, the second section of the present dissertation aims to further comprehend astrocyte peptidergic secretion, examining secretory dynamics in pure astroglial primary cultures in comparison with astrocytes into neural networks, a more physiological context.

Expression of exogenous ANP-EGFP/pHluorin in astrocytic and neuronal vesicular compartment

In order to study the peptidergic secretory pathway in astrocytes and compared it with the neuronal regulated profile, we produced AAV encoding ANP, a small peptide which is targeted to DCV in neurons, but also stored in similar vesicles in astrocytes (Kreft et al., 2004; Ramamoorthy & Whim, 2008). However, to evaluate secretory dynamics in each cellular type independently, we generated two variants of the construct: one in which ANP expression was controlled by GFAP promoter (to guarantee astrocytic targeting), and another Cre-dependent construct that we used in combination with a Cre-recombinase controlled by human Synapsin (hSyn) promoter (to ensure neuronal targeting). In **Figure 22A**, we illustrated a schematic plasmid map of ANP targeted to astrocytes. In addition, exogenous ANP was fused with two types of green florescent tags: EGFP and pHluorin. As represented in **Figure 22B**, the EGFP tag allows ANP visualization at the vesicular-targeted compartment and at the extracellular space, when fused with the plasma membrane; whereas fluorescence of pHluorin tag is only emitted after fusion, due to its sensitivity to changes in pH, which make it more appropriate to monitor secretory dynamics by imaging methods.

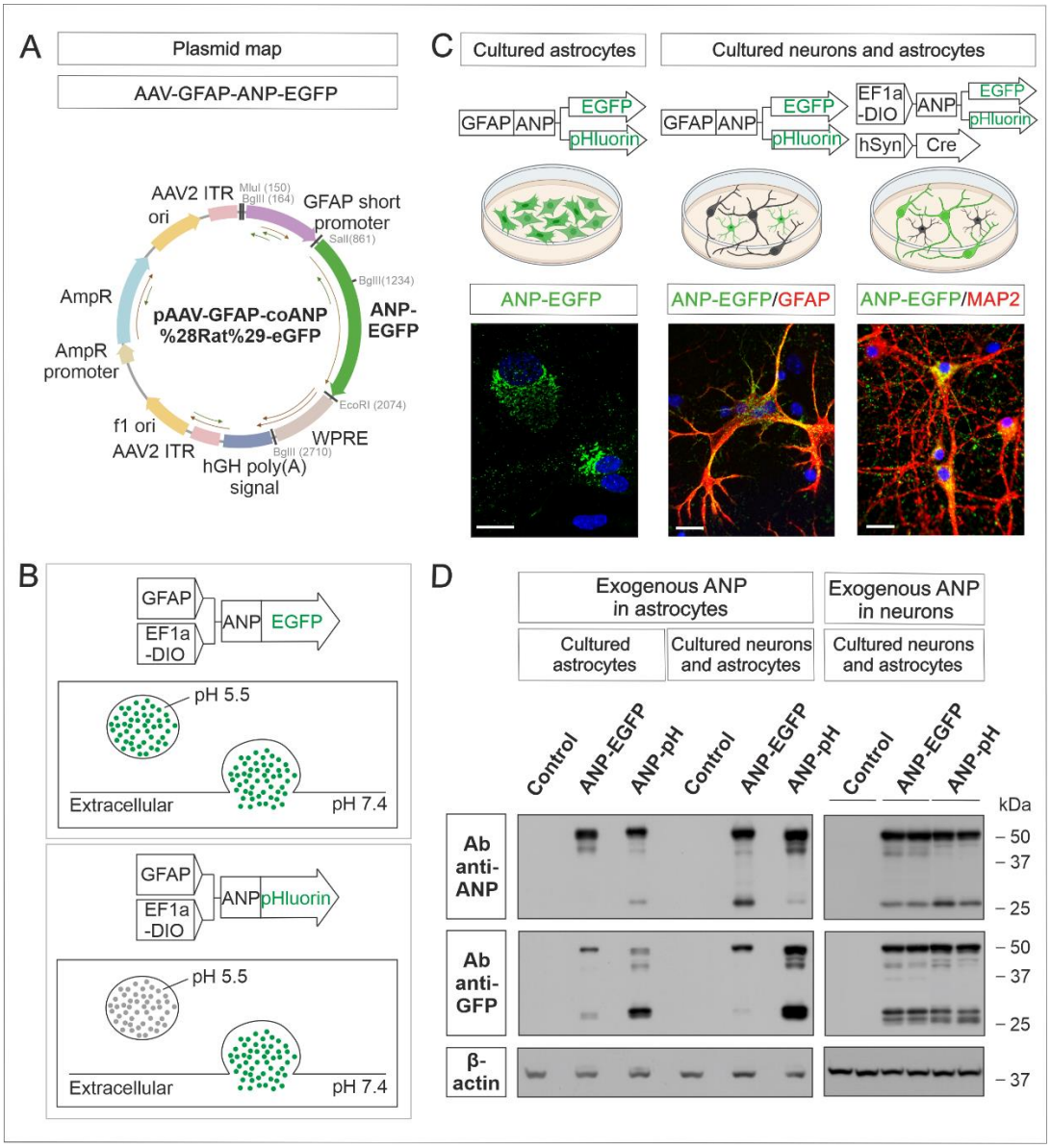

Figure 22. Exogeneous expression of DCV-stored ANP-EGFP/pHluorin in neurons and astrocytes. **(A)** Plasmid map of ANP-EGFP expression controlled by GFAP promoter. Restriction sites and antibiotic resistance are indicated. **(B)** Schemes illustrate fluorescent visualization of both EGFP and pHluorin tags. EGFP fluorescence is achieved at the vesicular compartment and the extracellular space, whereas fluorescence of pHluorin is only visualized at the extracellular space, at neutral pH. **(C)** Schematic and immunofluorescence images show astrocytic expression of ANP-EGFP construct in pure astrocytes cultures and in neuronal co-cultures, confirmed with GFAP labelling. Neuronal targeting of ANP-EGFP was determined with MAP2 labelling in co-cultures. Scale bars: 20 μm. **(D)** Immunoblots illustrate expression of astrocytic and neuronal ANP-EGFP, confirmed with ANP and GFP antibodies. Both conditions revealed a high-molecular-weight protein (~50 KDa), presumably consisting of the full form of ANP-EGFP, and a processed form of ~ 25 KDa, containing ANP and GFP sequences.

To evaluate the cellular-targeting of AAVs, the vector controlled by GFAP promoter was used in pure astroglial cultures (obtained from the cerebral cortex of early postnatal mice) and in co-cultures of neurons and astrocytes (obtained from E18-embryo hippocampi). The construct directed to neurons was only evaluated in co-cultures **(Figure 22C)**. Immunofluorescence analyses revealed an appropriate cellular targeting, visualizing astrocytes and neurons with GFAP

and MAP2 labelling, respectively. In detail, high fluorescence levels were observed in the reticular compartment and in puncta throughout cells, suggesting a vesicular targeting. Similar results were obtained with the pHluorin construct (data not shown). The molecular weight of ANP-EGFP and ANP-pHluorin expressed in both cell types was determined by western blotting analyses with antibodies against ANP and GFP (**Figure 22D**). Cell lysates from both cultures showed predominantly two molecular weights of the constructs: a high-molecular-weight form of approximately 50 KDa, and a low-molecular-weight protein consisting of 25 KDa. The 50 KDa-protein form would certainly represent the full form of ANP-GFP, as ANP molecular weight is approximately 17 KDa, and GFP, approximately 27 KDa. In addition, the low-molecular-weight protein would presumably consist of a fragment that contain both proteins, as it was detected with both antibodies.

Next, to ascertain if exogenous ANP-EGFP/pHluorin was properly destined to vesicles similar to DCV, we evaluated the colocalization of GFP with the DCV markers CPE, SgIII and SgII in pure astroglial cultures, as it has been described that peptidergic vesicles in astrocytes are provided with these sorting and processing components (Fischer-Colbrie et al., 1993; Klein & Fricker, 1992; Paco et al., 2010; Paco et al., 2009). Additionally, to discard an endosomal destiny, we assessed the colocalization with the markers EEA1 and LAMP1 **(Figure 23)**. Confocal immunofluorescence images displayed a poor colocalization of GFP with the DCV-contained CPE and SgIII. However, GFP highly colocalized with SgII, in accordance with previous results obtained from pure astrocytic cultures transfected with ANP.emd (Paco et al., 2009). Immunofluorescences of EEA1 and LAMP1 revealed that ANP-EGFP construct was not directed to the endosomal pathway, as expected **(Figure 23A).**

Then, to specifically evaluate the colocalization of ANP-EGFP with DCV markers in subcellular regions, we obtained Manders' coefficient values in the perinuclear areas, corresponding to ER, and in distal areas **(Figure 23B).** In general, colocalization was higher at the ER comparing to distal regions. At the ER, GFP exhibited a high overlap with SgII (Manders' coefficient of 0.807), although the colocalization with CPE was also relatively high (0.549). However, distal vesicles labelled with GFP predominantly contained SgII (0.698). Immunofluorescence analyses of ANP-pHluorin displayed similar results (data not shown). These results support the heterogeneity of peptidergic vesicles observed in neurons in the previous section.

In conclusion, exogenous ANP-EGFP/pHluorin was specifically expressed in astrocytes or in neurons, determined by the adjacent promoter. In detail, astrocytic fused-ANP was targeted to DCV-like vesicles that primarily contained SgII. Since DCV markers are located in neurons and astrocytes, it becomes challenging to specifically study DCV dynamics in a particular cell type in experimental approaches similar to *in vivo* conditions, where astrocytes are grown into neuronal networks. Therefore, our results showed that this construct could act as a potential tool to independently examine both peptidergic secretory pathways.

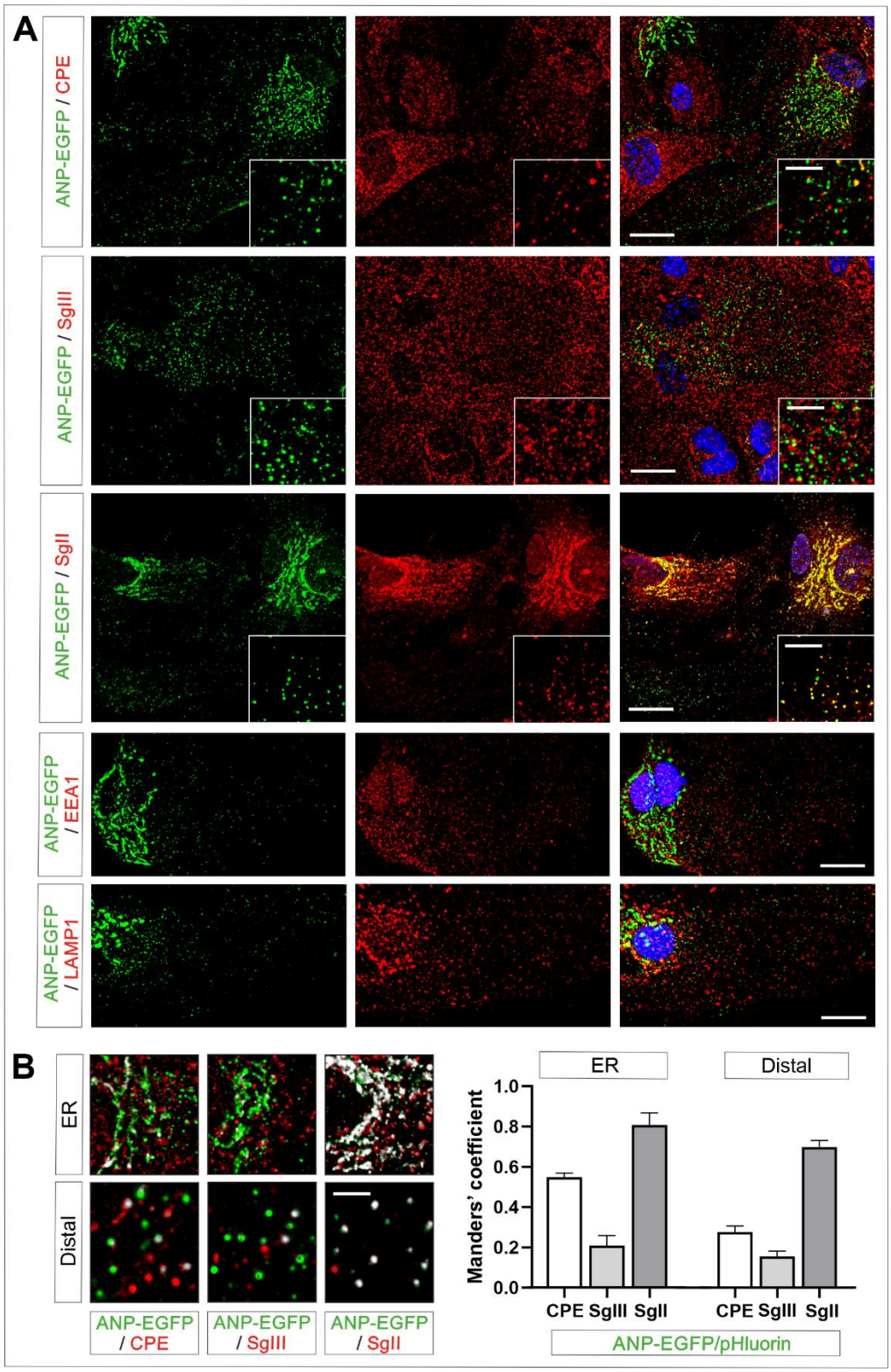

Figure 23. Distribution of astrocytic ANP-EGFP associated with DCV markers. **(A)** Confocal immunofluorescences performed in pure astroglial cultures show a poor colocalization of ANP-EGFP with DCV-contained proteins CPE and SgIII, but a high colocalization degree with SgII. Overlap with the endosomal markers EEA1 and LAMP1 is virtually null. **(B)** Representative confocal immunofluorescence images and histograms illustrate colocalization of ANP-EGFP with CPE, SgIII and SgII in proximal areas, corresponding to the ER, and in distal regions. Manders' coefficient (0 reflecting no-colocalization and 1 a total overlap) showed that colocalization at the ER was higher for SgII and CPE, whereas at distal areas ANP-EGFP primarily colocalized with SgII. Data are presented as the mean ± SEM. Scale bars in μm: A, 20; inset in A, 10; B, 5.

ANP-EGFP/pHluorin exhibit a robust regulated secretion in neurons

Before characterizing the secretory profile of the exogenous fused protein in astrocytes, we first performed secretion experiments in neurons to ensure that DCV-stored ANP-EGFP-pHluorin appropriately followed the regulated secretory pathway **(Figure 24)**. We carried out pharmacological stimulation procedures in co-cultures infected with the neuronal ANP-EGFP construct and evaluated the extracellular and intracellular content by western blotting **(Figure 24A)**. CPE release, examined as a control for DCV markers secretion, markedly increased in response to depolarization by KCl 55 mM for 15 min (529 %, $p=0.017$) and after exposure to 0.5 μM ionomycin (963%, $p=0.0003$) in comparison with the basal levels. Consequently, intracellular content clearly decreased in KCl (46 %, $p=0.018$) and ionomycin (32%, $p=0.005$) stimulations. Additionally, evoked secretion in presence of 2 μM TTX, a sodium channel blocker that preventing action potential generation and propagation, was slightly decreased, although it did not reach a significant difference.

To evaluate secretion of ANP-EGFP construct, we analyzed both 50-KDa- and the 25-KDa-forms independently, as both were robustly detected at the extracellular milieu using an antibody against GFP. Depolarization by KCl and exposure to 0.5 μM ionomycin for 15 min resulted in a dramatic enhancement of ANP-EGFP release for the 50 KDa form (KCl: 900%, $p<0.0001$; Iono: 668%, $p=0.001$) and the 25 KDa form (KCl 877%, $p=0.0003$; Iono 892%, $p=0.0003$). Similar results were obtained when using an antibody against ANP (data not shown). Moreover, as observed for CPE, ANP-EGFP secretion had a decreasing tendency in presence of TTX. In relation to the intracellular content, ANP-EGFP levels for both 50 KDa and 25 KDa forms significantly decreased in comparison with the basal situation after both KCl (50 KDa: 50%, $p=0.001$; 25 KDa: 48%, $p=0.018$) and ionomycin (50 KDa: 49%, $p=0.001$; 25 KDa: 33%, $p=0.004$) stimulations. As previously mentioned, differences were similarly observed using an antibody against ANP (data not shown).

To further determine ANP exocytosis in neurons, we evaluated neuronal ANP-pHluorin secretory dynamics by live-cell confocal imaging **(Figure 24B)**. Time-lapse data over a period of KCl-depolarization for 15 min revealed that, although some fusion events were already visible at the beginning, GFP puncta robustly increased throughout the extended neurons during stimulation. Interestingly, most exocytotic events were anchored to the plasma membrane, instead of rapidly dilute and disappear.

Taken together, these results showed that different secretagogues evaluated by pharmacological and live-cell imaging methods elicited ANP-EGFP/pHluorin Ca^{2+}-evoked secretion in neurons, following the expected regulated secretory pathway. Therefore, the exogenous vector was properly exocytosed.

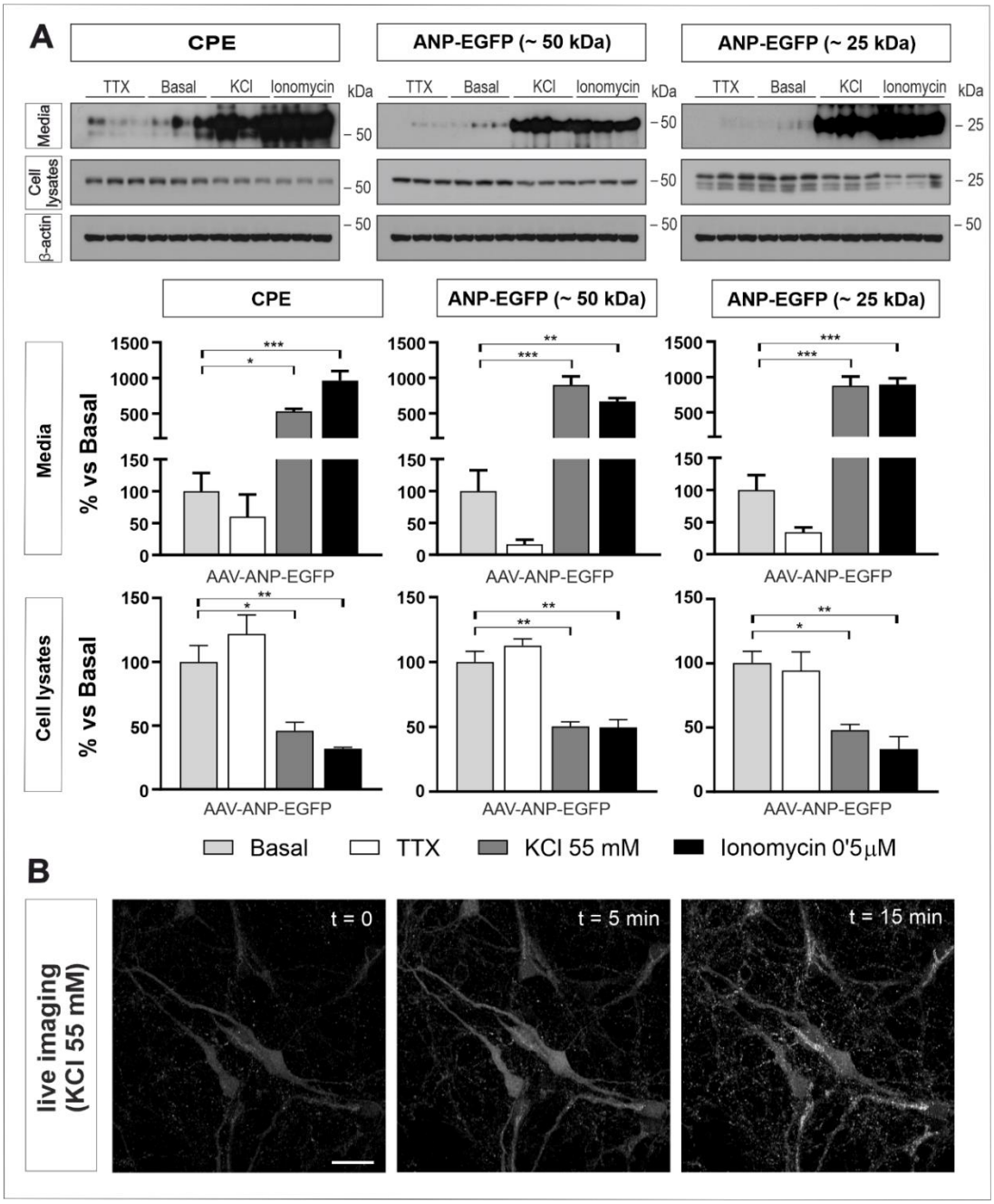

Figure 24. Exogenous ANP-EGFP follows the regulated secretory pathway in neurons. **(A)** Representative immunoblots showing media and cell-lysates levels of CPE and neuronal ANP-GFP in the same sample after 15 min of basal, 2 μM TTX, 55 mM KCl and 0.5 μM ionomycin. The mobility of molecular mass markers (in KDa) is indicated. Graph below summarizes blocked and evoked secretion of CPE and ANP-EGFP (50 KDa and 25 KDa forms). In all cases, extracellular levels were increased under both secretagogues. Consequently, intracellular content was diminished. Values represent percent variation compared with basal release (mean ± SEM). *$p < 0.05$; **$p < 0.01$; ***$p < 0.001$, Kruskal-Wallis test followed by Dunn's multiple comparisons test. **(B)** Confocal live cell imaging of ANP construct in neurons revealed and increase of anchored GFP puncta throughout the extended neurons after depolarization by KCl 55 mM for 15 min. Scale bar: 20 μm.

Astrocytic ANP-EGFP/pHluorin is secreted in a Ca^{2+}-dependent manner *in vitro*

We next assessed the peptidergic secretory pathway in astrocytes examining the release of ANP-EGFP/pHluorin in pure astroglial cultures and in co-cultures **(Figure 25)**. Noteworthy, neuronal co-cultures offer an appropriate *in vitro* scenario to study astrocytic function, as neuronal activity directly regulates the astrocytic transcriptome, inducing *in vivo*-like astrocytic phenotype (Hasel et al., 2017). In detail, we evaluated peptidergic secretion in astrocytic mono-cultures by pharmacological methods (infecting primary cultures with ANP-EGFP construction and stimulating with exposure to 1 μM ionomycin) and by confocal live cell imaging (infecting the cultures with ANP-pHluorin vector and stimulating with 1 μM ionomycin). Samples obtained by pharmacological approaches were examined performing western blotting procedures, whereas ANP-pHluorin exocytosis was analyzed in time-lapse images **(Figure 25A)**.

In control astrocytes which did not receive any AAV, forcing Ca^{2+} entry during 15 min by exposure to the ionophore resulted in a robust increase of extracellular CPE compared to basal levels (1903%, p=0.0022) and a reduction of the intracellular content (77%, p=0.026), as expected. Astrocytes infected with AAV responded in a similar manner, exhibiting an increase of extracellular CPE (2051%, p=0.0022) followed by a decrease of intracellular levels (72%, p=0.002 for CPE). Remarkably, both forms of ANP-EGFP exhibited a similar exocytotic profile than CPE (media: 50-KDa-form 695% p=0.002, 25-KDa-form 4519% p=0.002; cell lysates: 50-KDa 46% p=0,004, 25-KDa 37% p=0,002). In addition, exposure to 1 μM ionomycin in pure astrocytic cultures infected with ANP carrying the pHluorin reporter revealed increased exocytosis after a 15-min period. Indeed, shorter stimulation times (5 min) also showed increased secretory events. Notably, fusion events occurred mostly at perisomatic regions.

These results suggested that astrocytes from mono-cultures released DCV-stored ANP in a Ca^{2+}-dependent manner. However, we further examined the astrocytic peptidergic secretion in co-cultures. Similar than previously described, we performed pharmacological and live imaging approaches **(Figure 25B)**. To achieve astrocyte stimulation, we conducted two experimental approaches: we caused neuronal depolarization by addition of 55 mM KCl that, consequently, activates astrocytes; and we forced $[Ca^{2+}]_i$ elevation by exposure to 1 μM ionomycin, which directly influence both neuronal and astrocytic activity. In this experiment, extracellular media was evaluated by western blotting methods.

Similar to previous experiments, CPE levels were increased with both secretagogues compared to the basal situation (KCl: 701%, p=0.001; Iono: 1227%, p<0.0001). For astrocytic ANP-EGFP, we also observed evoked secretion under both stimulating conditions (50-KDa-form: KCl, 166%, p=0.0081; Iono, 224%, p=0.0017; 25-KDa-form: KCl, 269%, p=0.021; Iono: 687%, p<0.0001). However, inducing astrocytic secretion by neuronal stimulation resulted in a lower evoked secretion of the exogenous construct compared to ionomycin stimulation in pure astroglial and neuronal co-cultures, probably reflecting a more physiological secretory phenotype.

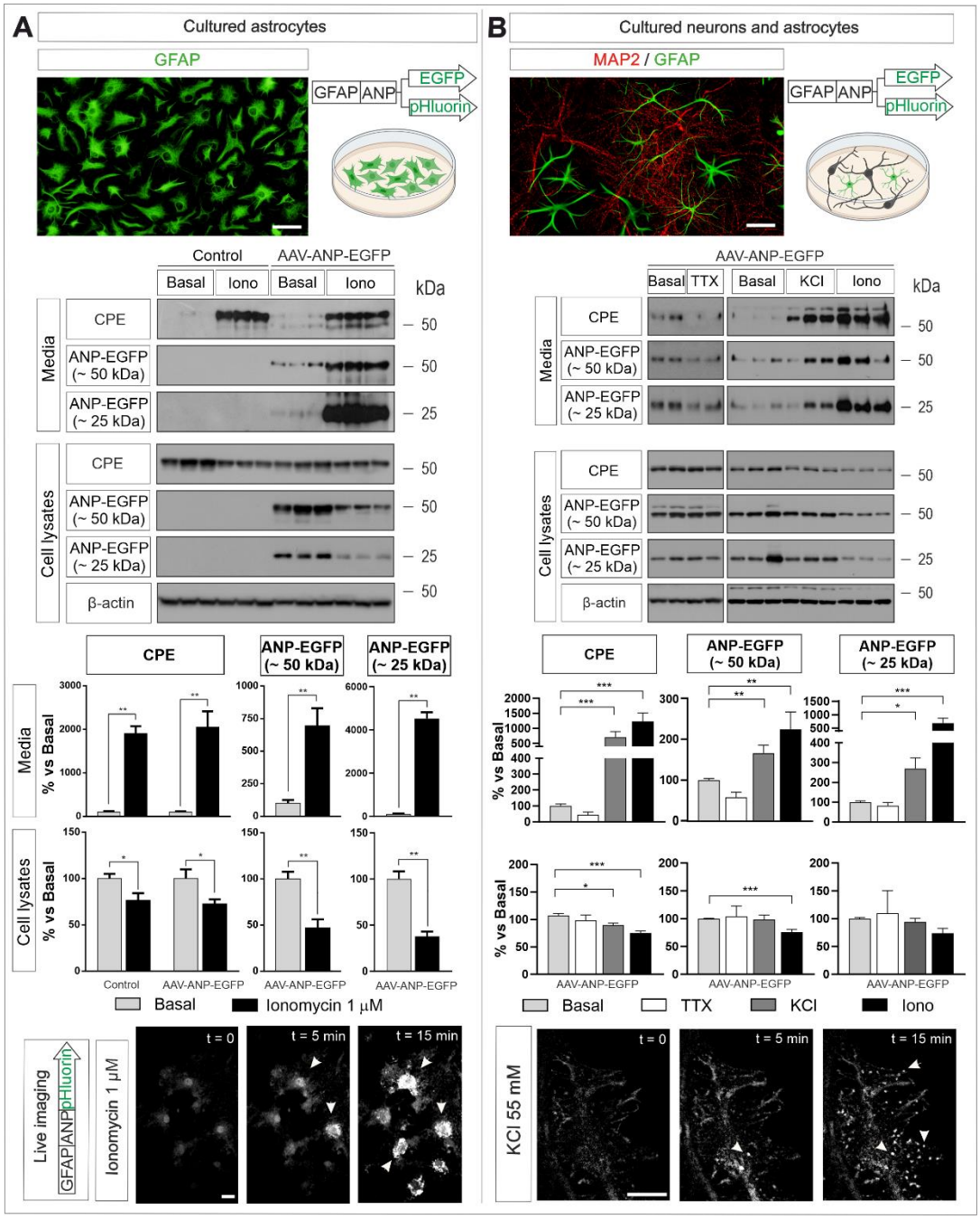

Figure 25. Exogenous ANP-EGFP/pHluorin in astrocytes exhibit a Ca^{2+}-dependent release *in vitro*. **(A)** Release of ANP-GFP in pure astroglial cultures by pharmacological and live-cell imaging methods. Representative immunoblots and histograms illustrate increased secretion of CPE and both forms of ANP-GFP (50 KDa and 25 KDa) under exposure to 1 μM ionomycin for 15 min. Consequently, intracellular content for secretory proteins decreased compared to the basal levels. Live-cell imaging of ANP-pHluorin after addition of an ionophore show increased exocytotic events, mostly in perisomatic regions. **(B)** Release of astrocytic ANP- EGFP/pHluorin in co-cultures of neurons and astrocytes by pharmacological and live-cell imaging approaches. Western blots and histograms show that ANP-EGFP in astrocytes followed an evoked release when inducing astrocytic secretion by neuronal stimulation (depolarizing with 55 mM KCl) or forcing Ca^{2+} entry in neurons and astrocytes by addition of 1 μM ionomycin for 15 min. Live-cell imaging reveals that ANP-pHluorin exocytosis was increased as a result of neuronal depolarization, exhibiting fusion events throughout astrocytic processes. For western blot, mobility of molecular mass markers (in KDa) is indicated. β-actin was used as a loading control. Graphs show the percent variation compared with basal conditions, presented as the mean ± SEM. *p < 0.05; **p < 0.01; ***p < 0.001 (A: Mann-Whitney test; B:Kruskal-Wallis test followed by Dunn's multiple comparisons test. Scale bars in μm: A,B top 50; A, B bottom 20.

Referring to the intracellular content, levels of CPE diminished during depolarization (89%, p=0.028) and with ionomycin (75%, p<0.0001). Levels of 50 KDa-ANP-EGFP in cell lysates were also reduced by exposure to ionomycin (75%, p=0.0007). Additionally, live cell imaging using ANP-pHluorin construct showed increased regions with GFP puncta over a depolarizing period of 15 min. As observed for neuronal ANP-pHluorin exocytosis, most fusion events were anchored in the plasma membrane during this period, suggesting that peptidergic vesicles could partially fuse with the plasma membrane and be retained for a long period of time.

Our results showed that astrocytes in mono-cultures released peptidergic vesicles in Ca^{2+}-dependent process, similar to previous investigations (Krzan et al., 2003; Paco et al., 2009). But, more interestingly, we demonstrated that astrocytes into cortical neural networks, which adopt the *in vivo*-like phenotype, also released DCV-like by Ca^{2+}-dependent exocytosis in response to neuronal activity.

Optogenetic regulation of peptidergic secretion in astrocytes and neurons

Secretory experiments in both astrocytic mono-cultures and neuronal co-cultures were performed by pharmacological manipulations. Although membrane depolarization by KCl or addition of ionomycin are broadly accepted as adequate secretagogues to cause Ca^{2+} influx and provoke exocytosis, they display poor cellular specificity and temporal control. Therefore, we next evaluated secretory dynamics by an optogenetic approach, a more precise method to regulate neuronal activity by light control resembling the timescale of relevant physiological processes **(Figure 26)**.

To achieve optogenetic stimulation *in vitro* and evaluate ANP-EGFP secretion in neurons and astrocytes, we used hippocampal co-cultures obtained from E18 embryos and infected them with an AAV of ChR2 carrying a mCherry reporter whose expression was regulated by the neuronal hSyn promoter **(Figure 26A).** Immunofluorescence analysis revealed that ChR2 was correctly targeted to neurons, labelled with MAP2. Of note, the light-gated cation channel ChR2 was widely distributed along neuronal processes.

To examine peptidergic secretion in astrocytes, we co-infected neuronal ChR2 with astrocytic ANP-EGFP and evaluated levels of secretory proteins by immunoblotting after photostimulating at frequencies between 5 and 40Hz **(Figure 26B)**. After a 15-min illumination with 10-ms blue-light pulses, CPE release was progressively enhanced as frequencies were higher, showing a significant increase at 20 Hz (449%, p=0.0324) and at 40 Hz (841%, p=0.0013). Interestingly, astrocytic ANP-EGFP evoked release was also achieved after neuronal photostimulation at 40 Hz (497%, p=0.0157). Noteworthy, detection of fused ANP was only achieved for the 50-KDa form. In addition, at higher frequencies, intracellular content of secretory proteins tended to decrease.

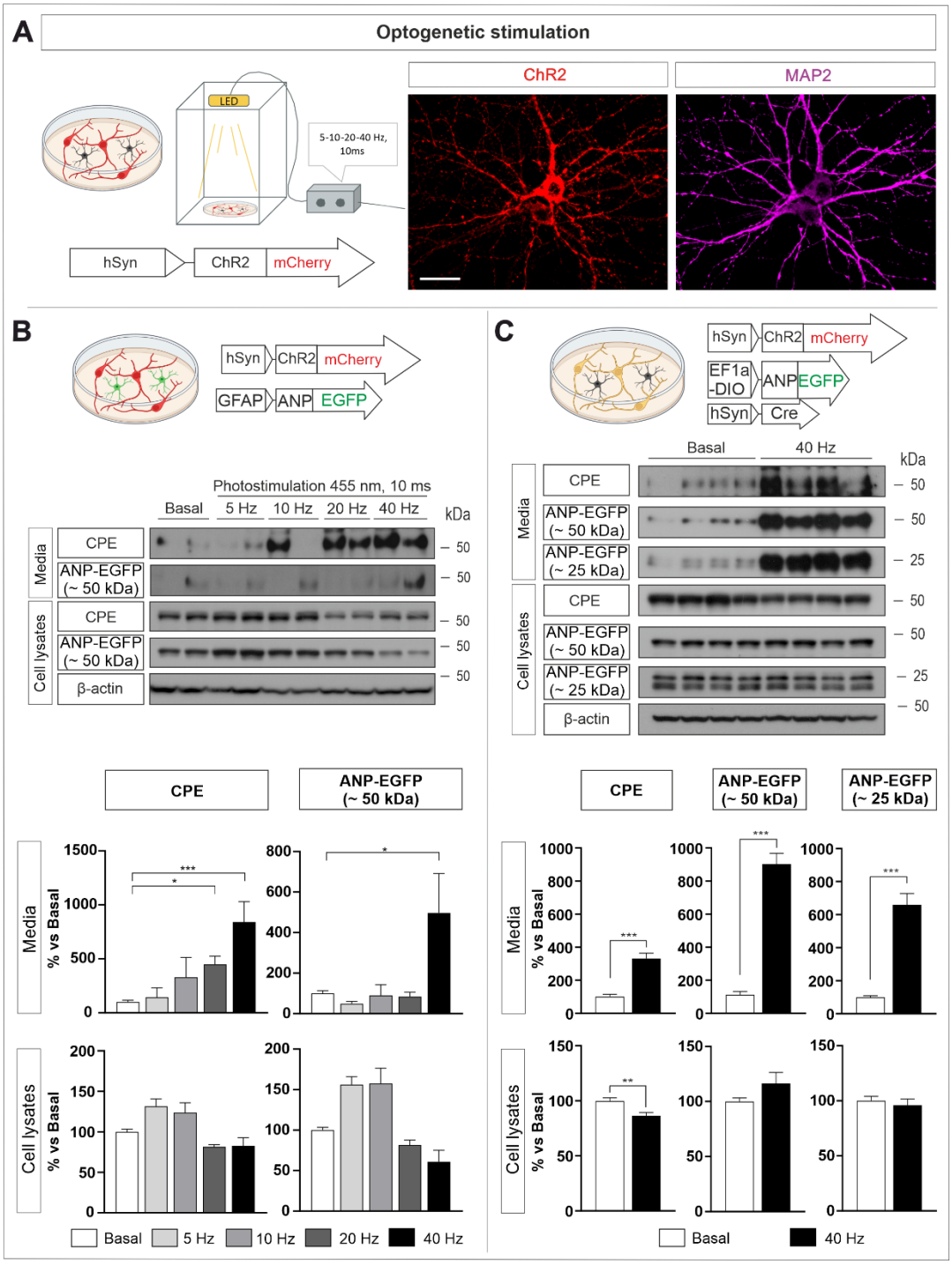

Figure 26. Optical control of ANP-EGFP secretion in astrocytes and neurons. **(A)** Schematic diagram showing vector carrying ChR2-mCherry for optical stimulation in a chamber control by blue-light pulses of 10 ms at different frequencies. Mixed hippocampal cultures expressed ChR2 in neurons, labelled with MAP2. Scale bar: 20 μm. **(B)** Representative immunoblots and histograms illustrate evoked secretion of CPE and astrocytic ANP-EGFP in cultures co-infected with ChR2 stimulating at 40 Hz for 15 min. **(C)** At 40 Hz, immunoblots and graphs show that optogenetic stimulation elicited regulated secretion of CPE and both forms of neuronal ANP-EGFP. Additionally, protein content of CPE in cell lysates decreased. For western blot, mobility of molecular mass markers is indicated in KDa, and β-actin used as a loading control. Graphs show the percent variation compared with basal conditions, presented as the mean ± SEM. *p < 0.05; **p < 0.01; ***p < 0.001 (A: Kruskal-Wallis test followed by Dunn's multiple comparisons test; B: Mann-Whitney test).

To compare astrocytic release of ANP construct with neuronal secretory dynamics, we next studied the effect of photostimulation in mixed cultures co-transfected with ChR2 and neuronal ANP-EGFP **(Figure 26C)**. At 40 Hz, levels of CPE and ANP-EGFP increased in comparison with basal release (CPE: 331%, ANP-EGFP 50-KDa: 902%, ANP-EGFP 25-KDa: 649%; all p=0.0002). Of note, here we successfully detected both forms of the exogenous fused protein. Moreover, enhanced of 50-KDa-form was higher comparing to astrocytic release. Regarding the intracellular content, a decrease compared to the basal situation was observed for CPE (86%, p=0.0047).

Overall, these results indicated that photostimulation with 10-ms blue-light pulses at 40 Hz, that mimic physiological activity, elicit regulated secretion of peptidergic vesicles in neurons, but also in astrocytes. However, as previously observed by pharmacological approaches, evoked secretion of secretory proteins was more notably in neurons.

Glutamate receptors contribution to peptidergic secretion in astrocytes

As formerly described, different approaches including pharmacological stimulation, live-cell imaging and optogenetic stimulation revealed that astrocytes release DCV-stored ANP in a Ca^{2+}-dependent manner *in vitro*, a release pattern observed in both pure astrocytic cultures and co-cultures of astrocytes and neurons.

In a physiological context, astrocytes are capable of sensing neuronal activity, as they express a wide array of membrane receptors, including purinergic, neurotransmitter and neuropeptide receptors (reviewed in Verkhratsky & Nedergaard, 2018). In particular, glutamate act as a key modulator in neuron-glia communication. Thus, to better understand the mechanism by which astrocytes release peptidergic vesicles, we evaluated the potential role of glutamate receptors **(Figure 27)**.

We transfected hippocampal co-cultures with the AAV encoding ANP-EGFP in astrocytes. Then, we evaluated astrocytic secretory dynamics in presence of glutamate receptors antagonists: APV (50 μM) to block NMDA receptor, CNQX (20 μM) to block AMPA/Kainate receptors and MCPG (1 mM) as an antagonist of metabotropic receptors **(Figure 27A)**. We examined protein release in response to neuronal KCl-depolarization for 15 min by western blotting procedures **(Figure 27B, C)**. For CPE, evoked secretion was observed in all conditions, except adding a mix of all inhibitors (untreated: 479%, p= 0.0009; APV: 312%, p=0.031; CNQX: 608%, p=0.0085; MCPG: 464%, p=0.0005; mix: ns). Interestingly, enhanced release of 50-KDa form of ANP-EGFP under depolarizing conditions was additionally blocked in presence of APV alone (untreated: 226%, p= 0.0.0351; APV: ns; CNQX: 264%, p=0.0033; MCPG: 216%, p=0.0235; mix: ns). Noteworthy, evoked secretion of the 25-KDa-form was only evidenced in untreated cells (186%, p=0.0351).

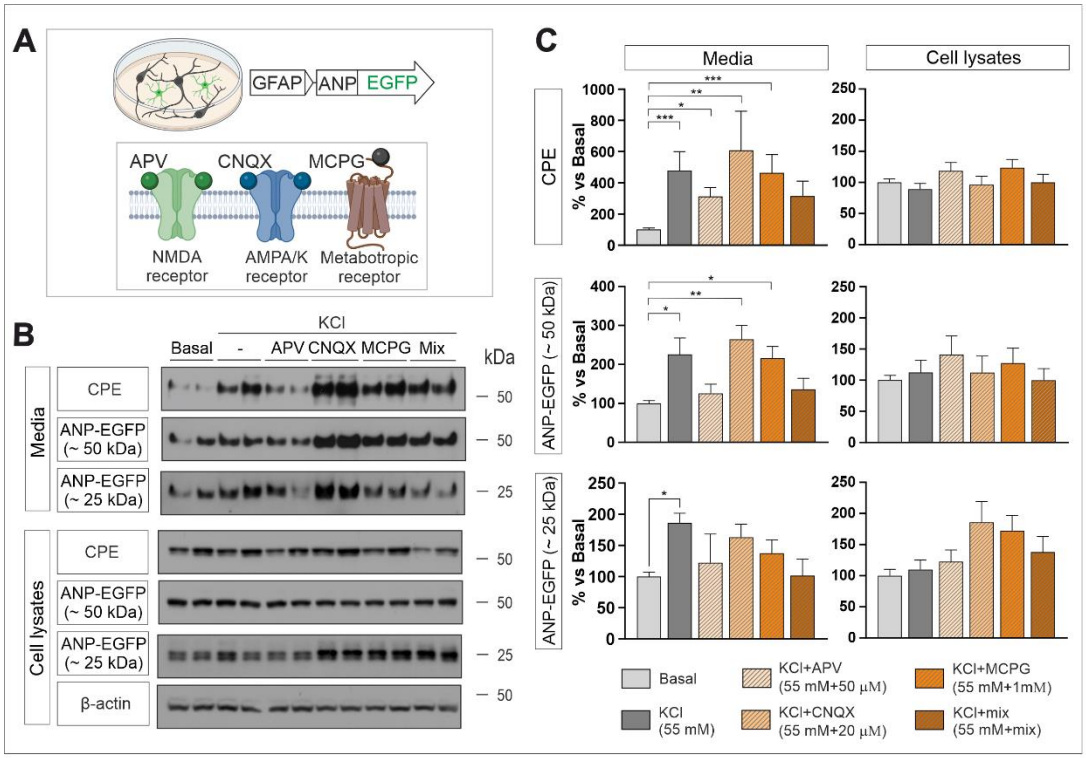

Figure 27. Role of glutamate receptors signalling for astrocyte peptidergic secretion. **(A)** Schemes illustrate secretory experiments evaluating astrocytic ANP-EGFP release in hippocampal co-cultures treated with APV (50 μM) as an antagonist of NMDA receptors, with CNQX (20 μM) for the blockade AMPA/Kainate receptors and MCPG (1 mM) for metabotropic receptors. **(B)** Western blots summarize extracellular and intracellular levels of DCV-stored proteins CPE and ANP-EGFP (for both 50-KDa and 25-KDa forms) in presence of glutamate receptors antagonists. β-actin was used as loading control. The mobility of molecular mass markers (in KDa) is indicated. **(C)** Histograms show that, while CPE evoked release in only blocked when a mix of all inhibitors is added, stimulated secretion of ANP-EGFP in astrocytes is also abolished in APV-treated cultures. Additionally, enhanced secretion of the 25-KDa-form is not achieved in any of the treatment conditions. Graphs show the percent variation compared with basal conditions, presented as the mean ± SEM. *p < 0.05; **p < 0.01; ***p < 0.001, Kruskal-Wallis test followed by Dunn's multiple comparisons test.

In conclusion, although all glutamate receptors apparently have a role in ANP-EGFP evoked release after neuronal depolarization, the most robust results were observed with the addition of APV. Therefore, these results suggest that NMDA receptors could play an important role in astrocytes peptidergic secretion in response to synaptic activity *in vitro*.

Ca^{2+}-dependent secretion of exogenous ANP-GFP in astrocytes *in situ*

To better understand peptidergic secretory dynamics in astrocytes, we performed *in vivo* experiments. We injected the AAV encoding the astrocytic ANP-pHluorin into mouse hippocampi. Then, we evaluated the secretory content in CSF collected from the cisterna magna, in blood samples collected from tail vein and in extracellular media collected from secretory experiments performed in acute brain slices **(Figure 28A).** In addition, to increase detection efficiency of the exogenous protein, we used an LPS-induced neuroinflammation model achieved by intraperitoneal injection of LPS no more than 24 hours before performing the experiment. The inflammatory environment increases GFAP expression that enhance exogenous ANP production (Brahmachari et al., 2016).

We first confirmed that the exogenous protein was targeted to astrocytes *in situ* **(Figure 28B)**. Immunohistochemical analysis of brain sections after 21 days of stereotaxic injection indicated that ANP-pHluorin was correctly directed to astrocytes, labelled with GFAP. Moreover, DCV-stored ANP partially colocalized with SgII, as previously observed in culture analyses. To further determine the most suitable conditions for detecting a robust signal in extracellular compartments, we performed time-course analyses of days post viral injection and of hours with LPS treatment. Levels of ANP-pHluorin in CSF from anesthetized mice were evaluated by western blotting procedures **(Figure 7C)**. Exogenous ANP reached the CSF after 10 days post-injection and from 7 hours of LPS treatment before collection. Of note, LCN2, a secretory protein mainly expressed by astrocytes whose expression is enhanced in neuroinflammation (Kang et al., 2018; Zamanian et al., 2012), was also detected from 4 hours of LPS treatment. Therefore, to ensure detection of ANP-pHluorin, we defined the experimental conditions as hippocampal injections maintained during 21 days in an LPS-induced neuroinflammation context in the last 24h.

To better determine the extracellular compartments that could reach secreted ANP-GFP in this experimental model, we analyzed secretory content in CSF and expanded to blood samples **(Figure 28D).** Immunoblots revealed that astrocytic construct successfully reached CSF, but also blood, in a similar manner than LCN2. Next, to evaluate secretion of ANP-pHluorin in astrocytes *in situ*, we performed secretory experiments in adult acute brain slices. In detail, to assess secretory dynamics in comparison of a control cell population, we split the coronal slices into left (control) and right (infected) hemispheres. Extracellular media was collected and concentrated, and secretory proteins were evaluated by immunoblotting **(Figure 28E).** After neuronal KCl-depolarization or stimulating both neurons and astrocytes adding ionomycin, levels of CPE were higher compared to the basal ones in both control and infected hemispheres. Interestingly, in the ipsilateral hemisphere, ANP-pHluorin was robustly detected in extracellular media and their levels increased with both secretagogues, suggesting a regulated secretion of peptidergic vesicles *in situ*. In contrast, other secretory proteins such as LCN2 or CysC did not show this secretory pattern.

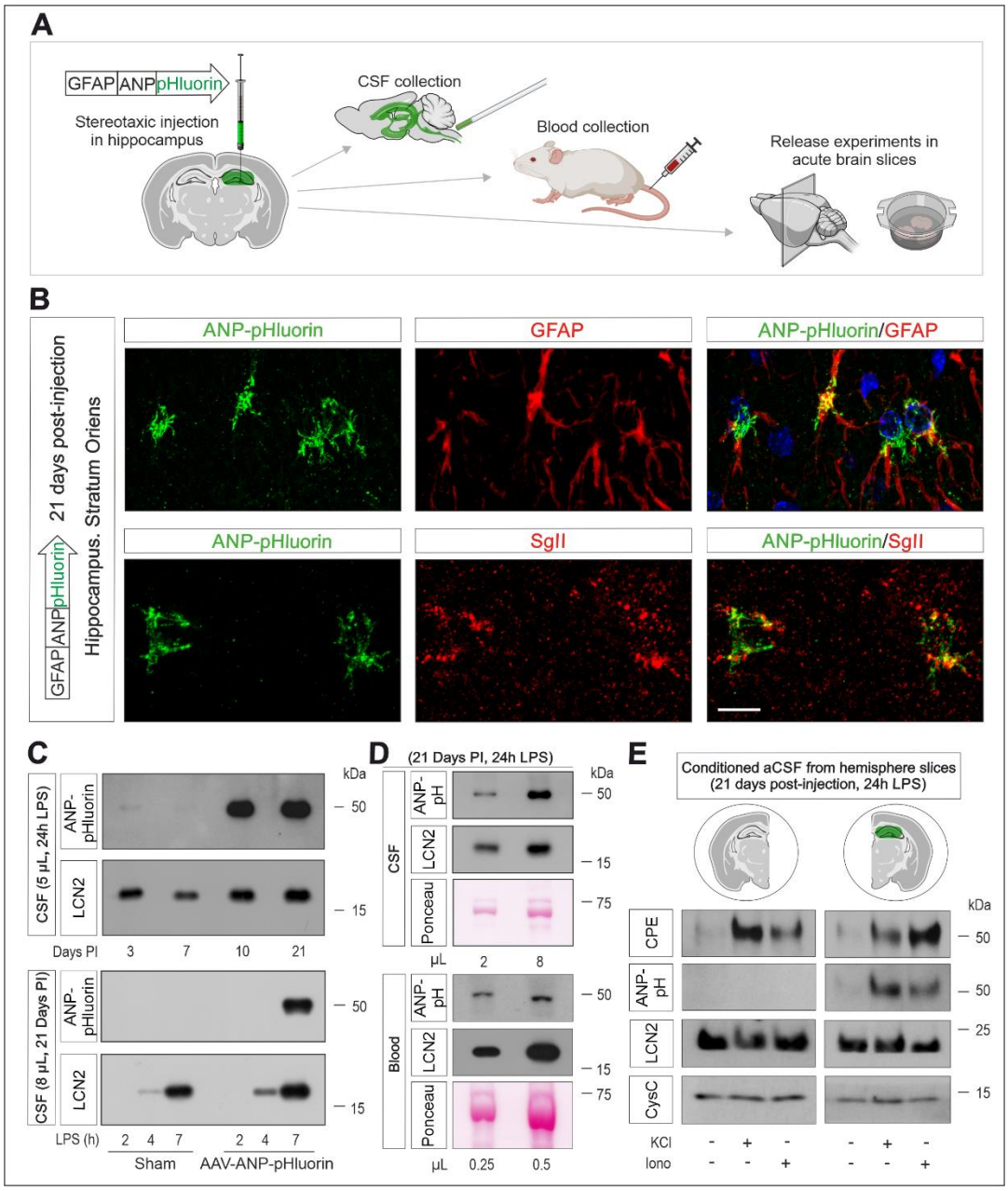

Figure 28. Secretory dynamics of exogenous ANP-EGFP in astrocytes *in situ*. **(A)** Schematic diagram showing the experimental design consisting of stereotaxic injection of ANP-pHluorin under GFAP promoter in the hippocampus, followed by CSF collection, blood collection and media collected from adult acute brain slices. **(B)** Immunofluorescence confocal images reveal that ANP-pHluorin was targeted to astrocytes, labelled with GFAP and partially colocalized with SgII. Scale bar: 20 µm. **(C)** Immunoblots illustrate release of ANP construct to CSF evaluated in a time-course of days post-injection and of hours with LPS treatment before the experiment. ANP-pHluorin was robustly detected after 10 days post-injection and from 7 hours of LPS treatment before collection. **(D)** Western blots of samples from injected maintained for 21 days and receiving 24h LPS treatment show that ANP-pHluorin successfully reached CSF and blood. Ponceau Stain was used as loading control. **(E)** Immunoblots show secretory proteins in aCSF from contralateral (control) and ipsilateral (injected) hemispheres after KCl-depolarization and exposure to 1 µM ionomycin for 15 min. CPE and, interestingly, astrocytic ANP-pHluorin were enhanced after stimulation with both secretagogues. In turn, levels of LCN2 and CysC are maintained in basal and stimulated conditions. Mobility of molecular mass markers (in KDa) is indicated.

Taken together, these results suggested that differentiated astrocytes *in vitro* and *in situ* release DCV-like vesicles in a Ca^{2+}-dependent manner, resembling the neuronal regulated secretory pathway, although in a lesser extent. In addition, secretory experiments in neuronal co-cultures proposed NMDA signalling as an important mediator of astrocytic peptidergic vesicles exocytosis. However, additional experiments are required to better determine the secretory profile in astroglial cells *in vivo*. Altogether, AAV expressing ANP-EGFP/pHluorin specifically in astrocytes or in neurons act as a key tool for studying peptidergic dynamics.

3. Protein changes in brain and CSF of an Alzheimer's disease rat model

Several processes as neurotransmission and neuron-glia communication are dramatically exposed by different insults in the central nervous system. Synaptic degeneration is a global neuropathological event in neurodegenerative disorders, such as Alzheimer's disease. This multifactorial disorder is associated with a progressive memory impairment, disorientation, apathy and depression that particularly cause a synaptic dysfunction as a result of an extracellular deposition of aggregated Aβ peptides that conforms the senile plaques, and an intracellular accumulation of hyperphosphorylated tau that produces neurofibrillary tangles (Hyman, 1997). Substantial efforts have been made to better understand the pathophysiology of AD to prevent the course of the disease. However, far too many questions remain to be answered.

Current research is now directed toward the identification of biomarkers to early detect synaptic dysfunction and loss. For this purpose, novel techniques are being developed to identify biomarkers from human fluid samples. In this context, animal models are essential to biological research. Although they do not fully recapitulate the complete spectrum of the disease, they enable a better understanding of the physiopathology to monitor disease progression and for pre-clinical AD research

Hence, the third and last section of this dissertation focuses on protein changes in the brain and CSF from TgF344-AD rats throughout the course of the disease with the aim of finding potential biomarkers, especially at early ages.

Accumulation of Aβ deposits in the TgF344-AD rat model

The TgF344-AD rat model express human APP with the Swedish mutation (KM670/671NL) and human PSEN1 with the Δ exon 9 mutation. In this way, they express 2.6 times more human APP and 6.2 times more human PSEN1 in the brain. Consequently, these rats exhibit an age-dependent accumulation of amyloid plaques in the hippocampus and the cortex from 6 months of age (Cohen et al., 2013).

In this study, we selected male and female rats that were grouped according to age: before appearance of Aβ plaques (4 months), after Aβ deposition (10'5 months) and at later stages of life and disease (16'5 months). Transgenic (TG) animals were determined by PCR amplification of APPswe and PSEN1ΔE9 mutations in DNA samples obtained from ear tissue **(Figure 29A)**. We evaluated Aβ deposition in TgF344-AD rats examining APP distribution in hippocampal sections by immunohistochemical analyses **(Figure 29B)**. In wild-type (WT) and TG male rats, pyramidal neurons from CA3 region of the hippocampus were strongly labelled with APP. At 4 months, hippocampi from both genotypes do not exhibit amyloid plaques. By contrast, Aβ deposits were clearly observed at 10'5- and 16'5-months transgenic rats, as described in the literature (Cohen et al., 2013). Similar results were obtained in hippocampal sections from female rats (data not shown). Additionally, we examined APP levels in hippocampal homogenates from the three experimental groups by western blotting procedures **(Figure 29C)**. Remarkably, APP

was robustly increased in hippocampus from TG male rats aged 4 to 16'5 months compared to WT rats, similar to analysis from female samples (data not shown).

These results showed that, although Aβ deposits in the hippocampus were clearly identified by immunohistochemical analyses in transgenic rats from 10'5 months of age, APP accumulation in hippocampus homogenates was already evidenced at 4 months, before appearance of Aβ plaques.

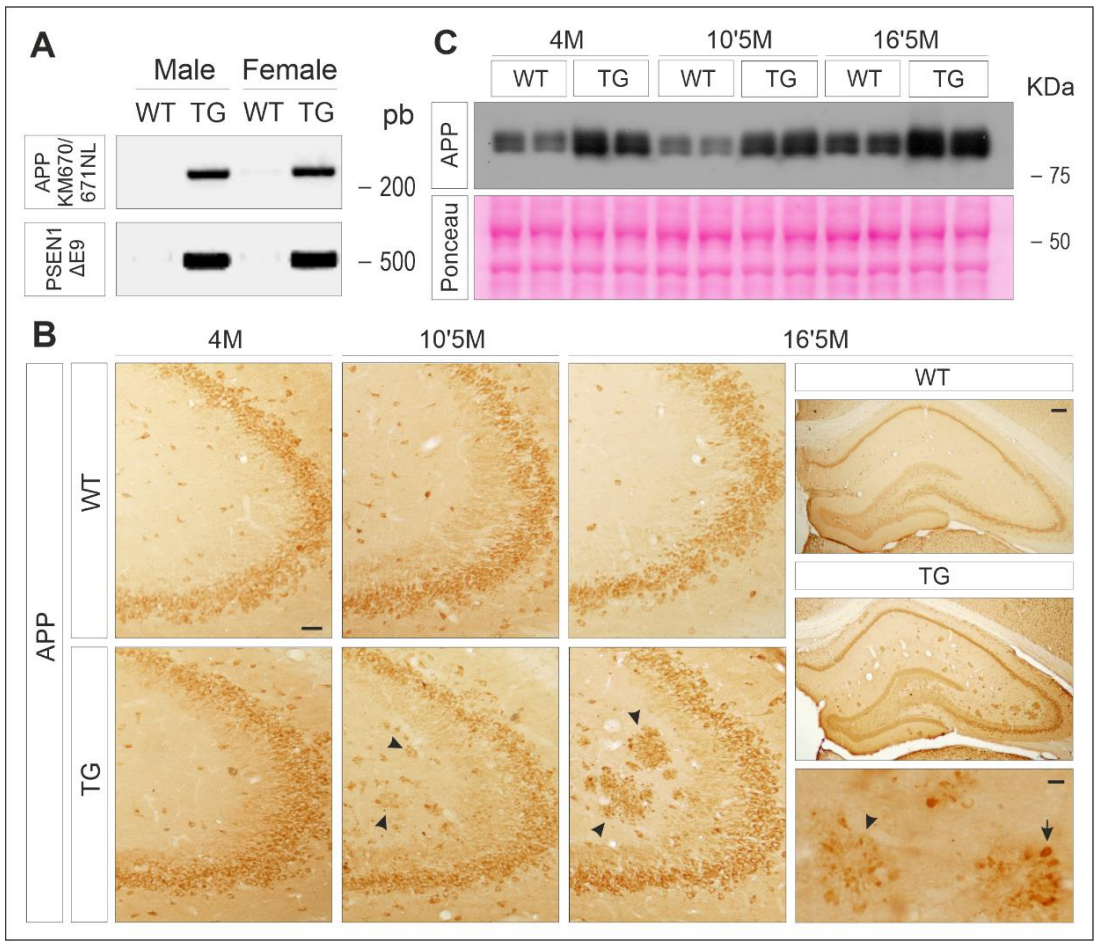

Figure 29. APP accumulation in Tg344-AD rats. **(A)** Rat genotypes were determined by PCR analyses of APPswe and PSEN1ΔE9 mutations in DNA samples from ear tissue. **(B)** Immunoperoxidase staining for APP in hippocampal sections of WT and TG rats from 4, 10'5 and 16'5 months. Although APP was widely distributed through pyramidal neurons of the CA3 region in WT and TG rats, Aβ deposition was observed in TG rats from 10'5 and 16'5 months (arrowheads). Lower magnification of hippocampus from 16'5-month WT and TG rats evidenced APP accumulation throughout TG section. Higher magnification in 16'5-month TG rats show Aβ plaques in detail. Scale bars in μm: C, left 10; C, top right 100; C, bottom right 50. **(C)** Immunoblots of hippocampal homogenates (20 μg) show that TG rats from 4, 10'5 and 16'5-month of age overexpressed APP. Ponceau Stain was used as loading control. Mobility of molecular mass markers (in KDa) is indicated.

Neuronal and glial secretory markers are altered in the brain of TgF344-AD rats

Aβ species dysregulate peptidergic transmission in neurons and astrocytes, leading to DCV accumulation in dystrophic neurites (Lassmann et al., 1992; Lechner et al., 2004; Plá et al., 2013, 2017). In fact, secreted DCV proteins have been identified as promising biomarkers of synaptic loss (Barranco et al., 2021; Blennow et al., 1995; Park et al., 2020). Hence, to investigate if the peptidergic secretory pathway is altered in TgF344-AD rats, we evaluated secretory protein levels in hippocampal homogenates of male and female WT and TG rats from 4, 10'5, 16'5-month of age by western blotting procedures **(Figure 30)**.

Hippocampal content of mature forms of neuronal DCV markers CgA and PC2 (normalized to membrane-transferred total protein) exhibited a sex-dependent dysregulation **(Figure 30A)**. In females TG rats, CgA significantly increased at 10'5 months comparing with WT rats (150%, p=0.010). In contrast, at 16'5 months CgA decreased (80%, p=0.0478). This reduction was also observed in males (44%, p=0.041). However, no differences were detected at 10'5 months. Interestingly, a decrease of CgA was also evidenced in male TG rats from 4 months, before Aβ plaque appearance (72%, p=0.014). Regarding PC2 content, female TG rats displayed an age-dependent regulation. At 4 and 10'5 months, levels of PC2 decreased in comparison to WTs (4 months: 69%, p=0.0079; 10'5 months: 78%, p=0.005), whereas a prominent increase was evident at 16'5 months (154%, p=0.004). In contrast, male TG rats at 16'5 months exhibited a reduction comparing with WT rats (71%, p=0.013).

Next, we evaluated the levels of Cys C, a protease inhibitor involved in AD (Mathews & Levy, 2016) that is contained in both neuronal and astrocytic compartments **(Figure 30B)**. Cys C exhibited a noticeable decrease in TG rats compared to WT at early stages (4 months) but only in males (61%, p=0.024). Additionally, we analyzed the levels of apoE **(Figure 30C)**, a component of lipoproteins that conforms the major genetic risk for AD and that is primarily produced in astrocytes (Pitas et al., 1987), although it is also expressed in neurons under conditions of injury and aging (Wang et al., 2018; Xu et al., 1999). apoE was highly regulated post Aβ plaques appearance in both sexes. In females, apoE content was enhanced 1.43-fold at 10'5 months (p=0.0016) and 1.55-fold at 16'5 months (p=0.0012). In the case of TG males, apoE was increased 1.35-fold at 10'5 months (p=0.0079) and 1.82-fold at 16'5 months (p=0.0022).

Therefore, DCV markers and other secretory proteins were altered in the brain of TgF344-AD rats, following a sex-dependent dysregulation in some cases. Remarkably, some protein changes were evidenced even prior to the appearance of Aβ plaques, especially in males. In addition, apoE was uniformly increased in hippocampus from TG rats after Aβ deposition.

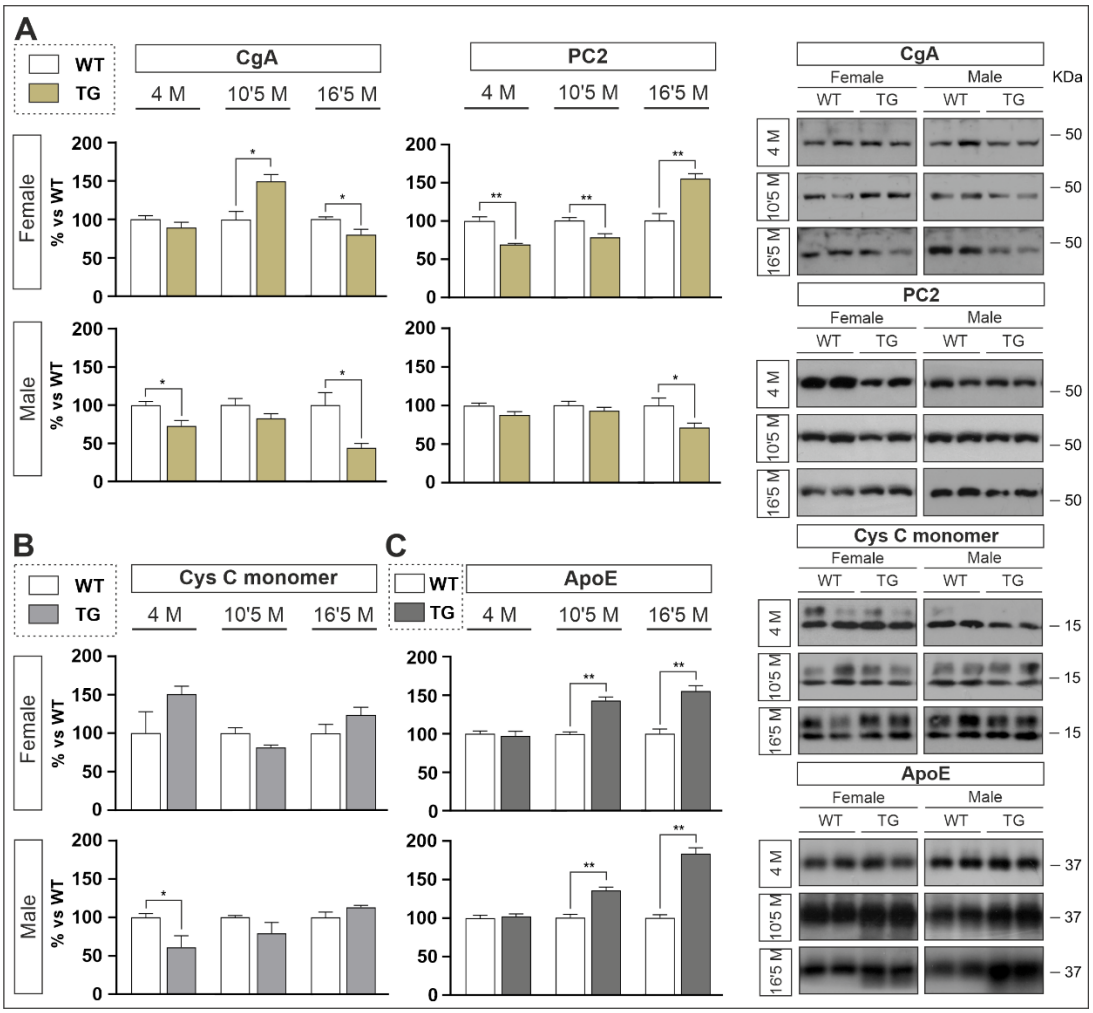

Figure 30. Secretory proteins are altered in hippocampi from TgF344-AD rats. **(A)** Histograms illustrate hippocampal levels of neuronal DCV markers CgA and PC2 from male and female TG rats compared to WT rats (referred as 100 %) at 4, 10'5 and 16'5-month (M) of age. Prior to Aβ deposits (4 months), levels of CgA in TG males and of PC2 in TG females were decreased. At later stages (16'5 months), CgA was also reduced in TG females and males and PC2 only in males. At intermediate stages (10'5 months), TG females exhibited an increase of CgA and a decrease of PC2. **(B)** Graphs summarize percentage of variation of TG versus WT rats of secretory proteins Cys C (contained in neurons and astrocytes). Cys C decreased only in TG male rats at 4 months. **(C)** Graphs showing percentage of variation of apoE, mainly expressed in astrocytes, in TG versus WT rats revealed a uniform and progressive accumulation in hippocampi from male and female rats, evidenced at 10'5 and 16'5 months. Results are normalized by total protein (Ponceau Stain) and data are presented as the mean ± SEM. *$p < 0.05$; **$p < 0.01$, Mann-Whitney test.

To further study the brain changes associated with the robust increase of apoE in hippocampus homogenates from male and female TG rats, we next determined the protein distribution *in situ* by immunohistochemical analyses **(Figure 31)**. Hippocampal brain sections from male rats at 4, 10'5 and 16'5 months of age showed that apoE was primarily expressed in astrocyte-like glial cells, as previously described (Pitas et al., 1987). In constrast, immunostaining throughout the cell bodies of pyramidal neurons in hippocampal CA1 region and throughout the neuropil were slightly observed at early stages (4 months) and more notably found at later stages. Noteworthy, apoE labelling in TG rats was associated with Aβ plaques at both 10'5 and 16'5 months. Similar results were obtained in females (data not shown).

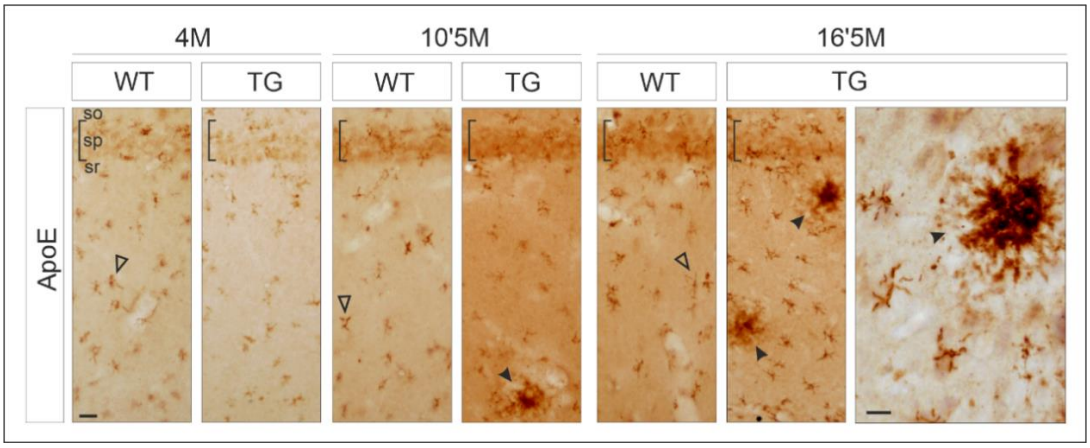

Figure 31. Distribution of apoE in hippocampal sections of TgF344-AD rats. Peroxidase immunohistochemistry in the CA1 region of the hippocampus from male rats aged 4, 10'5 and 16'5 months shows that apoE was predominantly expressed in astrocytes-like glial cells (empty arrowheads), although a slight immunolabelling was observed in the cell body of pyramidal neurons and in neuropil. Noteworthy, apoE in TG rats from 10'5 and 16'5 of age was robustly associated with Aβ plaques (arrowheads). In addition, immunolabelling of astroglial-like cells at later stages resembled a reactive phenotype. Scale bar: left, 10 μm; right 50 μm. Abbreviations: so, stratum oriens; sp, stratum pyramidale; sr, stratum radiatum.

Therefore, increased levels of apoE in hippocampus homogenates from TG rats after Aβ deposition (10'5 and 16'5 months of age) may be associated with Aβ accumulation and with astroglial apoE overexpression.

apoE immunostaining in aged TG rats evidenced a reactive morphology in astrocyte-like glial cells. Therefore, to corroborate that our TgF344-AD rats presented gliosis, we next examined the expression of GFAP (to detect astrocytes) and Iba1 (to identify microglia) in cortical sections by immunohistochemical analyses **(Figure 32)**. GFAP-immunoreactivity was markedly increased in the somatosensory cortex of male TG rats from 10'5 and 16'5 months compared to WT rats, noticeably in close vicinity of Aβ plaques. In detail, astrocytes exhibited hyperplasia and hypertrophy of soma and processes. Additionally, hippocampal microglia were also hyperplasic and hypertrophied at later stages of the TgF344-AD model, adopting an amoeaboid shape. In transgenic females, reactive phenotypes in both cell types were also noticeable (data not shown).

Considering that GFAP and Iba1 are typically overexpressed in reactive astrocytes and microglia, respectively (Ben Haim et al., 2015; Imai & Kohsaka, 2002), our TgF344-AD rats exhibited a robust neuroinflammation process associated with Aβ deposition, in accordance with previous results of the rat model (Cohen et al., 2013).

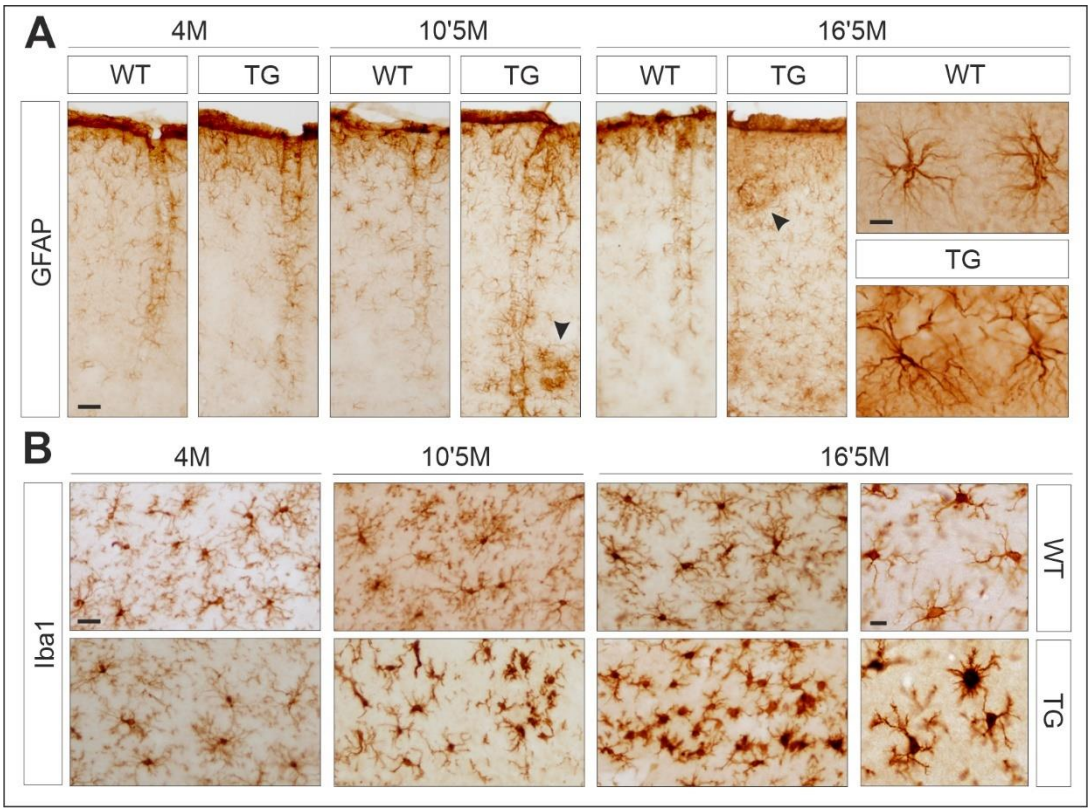

Figure 32. Distribution of neuroinflammatory cells in the cerebral cortex of TgF344-AD rats. **(A)** Immunoperoxidase staining for GFAP in somatosensory cortex sections performed in WT and TG male rats at 4, 10'5 and 16'5 months revealed that astrocytes were hyperplasic, especially in close vicinity of Aβ plaques (arrowheads), and hypertrophied in soma and processes. This reactive phenotype was observed at 10'5 months and, more notably at 16'5 months. **(A)** Peroxidase immunohistochemistry in hippocampal sections show that microglia, labelled with Iba1, were also hyperplasic and hypertrophied at 10'5 months, and in a greater degree at 16'5 months, acquiring an amoeaboid shape. Scale bars in μm: A, left 10; A, right 50; B, left 20; B, right 10.

Changes in secretory protein levels in the CSF of TgF344-AD rats

To investigate the relationship of brain content changes with the secreted amount in extracellular fluids, we next evaluated the levels of secretory proteins in CSF samples from female and male WT and TgF344-AD rats at 4, 10'5 and 16'5 months of age (n=8-12/group, total=107). As secretory proteins are also present in blood and plasma, all CSF samples were screened for blood contamination. Only visible clear samples with low concentration of IgM were considered for the study. Secretory proteins were evaluated in 4 μL of CSF samples by western blotting procedures **(Figure 33)**.

Referring to specific neuronal secretory proteins, CSF of TG rats from 4 months exhibited an increase of CgA precursor form compared to WT rats only in males (142%, p=0.0434). In the case of PC2 precursor form (~75 KDa), which is robustly detected in CSF samples, it decreased in 4-month TG males (58%, p=0.0014). Additionally, we evaluated PC1/3 in the same samples focusing on an apparent PC1/3 cleaved form that exhibited a lower electrophoretic mobility (~25 KDa). In this case, PC1/3 was increased in TG female rats from 10'5 months (208%, p=0.0205), whereas in TG males, this enhance was noticed earlier, at 4 months (264%, p=0.0062).

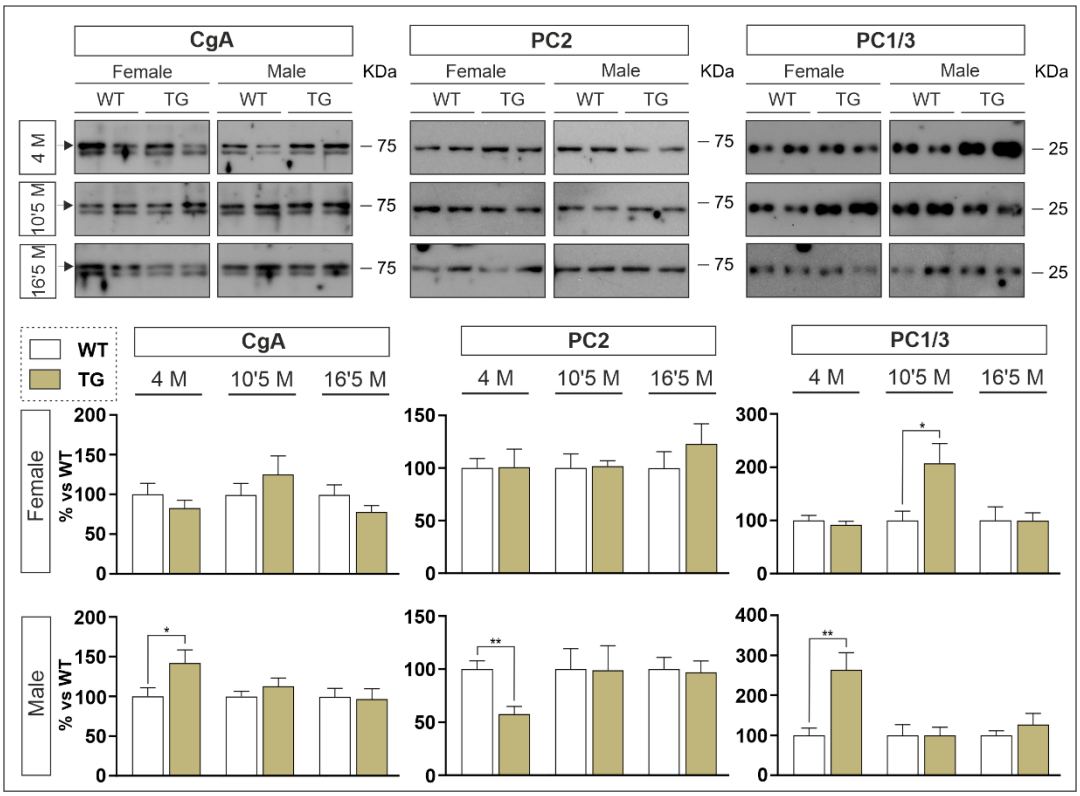

Figure 33. Changes in neuronal secretory proteins in the CSF of TgF344-AD rats. Representative immunoblots and histograms illustrate levels of precursor form of CgA (arrows) and PC2, and a processed form of PC1/3 in male and female rats from 4, 10'5 and 16'5 months (n=8-12/group, total=107). CgA was increased in TG males of 4 months, CgA was increased in TG females, whereas a robust reduction was observed in PC2. In addition, levels of PC1/3 increased at 10'5 months, whereas in TG males it occurred at 4-month-old. For western blots, mobility of molecular mass markers (in KDa) is indicated in KDa. Graphs show the percent variation in TG samples compared with WT rats (100%). Data are presented as the mean ± SEM. *p < 0.05; **p < 0.01, Mann-Whitney test.

Next, we further examined secretory proteins contained in neurons and astrocytes in the same CSF samples (4 μL) by western blot **(Figure 34)**. In addition to previous analyses performed in brain tissue, we evaluated the precursor form of SgIII (~ 53 KDa), also represented in astrocytes (Paco et al., 2010). At 4 months, SgIII precursor form was increased only in TG males (235%, p=0.0289). In the case of Cys C, an increase was observed at later stages (16'5 months) of TG males (229%, p=0.0068). In a similar manner, apoE was increased in TG males at 16'5 months (141%, p=0.0173), but also at 4-month TG males (146%, p=0.0379).

Taken together, apart from variations in the brain content, secretory proteins were also diversely altered in CSF samples from TgF344-AD rats, especially in males. Interestingly, some changes were early detected, prior to Aβ deposition. Being CSF a promise source of synaptic-derived proteins, as it is in direct contact with extracellular matrix in the brain, these results provided some candidates for biomarkers of synapse loss associated with AD neuropathology.

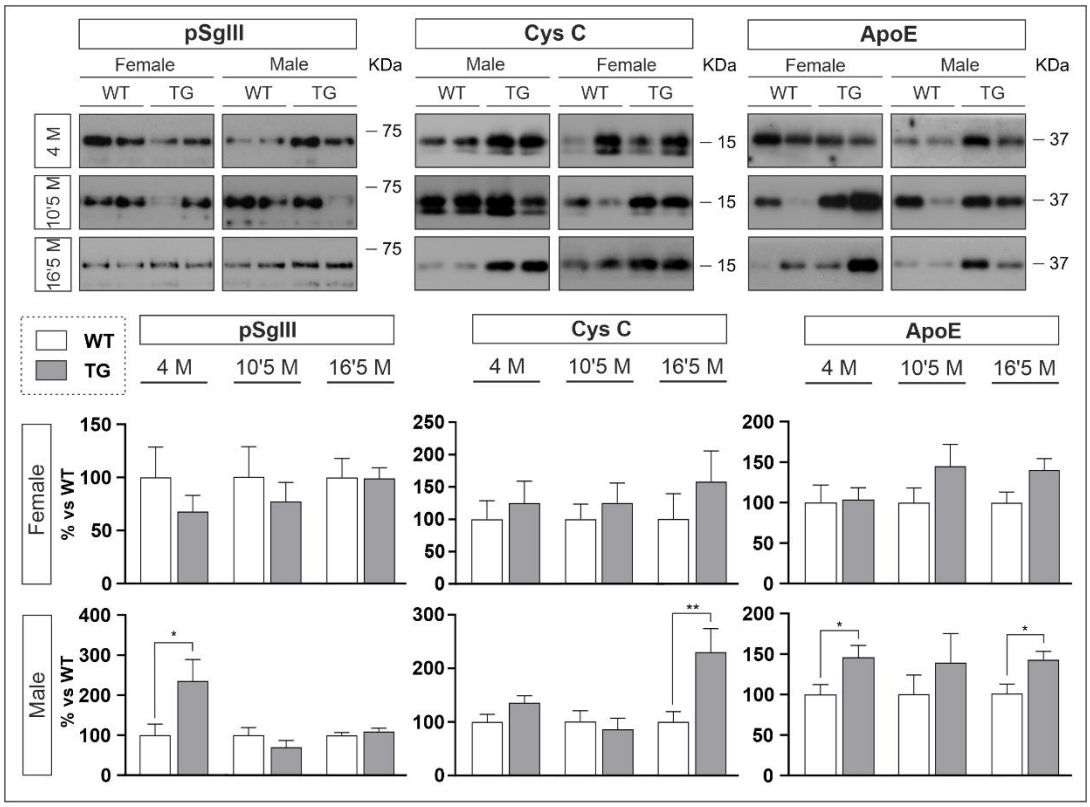

Figure 34. Variations in the levels of neuronal and glial secretory proteins in the CSF of TgF344-AD rats. Representative immunoblots and histograms illustrate levels of SgIII precursor form, Cys C and apoE in male and female rats from 4, 10'5 and 16'5 months (n=8-12/group, total=107). Precursor form of SgIII was increased in TG males from 4-month of age. For Cys C, there were a robust increase at 16'5 months in males. In the case of apoE, TG males from 4-month of age exhibited higher levels comparing with WT animals. This increase was maintained at 16'5 months. For Western blots, mobility of molecular mass markers (in KDa) is indicated in KDa. Graphs show the percent variation in TG samples compared with WT rats (100%). Data are presented as the mean ± SEM. *$p < 0.05$; **$p < 0.01$; ***$p < 0.001$, Mann-Whitney test.

Proteomic analysis of CSF from TgF344-AD rats

Western blotting analyses revealed that DCV-stored proteins, in addition to other secretory proteins, were altered in the CSF of TgF344-AD rats. Therefore, to further determine protein changes in a large-scale, we next performed a proteomic study **(Figure 35)**. A total of 60 validated CSF samples from WT and TG male and female rats at 4, 10'5 and 16'5 months were selected for the study (n=5/group, 35 μL). In summary, proteins in the CSF samples were extracted and diluted for LysC and trypsin digestion. Peptide mixes resulting from digestion were acidified and desalted prior to LC-MS/MS analysis. Acquired spectra were analyzed using the Proteome Discoverer software suite and the Mascot search engine. Then, data were searched against the reference proteome from Uniprot, UP_Rat, database. Peptide quantification data were retrieved from Proteome Discoverer, that matched to a total of 2040 proteins, which remained in 1802 after removal of contaminants.

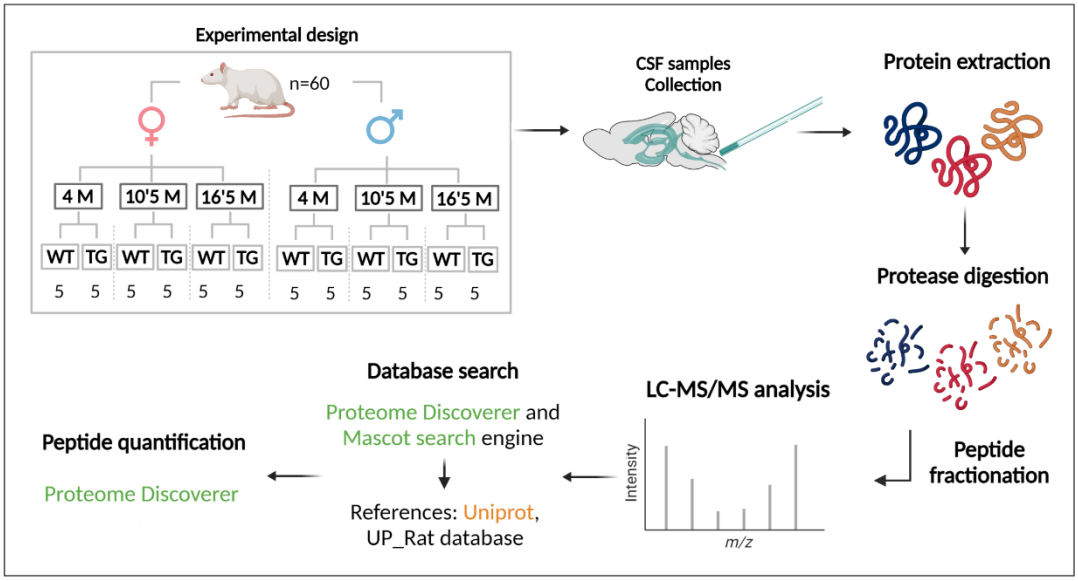

Figure 35. Schematic representation of proteomic analysis of CSF from TgF344-AD rats. CSF samples from 60 rats (WT and TG females and males from 4, 10'5 and 16'5 months, n=5/group, 35 µL) were particularly processed to finally obtain the proteome of each sample. Proteins were extracted from CSF samples and subsequently digested. Then, fractionated peptides followed a LC-MS/MS analysis. Data obtained from Proteome Discoverer software and the Mascot search engine were searched against the reference proteome (Uniprot, UP_Rat, database). Finally, peptide quantification data were retrieved from Proteome Discoverer.

To determine protein changes in the CSF proteome from TgF344-AD rats, we first compared TG versus WT samples at 4, 10'5 and 16'5 months in a sex-independent manner (n=10/group), similar to most proteomic investigations performed in human samples. Protein fold-changes and their corresponding adjusted p-values were obtained using MSqRob-VSN Shiny App and an FDR of 5%. Data were represented by Volcano plots and summarized in adjacent tables **(Figure 36)**.

Seven proteins were differentially adjusted in TG rats from 4 months, including downregulation of Tropomyosin-1 (Tpm1, A0A0G2JSQ4) and Brain acid soluble protein 1 (Basp1, Q05175), and upregulation of APP (P08592). At 10'5 months, a bigger number of protein changes were observed, nine protein changes corresponding to a decrease and three to an increase. Noteworthy, changes in Tpm1, Basp1 and APP were evidenced again. When examining the 16-month group, TG rats exhibited a greater number of protein changes compared to 4 and 10'5-month groups. In detail, five proteins were downregulated and twenty proteins followed an upregulation, including APP but also Basp1 and Tpm1, oppositely than previously observed. Interestingly, other relevant proteins were enhanced in the transgenic model, including Lysosome-associated membrane glycoprotein 1 (Lamp1, P145612), Lamp2, Superoxide dismutase 1 (Sod1, P07632), Cytocrome C Somatic (Cysc, P62898), Growth-associated protein 43 (Gap43, P07936), calmodulin-dependent protein kinase type II subunit alpha (Camk2a, P11275), Neurogranin (Nrgn, Q04940) and Neurofilament light polypeptide (Nefl, P19527).

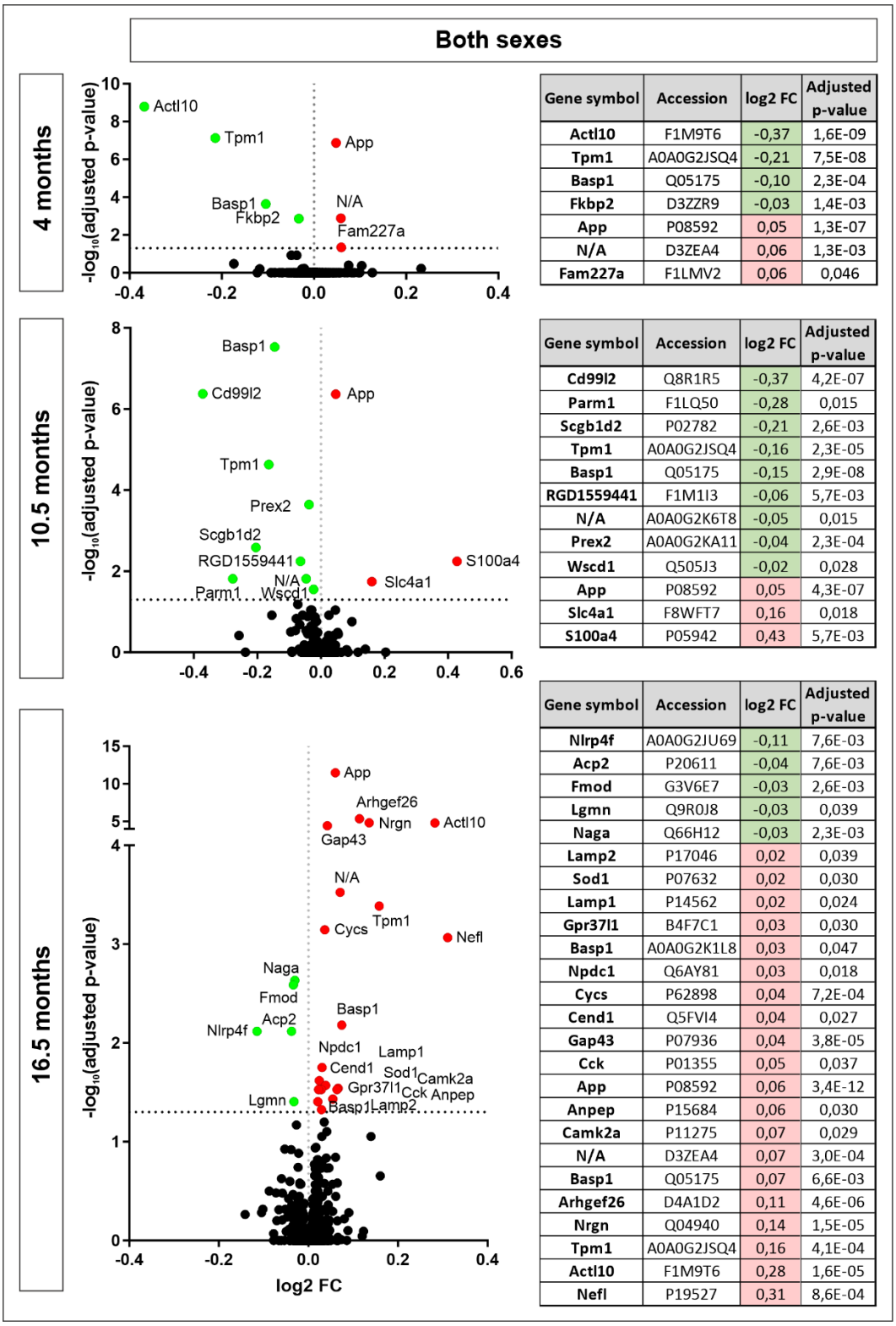

Gene symbol	Accession	log2 FC	Adjusted p-value
Actl10	F1M9T6	-0,37	1,6E-09
Tpm1	A0A0G2JSQ4	-0,21	7,5E-08
Basp1	Q05175	-0,10	2,3E-04
Fkbp2	D3ZZR9	-0,03	1,4E-03
App	P08592	0,05	1,3E-07
N/A	D3ZEA4	0,06	1,3E-03
Fam227a	F1LMV2	0,06	0,046

Gene symbol	Accession	log2 FC	Adjusted p-value
Cd99l2	Q8R1R5	-0,37	4,2E-07
Parm1	F1LQ50	-0,28	0,015
Scgb1d2	P02782	-0,21	2,6E-03
Tpm1	A0A0G2JSQ4	-0,16	2,3E-05
Basp1	Q05175	-0,15	2,9E-08
RGD1559441	F1M1I3	-0,06	5,7E-03
N/A	A0A0G2K6T8	-0,05	0,015
Prex2	A0A0G2KA11	-0,04	2,3E-04
Wscd1	Q505J3	-0,02	0,028
App	P08592	0,05	4,3E-07
Slc4a1	F8WFT7	0,16	0,018
S100a4	P05942	0,43	5,7E-03

Gene symbol	Accession	log2 FC	Adjusted p-value
Nlrp4f	A0A0G2JU69	-0,11	7,6E-03
Acp2	P20611	-0,04	7,6E-03
Fmod	G3V6E7	-0,03	2,6E-03
Lgmn	Q9R0J8	-0,03	0,039
Naga	Q66H12	-0,03	2,3E-03
Lamp2	P17046	0,02	0,039
Sod1	P07632	0,02	0,030
Lamp1	P14562	0,02	0,024
Gpr37l1	B4F7C1	0,03	0,030
Basp1	A0A0G2K1L8	0,03	0,047
Npdc1	Q6AY81	0,03	0,018
Cycs	P62898	0,04	7,2E-04
Cend1	Q5FVI4	0,04	0,027
Gap43	P07936	0,04	3,8E-05
Cck	P01355	0,05	0,037
App	P08592	0,06	3,4E-12
Anpep	P15684	0,06	0,030
Camk2a	P11275	0,07	0,029
N/A	D3ZEA4	0,07	3,0E-04
Basp1	Q05175	0,07	6,6E-03
Arhgef26	D4A1D2	0,11	4,6E-06
Nrgn	Q04940	0,14	1,5E-05
Tpm1	A0A0G2JSQ4	0,16	4,1E-04
Actl10	F1M9T6	0,28	1,6E-05
Nefl	P19527	0,31	8,6E-04

Figure 36. The CSF proteome from TgF344-AD rats. Volcano plots and data tables summarize protein changes in CSF from TG rats compared to WT rats at 4, 10'5 and 16'5 months of age. Data are depicted with the fold change and the adjusted p-value, both calculated with MSqRob-VSN Shiny App. Green circles show protein changes which have a significant decrease, whereas red circles indicate significant increases. Black circles are protein changes without any differences (adjusted p-value > 0.05). Remarkably, variations were already detected at early stages prior to Aβ deposition (4 months). Then, protein adjustments were progressively increased. At 4 and 10'5 months, most changes corresponded to a downregulated, whereas at 16'5 months proteins differently abundant in TG rats were mostly upregulated. Protein names from significant changes are indicated.

Therefore, CSF from TgF344-AD exhibited proteins changes during the course of the disease, displaying an age-dependent increase. Of note, at 4 and 10'5 months most protein changes followed a reduction. However, at 16'5 months most variations corresponded to an increase. At later stages, those changes reveal apoptotic and autofagic processes (Cycs, Lamp 1, Lamp2) and neuronal damage, as some cytoskeleton related-proteins (Tpm1, Nefl) and synaptic proteins (Basp1, GAP-43, Nrgn) reach the CSF in a greater amount.

To explore sex-related alterations in the CSF from TgF344-AD, we next analysed proteomic data considering female and male samples separately (n=5/group). Fold changes and their adjusted p-values were represented by Volcano plots **(Figure 37)** and summarized **Table 2**.

At 4 months, CSF from female and male TG rats displayed a similar number of proteins changes in comparison with WT samples (eleven in females, twelve in males). Similar to previous analysis, Tpm1 was downregulated and APP followed an upregulation in both sexes. However, decreased Basp1 levels were only observed in TG females. In addition, Neurofascin (Nfasc, P97685), which have a role in cell adhesion, was downregulated in CSF from TG females. Vitamin K-dependent protein Z (ProZ, G3V8K8), related to metabolic processes, was downregulated in TG males.

After Aβ deposition (10'5 months of age), protein changes in CSF from TG females and males were reduced in comparison with CSF samples from 4 months. Nine proteins were differentially abundant in CSF from TG females and seven proteins changes were all downregulated in TG males. In comparison with the sex-independent analysis, Tpm1 and Basp1 were also reduced in CSF from TG females and males. However, upregulation of APP was only evidenced in TG females. Additionally, Semaphorin-7A (Sema71, D3ZQP6), which play a role regulating cell migration and immune responses, was downregulated in TG females, whereas Profilin-2 (Pfn2, D3ZDU5), a cytoskeleton related-protein, was upregulated. In CSF from TG males, we observed a reduction in Innate immunity activator protein (Inava, D3ZL84), involved in metabolic cellular processes.

At later stages of the disease (16'5 months), we found a robust increase in protein variations, especially in males (fourteen differences in TG females and thirty-one in TG males, most of them corresponding to an upregulation). In comparison with previous results, differences in Tpm1 and APP were also evidenced in both female and male TG rats. However, other protein changes were only observed in one sex. In the case of Nefl and Nrgn, an upregulation was only identified in TG females, whereas enhanced GAP-43, Lamp1, Lamp2 and Cycs were only detected in TG males. In addition, Inava, Serine proteinase inhibitor clade A member 4 (Serpina4, Q5M8C3) and Serpina3m (F1LR92) were downregulated in TG males; and Myristoylated alanine-rich C-kinase substrate (Marcks, P30009), a synaptic protein, followed an upregulation.

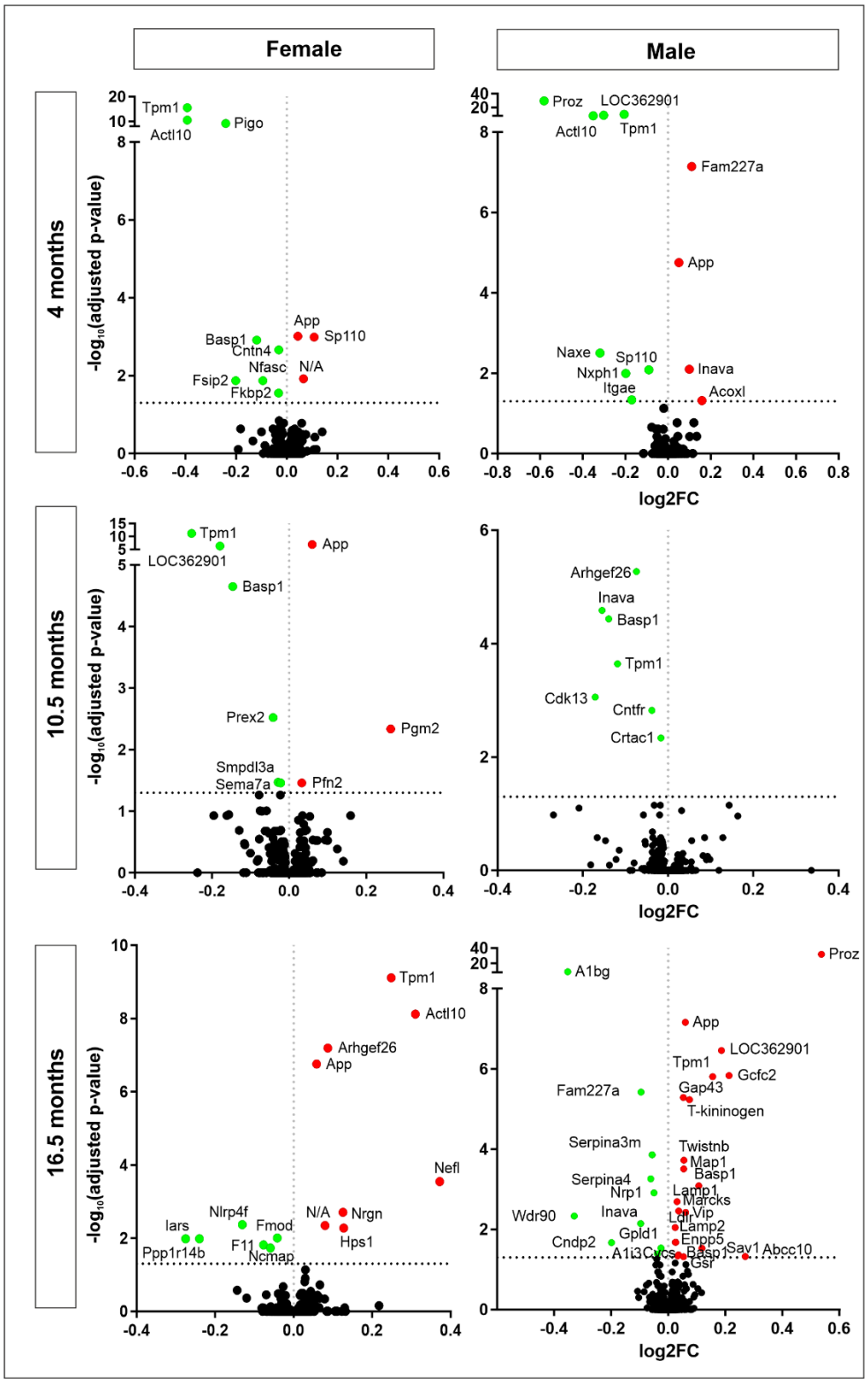

Figure 37. Proteomic analysis of CSF from sex-matched TgF344-AD rats. Volcano plots represent protein changes in CSF from TG female and male rats compared to WT rats at 4, 10'5 and 16'5 months of age. Green circles show protein changes which have a significant decrease, whereas red circles indicate significant increases. Black circles are protein changes without any differences (adjusted p-value > 0.05). Significant protein adjustments were observed at three developmental stages, prior to Aβ deposition (4 months), after Aβ plaques (10'5 months) and at later stages (16'5 months). Noteworthy, some variations were commonly found in both females and males, but others were only evidenced in one sex. Moreover, most protein changes at 4 and 10'5 months corresponded to a downregulation, whereas at 16'5 months variations predominantly evidenced an upregulation, especially evidenced in males. Protein names from significant changes are indicated.

		4 months				10.5 months				16.5 months			
		Female		Male		Female		Male		Female		Male	
Gene symbol	Accession	Log2 FC	Adjusted p-value	Log2 FC	Adjusted p-value	Log2 FC	Adjusted P value	Log2 FC	Adjusted p-value	Log2 FC	Adjusted p-value	Log2 FC	Adjusted P value
A1bg	Q9EPH1											-0,35	1,9E-09
A1i3	P14046											-0,04	0,040
Abcc10	D3ZX04											0,27	0,047
Acoxl	D4A257			0,16	0,048								
Actl10	F1M9T6	-0,39	3,2E-11	-0,35	6,5E-09					0,31	7,6E-09		
App	P08592	0,04	9,7E-04	0,05	1,8E-05	0,06	1,2E-07			0,06	1,8E-07	0,06	6,9E-08
Arhgef26	D4A1D2							-0,07	5,4E-06	0,09	6,5E-08		
Basp1	Q05175	-0,12	1,2E-03			-0,15	2,2E-05	-0,14	3,7E-05			0,11	8,2E-04
Basp1	A0A0G2K1L8											0,04	0,043
Cdk13	F1M1X9							-0,17	8,8E-04				
Cndp2	Q6Q0N1											-0,20	0,021
Cntfr	M0R9L2							-0,04	1,5E-03				
Cntn4	A0A0G2JVI9	-0,03	2,2E-03										
Crtac1	F1LQP7							-0,02	4,6E-03				
Cycs	P62898											0,03	0,046
Enpp5	P84039											0,03	0,021
F11	A0A0G2K4I9									-0,08	0,015		
Fam227a	F1LMV2			0,11	7,2E-08							-0,10	3,8E-06
Fkbp2	D3ZZR9	-0,03	0,028										
Fmod	G3V6E7									-0,04	0,010		
Fsip2	A0A096MJX4	-0,20	0,013										
N/A	D3ZEA4	0,07	0,012							0,08	4,5E-03		
Gap43	P07936											0,05	5,2E-06
Gcfc2	D4A3Z4											0,21	1,5E-06
Gpld1	G3V8B1											-0,02	0,029
Gsr	F1LRE1											0,05	0,048
Hps1	A0A0G2JXZ4									0,13	5,3E-03		
Iars	F1LS86									-0,27	0,010		
Inava	D3ZL84			0,10	8,0E-03			-0,15	2,6E-05			-0,10	7,2E-03
Itgae	M0R6T8			-0,17	0,0460								
Lamp1	P14562											0,03	2,0E-03
Lamp2	P17046											0,03	0,021
Ldlr	G3V7A5											0,02	9,0E-03
LOC362901	F7ESJ7			-0,30	1,3E-09	-0,18	0,000					0,19	3,5E-07
Map1	P01048											0,05	3,1E-04
Marcks	P30009											0,04	3,5E-03
Naxe	B0BNM1			-0,32	3,1E-03								
Ncmap	F1M2Z5									-0,06	0,019		
Nefl	P19527									0,37	2,9E-04		
Nfasc	P97685	-0,09	0,013										
Nlrp4f	A0A0G2JU69									-0,13	4,3E-03		
Nrgn	Q04940									0,13	2,0E-03		
Nrp1	Q9QWJ9											-0,05	1,2E-03
Nxph1	F1LRY8			-0,20	0,010								
Pfn2	D3ZDU5					0,03	0,035						
Pgm2	F7FLB2					0,26	4,6E-03						
Pigo	D3ZTP8	-0,24	7,3E-10										
Ppp1r14b	Q8K3F3									-0,24	0,010		
Prex2	A0A0G2KA11					-0,04	3,0E-03						
Proz	G3V8K8			-0,58	1,4E-30							0,54	1,1E-32
Sav1	A4V8B4											0,12	0,030
Sema7a	D3ZQP6					-0,02	0,035						
Serpina3m	F1LR92											-0,06	1,4E-04
Serpina4	Q5M8C3											-0,06	5,5E-04
Smpdl3a	Q641Z7					-0,03	0,034						
Sp110	R9PXZ9	0,11	1,0E-03	-0,09	8,2E-03								
T-kininogen 2	P08932											0,07	5,9E-06
Tpm1	A0A0G2JSQ4	-0,39	3,0E-16	-0,21	8,2E-11	-0,25	7,0E-12	-0,12	2,3E-04	0,25	7,7E-10	0,16	1,6E-06
Twistnb	D4ADH7											0,05	1,9E-04
Vip	B0BNF3											0,06	3,8E-03
Wdr90	D3ZMM2											-0,33	4,6E-03

Table 2. Protein changes in proteomic analysis of CSF from TG and WT female and male rats at 4, 10'5 and 16'5 months. Fold changes and their corresponding adjusted p-values from significant protein (< 0.05) comparing TG vs WT samples are summarized. Proteins are represented by gene symbol. Green data indicate fold changes corresponding to a decrease, whereas red fold changes evidence an increase. Additionally, accession data is indicated.

In conclusion, the proteome of CSF from TgF344-AD rats evidenced protein changes during the course of the disease as a result of an overexpression of APP and PSEN. However, analysing data from both sexes separately revealed a different variation profile. At early and intermediate stages (4 and 10'5 months of age), both TG female and male rats exhibited a similar number of protein changes but, at 16'5 months, TG males displayed a greater number of protein variations, most corresponding to an upregulation. In general, most deviations corresponded to proteins having a role in the cellular component, metabolic and inflammatory processes and synapsis.

To further investigate the functional annotations that characterized the list of proteins differentially expressed in the CSF proteome of Tg-F344-AD rats, we next performed a pathway enrichment analysis provided by PANTHER website **(Figure 38)**. To conduct this analysis, we used protein fold changes, independently of the statistical significance, comparing TG versus WT rats at 4, 10'5 and 16'5 months of age, considering both sexes together and independently.

At 4 months of age, analysing both sexes together, protein changes were not significantly clustered in any of the Panther annotations. However, significant results were obtained considering data from female and male separately. In females, 118 proteins were clustered into Panther GO-Slim Biological Process, all of them grouped in 1 cellular pathway. In males, 1980 proteins represented GO-Slim Cellular Components (50 %), GO-Slim Molecular Function (26%), GO-Slim Biological Process (22 %) and Panther Pathways (1 %), all related to 35 pathways.

Referring to changes at 10'5 months, 1857 proteins were categorized into GO-Slim Molecular Function (53 %), GO-Slim Cellular Components (23 %), Reactome Pathways (23 %) and Panther Pathways (1 %), corresponding to 42 pathways. However, total number of proteins and functional annotations decreased considering females alone. In this case, 706 proteins were grouped into Reactome Pathways (90 %) and GO-Slim Cellular Components (10 %) that were clustered into 18 pathways. Conversely, a huge number of proteins (4807) were categorized in males, corresponding to GO-Slim Biological Process (50 %), GO-Slim Cellular Components (25 %), GO-Slim Molecular Function (17%) and Reactome pathways (4%), all related to 68 pathways.

Finally, examining changes at 16'5 months, 403 proteins were significantly clustered into GO-Slim Molecular Function, where 1 cellular pathway was involved. Noteworthy, this group was lost considering only data from female rats. In the case of males, 643 proteins were categorized to GO-Slim Molecular Function (97%), but also to Reactome Pathways (3%). These functional annotations included 5 cellular pathways.

Taken together, the enrichment analysis performed by the Panther tools categorized functional annotations related to protein changes during the course of TgF344-AD rats' disease. As previously observed in western blotting and Volcano plots investigations, the number of protein changes varied in a sex-dependent manner. At early stages (4 months), most protein changes occurred in males, clustered into different functional annotations, whereas female variations were only categorized to biological processes. Later, after Aβ deposition (10'5 months), we observed a bigger number of protein changes that corresponded to several functional annotations. Finally, at later stages (16'5 months), proteins differentially expressed in

TG rats were predominantly associated with molecular functions, especially analysing male data or considering both sexes together.

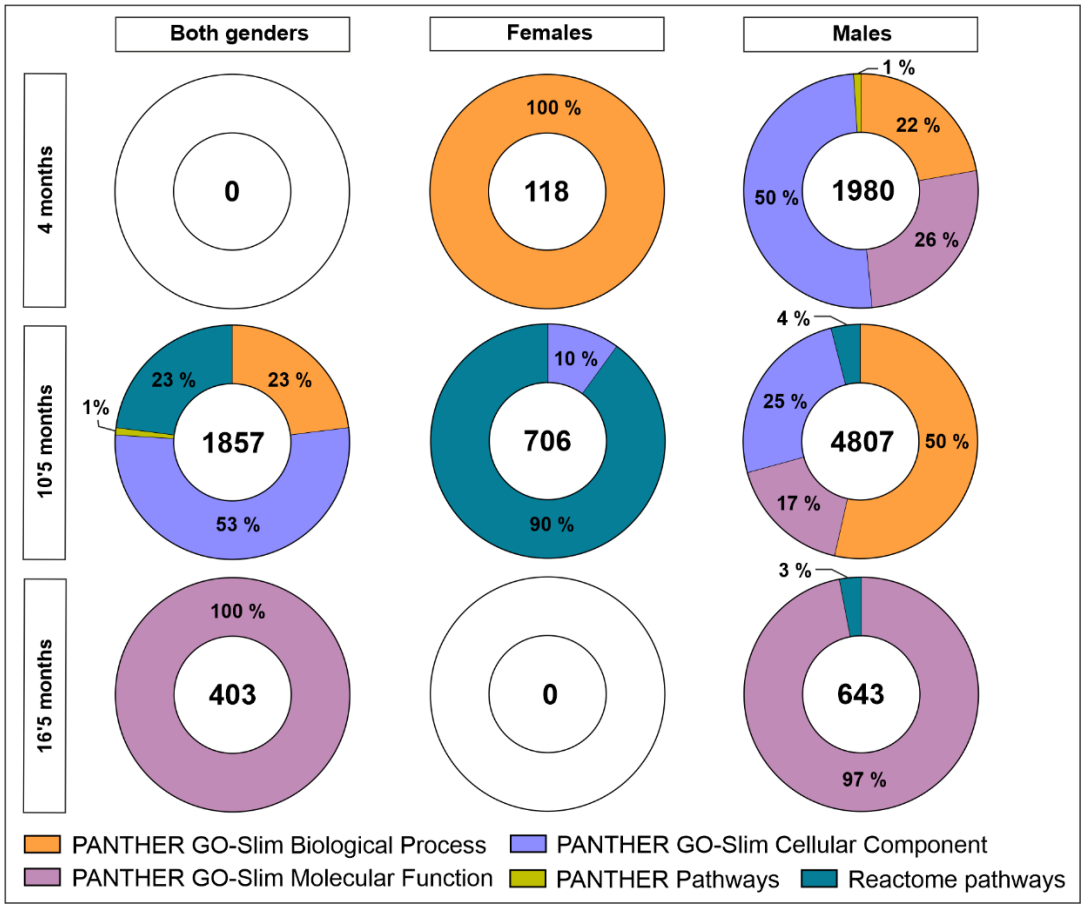

Figure 38. Functional enrichment analysis of variations in the CSF from TgF344-AD rats according to PANTHER classification. Donut charts showing functional annotations of the protein changes in the CSF of TG versus WT female and male rats (considering both sexes together or separately) at 4, 10'5 and 16'5 months of age. Charts show the proportion of proteins categorized in each functional annotation. Total number of protein variations is indicated in the centre of the graph.

Next, we focused on the most relevant biological pathways associated with protein changes **(Table 3)**. At 4 months, protein variations in the CSF of female TgF344-AD rats were associated only to an immune response. Instead, most relevant biological pathways in TG males corresponded to regulation of metabolic processes and cytoskeleton organization. At 10'5 months, protein changes analysing both sexes together represented glycolytic processes, ATP metabolic processes, glycolysis, detoxification of reactive oxygen species and apoptosis. However, in females the most relevant pathway was the classical antibody-mediated complement activation. In males, protein changes were related to cell adhesion, metabolic processes and glycolysis. Finally, at 16'5 months, the most relevant biological pathway linked to protein changes in CSF from TgF344-AD rats corresponded to catalytic activity, as observed analysing both sexes together or only in male samples.

Therefore, prior to Aβ deposition (4 months), proteins differentially expressed in the CSF of female rats participated in the immune response. However, in males most biological pathways represented metabolic processes and cytoskeleton organization. After appearance of Aβ plaques, variations in female CSF samples were related to immunological processes, where in males or considering both sexes together, the most important biological pathways included metabolic processes and apoptosis. At later stages, the major molecular function annotated was catalytic activity.

4 months

	GO Annotation	Pathway	Proteins	Raw p-value	FDR
F+M	-	-	-	-	-
F	**GO-Slim Biological Process**	**Immune response** (GO:0006955)	118 (Trem1, Adam15, C4a, Mog)	2.23E-05	3.80E-02
M	**GO-Slim Biological Process**	**Regulation of protein metabolic process** (GO:0051246)	48 (Cycs, Inava, Serpina4, Trem2)	3.16E-04	4.13E-02
		Cytoskeleton organization (GO:0007010)	52 (Marcks, Tpm1, Tpm3, Tpm4, Gsn)	3.60E-04	4.37E-02

10'5 months

	GO Annotation	Pathway	Proteins	Raw p-value	FDR
F+M	**GO-Slim Biological Process**	**Glycolytic process** (GO:0006096)	10 (Aldoa)	1.21E-04	3.03E-02
		ATP metabolic process (GO:0046034)	10 (Aldoa, Cycs)	2.14E-04	2.67E-02
	PANTHER Pathways	**Glycolysis** (P00024)	12 (Aldoa)	1.45E-04	1.57E-02
	Reactome pathways	**Detoxification of Reactive Oxygen Species** (R-RNO-3299685)	16 (Cycs, Sod1)	3.45E-04	2.97E-02
		Intrinsic Pathway for Apoptosis (R-RNO-109606)	7 (Cycs)	4.27E-04	3.17E-02
F	**Reactome pathways**	**Classical antibody-mediated complement activation** (R-RNO-173623)	39 (C1qa, C1qb)	6.52E-06	7.08E-03
M	**GO-Slim Biological Process**	**Cell adhesion** (GO:0007155)	71 (Nfasc, Robo1, Nrcam, Nlgn2, Cntn1, Cdh5)	4.48E-06	3.82E-03
		Metabolic process (GO:0008152)	442 (Adam10, Apoe, Capn12, Cycs, Lamp2, Lgmn, Sp110)	1.40E-04	1.99E-02
	Reactome pathways	**Glycolysis** (R-RNO-70171)	14 (Aldoa)	1.44E-06	3.95E-04

16'5 months

	GO Annotation	Pathway	Proteins	Raw p-value	FDR
F+M	**GO-Slim Molecular Function**	**Catalytic activity** (GO:0003824)	403 (Camk2a, Cflar, Epha7, F2, Naxe, Pigo)	3.12E-05	1.28E-02
F	**-**	-	-	-	-
M	**GO-Slim Molecular Function**	**Catalytic activity** (GO:0003824)	371 (Adam10, Camk2a, Epha7, Lgmn)	1.86E-05	7.47E-03

Table 3. List of relevant pathways associated with protein changes in the CSF of female and male TgF344-AD rats at 4, 10'5 and 16'5 months of age. Data were obtained performing functional enrichment analysis by the PANTHER tools. Biological pathways are associated with GO annotation and with total number of protein changes in each pathway. Additionally, some examples are indicated.

In order to identify pathways of relevance to the pathology of TgF344-AD rats, we next performed pathway analysis accounting for protein-protein interactions using pathfindR. The pathways associated with the differentially expressed proteins (adjusted p-value < 0.05) were analyzed by an active subnetwork enrichment analysis approach using the corresponding genes of those proteins. Top-10 ranked pathways and interactions between proteins in the datasets of rat samples from 10'5 months and 16'5 months are presented in **Figure 39** and **Figure 40**, respectively.

Endoplasmic reticulum lumen was the only significant pathway observed in CSF from TG rats at 4 months of age, obtained analysing only male data (data not shown). However, significant pathways were increased at 10'5 and 16'5 months. A total of 21 enriched terms were identified in TG rats from 10'5 months of age (12 considering both sexes, 8 only in female samples, 10 in male samples). Considering data from both sexes, most significant pathways included astrocyte and microglial activation, regulation of peptidyl-tyrosine phosphorylation and learning or memory, which were related to APP gene. In addition, positive regulation of stress fiber assembly and cellular response to reactive oxygen species were associated to TPM1 gene.

Analysing data in a sex-dependent manner, we obtained different enriched pathways, although significant results did not differ in female data respect to male data. APP gene was found to be related to amyloid fibril and formation, dendritic spine and trans-Golgi Network Vesicle Budding, whereas TPM1 was linked to positive regulation of stress fiber assembly but also to positive regulation of ATPase activity and cytoskeleton. Additionally, other distinguished genes included BASP1 (related to cytoskeleton and to RHOF GTPase cycle in male data), PFN2 (positive regulation of ATPase activity and positive regulation of stress fiber assembly) and SEMA7A (other semaphorin interactions).

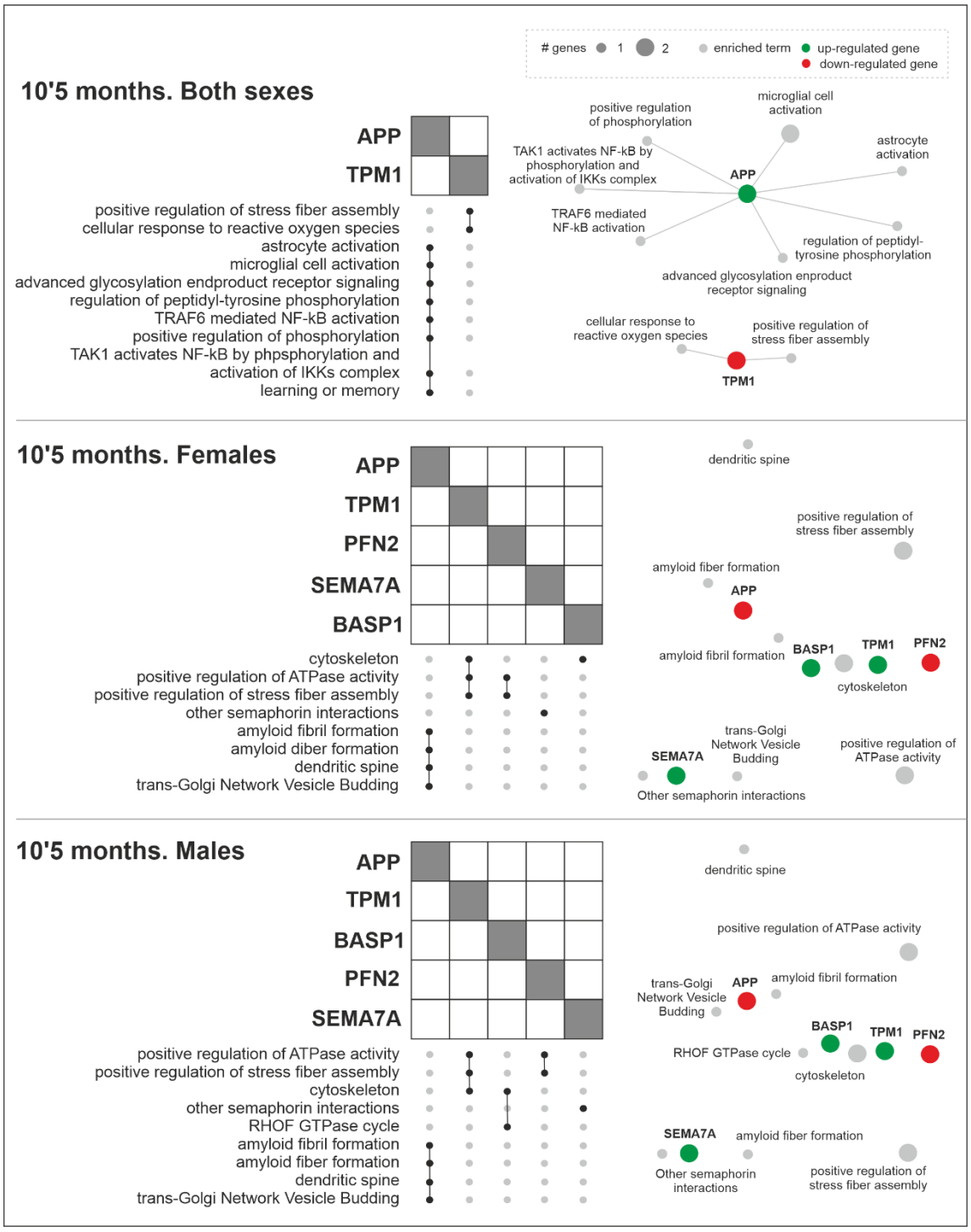

Figure 39. Enrichment analysis of significant protein changes in the CSF from 10'5-month-old TgF344-AD rats by pathfindR. Ranked pathway analysis via active subnetworks and protein interactions were determined in the CSF of TgF344-AD rats from 10'5 months of age considering both sexes together and separately. Left: upset plots indicate top-10 enriched terms in association with specific genes. Right: Network plot represents up-regulated (green) and down-regulated genes (red), and node size of the pathway terms represent the number of input genes implicated in the pathway.

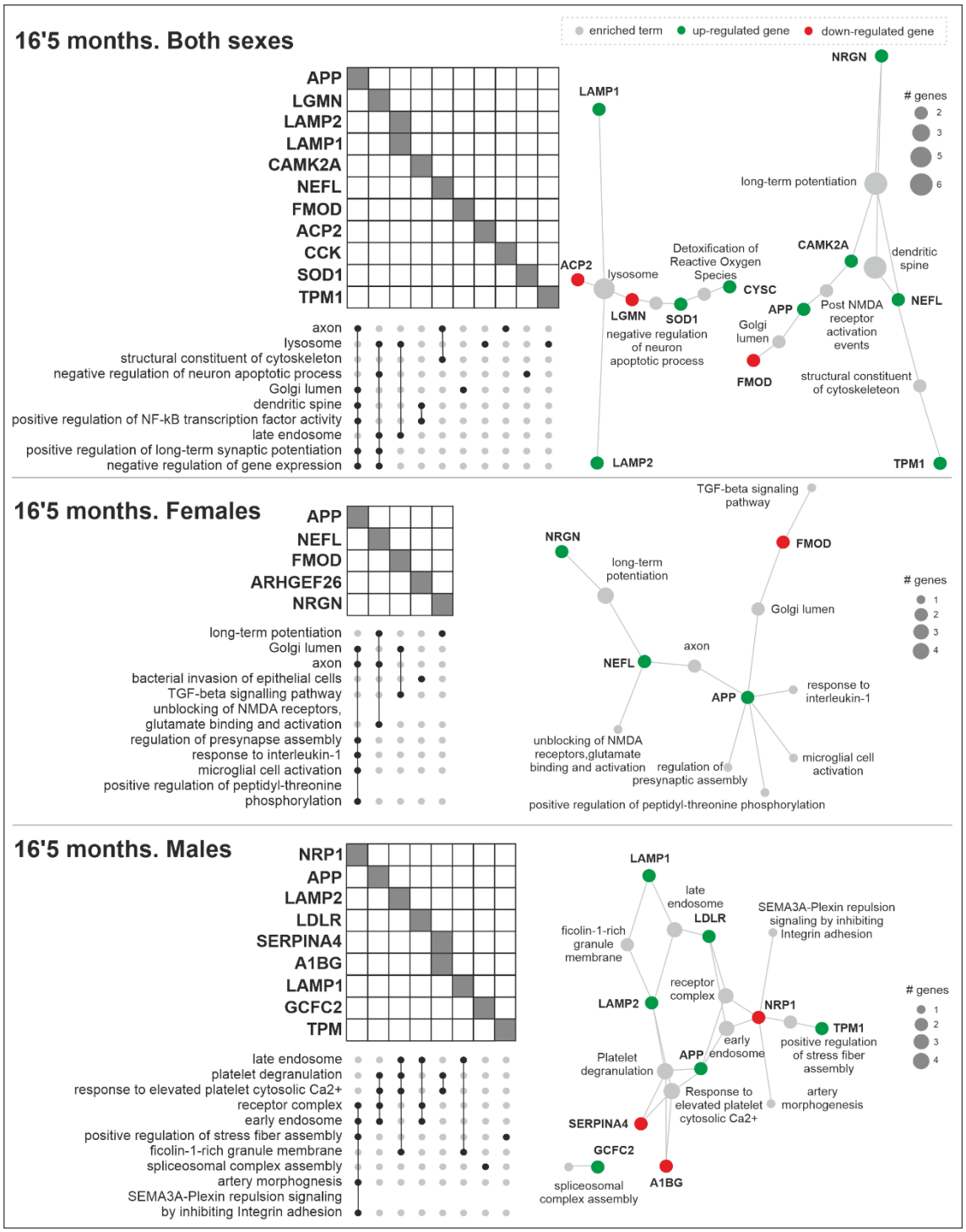

Figure 40. Enrichment analysis of significant protein changes in the CSF from 16'5-month-old TgF344-AD rats by pathfindR. Ranked pathway analysis via active subnetworks and protein interactions were determined in the CSF of TgF344-AD rats from 16'5 months of age considering both sexes together and separately. Left: upset plots indicate top-10 enriched terms in association with specific genes. Right: Network plot represents up-regulated (green) and down-regulated genes (red) and node size of the pathway terms represent the number of input genes implicated in the pathway.

In 16-month-old rats, a greater number of enriched terms were found to be involved in the pathology (a total of 94 which corresponded to 67 in both sexes, 11 in females and 42 in males). In both sexes, top-10 enriched terms were also associated to APP gene (axon, Golgi lumen, dendritic spine, positive regulation of NF-kappaB transcription factor and long-term synaptic potentiation) and TPM1 (cytoskeleton). Noteworthy, we additionally obtained enriched terms such as lysosome, negative regulation of neuron apoptotic process or late endosome that were linked to LGMN, LAMP1, LAMP2, ACP2, CCK and SOD1. Moreover, CAMK2A, NEFL and FMOD were linked to pathways previously mentioned for APP or TPM1.

Analysing both sexes separately, female data were associated with a considerably smaller number of enriched terms. The most significant pathway included Golgi lumen, axon, regulation of presynapse assembly, long-term potentiation and other relevant terms that were associated with APP, NEFL, FMOD, ARHGEF26 and NRGN. In contrast, the enrichment analysis in males revealed a larger number of significant pathways that included early and late endosome, integrin adhesion or spliceosomal complex assembly which were connected to genes such as APP, TPM1, NRP1, LAMP1, LAMP2, LDLR, SERPINA4, A1BG and GCFC2.

Therefore, the active-subnetwork-oriented enrichment analysis approach of pathfindR showed a list of ranked pathways particularly relevant in TgF344-AD rats from 10'5 and 16'5 months of age. Remarkably, enriched terms were considerably different using data from both sexes and from female and male separately. In addition, genes associated with significant pathways at 16'5 months also followed a sex-dependent deviation.

In summary, results obtained analysing brain and CSF samples from TgF344-AD by different techniques revealed that APP and PSEN mutations trigger a pathological profile that differs somewhat in each sex. Several biological processes such as glia-neuron communication, neuronal assembly, memory pathways or neuroinflammation were altered in this rat model, some of them robustly observed at early stages. Those changes are to a certain degree comparable to human alterations in Alzheimer's disease patients. Hence, we suggest that TgF344-AD rats act as a suitable model to investigate potential biomarkers which could have clinical value for monitoring disease progression and for pre-clinical AD trials.

DISCUSSION

DISCUSSION

This study characterizes the peptidergic secretory pathway in the physiology of the central nervous system and in Alzheimer's disease pathology. For the first time, we determined the temporal acquisition of peptidergic regulated secretion in developing neurons of the cerebral cortex *in situ* and *in vitro*. DCV markers exhibited an early non-conventional secretion that switched over the mature phenotype in a heterogeneous period according to vesicle subpopulations, which occurred in parallel to the decline of SytIV. In the mature brain, astroglial cells physiologically contribute to synaptic transmission. Here, we developed AAV encoding DCV-stored ANP fused with green fluorescent tags to evaluate how astrocyte release peptidergic vesicles in the environment of cortical neural networks by pharmacological and live-imaging methods. In response to neuronal activity, DCV-like in cortical astrocytes *in vitro* and, presumably, *in situ* were exocytosed strictly dependent on extracellular Ca^{2+} and probably mediated by NMDA receptor signalling.

Synapse dysfunction and loss is an early event in AD neuropathology which occur prior to neuronal death and precedes the onset of symptoms. Most efforts are now focused on identifying prognostic biomarkers to assess disease progression. This study describes the protein changes in brain and CSF associated with amyloid pathology in TgF344-AD rats. Additionally, we provide a wide spectrum of protein deviations characterizing the CSF proteome of this AD rat model. Interestingly, secretory proteins and other synaptic components involved in several biological processes such as glia-neuron communication, neuronal assembly, memory pathways or neuroinflammation were altered in TgF344-AD, even prior to Aβ deposition, relevant for pre-clinical AD research.

Developmental acquisition of peptidergic secretion in cortical neurons

To our knowledge, there is only one study that investigates the maturation of the peptidergic regulated secretory pathway (Emperador Melero et al., 2017). This work analyzed the regulated secretion of SV and DCV in micro-networks of human iPSC-derived neurons. Interestingly, they suggest that secretion efficiency of the two secretory pathways exhibit different maturation processes. However, these results were obtained in culture conditions of cells which has been genetically modified. Thus, more investigations are needed to establish the maturation of regulated secretory pathways in the physiology of the central nervous system. Understanding the peptidergic secretory phenotype is of particular interest considering that DCV-stored peptidergic transmitters represent by far the largest and most diverse group of chemical signals in the brain playing essential roles in neuronal circuit development and function (Hökfelt et al., 2000; Merighi et al., 2011). Here, we determined the temporal acquisition of peptidergic regulated secretion in cortical developing neurons *in vitro*, but also *in situ*.

To examine peptidergic vesicles secretory profile, we mainly evaluated levels of SgIII, CPE and PC1/3, the molecular machinery of DCV involved in the sorting and processing of peptide hormones and neuropeptides. In the mature brain, neurons release DCV in a regulated-dependent fashion as a result of a massive Ca^{2+} influx (Brion et al., 1992; Burgoyne & Morgan, 2003). However, a surprising result in our data from developing cortical neurons *in situ*, was that the release of PC1/3 was dramatically reduced under stimulating conditions compared to basal secretion until the first

postnatal week, where a switch in the secretory dynamics elicited the classical regulated secretion. Additionally, hippocampal cultured neurons, which achieve more immature stages, CPE also exhibited a non-conventional release at early stages (3-5 DIV). Progressively, the release pattern was adjusted over the mature phenotype, evidenced at 12-15 DIV for PC1/3, at 10-11 DIV for CPE and at 8-9 DIV for SgIII.

In differentiated neurons, the key messenger that trigger SV and DCV exocytosis is the elevation of the cytosolic calcium concentration in response to the arrival of the action potential. Thus, we examined the role of extracellular calcium in the developmental secretory profile of peptidergic vesicles. KCl-depolarization in a nominally Ca^{2+}-free medium (0 mM $[Ca^{2+}]_0$) did not shift the early evoked reduction. Again, cortical neurons diminished CPE and PC1/3 secretion in stimulating conditions at early development. In this way, the early secretory dynamic seemed independent of extracellular calcium. However, forcing Ca^{2+} entry by exposure to ionomycin robustly reduced DCV secretion, giving intracellular calcium elevation a major role in early diminished secretion. We suggest that small amounts of calcium that may remained unchelated in the experiments carried out with a calcium-free medium could be sufficient to trigger the non-conventional release. Small calcium influx could promotes the release of calcium from intracellular stores, that have been described to be more sensitive to calcium oscillations at early stages of maturation, which facilitates neuronal migration and differentiation (Hollliday et al., 1991; Platel et al., 2008; Spitzer, 1994). Moreover, elevations of intracellular calcium are shown to last for long periods of time in undifferentiated cells (Gu et al., 1994). Therefore, we propose that calcium must be influencing in some way the mode of VCD release at early stages.

The frequency of spikes in neurons has been described to follow a developmental regulation, exhibiting high frequency in the soma, which decreases with time in cell cultures (Spitzer, 1994). Calcium oscillations in the soma may have a particular impact on the release of DCV, as exocytosis of these organelles have been described in the perisynaptic membrane of axonal boutons, but also in dendrites and soma (Ludwig & Leng, 2006; Thureson-Klein & Klein, 1990; van den Pol, 2012). Previous studies determined that, although peptidergic vesicles are widely distributed throughout the neuronal cell body and processes, they preferentially fuse at axons (Persoon et al., 2018). However, these results were obtained from differentiated neurons. In this study, we have described that DCV subpopulations only colocalized with SV2-containing presynaptic terminals in the mature brain. By contrast, they were variable distributed in the subcellular domains at early stages of development, where they could be more sensitive to changes in intracellular calcium levels causing non-expected secretion patterns. Moreover, the heterogeneity of peptidergic vesicles demonstrated *in situ* and *in vitro*, similar to previous investigations (Landry et al., 2003; Plá et al., 2013), probably favors particular vesicle subpopulations to be more sensitive to certain secretory patterns. In addition, we support that this developmental acquisition of regulated secretion is specific for DCV, as it was not observed evaluating the release of SV, in accordance with previous studies (Andreae et al., 2012). Of note, SV exclusively fuse at the presynaptic active zone (Südhof, 2004).

SytIV as a potential mediator in maturation of peptidergic regulated secretion

The core of DCV vesicular machinery in mammalian neurons involved in exocytosis includes VAMP2, SNAP25, SNAP47, Munc18-1, syntaxin1, SytVI and SytIV (Arora et al., 2017; Hoogstraaten et al., 2020; Puntman et al., 2021; Shimojo et al., 2015; Wong et al., 2015). Synaptotagmins act most likely as calcium sensors controlling calcium-dependent exocytosis of secretory vesicles (Fukuda, 2007; Mori and Fukuda, 2011). Synaptic function of SytI has been well-established, which mainly mediates synchronous neurotransmitter release (Geppert, et al., 1994; Mori & Fukuda, 2011). By contrast, the role of SytIV caused some discrepancies in the literature. However, mammalian SytIV has been interestingly associated to negatively regulate calcium-dependent exocytosis. This effect has been observed for BDNF secretion in axons and dendrites (Dean et al., 2009; López-Benito et al., 2018), for oxytocin release in hypothalamic neurons (Zhang et al., 2011) and for insulin secretion in mature β cells (Huang et al., 2018).

In our study, we show that levels of SytIV are regulated during brain development, exhibiting higher expression during the first postnatal week which then decline, consistent with previous results from the nervous system (Berton et al., 1997, 2000), but in contrast with developmental expression in β cells (Huang et al., 2018). In our results, a dramatic reduction of SytIV from 4 DIV to 11 DIV was clearly evidenced in our hippocampal cell lysates. In this way, the developmental profile of SytIV perfectly matched with the switch of peptidergic regulated dynamics in some DV subpopulations: when DCV evoked secretion was restrained, SytIV exhibited higher levels, and when there was a switch to the classical regulated secretion, SytIV levels dropped. These data encouraged us to investigate whether there was a relationship in vesicle subpopulations containing SytIV and determined DCV markers. From colocalization analyses in cortical cultured neurons, we concluded that at early stages (4 DIV), SytIV was more associated with PC1/3 and CPE than with SgIII, at the same moment that PC1/3 and CPE displayed an evoked reduction during depolarization. By contrast, colocalization was poorly observed at mature stages, where all DCV subpopulations acquired the mature phenotype. For SV, whose secretory dynamic has been studied for several decades, specific pools of SV have been proposed to follow different secretory dynamics apparently depending on the molecular identity of membrane proteins, such as SNAREs (Raingo et al., 2012; Ramirez et al., 2012; Takamori et al., 2000). Therefore, in the case of DCV, SytIV, differently abundant in some vesicle subpopulations, could be mediating the acquisition of a mature regulated secretion.

Taken together, we suggest that release of heterogenous DCV subpopulations could be regulated in early neuronal development by synaptotagmin-IV, which determines the temporal acquisition of peptidergic regulated secretion, established for all DCV markers after the first postnatal week in cortical neurons *in situ*. Opposed to these results, investigations revealed a major role of SytIV in mature β-pancreatic cells, reducing the number of readily releasable vesicles (Huang et al., 2018). Therefore, although the secretory granules in brain and β-pancreatic cells contain a similar molecular machinery, they play key roles at different developmental stages. Refinement of projections in the cerebral cortex is established during the final days of the prenatal period (de Carlos & O'leary, 1992). In this way, DCV subpopulations may be particularly relevant in the early development ensuring the sorting, processing and release of peptidergic transmitters playing crucial roles during critical points as cell motility, neurite outgrowth, synaptogenesis or neuronal differentiation (Emerit et al., 1992; Johnston & Coyle, 1981; Lauder, 1993; Shuey et al., 1993).

Neuronal activity triggers astroglial DCV-like exocytosis in physiological neuro-glial networks

Astroglial cells are intimately involved in synaptic transmission, as they sense neuronal activity, triggering the release of transmitters that causes feedback influencing neuronal activity and synaptic strength (Halassa & Haydon, 2009; Jordain et al., 2007; Perea et al., 2009). To date, most studies evaluated the synaptic contribution of glial glutamate, stored in SLMVs, which is assumed that is release in a calcium-dependent manner (Araque et al., 2000). However, the mechanisms of astrocytic peptidergic secretion and its relevance in synaptic networks has been determined to a lesser extent. Of note, the existing studies were performed in astrocytic mono-cultures (Krzan et al., 2003; Paco et al., 2009), which exhibit a morphology, molecular composition, and physiology far away from *in vivo* conditions.

DCV in astrocytes contain similar components as peptidergic vesicles in neurons, exhibiting members of the molecular machinery of DCV, such as secretogranin II, secretogranin III and CPE (Calegari et al., 1999; Klein & Fricker, 1992; Paco et al., 2009, 2010; Plá et al., 2017) and peptidergic transmitters as NPY and ANP (Kreft et al., 2004; Paco et al., 2009; Ramamoorthy & Whim, 2008; Zafra et al., 1992). In this way, it remains a challenge to investigate dynamics of endogenous components of DCV specifically in each cell-type in experimental conditions which include both neurons and astrocytes, the basic scenario of brain network. In the present study, we developed AAVs encoding ANP, a diuretic vasorelaxant hormone having major roles in cerebral blood regulation (McKenzie et al., 2001). To specifically evaluate astrocytic peptidergic secretion, we generated an AAV where ANP expression was controlled by GFAP promoter. In addition, we developed a Cre-dependent construct which we combined with a Cre-recombinase expressed under hSyn promoter for ensuring ANP expression in neurons as a hallmark for regulated secretion. In both cases, the exogenous protein can be monitored by two fluorescent tags: EGFP and pHluorin. From *in vitro* and *in situ* experiments we conclude that: (i) adeno-associated vectors expressing ANP follow the cell-type-specific targeting; (ii) exogenous ANP is directed to vesicles that primarily contain SgII, in agreement with previous studies using the construct ANP.emd (Paco et al., 2009); (iii) vesicles containing fused ANP are properly exocytosed in neurons, following the classical regulated secretory pattern, evidenced by pharmacological and live-cell imaging methods. Therefore, our AAVs acted as suitable tools to examine astrocytic peptidergic secretion in comparison with the neuronal secretory profile.

In previous studies from pure astroglial cultures, ANP.emd was observed to be released by regulated calcium-dependent exocytosis (Krzan et al., 2003; Paco et al., 2009). We supported this secretory profile in our glial mono-cultures by pharmacological and live-cell imaging methods However, astrocytes alone in culture exhibit a non-fully differentiated phenotype (Kettenmann & Ransom, 2005). Therefore, we improved experimental conditions performing secretory experiments in astrocytes and neuronal co-cultures, where astrocytes vary their gene expression profile exhibiting an *in vivo*-like phenotype induced by synaptic activity (Hasel et al., 2017). We demonstrated that neuronal stimulation achieved by pharmacological and optogenetic methods and evaluated by western blotting and confocal live-cell imaging triggered astrocytic ANP regulated secretion.

However, the evoked secretion was elicited to a lesser degree compared with the neuronal secretory profile, suggesting that mechanisms that trigger astrocyte regulated secretion are more limited comparing to those in neurons, even though astrocytes translate extracellular signals to intracellular Ca^{2+} codes and release gliotransmitters via SNARE mechanisms (Araque et al., 2000; Verkhratsky et al., 2016). One of the critical tools by which astrocytes release peptidergic transmitters are neurotransmitter receptors placed on astrocytic cell membrane (Verkhratsky & Nedergaard, 2018). Here we show that secretion of peptidergic vesicles in astrocytic into neural networks could be to a greater extent mediated by NMDAR signalling, as release of fused-ANP was ANP is largely blocked by APV. In contrast to other glutamate receptors, NMDAR has been relatively less explored. Although first investigations failed to establish the presence of functional NMDA receptors on astrocytes, glutamate-mediated responses have been carefully recorded (Lalo et al., 2006; Schipke et al., 2001; Skowrońska et al., 2019), and here we propose that this receptor could play a key role in astrocyte peptidergic secretion.

Results obtained in co-cultures of neurons and astrocytes prompted us to monitor astrocytic peptidergic secretion even in a more physiological context. By injecting AAV in mouse hippocampi, we evaluated astrocytic ANP dynamics *in vivo*. After three weeks post-injection, hippocampal astrocytes exposed to LPS for 24 h successfully expressed fused-ANP. LPS crosses the blood-brain barrier and mediate inflammatory responses (Banks & Robinson, 2010), increasing GFAP expression (Brahmachari et al., 2006) which, in turn, enhanced exogenous ANP production. Interestingly, in our model, ANP successfully reached the CSF and blood. Although the majority of CSF is produced by the choroid plexus, the capillary-astrocyte complex in the blood-brain barrier actively produces interstitial fluid, closely related to CSF composition (Abbott, 2004; Cserr, 1988; Johanson et al., 2008). Moreover, astrocyte end-feet surround microvessels, which make them key elements for information transfer to microcirculation (Abbott et al., 2006; Anderson & Nedergaard, 2003). Therefore, our results support the functional gliovascular unit.

For the first time, we evaluated glial peptidergic secretory dynamics *in situ*: in acute brain slices of injected mice. Clearly, in the neuroinflammatory-induced model, astrocytic ANP increased after neuronal depolarization and after Ca^{2+} influx provoked by exposure to ionomycin. It has been previously demonstrated that neuronal activity increases intracellular calcium concentration in astrocytes (J.Kang et al., 1998; Perea et al., 2009; Porter & Mccarthy, 1996). Our preliminar data provide relevant results adding that, in response to this elevated $[Ca^{2+}]_i$, astrocytes *in situ* are able to release peptidergic vesicles containing ANP. Secretory experiments performed in acute brain slices were analyzed by western blotting procedures. Nevertheless, our adeno-associated vectors provide a key tool to monitor vesicular dynamics by confocal and high-resolution two-photon microscopy. After numerous attempts, several technical limitations prevented us to obtain valuable conclusions. Much evidence supports that astrocytes *in situ* express neurotransmitter receptors and respond to synaptic activity increasing intracellular calcium concentrations. Therefore, although some studies questions whether astrocytic stimulation affects neuronal activity (Fiacco et al., 2007), other investigations support that astroglial cells controls synaptic activity and plasticity (Henneberger et al., 2010; Jourdain et al., 2007; Navarrete et al., 2012; Navarrete & Araque, 2010; Panatier et al., 2006; Perea & Araque, 2007). Hence, our results, in addition to future investigations, address key issues in neuronal-astrocytic network relevant for brain physiology.

Protein changes associated with Alzheimer's disease pathology in the brain and CSF of TgF344-AD rats

Central nervous system insults, including Alzheimer's disease, cause dysfunctional molecular mechanisms that lead to a defective cellular communication network. Pathogenesis of AD is associated with synaptic dysfunction and loss, an early feature which strongly correlate with cognitive impairment (Forner et al., 2017; Terry et al., 1991). Most efforts are currently focused on identifying prodromal biomarkers for an early intervention of the disease (Lleó et al., 2019). In this context, the use of animal models is relevant for deconstructing pathological mechanisms underlying the disease and for addressing intervention strategies.

To our knowledge, the present study is the first that extensively characterize the secretory proteins in brain and CSF of male and female TgF344-AD rats before Aβ deposition (4 months), after Aβ deposits (10'5 months) and at later stages of life and disease (16'5 months), focusing on the influence of sex and genotype over the course of rat's lifetime. This transgenic model only express mutant APP and PS1 but remarkably recapitulates almost the whole spectrum of Alzheimer's neuropathology, including age-dependent accumulation of amyloid plaques, emerging neuritic dystrophies, tau pathology, gliosis, neuronal loss and cognitive impairment (Cohen et al., 2013), although some aspects are undergoing further testing. This complete phenotype, together with the genetical and behavioural features which place them closer to humans (Ellenbroek & Youn, 2016), make TgF344-AD rats particularly relevant for AD research, in contrast to mouse models which display a limited continuum model of the disease (Borchelt et al., 1996; Games et al., 1995; Oakley et al., 2006).

As synaptic dysfunction has been proposed as an early event preceding neuronal damage and symptoms onset, in this study we evaluated the peptidergic secretory pathway and other secretory components in the brain and CSF of this rat transgenic model. CSF clearly represents the composition of the extracellular fluid in the central nervous system (Johanson et al., 2008), so in conjunction with molecular brain imaging, it conforms a key fluid for identifying synaptic dysfunction. In mice, the volume of CSF collected is limited, so drawing conclusions from these models is challenging. Instead, the rat model has a great advantage: they have larger volume amenable to replicate sampling (Barten et al., 2017). For this purpose, we optimized a protocol to efficiently collect a large amount of CSF samples in rats which were discarded in case of blood contamination. Our results show that DCV proteins and other secretory components are diversely altered in hippocampal homogenates and CSF samples from TgF344-AD rats, following a sex-dependent dysregulation. Interestingly, before Aβ deposition some neuronal DCV markers decreased in brain tissue (PC2 and CgA) and increased in CSF samples (CgA, PC1/3), especially in males.

Synaptic defects in the hippocampus have been classically related to changes in presynaptic proteins such as synaptophysin, whose reduction correlate with severity of AD pathology (Sze et al., 1997; Terry et al., 1991). Therefore, decreased intracellular content of synaptic proteins frequently represent synaptic and neuronal loss. In TgF344-AD rats, first studies evidenced a progressive neuronal loss in the hippocampus of rats from 16 and 26 months of age (Cohen et al., 2013),

supported by other studies where loss of neurons were observed in some regions of the hippocampus and the cortex at 18 months (Leplus et al., 2019) and others where it was shown in the hippocampus but not in the cortex at 24 months of age (Voorhees et al., 2018). In any case, this feature represents a phenotypic advantage compared to mouse transgenic models, which do not demonstrate a robust neuronal loss. Thus, our results of reduced secretory content in hippocampus homogenates and an increase in the CSF could reflect the neuronal damage occurring as early as 4 months of age. At later stages after Aβ deposition, PC2 and CgA decreased, whereas in females transgenic rats PC2 robustly increased. Those differences were evidenced in hippocampal tissue, but which did not alter the CSF composition. In fact, intracellular differences might not always be substantiated in CSF samples. Impaired peripheral lymphatic function could influence CSF outflow, which has been previously reported for mouse models of AD (Kwon et al., 2019), but not yet for TgF344-AD rats. However, alterations to blood-brain barrier water permeability were demonstrated in transgenic rats aged 13 months or older. In this way, a huge number of proteins abundantly contained in plasma may interfere CSF composition.

In humans, we recently reported an increase of PC2 precursor form in the parietal cortex and, more notably, in the hippocampus of AD patients (Barranco et al., 2021). An accumulation of the precursor form could imply a reduction of mature form, as observed in our samples. Barranco et al. also reported deposits of DCV cargoes, including PC2, in granulovacuolar degeneration bodies. Although we did not successfully label similar structures in TgF344-AD animals, female rats at 16'5 months when PC2 exhibited an increase in hippocampal homogenates could be more likely associated with the accumulation of soluble components such as PC2 in neuronal projections. Nevertheless, we cannot exclude that certain changes may be associated with post-transcriptional modifications. Regarding the CSF content, some discrepancies were obtained in analyses from human samples, but most studies also reported a reduction of different DCV cargoes in AD condition, including CgA, PC2 and PC1/3 (Barranco et al., 2021; Brinkmalm et al., 2018; Camporesi et al., 2020; Pedrero-Prieto et al., 2020).

Interestingly, our results showing secretory proteins dysregulation prior to Aβ deposition (4 months), provide an encouraging picture in the search for early biomarkers. Although there is no evidence for neuronal loss at early stages, decreased secretory components, robustly marked in male rats, could imply reduce functioning of DCVs and other secretory components basic for synaptic function, which could predict synaptic loss. This is supported by recent investigations where TgF344-AD rats from 4 months displayed cognitive disturbance, with impairments in long-term spatial reference memory (Fowler et al., 2022; Proskauer Pena et al., 2021). Soon after, at the age of 5-6 months, others reported disruption in hippocampal connectivity, dysfunction of the noradrenergic system and loss of connectivity before significant Aβ deposition (Anckaerts et al., 2019; Muñoz-Moreno et al., 2018; Stoiljkovic et al., 2019).

CysC in male transgenic rats from 4 months was also diminished in hippocampal tissue, in a similar manner than PC2. However, differences in the levels of CysC progressively disappeared, even tended to increase at 16'5 months, where CSF analyses evidenced an increase. Although we did not report any changes in the levels of CysC from human AD brains (Barranco et al., 2021), others evidenced an increased (Deng et al., 2001; Levy et al., 2001). In fact, CysC, which favours proteolytic elimination of autophagy products by lysosomes (Tizon et al., 2010), has been observed in close

association with amyloid deposits in the brain, playing a protective role against neurodegeneration (Nixon, 2013). Moreover, CysC is also contained in the astrocytic compartments. Hence, their levels are expected to increase in parallel with activation of microglia and astrocytes, previously described in TgF344-AD rats after β-amyloid deposits (Cohen et al., 2013) and confirmed in our study. Therefore, early dysregulation of CysC could be masked at later stages by reactive gliosis. This process is supported by our findings showing a remarkable increase of apoE in female and male hippocampal homogenates from 10'5 and 16'5 months of age, expressed primarily in astroglial cells.

In our study, we evaluated secretory proteins in the CSF contained in astroglial cells (pSgIII, CysC and apoE), all displaying increased levels in transgenic animals but at different stages. Noteworthy, most notable increases occurred for apoE in males. ApoE, and specifically apoE4, the strongest genetic risk factor for AD in humans (Strittmatter et al., 1993), aggregates in amyloid plaques AD brain (Martens et al., 2022), also evidenced in section of our transgenic rats. Moreover, apoE influences amyloid-β and tau pathology and disrupts immunomodulating functions contributing to neurodegeneration (Parhizkar & Holtzman, 2022). Therefore, apoE could early influence pathogenesis in TgF344-AD rats as early as 4 months of age.

The results presented in this study support a synaptic alteration in TgF344-AD early in the disease. Protein changes that were more robustly observed in males than in females. Noteworthy, particular dysregulations were efficiently detected in CSF samples, a more suitable source for biomarker discovery than brain tissue. Hence, we employed a large-scale approach to further search for relevant CSF biomarkers related to AD neuropathology.

Pre-synaptic components are altered in the CSF of TgF344-AD rats

For the first time, we described sex and age-dependent alterations in the CSF proteome analyzed by MSqRob Shiny App using Variance Stabilizing Normalization. Although some protein changes differed considering samples from both sexes together or independently, in general terms, protein content in the CSF of TgF344-AD primarily exhibited a reduction at 4 and at 10'5 months, which culminated in a greater number of protein variations at 16'5 months, mostly corresponding to an upregulation. This protein profile occurred in a similar manner than proteomic analyses of the synaptic compartment performed in human samples, where preclinical stages of AD followed reduced levels that progressively switch to an increase (Lleó et al., 2019).

Highlighted proteins diversely altered during the course of disease in TgF344-AD rats comprised components concerning the cytoskeleton. Tpm1 is actin-associated protein involved in stabilising actin filaments and regulating the interaction with other actin binding proteins (Gunning et al., 2008). Tpm was first discovered in striated muscle (Bailey, 1946), where it regulates the interaction between actin and myosin in muscle contraction. However, several isoforms of TPM, including Tpm1, are found in the nervous system (Geeves et al., 2015). In neurons, Tpm is implicated in neurite outgrowth, branching and synapse formation. Particularly, some isoforms of Tpm1 are primarily found in the presynaptic and may have an important role regulating neurotransmitter release and recycling (Brettle et al., 2016). In AD pathology, Tpm was detected in the neurofibrillary tangles and proteomic data revealed that some Tpm1 and Tpm3 gene products were increased in the white matter of AD patients compared with controls (Castaño et al., 2013; Galloway et al., 1990). In our

results from the sex-dependent and independent analyses, Tpm1 in the CSF of transgenic rats was initially diminished (at 4 and 10'5 months) and then enhanced (at 16'5 months). Dysregulation in synaptic processes may retain some components resulting in reduced CSF levels. However, at later stages, the neuronal damage and loss may lead to increased concentrations. Additionally, the proteomic results analysed in a sex-independent manner, revealed that Tpm1 fold-changes were higher in females than in males, similar to other studies where proteomic AD platelet biomarker Tpm1 was enhanced only in females (Reumiller et al., 2018). Therefore, taking into account that incidence of AD is higher in women than in men, is important to highlight the sex-related influence of some biomarkers.

In this study, Basp1 exhibited alterations in the CSF from TgF344-AD rats in the same direction than Tpm1. In neurons, Basp1 is a membrane-associated protein located mainly in axon terminals (Widmer & Caroni, 1990), having important roles in neurodevelopment, synaptic function, and nerve regeneration (Chung et al., 2020; Mosevitsky, 2005). The CSF proteome of human AD samples compared to controls revealed an increase of Basp1 (Guerreiro et al., 2009). Our transgenic rats firstly showed a downregulation of Basp1 in CSF samples, probably reflecting earlier dysregulations, but at 16'5 months, Basp1 increased in the CSF from transgenic rats, strongly found in males alone. Interestingly, the sex-independent analysis revealed that enhanced Basp1 in males was accompanied by an increase in the levels of GAP-43 and Marcks. Noteworthy, the three components play synergic roles at the presynaptic compartment. GAP-43 and Basp1 together regulate actin dynamics, presynaptic vesicle cycling and neuronal plasticity processes, some of them counteracted with Marcks function (Chung et al., 2020; Mosevitsky, 2005). Of note, defects in axon guidance and synaptic plasticity are attributed to AD pathology (Lacor et al., 2004, 2007; Stokin & Goldstein, 2006), where GAP-43, Basp1 and Marcks could be clearly implicated. In fact, GAP-43 has been found to be significantly increased in the CSF of patients with AD (Sandelius et al., 2019; Sjögren et al., 2001) and reduced in cortical brain (Davidsson et al., 1998). In addition, Marcks has recently be associated with amyloid pathology, undergoing an upregulation in the CSF (Pedrero-Prieto et al., 2021).

Opposite to the presynaptic terminal, Nrgn is a calmodulin-binding substrate associated with the postsynaptic density that is involved in synaptic plasticity, crucial in learning and memory processes (Takeuchi et al., 2014; Watson et al., 1994). Levels of Nrgn in the CSF correlates with the severity of cognitive decline in the AD spectrum (Remnestål et al., 2016; Yoong et al., 2021). Thus, Nrgn has recently been considered as a potential biomarker to predict AD progression, in contrast with well-established biomarkers Aβ42, T-Tau and P-Tau. Elevated Nrgn in the CSF of AD patient are in line with our results, where TgF344-AD rats exhibited increased levels of Nrgn compared to WT littermates at 16'5 months, but considering both sexes together and only in females separately. In humans, although Nrgn has been found to increase in both female in male subjects, it was particularly higher in females with mild-cognitive impairment (Wang, 2019). Differences could be explained by hormonal mechanisms, having estrogen relevant roles in synapse formation and hippocampal function that could be a compromised target with the decline of estrogen in menopause (Mielke et al., 2014). Quantifying the intensity of neuronal injury is relevant for monitoring pathological processes. In detail, neurofilament light protein has been proposed as a biomarker of neuroaxonal damage (Bridel et al., 2019; Yuan & Nixon, 2021). Increased levels of Nf-L have been described in several neurodegenerative diseases, including Alzheimer's disease. Even at very early

stages, Nf-L is increased in AD pathology (Antonell et al., 2020). In our proteomic approach, we observed an upregulation of Nf-L in the CSF of transgenic rats at 16'5 months of age considering both sexes together and in females alone.

PANTHER and PathfindR analyses were performed to complement proteomic findings by recognizing common functional pathways that could be specifically associated to pathological events in TgF344-AD. According to these functional enrichment analyses, we identified a few pathways that play key roles from very early stages: immunological and metabolic processes, and cytoskeleton organizations, which were also relevant for advanced stages. The immunological response is one of the most important relevant biological processes involved in AD (Calabrò et al., 2021; Heneka, 2015). The environment accomplished in a neuroinflammatory context increases the severity of the AD disease intensifying Aβ and Tau pathologies (Zotova et al., 2010). Moreover, activation of the immune system causes, in turn, an increase of proinflammatory cytokines, those provoking damaging consequences such as the increase of oxidative stress (Calabrò et al., 2021), observed in the analysis of 10'5-month-old rats.

Ensuring a proper control of oxidative stress is relevant in brain physiology. In neurons, reduction oxidation signalling regulates cytoskeletal dynamics, cellular communication, and neuronal plasticity (Franco & Vargas, 2018; Muñoz et al., 2020; Quintanilla et al., 2012). These processes which are known to be impaired in AD are probably influenced by increased oxidative stress. Linked to this increase, a great number of mediators are concerned, including NF-κB (Chen et al., 2019), which appears to be positive regulated in our functional analyses. In addition, reactive oxygen species are also related to energy metabolism, indirectly regulating glucose dynamics (Calabrò et al., 2021). According to our functional approach, some metabolic processes, including glycolysis are featured in rat pathology.

Among the biological pathways behind AD pathology, dysregulation of autophagy is emerging as a relevant process in neurodegeneration (Llanos-González et al., 2020). Several factors such as increased oxidative stress and overexpression of apoE4 exacerbates lysosomal dysfunction, which is associated with cognitive deficits (Belinson et al., 2008; Ji et al., 2002). Moreover, increased oxidative stress is also involved in the inhibition of fusion events between autophagosomes and lysosomes (Llanos-González et al., 2020). Noteworthy, our results from proteomic and functional analyses revealed that lysosomal pathway played key roles in the rat amyloid pathology at later stages, being Legumain, Lamp1 and Lamp2 directly involved in this deregulation. Remarkably, Lamp1 and Lamp2 were upregulated in the CSF of TgF344-AD rats. At later stages of the disease, apoptosis was another relevant pathway compromised in our results. Indeed, increased oxidative stress also imbalance apoptotic processes, leading to neurodegeneration (Swerdlow & Khan, 2004). Further, Cytochrome c, which is directly involved with apoptosis (Putcha et al., 1999), was enhanced in the CSF of our transgenic rats. This process clearly reflects the neuronal loss presented in the late stages of AD.

In summary, as confirmed in functional enrichment studies, transgenic rats largely reproduced AD pathology. The CSF proteome revealed a great number of protein changes involved with the amyloid pathology in TgF344-AD rats, which follow a sex-related influence. Although a

substantial amount of data is produced with proteomics, clear translational biomarkers are hard to detect. However, this study provides a considerable list of candidates, some in line with emerging biomarkers in human studies. Of note, several synaptic components are proposed as relevant targets to monitor synaptic dysfunction in Alzheimer's disease. Taken together, we consider TgF344-AD rats as a suitable model to find potential biomarkers and to predict therapeutic responses before human investigations.

Closing remarks

The present dissertation addresses essential aspects in the physiology of the central nervous system with particular emphasis on intercellular communication, fundamental to brain function. Our findings demonstrate the temporal acquisition of peptidergic regulated secretion in the maturation of cortical neurons, which is achieved heterogeneously depending on DCV subpopulations during the first postnatal week, possibly mediated to some extent by synaptotagmin-IV. In this way, the maturation of this regulated secretory pathway is accomplished during synaptogenesis, when DCV subpopulations may play critical roles regulating cell motility, neurite outgrowth and neuronal differentiation. Moreover, this thesis focused on astrocyte active contribution to synaptic transmission monitoring peptidergic vesicles as a relevant organelle in evoked calcium responses. Noteworthy, our results provide new insights into astrocytic secretory phenotype into physiological neural networks, the environment of brain function. In addition, in this dissertation we have shed some light on the molecular evidence for synaptic dysfunction caused in early AD pathogenesis. Using the TgF344-AD rat model, we have characterized age- and sex-amyloid-associated secretory impairments and synaptic defects by immunological approaches and proteomic analyses, to a certain degree comparable to human alterations. Hence, we propose TgF344-AD rats as a suitable source for the search of fluid biomarkers that support the development of new therapeutic strategies for pre-clinical AD interventions.

CONCLUSIONS

CONCLUSIONS

From the results presented in this dissertation it can be concluded that:

1. *In situ* and *in vitro* studies on cortical neurons show that competence for regulated secretion is sequentially acquired for different DCV subsets during the first postnatal week.

2. At early developmental stages, before displaying the typical evoked secretion, depolarization of cortical neurons consistently elicits an unconventional decrease of DCV exocytosis, likely in a calcium-dependent manner.

3. The strong correlation between the acquisition of regulated secretion competence and the downregulation of synaptotagmin-IV levels in DCV suggest a key role for this vesicular component in the maturation of the peptidergic secretory pathway in cortical neurons.

4. New generated adeno-associated vectors targeting ANP fused with fluorescent tags specifically to astrocytes or neurons are suitable tools to study peptidergic secretory pathways in co-cultures and *in vivo*.

5. Astrocytes grown in mono-cultures and into neural networks (*in vitro* and *in situ*) release peptidergic vesicles in a calcium-dependent fashion, although to a lesser extent than neuronal regulated secretion.

6. Astrocytic peptidergic secretion is evoked by pharmacological and optogenetic activation of neurons in co-cultures. This effect is mainly linked to NMDA receptors, suggesting a neuron-astrocyte communication mediated by glutamate.

7. TgF344-AD rats, an animal model of Alzheimer's disease, show notable sex- and age-dependent changes of peptidergic and other secretory components in the brain and CSF, beginning even prior to Aβ deposition, markedy in male rats.

8. Synaptic components having significant regard in CSF from AD patients, such as Neurogranin, Nf-L, Basp1 or GAP-43, and interesting new candidates as Tpm1, are altered in the CSF of TgF344-AD rats.

9. The wide spectrum of protein changes revealed in the CSF proteome of transgenic rats suggest a differential impact on biological pathways, such as glia-neuron communication, neuronal assembly, memory pathways or neuroinflammation in males and females.

10. These findings point to TgF344-AD rats as a suitable pre-clinical model for the investigation of fluid biomarkers that sustain the development of new therapeutic strategies for early clinical interventions.

REFERENCES

REFERENCES

Abbott, N. J. (2004). Evidence for bulk flow of brain interstitial fluid: significance for physiology and pathology. *Neurochemistry International*, 45(4), 545–552.

Abbott, N. J., Rönnbäck, L., & Hansson, E. (2006). Astrocyte-endothelial interactions at the blood-brain barrier. *Nature Reviews Neuroscience*, 7(1), 41–53.

Abbracchio, M. P., Burnstock, G., Verkhratsky, A., & Zimmermann, H. (2009). Purinergic signalling in the nervous system: an overview. *Trends in Neurosciences*, 32(1), 19–29.

Aguado, F., Espinosa-Parrilla, J. F., Carmona, M. A., & Soriano, E. (2002). Neuronal activity regulates correlated network properties of spontaneous calcium transients in astrocytes in situ. *Journal of Neuroscience*, 22(21), 9430-9444.

Ahmad, M. H., Fatima, M., & Mondal, A. C. (2019). Influence of microglia and astrocyte activation in the neuroinflammatory pathogenesis of Alzheimer's disease: rational insights for the therapeutic approaches. *Journal of Clinical Neuroscience*, 59, 6–11.

Ahras, M., Otto, G. P., & Tooze, S. A. (2006). Synaptotagmin IV is necessary for the maturation of secretory granules in PC12 cells. *Journal of Cell Biology*, 173(2), 241–251.

Akiyama, H., Barger, S., Barnum, S., Bradt, B., Bauer, J., Cole, G. M., Cooper, N. R., Eikelenboom, P., Emmerling, M., Fiebich, B. L., Finch, C. E., Frautschy, S., Griffin, W. S. T., Hampel, H., Hull, M., Landreth, G., Lue, L.-F., Mrak, R., Mackenzie, I. R., … Wyss-Coray, T. (2000). Inflammation and Alzheimer's disease. *Neurobiology of aging*, 21(3), 383-421.

Akram, A., Christoffel, D., Rocher, A. B., Bouras, C., Kövari, E., Perl, D. P., Morrison, J. H., Herrmann, F. R., Haroutunian, V., Giannakopoulos, P., & Hof, P. R. (2008). Stereologic estimates of total spinophilin-immunoreactive spine number in area 9 and the CA1 field: Relationship with the progression of Alzheimer's disease. *Neurobiology of Aging*, 29(9), 1296–1307.

Albert, M. S., Dekosky, S. T., Dickson, D., Dubois, B., Feldman, H. H., Fox, N. C., Gamst, A., Holtzman, D. M., Jagust, W. J., Petersen, R. C., Snyder, P. J., Carrillo, M. C., Thies, B., & Phelps, C. H. (2013). The diagnosis of mild cognitive impairment due to Alzheimer's disease: recommendations from the National Institute on Aging-Alzheimer's Association workgroups on diagnostic guidelines for Alzheimer's disease. *Focus*, 11(1), 96–106.

Anckaerts, C., Blockx, I., Summer, P., Michael, J., Hamaide, J., Kreutzer, C., Boutin, H., Couillard-Després, S., Verhoye, M., & van der Linden, A. (2019). Early functional connectivity deficits and progressive microstructural alterations in the TgF344-AD rat model of Alzheimer's Disease: A longitudinal MRI study. *Neurobiology of Disease*, 124, 93–107.

Andersen, J. v., Markussen, K. H., Jakobsen, E., Schousboe, A., Waagepetersen, H. S., Rosenberg, P. A., & Aldana, B. I. (2021). Glutamate metabolism and recycling at the excitatory synapse in health and neurodegeneration. *Neuropharmacology*, 196, 108719.

Anderson, C. M., Bergher, J. P., & Swanson, R. A. (2004). ATP-induced ATP release from astrocytes. *Journal of neurochemistry*, 88(1), 246–256.

Anderson, C. M., & Nedergaard, M. (2003). Astrocyte-mediated control of cerebral microcirculation. *Trends in Neurosciences*, 26(7), 340–344.

Andreae, L. C., Fredj, N. B., & Burrone, J. (2012). Independent vesicle pools underlie different modes of release during neuronal development. *Journal of Neuroscience*, 32(5), 1867–1874.

Antonell, A., Tort-Merino, A., Ríos, J., Balasa, M., Borrego-Écija, S., Auge, J. M., Muñoz-García, C., Bosch, B., Falgàs, N., Rami, L., Ramos-Campoy, O., Blennow, K., Zetterberg, H., Molinuevo, J. L., Lladó, A., & Sánchez-Valle, R. (2020). Synaptic, axonal damage and inflammatory cerebrospinal fluid biomarkers in neurodegenerative dementias. *Alzheimer's and Dementia*, 16(2), 262–272.

Araque, A., Carmignoto, G., & Haydon, P. G. (2001). Dynamic signaling between astrocytes and neurons. *Annual review of physiology*, 63(1), 795-813

Araque, A., Li, N., Doyle, R. T., & Haydon, P. G. (2000). SNARE protein-dependent glutamate release from astrocytes. Journal of Neuroscience, 20(2), 666-673.

Araque, A., Parpura, V., Sanzgiri, R. P., & Haydon, P. G. (1998). Glutamate-dependent astrocyte modulation of synaptic transmission between cultured hippocampal neurons. *European Journal of Neuroscience*, 10(6), 2129–2142.

Araque, A., Parpura, V., Sanzgiri, R. P., & Haydon, P. G. (1999). Tripartite synapses: glia, the unacknowledged partner. *Trends in Neurosciences*, 22(5), 208–215.

Armstrong, W. E., Rubrum, A., Teruyama, R., Bond, C. T., & Adelman, J. P. (2005). Immunocytochemical localization of small-conductance, calcium-dependent potassium channels in astrocytes of the rat supraoptic nucleus. *Journal of Comparative Neurology*, 491(3), 175–185.

Arnaoutova, I., Smith, A. M., Coates, L. C., Sharpe, J. C., Dhanvantari, S., Snell, C. R., Birch, N. P., & Loh, Y. P. (2003). The prohormone processing enzyme PC3 is a lipid raft-associated transmembrane protein. *Biochemistry*, 42(35), 10445–10455.

Arnold, S. E., Hyman, B. T., Flory, J., Damasio, A. R., & van Hoesen, G. W. (1991). The topographical and neuroanatomical distribution of neurofibrillary tangles and neuritic plaques in the cerebral cortex of patients with Alzheimer's disease. *Cerebral Cortex*, 1(1), 103–116.

Arora, S., Saarloos, I., Kooistra, R., van de Bospoort, R., Verhage, M., & Toonen, R. F. (2017). SNAP-25 gene family members differentially support secretory vesicle fusion. *Journal of Cell Science*, 130 (11), 1877–1889.

Arvan, P., & Castle, D. (1998). Sorting and storage during secretory granule biogenesis: looking backward and looking forward. *Biochemical Journal*, 332(3), 593-610.

Arvan, P., Kuliawat, R., Prabakaran, D., Zavacki, A. M., Elahi, D., Wang, S., & Pilkey, D. (1991). Protein discharge from immature secretory granules displays both regulated and constitutive characteristics. *Journal of Biological Chemistry*, 266(22), 14171–14174.

Bai, B., Wang, X., Li, Y., Chen, P. C., Yu, K., Dey, K. K., Yarbro, J. M., Han, X., Lutz, B. M., Rao, S., Jiao, Y., Sifford, J. M., Han, J., Wang, M., Tan, H., Shaw, T. I., Cho, J. H., Zhou, S., Wang,

H., … Peng, J. (2020). Deep Multilayer Brain Proteomics Identifies Molecular Networks in Alzheimer's Disease Progression. *Neuron*, 105(6), 975-991.

Bailey, K. (1946). Tropomyosin: a new asymmetric protein component of muscle. *Nature*, 157(3986), 368–369.

Ballatore, C., Lee, V. M. Y., & Trojanowski, J. Q. (2007). Tau-mediated neurodegeneration in Alzheimer's disease and related disorders. *Nature Reviews Neuroscience* (Vol. 8, Issue 9, pp. 663–672).

Bancher, C., Braak, H., Fischer, P., & Jellinger, K. A. (1993). Neuropathological staging of Alzheimer lesions and intellectual status in Alzheimer's and Parkinson's disease patients. *Neuroscience letters*, 162(1-2), 179-182.

Banks, W. A., & Robinson, S. M. (2010). Minimal penetration of lipopolysaccharide across the murine blood-brain barrier. *Brain, Behavior, and Immunity*, 24(1), 102–109.

Barranco, N., Plá, V., Alcolea, D., Sánchez-Domínguez, I., Fischer-Colbrie, R., Ferrer, I., Lleó, A., & Aguado, F. (2021). Dense core vesicle markers in CSF and cortical tissues of patients with Alzheimer's disease. *Translational Neurodegeneration*, 10(1), 1-15.

Barten, D. M., Cadelina, G. W., & Weed, M. R. (2017). Dosing, collection, and quality control issues in cerebrospinal fluid research using animal models. *Handbook of Clinical Neurology*, 146, 47-64.

Bartolomucci, A., Possenti, R., Mahata, S. K., Fischer-Colbrie, R., Loh, Y., & Salton, S. (2011). The extended granin family: structure, function, and biomedical implications. *Endocrine Reviews*, 32(6), 755–797.

Belinson, H., Lev, D., Masliah, E., & Michaelson, D. M. (2008). Activation of the amyloid cascade in apolipoprotein E4 transgenic mice induces lysosomal activation and neurodegeneration resulting in marked cognitive deficits. *Journal of Neuroscience*, 28(18), 4690–4701.

Ben Haim, L., Carrillo-de Sauvage, M. A., Ceyzériat, K., & Escartin, C. (2015). Elusive roles for reactive astrocytes in neurodegenerative diseases. Frontiers in cellular neuroscience, 9, 278.

Benedikz, E., Kloskowska, E., & Winblad, B. (2009). The rat as an animal model of Alzheimer's disease. *Journal of cellular and molecular medicine*, 13(6), 1034–1042.

Bergersen, L. H., Morland, C., Ormel, L., Rinholm, J. E., Larsson, M., Wold, J. F. H., Røe, A. T., Stranna, A., Santello, M., Bouvier, D., Ottersen, O. P., Volterra, A., & Gundersen, V. (2012). Immunogold detection of L-glutamate and D-serine in small synaptic-like microvesicles in adult hippocampal astrocytes. *Cerebral Cortex*, 22(7), 1690–1697.

Berton, F., Cornet, V., Iborra, C., Garrido, J., Dargent, B., Fukuda, M., Seagar, M., & Marquèze, B. (2000). Synaptotagmin I and IV define distinct populations of neuronal transport vesicles. *European Journal of Neuroscience*, 12(4), 1294–1302.

Berton, F., Iborra, C., Boudier, J. A., Seagar, M. J., & Marquèze, B. (1997). Developmental regulation of synaptotagmin I, II, III, and IV mRNAs in the rat CNS. *Journal of Neuroscience*, 17(4), 1206–1216.

Bettens, K., Sleegers, K., & van Broeckhoven, C. (2010). Current status on Alzheimer disease molecular genetics: from past, to present, to future. *Human Molecular Genetics*, 19(R1) R4-R11.

Bezzi, P., Carmignoto, G., Pasti, L., Vesce, S., Rossi, D., Rizzini, B. L., & Pozzan, T. & V. A. (1998). Prostaglandins stimulate calcium-dependent glutamate release in astrocytes. *Nature*, 391(6664), 281–285.

Bezzi, P., Gundersen, V., Galbete, J. L., Seifert, G., Steinhäuser, C., Pilati, E., & Volterra, A. (2004). Astrocytes contain a vesicular compartment that is competent for regulated exocytosis of glutamate. *Nature Neuroscience*, 7(6), 613–620.

Bezzi, P., & Volterra, A. (2001). A neuron–glia signalling network in the active brain. *Current opinion in neurobiology*, 11(3), 387–394.

Biber, K., Lubrich, B., Fiebich, B. L., Boddeke, H. W. G. M., & van Calker, D. (2001). Interleukin-6 enhances expression of adenosine A1 receptor mRNA and signaling in cultured rat cortical astrocytes and brain slices. *Neuropsychopharmacology*, 24(1), 86-96.

Billings, L. M., Oddo, S., Green, K. N., McGaugh, J. L., & LaFerla, F. M. (2005). Intraneuronal Aβ causes the onset of early Alzheimer's disease-related cognitive deficits in transgenic mice. *Neuron*, 45(5), 675–688.

Blázquez, M., Thiele, C., Huttner, W. B., Docherty, K., & Shennan, K. I. J. (2000). Involvement of the membrane lipid bilayer in sorting prohormone convertase 2 into the regulated secretory pathway. *Biochemical Journal*, 349(3), 843-852.

Blennow, K., Davidsson, P., Wallin, A., & Ekman, R. (1995). Chromogranin A in cerebrospinal fluid: a biochemical marker for synaptic degeneration in Alzheimer's disease? *Dementia and Geriatric Cognitive Disorders*, 6(6), 306–311.

Blennow, K., & Hampel, H. (2003). CSF markers for incipient Alzheimer's disease. *The Lancet Neurology*, 2(10), 605-613.

Blott, E. J., & Griffiths, G. M. (2002). Secretory lysosomes. *Nature reviews Molecular cell biology*, 3(2), 122-131.

Boncristiano, S., Calhoun, M. E., Howard, V., Bondolfi, L., Kaeser, S. A., Wiederhold, K. H., Staufenbiel, M., & Jucker, M. (2005). Neocortical synaptic bouton number is maintained despite robust amyloid deposition in APP23 transgenic mice. *Neurobiology of Aging*, 26(5), 607–613.

Bonneh-Barkay, D., Bissel, S. J., Wang, G., Fish, K. N., Nicholl, G. C. B., Darko, S. W., Medina-Flores, R., Murphey-Corb, M., Rajakumar, P. A., Nyaundi, J., Mellors, J. W., Bowser, R., & Wiley, C. A. (2008). YKL-40, a marker of simian immunodeficiency virus encephalitis, modulates the biological activity of basic fibroblast growth factor. *The American journal of pathology*, 173(1), 130–143.

Bonnemaison, M. L., Eipper, B. A., & Mains, R. E. (2013). Role of adaptor proteins in secretory granule biogenesis and maturation. *Frontiers in Endocrinology*, 4, 101.

Borchelt, D. R., Thinakaran, G., Eckman, C. B., Lee, M. K., Davenport, F., Ratovitsky, T., & ... & Sisodia, S. S. (1996). Familial Alzheimer's disease–linked presenilin 1 variants elevate Aβ1–42/1–40 ratio in vitro and in vivo. *Neuron*, 17(5), 1005-1013

Bowser, D. N., & Khakh, B. S. (2007). Vesicular ATP is the predominant cause of intercellular calcium waves in astrocytes. Journal of General Physiology, 129(6), 485–491.

Braak, H., & Braak, E. (1991a). Demonstration of amyloid deposits and neurofibrillary changes in whole brain sections. *Brain Pathology*, 1(3), 213–216.

Braak, H., & Braak, E. (1991b). Neuropathological stageing of Alzheimer-related changes. *Acta Neuropathologica*, 82(4), 239–259.

Braakman, I., & Bulleid, N. J. (2011). Protein folding and modification in the mammalian endoplasmic reticulum. *Annual Review of Biochemistry*, 80, 71–99.

Brahmachari, S., Fung, Y. K., & Pahan, K. (2006). Induction of glial fibrillary acidic protein expression in astrocytes by nitric oxide. *Journal of Neuroscience*, 26(18), 4930–4939.

Braks, J. A. M., & Martens, G. J. M. (1994). 7B2 is a neuroendocrine chaperone that transiently interacts with prohormone convertase PC2 in the secretory pathway. *Cell*, 78(2), 263-273.

Brambilla, R., Burnstock, G., Bonazzi, A., Ceruti, S., Cattabeni, F., & Abbracchio, M. P. (1999). Cyclo-oxygenase-2 mediates P2Y receptor-induced reactive astrogliosis. *British Journal of Pharmacology*, 126(3), 563–567.

Brettle, M., Patel, S., & Fath, T. (2016). Tropomyosins in the healthy and diseased nervous system. *Brain Research Bulletin*, 126, 311–323.

Bridel, C., van Wieringen, W. N., Zetterberg, H., Tijms, B. M., Teunissen, C. E., Alvarez-Cermeño, J. C., Andreasson, U., Axelsson, M., Bäckström, D. C., Bartos, A., Bjerke, M., Blennow, K., Boxer, A., Brundin, L., Burman, J., Christensen, T., Fialová, L., Forsgren, L., Frederiksen, J. L., … Wild, E. J. (2019). Diagnostic value of cerebrospinal fluid neurofilament light protein in neurology: a systematic review and meta-analysis. *JAMA neurology*, 76(9), 1035-1048.

Brinkmalm, A., Brinkmalm, G., Honer, W. G., Frölich, L., Hausner, L., Minthon, L., Hansson, O., Wallin, A., Zetterberg, H., Blennow, K., & Öhrfelt, A. (2014). SNAP-25 is a promising novel cerebrospinal fluid biomarker for synapse degeneration in Alzheimer's disease. *Molecular Neurodegeneration*, 9(1), 1-13.

Brinkmalm, G., Sjödin, S., Simonsen, A. H., Hasselbalch, S. G., Zetterberg, H., Brinkmalm, A., & Blennow, K. (2018). A parallel reaction monitoring mass spectrometric method for analysis of potential CSF biomarkers for Alzheimer's disease. PROTEOMICS–Clinical Applications, 12(1), 1700131.

Brion, C., Miller, S., & Moore, H. (1992). Regulated and constitutive secretion. Differential effects of protein synthesis arrest on transport of glycosaminoglycan chains to the two secretory pathways. *Journal of Biological Chemistry*, 267(3), 1477-1483

Burgess, T. L., & Kelly, R. B. (1987). Constitutive and regulated secretion of proteins. Annual review of cell biology, 3(1), 243-293.

Burgoyne, R. D., & Morgan, A. (2003). Secretory Granule Exocytosis. *Physiological Reviews*, 83(2), 581–632.

Butt, A. M. (2011). ATP: A ubiquitous gliotransmitter integrating neuron-glial networks. In *Seminars in Cell and Developmental Biology* (Vol. 22, Issue 2, pp. 205–213). Academic Press.

Cai, Z., Schools, G. P., & Kimelberg, H. K. (2000). Metabotropic glutamate receptors in acutely isolated hippocampal astrocytes: developmental changes of mGluR5 mRNA and functional expression. Glia, 29(1), 70-80.

Calabrò, M., Rinaldi, C., Santoro, G., & Crisafulli, C. (2021). The biological pathways of Alzheimer disease: a review. *AIMS Neuroscience*, 8(1), 86–132.

Calegari, F., Coco, S., Taverna, E., Bassetti, M., Verderio, C., Corradi, N., Matteoli, M., & Rosa, P. (1999). A regulated secretory pathway in cultured hippocampal astrocytes. *Journal of Biological Chemistry*, 274(32), 22539–22547.

Cameron, A., Fortenberry, Y., & Lindberg, I. (2000). The SAAS granin exhibits structural and functional homology to 7B2 and contains a highly potent hexapeptide inhibitor of PC1. *FEBS Letters*, 473(2), 135–138.

Camporesi, E., Nilsson, J., Brinkmalm, A., Becker, B., Ashton, N. J., Blennow, K., & Zetterberg, H. (2020). Fluid Biomarkers for Synaptic Dysfunction and Loss. *Biomarker Insights*, 15.

Castaño, E. M., Maarouf, C. L., Wu, T., Leal, M. C., Whiteside, C. M., Lue, L. F., Kokjohn, T. A., Sabbagh, M. N., Beach, T. G., & Roher, A. E. (2013). Alzheimer disease periventricular white matter lesions exhibit specific proteomic profile alterations. *Neurochemistry International*, 62(2), 145–156.

Cawley, N. X., Wetsel, W. C., Murthy, S. R. K., Park, J. J., Pacak, K., & Loh, Y. P. (2012). New roles of carboxypeptidase E in endocrine and neural function and cancer. *Endocrine Reviews*, 33(2), 216–253.

Chanat, E., & Huttner, W. B. (1991). Milieu-induced, selective aggregation of regulated secretory proteins in the trans-Golgi network. The Journal of cell biology, 115(6), 1505-1519.

Chen, G., Chen, K. S., Knox, J., Inglis, J., Bernard, A., Martin, S. J., & ... & Morris, R. G. (2000). A learning deficit related to age and β-amyloid plaques in a mouse model of Alzheimer's disease. *Nature*, 408(6815), 975–979.

Chen, Y., Rathbone, M. P., & Hertz, L. (2001). Guanosine-induced increase in free cytosolic calcium concentration in mouse astrocytes in primary cultures: Does it act on an A3 adenosine receptor?. Journal of neuroscience research, 65(2), 184-189.

Chen, Y. Y., Yu, X. Y., Chen, L., Vaziri, N. D., Ma, S. C., & Zhao, Y. Y. (2019). Redox signaling in aging kidney and opportunity for therapeutic intervention through natural products. *Free Radical Biology and Medicine*, 141, 141–149.

Chung, D., Shum, A., & Caraveo, G. (2020). GAP-43 and BASP1 in axon regeneration: implications for the treatment of neurodegenerative diseases. Frontiers in Cell and Developmental Biology, 8.

Citron, M., Diehl, T. S., Gordon, G., Biere, A. L., Seubert, P., & Selkoe, D. J. (1996). Evidence that the 42-and 40-amino acid forms of amyloid protein are generated from the-amyloid precursor protein by different protease activities. Proceedings of the National Academy of Sciences, 93(23), 13170-13175.

Coco, S., Calegari, F., Pravettoni, E., Pozzi, D., Taverna, E., Rosa, P., Matteoli, M., & Verderio, C. (2003). Storage and release of ATP from astrocytes in culture. *Journal of Biological Chemistry*, 278(2), 1354–1362.

Cohen, R. M., Rezai-Zadeh, K., Weitz, T. M., Rentsendorj, A., Gate, D., Spivak, I., Bholat, Y., Vasilevko, V., Glabe, C. G., Breunig, J. J., Rakic, P., Davtyan, H., Agadjanyan, M. G., Kepe, V., Barrio, J. R., Bannykh, S., Szekely, C. A., Pechnick, R. N., & Town, T. (2013). A transgenic alzheimer rat with plaques, tau pathology, behavioral impairment, oligomeric Aβ, and frank neuronal loss. *Journal of Neuroscience*, 33(15), 6245–6256.

Conti, F., Barbaresi, P., Melone, M., & Ducati, A. (1999). Neuronal and glial localization of NR1 and NR2A/B subunits of the NMDA receptor in the human cerebral cortex. *Cerebral Cortex*, 9(2), 110–120.

Conti, F., Minelli, A., & Brecha, N. C. (1994). Cellular localization and laminar distribution of AMPA glutamate receptor subunits mRNAs and proteins in the rat cerebral cortex. Journal of Comparative Neurology, 350(2), 241-259.

Cool, D. R., & Loh, Y. P. (1998). Carboxypeptidase E is a sorting receptor for prohormones: Binding and kinetic studies. *Molecular and cellular endocrinology*, 139(1-2), 7-13.

Cornell-Bell, A. H., Finkbeiner, S. M., Cooper, M. S., & Smith, S. J. (1990). Glutamate induces calcium waves in cultured astrocytes: long-range glial signaling. *Science*, 247(4941), 470–473.

Craig-Schapiro, R., Perrin, R. J., Roe, C. M., Xiong, C., Carter, D., Cairns, N. J., Mintun, M. A., Peskind, E. R., Li, G., Galasko, D. R., Clark, C. M., Quinn, J. F., D'Angelo, G., Malone, J. P., Townsend, R. R., Morris, J. C., Fagan, A. M., & Holtzman, D. M. (2010). YKL-40: A novel prognostic fluid biomarker for preclinical Alzheimer's disease. *Biological Psychiatry*, 68(10), 903–912.

Creemers, J. W. M., Usac, E. F., Bright, N. A., van de Loo, J. W., Jansen, E., van de Ven, W. J. M., & Hutton, J. C. (1996). Identification of a transferable sorting domain for the regulated pathway in the prohormone convertase PC2. *Journal of Biological Chemistry*, 271(41), 25284–25291.

Crimins, J. L., Pooler, A., Polydoro, M., Luebke, J. I., & Spires-Jones, T. L. (2013). The intersection of amyloid beta and tau in glutamatergic synaptic dysfunction and collapse in Alzheimer's disease. Ageing research reviews, 12(3), 757–763.

Cserr, H. F. (1988). Role of Secretion and Bulk Flow of Brain Interstitial Fluid in Brain Volume Regulation. *Annals of the New York Academy of Sciences*, 529(1), 9–20.

Curtis, D. R., & Johnston, G. A. (1974). Amino acid transmitters in the mammalian central nervous system. Ergebnisse der Physiologie Reviews of Physiology, Volume 69, 97-188.

Czirr, E., Castello, N. A., Mosher, K. I., Castellano, J. M., Hinkson, I. v., Lucin, K. M., Baeza-Raja, B., Ryu, J. K., Li, L., Farina, S. N., Belichenko, N. P., Longo, F. M., Akassoglou, K., Britschgi,

M., Cirrito, J. R., & Wyss-Coray, T. (2017). Microglial complement receptor 3 regulates brain Aβ levels through secreted proteolytic activity. *Journal of Experimental Medicine*, 214(4), 1081–1092.

D'Amelio, M., Cavallucci, V., Middei, S., Marchetti, C., Pacioni, S., Ferri, A., Diamantini, A., de Zio, D., Carrara, P., Battistini, L., Moreno, S., Bacci, A., Ammassari-Teule, M., Marie, H., & Cecconi, F. (2011). Caspase-3 triggers early synaptic dysfunction in a mouse model of Alzheimer's disease. Nature Neuroscience, 14(1), 69–79.

Danbolt, N. C. (2001). Glutamate uptake. Progress in Neurobiology, 65(1), 1-105.

Daré, E., Schulte, G., Karovic, O., Hammarberg, C., & Fredholm, B. B. (2007). Modulation of glial cell functions by adenosine receptors. *Physiology and Behavior*, 92(1–2), 15–20.

D'Ascenzo, M., Fellin, T., Terunuma, M., Revilla-Sanchez, R., Meaney, D. F., Auberson, Y. P., Moss, S. J., & Haydon, P. G. (2007). mGluR5 stimulates gliotransmission in the nucleus accumbens. *Proceedings of the National Academy of Sciences*, 104(6), 1995-2000.

Davidsson, P., Blennow, K., Davidsson, S. P., & Blennow, K. (1998). Neurochemical dissection of synaptic pathology in Alzheimer's disease. International psychogeriatrics, 10(1), 11-23.

Day, R., K-H Schafer, M., Watson, S. J., Chrbtien, M., & Seidah J A, N. G. (1992). Distribution and Regulation of the Prohormone Convertases PC1 and PC2 in the Rat Pituitary. Molecular Endocrinology, 6(3), 485-497.

De Camilli, P., & Navone, F. (1987). Regulated secretory pathways of neurons and their relation to the regulated secretory pathway of endocrine cells. *Annals of the New York Academy of Sciences,* 493(1), 461–479.

De Carlos, J. A., & O'leary, D. D. M. (1992). Growth and targeting of subplate axons and establishment of major cortical pathways [published erratum appears in J Neurosci 1993 Mar; 13 (3): following table of contents]. *Journal of Neuroscience*, 12(4), 1194-1211.

De Duve, C., & Wattiaux, R. (1966). Functions of lysosomes. *Annual review of physiology*, 28(1), 435-492.

De Felice, F. G., Velasco, P. T., Lambert, M. P., Viola, K., Fernandez, S. J., Ferreira, S. T., & Klein, W. L. (2007). Aβ oligomers induce neuronal oxidative stress through an N-methyl-D-aspartate receptor-dependent mechanism that is blocked by the Alzheimer drug memantine. *Journal of Biological Chemistry*, 282(15), 11590–11601.

De Felice, F. G., Wu, D., Lambert, M. P., Fernandez, S. J., Velasco, P. T., Lacor, P. N., Bigio, E. H., Jerecic, J., Acton, P. J., Shughrue, P. J., Chen-Dodson, E., Kinney, G. G., & Klein, W. L. (2008). Alzheimer's disease-type neuronal tau hyperphosphorylation induced by Aβ oligomers. *Neurobiology of Aging*, 29(9), 1334–1347.

Dean, C., Liu, H., Dunning, F. M., Chang, P. Y., Jackson, M. B., & Chapman, E. R. (2009). Synaptotagmin-IV modulates synaptic function and long-term potentiation by regulating BDNF release. *Nature Neuroscience*, 12(6), 767–776.

Decker, H., Jürgensen, S., Adrover, M. F., Brito-Moreira, J., Bomfim, T. R., Klein, W. L., Epstein, A. L., de Felice, F. G., Jerusalinsky, D., & Ferreira, S. T. (2010). N-Methyl-d-aspartate receptors are required for synaptic targeting of Alzheimer's toxic amyloid-β peptide oligomers. *Journal of Neurochemistry*, 115(6), 1520–1529.

Dekosky, S. T., & Scheff, S. W. (1990). Synapse loss in frontal cortex biopsies in Alzheimer's disease: correlation with cognitive severity. *Annals of Neurology: Official Journal of the American Neurological Association and the Child Neurology Society*, 27(5), 457-464.

DeMattos, R. B., Bales, K. R., Parsadanian, M., O'dell, M. A., Foss, E. M., Paul, S. M., & Holtzman, D. M. (2002). Plaque-associated disruption of CSF and plasma amyloid-β (Aβ) equilibrium in a mouse model of Alzheimer's disease. *Journal of neurochemistry*, 81(2), 229-236.

Deng, A., Irizarry, M. C., Nitsch, R. M., Growdon, J. H., & Rebeck, G. W. (2001). Elevation of cystatin C in susceptible neurons in Alzheimer's disease. *The American journal of pathology*, 159(3), 1061-1068

Dhanvantari, S., & Loh, Y. P. (2000). Lipid raft association of carboxypeptidase E is necessary for its function as a regulated secretory pathway sorting receptor. *Journal of Biological Chemistry*, 275(38), 29887–29893.

Di Scala-Guenot, D., Mouginot, D., & Strosser, M.-T. (1994). Increase of intracellular calcium induced by oxytocin in hypothalamic cultured astrocytes. *Glia*, 11(3), 269-276

Dickerson, B. C., Goncharova, I., Sullivan, M. P., Forchetti, C., Wilson, R. S., Bennett, D. A., Beckett, L. A., & Detoledo-Morrell, L. (2001). MRI-derived entorhinal and hippocampal atrophy in incipient and very mild Alzheimer's disease. *Neurobiology of aging*, 22(5), 747-754.

Dineley, K. T., Westerman, M., Bui, D., Bell, K., Ashe, K. H., & Sweatt, J. D. (2001). β-Amyloid activates the mitogen-activated protein kinase cascade via hippocampal α7 nicotinic acetylcholine receptors: in vitro and in vivo mechanisms related to Alzheimer's disease. Journal of Neuroscience, 21(12), 4125-4133.

Dixit, R., Ross, J. L., Goldman, Y. E., & Holzbaur, E. L. (2008). Differential regulation of dynein and kinesin motor proteins by tau. Science, 319(5866), 1086-1089.

Doengi, M., Deitmer, J. W., & Lohr, C. (2008). New evidence for purinergic signaling in the olfactory bulb: A 2A and P2Y 1 receptors mediate intracellular calcium release in astrocytes. *The FASEB Journal,* 22(7), 2368–2378.

Duff, K., & Suleman, F. (2004). Transgenic mouse models of Alzheimer's disease: How useful have they been for therapeutic development? *Briefings in Functional Genomics*, 3(1), 47–59.

Durkee, C. A., & Araque, A. (2019). Diversity and specificity of astrocyte–neuron communication. *Neuroscience*, 396, 73-78.

Eaton, B. A., Haugwitz, M., Lau, D., & Moore, H.-P. H. (2000). Biogenesis of regulated exocytotic carriers in neuroendocrine cells. Journal of Neuroscience, 20(19), 7334-7344.

Ellenbroek, B., & Youn, J. (2016). Rodent models in neuroscience research: is it a rat race? *Disease Models & Mechanisms*, 9(10), 1079–1087.

Emerit, M. B., Riad, M., & Hamon, M. (1992). Trophic effects of neurotransmitters during brain maturation. *Neonatology*, 62(4), 193-201.

Emperador Melero, J., Nadadhur, A. G., Schut, D., Weering, J. v., Heine, V. M., Toonen, R. F., & Verhage, M. (2017). Differential Maturation of the Two Regulated Secretory Pathways in Human iPSC-Derived Neurons. *Stem Cell Reports*, 8(3), 659–672.

Emperador-Melero, J., & Kaeser, P. S. (2020). Assembly of the presynaptic active zone. *Current opinion in neurobiology*, 63, 95-103.

Esquerda-Canals, G., Montoliu-Gaya, L., Güell-Bosch, J., & Villegas, S. (2017). Mouse Models of Alzheimer's Disease. *Journal of Alzheimer's Disease*, 57(4), 1171–1183.

Feijoo, C., Campbell, D. G., Jakes, R., Goedert, M., & Cuenda, A. (2005). Evidence that phosphorylation of the microtubule-associated protein Tau by SAPK4/p38δ at Thr50 promotes microtubule assembly. *Journal of Cell Science*, 118(2), 397–408.

Fiacco, T. A., Agulhon, C., Taves, S. R., Petravicz, J., Casper, K. B., Dong, X., Chen, J., & McCarthy, K. D. (2007). Selective Stimulation of Astrocyte Calcium In Situ Does Not Affect Neuronal Excitatory Synaptic Activity. *Neuron*, 54(4), 611–626.

Fiacco, T. A., & McCarthy, K. D. (2018). Multiple lines of evidence indicate that gliotransmission does not occur under physiological conditions. *Journal of Neuroscience*, 38(1), 3–13.

Finkbeiner, S. (1992). Calcium waves in astrocytes-filling in the gaps. Neuron, 8(6), 1101-1108.

Fischer-Colbrie, R., Kirchmair, R., Elika Schobert, A., Olenik, C., Meyer, D. K., & Winkler, H. (1993). Secretogranin II is synthesized and secreted in astrocyte cultures. Journal of neurochemistry, 60(6), 2312-2314.

Formichi, P., Battisti, C., Radi, E., & Federico, A. (2006). Cerebrospinal fluid tau, Aβ, and phosphorylated tau protein for the diagnosis of Alzheimer's disease. *Journal of Cellular Physiology,* 208(1), 39–46.

Forner, S., Baglietto-Vargas, D., Martini, A. C., Trujillo-Estrada, L., & LaFerla, F. M. (2017). Synaptic impairment in Alzheimer's disease: a dysregulated symphony. Trends in neurosciences, 40(6), 347-357.

Foster, N. L., Heidebrink, J. L., Clark, C. M., Jagust, W. J., Arnold, S. E., Barbas, N. R., DeCarli, C. S., Scott Turner, R., Koeppe, R. A., Higdon, R., & Minoshima, S. (2007). FDG-PET improves accuracy in distinguishing frontotemporal dementia and Alzheimer's disease. *Brain*, 130(10), 2616–2635.

Fowler, C. F., Goerzen, D., Devenyi, G. A., Madularu, D., Chakravarty, M. M., & Near, J. (2022). Neurochemical and cognitive changes precede structural abnormalities in the TgF344-AD rat model. *Brain Communications*, 4(2).

Franco, R., & Vargas, M. R. (2018). Redox biology in neurological function, dysfunction, and aging. Antioxidants & redox signaling, 28(18), 1583-1586.

Franke, H., Verkhratsky, A., Burnstock, G., & Illes, P. (2012). Pathophysiology of astroglial purinergic signalling. *Purinergic Signalling*, 8(3), 629–657.

Fricker, L. D. (2004). Carboxypeptidase E. In *Handbook of proteolytic enzymes* (pp. 840–844). Academic Press

Fricker, L. D., McKinzie, a a, Sun, J., Curran, E., Qian, Y., Yan, L., Patterson, S. D., Courchesne, P. L., Richards, B., Levin, N., Mzhavia, N., Devi, L. A., & Douglass, J. (2000). Identification and characterization of proSAAS, a granin-like neuroendocrine peptide precursor that inhibits prohormone processing. *Journal of Neuroscience*, 20(2), 639–648.

Fricker, L. D., & Snyder, S. H. (1982). Enkephalin convertase: Purification and characterization of a specific enkephalin-synthesizing carboxypeptidase localized to adrenal chromaffin granules. Proceedings of the National Academy of Sciences, 79(12), 3886-3890.

Frickersg, L. D., Da&, B., & Angelettiil, R. H. (1990). Identification of the pH-dependent membrane anchor of carboxypeptidase E (EC 3.4. 17.10). *Journal of Biological Chemistry*, 265(5), 2476–2482.

Frisoni, G. B., Fox, N. C., Jack, C. R., Scheltens, P., & Thompson, P. M. (2010). The clinical use of structural MRI in Alzheimer disease. *Nature Reviews Neurology*, 6(2), 67–77.

Fukuda, M., & Mikoshiba, K. (1999). A novel alternatively spliced variant of synaptotagmin VI lacking a transmembrane domain: Implications for distinct functions of the two isoforms. *Journal of Biological Chemistry*, 274(44), 31428–31434.

Fukuda, M. (2007). The role of synaptotagmin and synaptotagmin-like protein (Slp) in regulated exocytosis. *Molecular mechanisms of exocytosis* (pp. 42-61).

Fukuyama, R., Izumoto, T., & Fushiki, S. (2001). The cerebrospinal fluid level of glial fibrillary acidic protein is increased in cerebrospinal fluid from Alzheimer's disease patients and correlates with severity of dementia. *European neurology*, 46(1), 35-38.

Galasko, D., Xiao, M., Xu, D., Smirnov, D., Salmon, D. P., Dewit, N., Vanbrabant, J., Jacobs, D., Vanderstichele, H., Vanmechelen, E., & Worley, P. (2019). Synaptic biomarkers in CSF aid in diagnosis, correlate with cognition and predict progression in MCI and Alzheimer's disease. *Alzheimer's and Dementia: Translational Research and Clinical Interventions*, 5, 871–882.

Galloway, P. G., Mulvihill, P., Siedlak, S., Mijares, M., Kawai, M., Padget, H., Kim, R., & Perry, G. (1990). Immunochemical demonstration of tropomyosin in the neurofibrillary pathology of Alzheimer's disease. *The American journal of pathology*, 137(2), 291.

Games, D., Adams, D., Alessandrini, R., Barbour, R., Borthelette, P., Blackwell, C., & ... & Zhao, J. (1995). Alzheimer-type neuropathology in transgenic mice overexpressing V717F β-amyloid precursor protein. *Nature*, 373(6514), 523–527.

Gebremedhin, D., Yamaura, K., Zhang, C., Bylund, J., Koehler, R. C., & Harder, D. R. (2003). Metabotropic Glutamate Receptor Activation Enhances the Activities of Two Types of Ca2+-Activated K+Channels in Rat Hippocampal Astrocytes. *Journal of Neuroscience*, 23(5), 1678–1687.

Geeves, M. A., Hitchcock-DeGregori, S. E., & Gunning, P. W. (2015). A systematic nomenclature for mammalian tropomyosin isoforms. Journal of muscle research and cell motility, 36(2), 147-153.

Geppert, M., Goda, Y., Hammer, R. E., Li, C., Rosahl, T. W., Stevens, C. F., & Südhof, T. C. (1994). Synaptotagmin I: a major Ca2+ sensor for transmitter release at a central synapse. *Cell*, 79(4), 717-727.

Gerdes, H. H., Rosa, P., Phillips, E., Baeuerle, P. A., Frank, R., Argos, P., & Huttner, W. B. (1989). The primary structure of human secretogranin II, a widespread tyrosine-sulfated secretory granule protein that exhibits low pH- and calcium-induced aggregation. *Journal of Biological Chemistry*, 264(20), 12009–12015.

Glombik, M. M., Krö Mer, A., Salm, T., Huttner, W. B., Gerdes, H.-H., Glombik, M. M., & Krömer, A. (1999). The disulfide-bonded loop of chromogranin B mediates membrane binding and directs sorting from the trans-Golgi network to secretory granules. The EMBO Journal, 18(4), 1059-1070.

Goeminne, L. J. E., Gevaert, K., & Clement, L. (2018). Experimental design and data-analysis in label-free quantitative LC/MS proteomics: A tutorial with MSqRob. *Journal of Proteomics*, 171, 23–36.

Griffiths, G., & Simons, K. (1986). The trans Golgi network: sorting at the exit site of the Golgi complex. Science, 234(4775), 438-443.

Grundke-Iqbal, I., Iqbal, K., Quinlan, M., Tung, Y.-C., Zaidi, M. S., & Wisniewski, H. M. (1986). Microtubule-associated protein tau. A component of Alzheimer paired helical filaments. *Journal of Biological Chemistry*, 261(13), 6084–6089.

Gu, X., Olson, E. C., & Spitzer, N. C. (1994). Spontaneous neuronal calcium spikes and waves during early differentiation. Journal of Neuroscience, 14(11), 6325-6335.

Guerreiro, N., Gomez-Mancilla, B., Williamson, B., Minkoff, M., & Guertin, S. (2009). Proteomic profiling of cerebrospinal fluid by 8-plex iTRAQ reveals potential biomarker candidates of alzheimer's disease. *Clinical Proteomics*, 5(2), 114–124.

Guerreiro, R., & Bras, J. (2015). The age factor in Alzheimer's disease. *Genome Medicine*, 7(1), 1–3.

Guerrero-Muñoz, M. J., Gerson, J., & Castillo-Carranza, D. L. (2015). Tau oligomers: the toxic player at synapses in Alzheimer's disease. Frontiers in cellular neuroscience, 9, 464.

Guescini, M., Genedani, S., Stocchi, V., & Agnati, L. F. (2010). Astrocytes and Glioblastoma cells release exosomes carrying mtDNA. *Journal of Neural Transmission*, 117(1), 1–4.

Gunning, P., O'Neill, G., & Hardeman, E. (2008). Tropomyosin-based regulation of the actin cytoskeleton in time and space. Physiological reviews, 88(1), 1-35.

Guo, T., Zhang, D., Zeng, Y., Huang, T. Y., Xu, H., & Zhao, Y. (2020). Molecular and cellular mechanisms underlying the pathogenesis of Alzheimer's disease. Molecular neurodegeneration, 15(1), 1-37.

Gut, A., Kiraly, C. E., Fukuda, M., Mikoshiba, K., Wollheim, C. B., & Lang, J. (2001). Expression and localisation of synaptotagmin isoforms in endocrine (β)-cells: their function in insulin exocytosis. *Journal of Cell Science*, 114(9), 1709-1716.

Halassa, M. M., Fellin, T., & Haydon, P. G. (2007). The tripartite synapse: roles for gliotransmission in health and disease. *Trends in Molecular Medicine*, 13(2), 54–63.

Halassa, M. M., & Haydon, P. G. (2009). Integrated brain circuits: astrocytic networks modulate neuronal activity and behavior. Annual review of physiology, 72, 335.

Hanger, D. P., Hughes, K., Woodgett, J. R., Brion, J.-P., & Anderton, B. H. (1992). Glycogen synthase kinase-3 induces Alzheimer's disease-like phosphorylation of tau: generation of paired helical filament epitopes and neuronal localisation of the kinase. Neuroscience Letters, 147(1), 58-62.

Hansson, O., Zetterberg, H., Buchhave, P., Andreasson, U., Londos, E., Minthon, L., & Blennow, K. (2007). Prediction of Alzheimer's disease using the CSF Aβ42/Aβ40 ratio in patients with mild cognitive impairment. Dementia and geriatric cognitive disorders, 23(5), 316-320.

Hansson, O., Zetterberg, H., Buchhave, P., Londos, E., Blennow, K., & Minthon, L. (2006). Association between CSF biomarkers and incipient Alzheimer's disease in patients with mild cognitive impairment-a follow-up study. *The Lancet Neurology*, 5(3), 228–234.

Hardy, J., & Allsop, D. (1991). Amyloid deposition as the central event in the aetiology of Alzheimer's disease. *Trends in Pharmacological Sciences*, 12, 383–388.

Hasel, P., Dando, O., Jiwaji, Z., Baxter, P., Todd, A. C., Heron, S., ... & Hardingham, G. E. (2017). Neurons and neuronal activity control gene expression in astrocytes to regulate their development and metabolism. *Nature communications*, 8(1), 1-18.

Heneka, M. T., Carson, M. J., El Khoury, J., Landreth, G. E., Brosseron, F., Feinstein, D. L., ... & Kummer, M. P. (2015). Neuroinflammation in Alzheimer's disease. *The Lancet Neurology*, 14(4), 388-405.

Henneberger, C., Papouin, T., Oliet, S. H. R., & Rusakov, D. A. (2010). Long-term potentiation depends on release of d-serine from astrocytes. *Nature*, 463(7278), 232–236.

Henstridge, C. M., Hyman, B. T., & Spires-Jones, T. L. (2019). Beyond the neuron–cellular interactions early in Alzheimer disease pathogenesis. Nature Reviews Neuroscience, 20(2), 94-108.

Henstridge, C. M., Pickett, E., & Spires-Jones, T. L. (2016). Synaptic pathology: a shared mechanism in neurological disease. Ageing Research Reviews, 28, 72–84.

Hirase, H., Qian, L., Barthó, P., & Buzsáki, G. (2004). Calcium dynamics of cortical astrocytic networks in vivo. *PLoS Biology*, 2(4), e96.

Hodes, A., & Lichtstein, D. (2014). Natriuretic hormones in brain function. *Frontiers in Endocrinology*, 5, 201.

Hökfelt, T. (1991). Neuropeptides in perspective: the last ten years. Neuron, 7(6), 867-879.

Hökfelt, T., Broberger, C., David Xu, Z.-Q., Sergeyev, V., Ubink, R., & Diez, M. (2000). Neuropeptides-an overview. Neuropharmacology, 39(8), 1337-1356.

Holcomb, L., Gordon, M. N., McGowan, E., Yu, X., Benkovic, S., Jantzen, P., & ... & Duff, K. (1998). Accelerated Alzheimer-type phenotype in transgenic mice carrying both mutant amyloid precursor protein and presenilin 1 transgenes. *Nature Medicine*, 4(1), 97–100.

Holliday, J., Adams, R. J., Sejnowski, T. J., & Spitzer, N. C. (1991). Calcium-induced release of calcium regulates differentiation of cultured spinal neurons. Neuron, 7(5), 787-796.

Holmes, B. B., & Diamond, M. I. (2014). Prion-like properties of Tau protein: the importance of extracellular Tau as a therapeutic target. Journal of Biological Chemistry, 289(29), 19855-19861.

Holmes, C., Boche, D., Wilkinson, D., Yadegarfar, G., Hopkins, V., Bayer, A., Jones, R. W., Bullock, R., Love, S., Neal, J. W., Zotova, E., & Nicoll, J. A. R. (2008). Long-term effects of Aβ42 immunisation in Alzheimer's disease: follow-up of a randomised, placebo-controlled phase I trial. *The Lancet*, 372(9634), 216–223.

Hoogstraaten, R. I., van Keimpema, L., Toonen, R. F., & Verhage, M. (2020). Tetanus insensitive VAMP2 differentially restores synaptic and dense core vesicle fusion in tetanus neurotoxin treated neurons. *Scientific Reports*, 10(1), 1-14.

Hook, V. Y., & Loh, Y. P. (1984). Carboxypeptidase B-like converting enzyme activity in secretory granules of rat pituitary. Proceedings of the National Academy of Sciences, 81(9), 2776-2780.

Hoozemans, J. J. M., Veerhuis, R., Rozemuller, J. M., & Eikelenboom, P. (2006). Neuroinflammation and regeneration in the early stages of Alzheimer's disease pathology. *International Journal of Developmental Neuroscience*, 24(2–3), 157–165.

Hosaka, M., Watanabe, T., Sakai, Y., Uchiyama, Y., & Takeuchi, T. (2002). Identification of a chromogranin A domain that mediates binding to secretogranin III and targeting to secretory granules in pituitary cells and pancreatic β-cells. *Molecular Biology of the Cell*, 13(10), 3388–3399.

Hösli, E., & Hösli, L. (1991). Autoradiographic evidence for endothelin receptors on astrocytes in cultures of rat cerebellum, brainstem and spinal cord. Neuroscience Letters, 129(1), 55-58.

Hsia, A. Y., Masliah, E., Mcconlogue, L., Tatsuno, G., Kholodenko, D., Malenka, R. C., Nicoll, R. A., & Mucke, L. (1999). Plaque-independent disruption of neural circuits in Alzheimer's disease mouse models. *Proceedings of the National Academy of Sciences*, 96(6), 3228–3233.

Hsiao, K., Chapman, P., Nilsen, S., Ec Kman, ', C., Harigaya, Y., Younkin, S., Yang, F., & Cole, G. (1996). Correlative Memory Deficits, AP Elevation, and Amyloid Plaques in Transgenic Mice. *Science*, 274(5284), 99–103.

Hsieh, H., Boehm, J., Sato, C., Iwatsubo, T., Tomita, T., Sisodia, S., & Malinow, R. (2006). AMPAR Removal Underlies Aβ-Induced Synaptic Depression and Dendritic Spine Loss. *Neuron*, 52(5), 831–843.

Hua, X., Malarkey, E. B., Sunjara, V., Rosenwald, S. E., Li, W. H., & Parpura, V. (2004). Ca2+-dependent glutamate release involves two classes of endoplasmic reticulum Ca2+ stores in astrocytes. Journal of neuroscience research, 76(1), 86-97.

Huang, C., Walker, E. M., Dadi, P. K., Hu, R., Xu, Y., Zhang, W., ... & Gu, G. (2018). Synaptotagmin 4 regulates pancreatic β cell maturation by modulating the Ca2+ sensitivity of insulin secretion vesicles. Developmental cell, 45(3), 347-361.

Huang, E. J., & Reichardt, L. F. (2001). Neurotrophins: roles in neuronal development and function. Annual review of neuroscience, 24, 677.

Hur, Y. S., Kim, K. D., Paek, S. H., & Yoo, S. H. (2010). Evidence for the existence of secretory granule (dense-core vesicle)-based inositol 1,4,5-trisphosphate-dependent Ca2+ signaling system in astrocytes. *PLoS One*, 5(8), e11973.

Hyman, B. T. (1997). The neuropathological diagnosis of Alzheimer's disease: clinical-pathological studies. Neurobiology of aging, 18(4), S27-S32.

Hyman, B. T. (2014). Tau propagation, different tau phenotypes, and prion-like properties of tau. Neuron, 82(6), 1189-1190.

Imai, Y., & Kohsaka, S. (2002). Intracellular signaling in M-CSF-induced microglia activation: role of Iba1. Glia, 40(2), 164-174.

Iqbal, K., Liu, F., & Gong, C. X. (2018). Recent developments with tau-based drug discovery. In Expert Opinion on Drug Discovery, 13(5), 399-410.

Irizarry, M. C. (2004). Biomarkers of Alzheimer Disease in Plasma. *NeuroRx*, 1(2), 226–234.

Ittner, L. M., Ke, Y. D., Delerue, F., Bi, M., Gladbach, A., van Eersel, J., Wölfing, H., Chieng, B. C., Christie, M. J., Napier, I. A., Eckert, A., Staufenbiel, M., Hardeman, E., & Götz, J. (2010). Dendritic function of tau mediates amyloid-β toxicity in Alzheimer's disease mouse models. *Cell*, 142(3), 387–397.

Jack, C. R., Bennett, D. A., Blennow, K., Carrillo, M. C., Dunn, B., Haeberlein, S. B., Holtzman, D. M., Jagust, W., Jessen, F., Karlawish, J., Liu, E., Molinuevo, J. L., Montine, T., Phelps, C., Rankin, K. P., Rowe, C. C., Scheltens, P., Siemers, E., Snyder, H. M., … Silverberg, N. (2018). NIA-AA Research Framework: Toward a biological definition of Alzheimer's disease. *Alzheimer's & Dementia*, 14(4), 535-562.

Jack, C. R., Bennett, D. A., Blennow, K., Carrillo, M. C., Feldman, H. H., Frisoni, G. B., Hampel, H., Jagust, W. J., Johnson, K. A., Knopman, D. S., Petersen, R. C., Scheltens, P., Sperling, R. A., & Dubois, B. (2016). A/T/N: an unbiased descriptive classification scheme for Alzheimer disease biomarkers. *Neurology*, 87(5), 539–547.

Jahn, R., & Südhof, T. C. (1994). Synaptic vesicles and exocytosis. Annual review of neuroscience, 17(1), 219-246.

Jansson, A., Descarries, L., Cornea-Hebert, V., Riad, M., Verge, D., Bancila, M., Agnati, L. F., & Fuxe, K. (2002). Transmitter-receptor mismatches in central dopamine, serotonin, and neuropeptide systems. In *The Neuronal Environment* (pp. 83–108).

Ji, L., Wu, H. T., Qin, X. Y., & Lan, R. (2017). Dissecting carboxypeptidase E: Properties, functions and pathophysiological roles in disease. *Endocrine Connections*, 6(4), R18-R38.

Ji, Z. S., Dennis Miranda, R., Newhouse, Y. M., Weisgraberyadong Huang, K. H., & Mahley, R. W. (2002). Apolipoprotein E4 potentiates amyloid β peptide-induced lysosomal leakage and apoptosis in neuronal cells. *Journal of Biological Chemistry*, 277(24), 21821–21828.

Johanson, C. E., Duncan, J. A., Klinge, P. M., Brinker, T., Stopa, E. G., & Silverberg, G. D. (2008). Multiplicity of cerebrospinal fluid functions: new challenges in health and disease. Cerebrospinal fluid research, 5(1), 1-32.

Johansson, P., Mattsson, N., Hansson, O., Wallin, A., Johansson, J. O., Andreasson, U., Zetterberg, H., Blennow, K., & Svensson, J. (2011). Cerebrospinal fluid biomarkers for Alzheimer's disease: Diagnostic performance in a homogeneous mono-center population. *Journal of Alzheimer's Disease*, 24(3), 537–546.

Johnston, M. v., & Coyle, J. T. (1981). Development of Central Neurotransmitter Systems. *Ciba Foundation Symposium*, 86, 251-270)

Joo, K. M., Chung, Y. H., Kim, M. K., Nam, R. H., Lee, B. L., Lee, K. H., & Cha, C. I. (2004). Distribution of vasoactive intestinal peptide and pituitary adenylate cyclase-activating polypeptide receptors (VPAC1, VPAC2, and PAC1 receptor) in the rat brain. *Journal of Comparative Neurology*, 476(4), 388–413.

Jourdain, P., Bergersen, L. H., Bhaukaurally, K., Bezzi, P., Santello, M., Domercq, M., Matute, C., Tonello, F., Gundersen, V., & Volterra, A. (2007). Glutamate exocytosis from astrocytes controls synaptic strength. *Nature Neuroscience*, 10(3), 331–339.

Jurzak, M., Muller, A. R., & Gerstberger, R. (1995). Characterization of vasopressin receptors in cultured cells derived from the region of rat brain circumventricular organs. *Neuroscience*, 65(4), 1145-1159.

Kang, J., Jiang, L., Goldman, S. A., & Nedergaard, M. (1998). Astrocyte-mediated potentiation of inhibitory synaptic transmission. *Nature Neuroscience*, 1(8), 683–692.

Kang, S. S., Ren, Y., Liu, C. C., Kurti, A., Baker, K. E., Bu, G., Asmann, Y., & Fryer, J. D. (2018). Lipocalin-2 protects the brain during inflammatory conditions. *Molecular Psychiatry*, 23(2), 344–350.

Katz B. (1969). The release of neural transmitter substances. *Liverpool University Press*, 5-39

Kester, M. I., Teunissen, C. E., Crimmins, D. L., Herries, E. M., Ladenson, J. K. H., Scheltens, P., van der Flier, W. M., Morris, J. C., Holtzman, D. M., & Fagan, A. M. (2015). Neurogranin as a cerebrospinal fluid biomarker for synaptic loss in symptomatic Alzheimer disease. *JAMA Neurology*, 72(11), 1275–1280.

Kettenmann, H., & Ransom, B. R. (2005). Neuroglia. Oxford University Press.

Khakh, B. S. (2019). Astrocyte–neuron interactions in the striatum: insights on identity, form, and function. *Trends in neurosciences*, 42(9), 617-630.

Kim, T., Gondré-lewis, M. C., Arnaoutova, I., Loh, Y. P., Kim, T., & Gondré-, M. C. (2006). Dense-Core Secretory Granule Biogenesis. *Physiology*, 21 (2), 124–133.

Kimelberg, H. K., Goderie, S. K., Higman, S, Pang, S, & Waniewski4, R. A. (1990). Swelling-induced release of glutamate, aspartate, and taurine from astrocyte cultures. *Journal of Neuroscience*, 10(5), 1583-1591.

Kimura, T., Whitcomb, D. J., Jo, J., Regan, P., Piers, T., Heo, S., Brown, C., Hashikawa, T., Murayama, M., Seok, H., Sotiropoulos, I., Kim, E., Collingridge, G. L., Takashima, A., & Cho, K. (2014). Microtubule-associated protein tau is essential for long-term depression in the

hippocampus. *Philosophical Transactions of the Royal Society B: Biological Sciences*, 369(1633), 20130144.

Kitazawa, M., Medeiros, R., & Laferla, F. M. (2012). Transgenic mouse models of Alzheimer disease: developing a better model as a tool for therapeutic interventions. Current pharmaceutical design, 18(8), 1131-1147.

Klafki, H. W., Abramowski, D., Swoboda, R., Paganetti, P. A., & Staufenbiel, M. (1996). The carboxyl termini of β-amyloid peptides 1-40 and 1-42 are generated by distinct γ-secretase activities. *Journal of Biological Chemistry*, 271(45), 28655–28659.

Klein, R. S., & Fricker, L. D. (1992). Heterogeneous expression of carboxypeptidase E and proenkephalin mRNAs by cultured astrocytes. *Brain research*, 569(2), 300-310.

Klunk, W. E., Engler, H., Nordberg, A., Wang, Y., Blomqvist, G., Holt, D. P., Bergström, M., Savitcheva, I., Huang, G.-F., Estrada, S., Ausén, B., Debnath, M. L., Barletta, J., Price, J. C., Sandell, J., Lopresti, B. J., Wall, A., Koivisto, P., Antoni, G., … Långström, B. (2004). Imaging Brain Amyloid in Alzheimer's Disease with Pittsburgh Compound-B. *Annals of Neurology: Official Journal of the American Neurological Association and the Child Neurology Society*, 55(3), 306-319.

Knowles, R. B., Wyart, C., Buldyrev, S. v, Cruz, L., Urbanc, B., Hasselmo, M. E., Eugene Stanley, H., & Hyman, B. T. (1999). Plaque-induced neurite abnormalities: Implications for disruption of neural networks in Alzheimer's disease Proceedings of the National Academy of Sciences, 96(9), 5274-5279.

Kögel, T., & Gerdes, H.-H. (2009). Maturation of secretory granules. Cellular Peptide Hormone Synthesis and Secretory Pathways, 137-184.

Kopeikina, K. J., Hyman, B. J., & Spires-Jones, T. L. (2012). Soluble forms of tau are toxic in alzheimer's disease. *Translational Neuroscience*, 3(3), 223–233.

Kopelman, M. D. (1986). The cholinergic neurotransmitter system in human memory and dementia: a review. *The Quarterly Journal of Experimental Psychology*, 38(4), 535-573.

Kornfeld, S., & Mellman, I. (1989). The biogenesis of lysosomes. Annual review of cell biology, 5(1), 483-525.

Krasemann, S., Madore, C., Cialic, R., Baufeld, C., Calcagno, N., el Fatimy, R., Beckers, L., O'Loughlin, E., Xu, Y., Fanek, Z., Greco, D. J., Smith, S. T., Tweet, G., Humulock, Z., Zrzavy, T., Conde-Sanroman, P., Gacias, M., Weng, Z., Chen, H., … Butovsky, O. (2017). The TREM2-APOE Pathway Drives the Transcriptional Phenotype of Dysfunctional Microglia in Neurodegenerative Diseases. *Immunity*, 47(3), 566-581.e9.

Kreft, M., Stenovec, M., Rupnik, M., Grilc, S., Kržan, M., Potokar, M., Pangršič, T., Haydon, P. G., & Zorec, R. (2004). Properties of Ca2+-dependent exocytosis in cultured astrocytes. *Glia*, 46(4), 437–445.

Krisch, B., Buchholz, C., & Mentlein, R. (1991). Somatostatin binding sites on rat diencephalic astrocytes. *Cell and tissue research*, 263(2), 253–263.

Krisch, B., & Mentlein, R. (1994). Neuropeptide receptors and astrocytes. International review of cytology, 148, 119-169.

Krzan, M., Stenovec, M., Kreft, M., Pangršič, T., Grilc, S., Haydon, P. G., & Zorec, R. (2003). Calcium-dependent exocytosis of atrial natriuretic peptide from astrocytes. *Journal of Neuroscience*, 23(5), 1580–1583.

Kuchibhotla, K. v., Lattarulo, C. R., Hyman, B. T., & Bacskai, B. J. (2009). Synchronous hyperactivity and intercellular calcium waves in astrocytes in Alzheimer mice. *Science*, 323(5918), 1211–1215.

Kuliawat, R., Klumperman, J., Ludwig, T., & Arvan, P. (1997). Differential sorting of lysosomal enzymes out of the regulated secretory pathway in pancreatic β-cells. *The Journal of cell biology*, 137(3), 595-608.

Kwon, S., Moreno-Gonzalez, I., Taylor-Presse, K., Edwards, G., Gamez, N., Calderon, O., Zhu, B., Velasquez, F. C., Soto, C., & Sevick-Muraca, E. M. (2019). Impaired peripheral lymphatic function and cerebrospinal fluid outflow in a mouse model of Alzheimer's disease. Journal of Alzheimer's Disease, 69(2), 585-593.

Lacor, P. N., Buniel, M. C., Chang, L., Fernandez, S. J., Gong, Y., Viola, K. L., Lambert, M. P., Velasco, P. T., Bigio, E. H., Finch, C. E., Krafft, G. A., & Klein, W. L. (2004). Synaptic targeting by Alzheimer's-related amyloid β oligomers. *Journal of Neuroscience*, 24(45), 10191–10200.

Lacor, P. N., Buniel, M. C., Furlow, P. W., Clemente, A. S., Velasco, P. T., Wood, M., Viola, K. L., & Klein, W. L. (2007). Aβ oligomer-induced aberrations in synapse composition, shape, and density provide a molecular basis for loss of connectivity in Alzheimer's disease. *Journal of Neuroscience*, 27(4), 796–807.

Lalo, U., Pankratov, Y., Kirchhoff, F., North, R. A., & Verkhratsky, A. (2006). NMDA receptors mediate neuron-to-glia signaling in mouse cortical astrocytes. *Journal of Neuroscience*, 26(10), 2673–2683.

Landry, M., Vila-Porcile, E., Hökfelt, T., & Calas, A. (2003). Differential routing of coexisting neuropeptides in vasopressin neurons. *European Journal of Neuroscience*, 17(11), 579–589.

Lanoiselée, H. M., Nicolas, G., Wallon, D., Rovelet-Lecrux, A., Lacour, M., Rousseau, S., Richard, A. C., Pasquier, F., Rollin-Sillaire, A., Martinaud, O., Quillard-Muraine, M., de la Sayette, V., Boutoleau-Bretonniere, C., Etcharry-Bouyx, F., Chauviré, V., Sarazin, M., le Ber, I., Epelbaum, S., Jonveaux, T., … Campion, D. (2017). APP, PSEN1, and PSEN2 mutations in early-onset Alzheimer disease: A genetic screening study of familial and sporadic cases. *PLoS medicine*, 14(3), e1002270.

Lasagna-Reeves, C. A., Castillo-Carranza, D. L., Sengupta, U., Sarmiento, J., Troncoso, J., Jackson, G. R., & Kayed, R. (2012). Identification of oligomers at early stages of tau aggregation in Alzheimer's disease. *The FASEB Journal*, 26(5), 1946–1959.

Lassmann, H., Weiler, R., Fischer, P., Bancher, C., Jellinger, K., Floor, E., ... & Winkler, H. (1992). Synaptic pathology in Alzheimer's disease: immunological data for markers of synaptic and large dense-core vesicles. *Neuroscience*, 46(1), 1-8.

Lauder, J. M. (1993). Neurotransmitters as growth regulatory signals: role of receptors and second messengers. *Trends in Neurosciences*, 16(6), 233–240.

Lechner, T., Adlassnig, C., Humpel, C., Kaufmann, W. A., Maier, H., Reinstadler-Kramer, K., ... & Marksteiner, J. (2004). Chromogranin peptides in Alzheimer's disease. *Experimental gerontology*, 39(1), 101-113.

Lee, M. C., Ting, K. K., Adams, S., Brew, B. J., Chung, R., & Guillemin, G. J. (2010). Characterisation of the expression of NMDA receptors in human astrocytes. *PLoS one*, 5(11), e14123.

Lee, S.N., Prodhomme, E., & Lindberg, I. (2004). Prohormone convertase 1 (PC1) processing and sorting: effect of PC1 propeptide and proSAAS. *Journal of endocrinology*, 182(2), 353-364.

Leng, G. (2018). The endocrinology of the brain. *Endocrine connections*, 7(12), R275-R285.

Leon, W. C., Canneva, F., Partridge, V., Allard, S., Ferretti, M. T., Dewilde, A., Vercauteren, F., Atifeh, R., Ducatenzeiler, A., Klein, W., Szyf, M., Alhonen, L., & Cuello, A. C. (2010). A novel transgenic rat model with a full alzheimer's - Like amyloid pathology displays pre - Plaque intracellular amyloid -β- Associated cognitive impairment. *Journal of Alzheimer's Disease*, 20(1), 113–126.

Leplus, A., Lauritzen, I., Melon, C., Kerkerian-Le Goff, L., Fontaine, D., & Checler, F. (2019). Chronic fornix deep brain stimulation in a transgenic Alzheimer's rat model reduces amyloid burden, inflammation, and neuronal loss. *Brain Structure and Function*, 224(1), 363–372.

Lesné, S., Ming, T. K., Kotilinek, L., Kayed, R., Glabe, C. G., Yang, A., Gallagher, M., & Ashe, K. H. (2006). A specific amyloid-β protein assembly in the brain impairs memory. *Nature*, 440(7082), 352–357.

Levy, E., Sastre, M., Kumar, A., Gallo, G., Piccardo, P., Ghetti, B., & Tagliavini, F. (2001). Codeposition of cystatin C with amyloid-β protein in the brain of Alzheimer disease patients. Journal of Neuropathology & Experimental Neurology, 60(1), 94-104.

Lewis, J., Dickson, D. W., Lin, W.-L., Chisholm, L., Corral, A., Jones, G., Yen, S.-H., Sahara, N., Skipper, L., Yager, D., Eckman, C., Hardy, J., Hutton, M., & McGowan, E. (2001). Enhanced Neurofibrillary Degeneration in Transgenic Mice Expressing Mutant Tau and APP. *Science*, 293(5534), 1487–1491.

Lewis, J., Mcgowan, E., Rockwood, J., Melrose, H., Nacharaju, P., van Slegtenhorst, M., Gwinn-Hardy, K., Murphy, M. P., Baker, M., Yu, X., Duff, K., Hardy, J., Corral, A., Lin, W.-L., Yen, S.-H., Dickson, D. W., Davies, P., & Hutton, M. (2000). Neurofibrillary tangles, amyotrophy and progressive motor disturbance in mice expressing mutant (P301L) tau protein. *Nature genetics*, 25(4), 402-405.

Li, X., Kumar, Y., Zempel, H., Mandelkow, E. M., Biernat, J., & Mandelkow, E. (2011). Novel diffusion barrier for axonal retention of Tau in neurons and its failure in neurodegeneration. *The EMBO Journal*, 30(23), 4825–4837.

Li, Z., Jo, J., Jia, J. M., Lo, S. C., Whitcomb, D. J., Jiao, S., Cho, K., & Sheng, M. (2010). Caspase-3 activation via mitochondria is required for long-term depression and AMPA receptor internalization. *Cell*, 141(5), 859–871.

Liaoi, Y. F., Wang, B. J., Cheng, H. T., Kuo, L. H., & Wolfe, M. S. (2004). Tumor necrosis factor-α, interleukin-1β, and interferon-γ stimulate γ-secretase-mediated cleavage of amyloid precursor protein through a JNK-dependent MAPK pathway. *Journal of Biological Chemistry*, 279(47), 49523–49532.

Liddelow, S. A., Guttenplan, K. A., Clarke, L. E., Bennett, F. C., Bohlen, C. J., Schirmer, L., Bennett, M. L., Münch, A. E., Chung, W. S., Peterson, T. C., Wilton, D. K., Frouin, A., Napier, B. A., Panicker, N., Kumar, M., Buckwalter, M. S., Rowitch, D. H., Dawson, V. L., Dawson, T. M., … Barres, B. A. (2017). Neurotoxic reactive astrocytes are induced by activated microglia. *Nature*, 541(7638), 481–487.

Lim, D., Iyer, A., Ronco, V., Grolla, A. A., Canonico, P. L., Aronica, E., & Genazzani, A. A. (2013). Amyloid beta deregulates astroglial mGluR5-mediated calcium signaling via calcineurin and Nf-kB. *Glia*, 61(7), 1134–1145.

Llanos-González, E., Henares-Chavarino, Á. A., Pedrero-Prieto, C. M., García-Carpintero, S., Frontiñán-Rubio, J., Sancho-Bielsa, F. J., Alcain, F. J., Peinado, J. R., Rabanal-Ruíz, Y., & Durán-Prado, M. (2020). Interplay between mitochondrial oxidative disorders and proteostasis in Alzheimer's disease. Frontiers in Neuroscience, 13, 1444.

Lleó, A., Cavedo, E., Parnetti, L., Vanderstichele, H., Herukka, S. K., Andreasen, N., Ghidoni, R., Lewczuk, P., Jeromin, A., Winblad, B., Tsolaki, M., Mroczko, B., Visser, P. J., Santana, I., Svenningsson, P., Blennow, K., Aarsland, D., Molinuevo, J. L., Zetterberg, H., & Mollenhauer, B. (2015). Cerebrospinal fluid biomarkers in trials for Alzheimer and Parkinson diseases. Nature Reviews Neurology, 11(1), 41-55.

Lleó, A., Núñez-Llaves, R., Alcolea, D., Chiva, C., Balateu-Paños, D., Colom-Cadena, M., Gomez-Giro, G., Muñoz, L., Querol-Vilaseca, M., Pegueroles, J., Rami, L., Lladó, A., Molinuevo, J. L., Tainta, M., Clarimón, J., Spires-Jones, T., Blesa, R., Fortea, J., Martínez-Lage, P., … Belbin, O. (2019). Changes in synaptic proteins precede neurodegeneration markers in preclinical Alzheimer's disease cerebrospinal fluid. *Molecular and Cellular Proteomics*, 18(3), 546–560.

López-Benito, S., Sánchez-Sánchez, J., Brito, V., Calvo, L., Lisa, S., Torres-Valle, M., Palko, M. E., Vicente-García, C., Fernández-Fernández, S., Bolaños, J. P., Ginés, S., Tessarollo, L., & Arévalo, J. C. (2018). Regulation of BDNF release by ARMS/Kidins220 through modulation of synaptotagmin-IV levels. *Journal of Neuroscience*, 38(23), 5415–5428.

Ludwig, M., Apps, D., Menzies, J., Patel, J. C., & Rice, M. E. (2017). Dendritic release of neurotransmitters. *Comprehensive Physiology*, 7(1), 235–252.

Ludwig, M., & Leng, G. (2006). Dendritic peptide release and peptide-dependent behaviours. *Nature Reviews Neuroscience*, 7(2), 126-136.

Luisa Cotrina, M., H-C Lin, J., Carlos Ló pez-García, J., G Naus, C. C., & Nedergaard, M. (2000). ATP-mediated glia signaling. Journal of Neuroscience, 20(8), 2835-2844.

Luzio, J. P., Pryor, P. R., & Bright, N. A. (2007). Lysosomes: fusion and function. Nature reviews Molecular cell biology, 8(8), 622-632.

Maeda, J., Ji, B., Irie, T., Tomiyama, T., Maruyama, M., Okauchi, T., Staufenbiel, M., Iwata, N., Ono, M., Saido, T. C., Suzuki, K., Mori, H., Higuchi, M., & Suhara, T. (2007). Longitudinal, quantitative assessment of amyloid, neuroinflammation, and anti-amyloid treatment in a living mouse model of Alzheimer's disease enabled by positron emission tomography. *Journal of Neuroscience*, 27(41), 10957–10968.

Maji, S. K., Anoop, A., Singh, P. K., & Jacob, R. S. (2010). CSF biomarkers for Alzheimer's disease diagnosis.*International Journal of Alzheimer's Disease*, 2010.

Malarkey, E. B., & Parpura, V. (2008). Mechanisms of glutamate release from astrocytes. Neurochemistry international, 52(1-2), 142-154.

Mandelkow, E., Biernat, J., Drewes, G., Gustke, N., Trinczek, B., & Mandelkow, E. (1995). Tau domains, phosphorylation, and interactions with microtubules. Neurobiology of aging, 16(3), 355-362.

Mandelkow, E. M., & Mandelkow, E. (1998). Tau in Alzheimer's disease. *Trends in Cell Biology*, 8(11), 425–427.

Manders, E. M. M., Verbeek, F. J., & Aten, J. A. (1993). Measurement of co-localization of objects in dual-colour confocal images. *Journal of Microscopy*, 169(3), 375–382.

Martens, Y. A., Zhao, N., Liu, C. C., Kanekiyo, T., Yang, A. J., Goate, A. M., Holtzman, D. M., & Bu, G. (2022). ApoE Cascade Hypothesis in the pathogenesis of Alzheimer's disease and related dementias. *Neuron*, 110(8), 1304–1317.

Martineau, M., Galli, T., Baux, G., & Mothet, J. P. (2008). Confocal imaging and tracking of the exocytotic routes for D-serine-mediated gliotransmission. *Glia*, 56(12), 1271–1284.

Martineau, M., Shi, T., Puyal, J., Knolhoff, A. M., Dulong, J., Gasnier, B., Klingauf, J., Sweedler, J. v., Jahn, R., & Mothet, J. P. (2013). Storage and uptake of D-serine into astrocytic synaptic-like vesicles specify gliotransmission. *Journal of Neuroscience*, 33(8), 3413–3423.

Mathews, P. M., & Levy, E. (2016). Cystatin C in aging and in Alzheimer's disease. *Ageing research reviews*, 32, 38-50.

Matos, M., Augusto, E., Agostinho, P., Cunha, R. A., & Chen, J. F. (2013). Antagonistic interaction between adenosine A2A Receptors and Na+/K+-ATPase-α2 controlling glutamate uptake in astrocytes. *Journal of Neuroscience*, 33(47), 18492–18502.

Mattsson, N., Insel, P. S., Palmqvist, S., Portelius, E., Zetterberg, H., Weiner, M., Blennow, K., & Hansson, O. (2016). Cerebrospinal fluid tau, neurogranin, and neurofilament light in Alzheimer's disease. *EMBO Molecular Medicine*, 8(10), 1184–1196.

Maycox, P. R., Hell, J. W., & Jahn, R. (1990). Amino acid neurotransmission: spotlight on synaptic vesicles. Trends in neurosciences, 13(3), 83-87.

Mbikay, M., Seidah, N. G., Chrétien, M. (2001). Neuroendocrine secretory protein 7B2: structure, expression and functions. *Biochemical Journal*, 357(2), 329-342.

McKenzie, J. C. (1992). Atrial natriuretic peptide-like immunoreactivity in astrocytes of parenchyma and glia limitans of the canine brain. *Journal of Histochemistry & Cytochemistry*, 40(8), 1211–1222.

McKenzie, J. C., Juan, Y.-W., Thomas, C. R., Berman, N. E. J., & Klein, R. M. (2001). Atrial natriuretic peptide-like immunoreactivity in neurons and astrocytes of human cerebellum and inferior olivary complex. Journal of Histochemistry & Cytochemistry, 49(11), 1453-1467.

McKhann, G. M., Knopman, D. S., Chertkow, H., Hyman, B. T., Jack, C. R., Kawas, C. H., Klunk, W. E., Koroshetz, W. J., Manly, J. J., Mayeux, R., Mohs, R. C., Morris, J. C., Rossor, M. N., Scheltens, P., Carrillo, M. C., Thies, B., Weintraub, S., & Phelps, C. H. (2011). The diagnosis of dementia due to Alzheimer's disease: Recommendations from the National Institute on Aging-Alzheimer's Association workgroups on diagnostic guidelines for Alzheimer's disease. Alzheimer's & dementia, 7(3), 263-269.

Mehta, P. D., Pirttilä, T., Mehta, S. P., Sersen, E. A., Aisen, P. S., & Wisniewski, H. M. (2000). Plasma and cerebrospinal fluid levels of amyloid β proteins 1-40 and 1-42 in Alzheimer disease. *Archives of Neurology*, 57(1), 100–105.

Merighi, A. (2002). Costorage and coexistence of neuropeptides in the mammalian CNS. *Progress in neurobiology*, 66(3), 161-190.

Merighi, A., Salio, C., Ferrini, F., & Lossi, L. (2011). Neuromodulatory function of neuropeptides in the normal CNS. Journal of chemical neuroanatomy, 42(4), 276-287.

Meyer-Luehmann, M., Spires-Jones, T. L., Prada, C., Garcia-Alloza, M., de Calignon, A., Rozkalne, A., Koenigsknecht-Talboo, J., Holtzman, D. M., Bacskai, B. J., & Hyman, B. T. (2008). Rapid appearance and local toxicity of amyloid-β plaques in a mouse model of Alzheimer's disease. *Nature*, 451(7179), 720–724.

Mi, H., Dong, Q., Muruganujan, A., Gaudet, P., Lewis, S., & Thomas, P. D. (2009). PANTHER version 7: Improved phylogenetic trees, orthologs and collaboration with the Gene Ontology Consortium. *Nucleic Acids Research*, 38(suppl_1), D204-D210.

Mielke, M. M., Hagen, C. E., Xu, J., Chai, X., Vemuri, P., Lowe, V. J., Airey, D. C., Knopman, D. S., Roberts, R. O., Machulda, M. M., Jack, C. R., Petersen, R. C., & Dage, J. L. (2018). Plasma phospho-tau181 increases with Alzheimer's disease clinical severity and is associated with tau- and amyloid-positron emission tomography. *Alzheimer's and Dementia*, 14(8), 989–997.

Mielke, M. M., Vemuri, P., & Rocca, W. A. (2014). Clinical epidemiology of Alzheimer's disease: Assessing sex and gender differences. *Clinical epidemiology*, 6, 37.

Moghadam, P. K., & Jackson, M. B. (2013). The functional significance of synaptotagmin diversity in neuroendocrine secretion. *Frontiers in endocrinology*, 4, 124.

Mondragón-Rodríguez, S., Trillaud-Doppia, E., Dudilot, A., Bourgeois, C., Lauzon, M., Leclerc, N., & Boehm, J. (2012). Interaction of endogenous tau protein with synaptic proteins is regulated by N-methyl-D-aspartate receptor-dependent tau phosphorylation. *Journal of Biological Chemistry*, 287(38), 32040–32053.

Montana, V., Malarkey, E. B., Verderio, C., Matteoli, M., & Parpura, V. (2006). Vesicular transmitter release from astrocytes. *Glia*, 54(7), 700–715.

Montana, V., Ni, Y., Sunjara, V., Hua, X., & Parpura, V. (2004). Vesicular Glutamate Transporter-Dependent Glutamate Release from Astrocytes. *Journal of Neuroscience*, 24(11), 2633–2642.

Moreno, H., Morfini, G., Buitrago, L., Ujlaki, G., Choi, S., Yu, E., Moreira, J. E., Avila, J., Brady, S. T., Pant, H., Sugimori, M., & Llinás, R. R. (2016). Tau pathology-mediated presynaptic dysfunction. *Neuroscience*, 325, 30–38.

Mori, Y., & Fukuda, M. (2011). Synaptotagmin IV acts as a multi-functional regulator of Ca2+-dependent exocytosis. *Neurochemical research*, 36(7), 1222-1227.

Morris, M., Knudsen, G. M., Maeda, S., Trinidad, J. C., Ioanoviciu, A., Burlingame, A. L., & Mucke, L. (2015). Tau post-translational modifications in wild-type and human amyloid precursor protein transgenic mice. *Nature Neuroscience*, 18(8), 1183–1189.

Mosevitsky, M. I. (2005). Nerve ending "signal" proteins GAP-43, MARCKS, and BASP1. *International review of cytology*, 245, 245-325.

Mothet, J.-P., Pollegioni, L., Ouanounou, G., Martineau, M., Fossier, P., & Rard Baux, G. (2005). Glutamate receptor activation triggers a calcium-dependent and SNARE protein-dependent release of the gliotransmitter D-serine. *Proceedings of the National Academy of Sciences*, 102(15), 5606-5611.

Motter, R., Vigo-Pelfrey, C., Kholodenko, D., Barbour, R., Johnson-Wood, K., Galasko, D., Chang, L., Miller, B., Clark, C., Green, Q. R., Olson, M. D., Southwick, P., Wolfert, R., Munroe, B., Lieberburg, I., Seubert, P., & Schenk, D. (1995). Reduction of β-amyloid peptide42 in the cerebrospinal fluid of patients with Alzheimer's disease. *Annals of Neurology: Official Journal of the American Neurological Association and the Child Neurology Society*, 38(4), 643-648.

Mulder, S. D., Veerhuis, R., Blankenstein, M. A., & Nielsen, H. M. (2012). The effect of amyloid associated proteins on the expression of genes involved in amyloid-β clearance by adult human astrocytes. *Experimental Neurology*, 233(1), 373–379.

Muller, L., Cameron, A., Fortenberry, Y., Apletalina, E. v., & Lindberg, I. (2000). Processing and sorting of the prohormone convertase 2 propeptide. *Journal of Biological Chemistry*, 275(50), 39213–39222.

Muller, L., Zhu, X., & Lindberg, I. (1997). Mechanism of the facilitation of PC2 maturation by 7B2: involvement in ProPC2 transport and activation but not folding. *The Journal of cell biology*, 139(3), 625-638.

Muñoz, P., Ardiles, Á. O., Pérez-Espinosa, B., Núñez-Espinosa, C., Paula-Lima, A., González-Billault, C., & Espinosa-Parrilla, Y. (2020). Redox modifications in synaptic components as biomarkers of cognitive status, in brain aging and disease. *Mechanisms of Ageing and Development*, 189, 111250.

Muñoz-Moreno, E., Tudela, R., López-Gil, X., & Soria, G. (2018). Early brain connectivity alterations and cognitive impairment in a rat model of Alzheimer's disease. *Alzheimer's Research and Therapy*, 10(1), 1-17.

Navarrete, M., & Araque, A. (2010). Endocannabinoids potentiate synaptic transmission through stimulation of astrocytes. *Neuron*, 68(1), 113–126.

Navarrete, M., Perea, G., de Sevilla, D. F., Gómez-Gonzalo, M., Núñez, A., Martín, E. D., & Araque, A. (2012). Astrocytes mediate in vivo cholinergic-induced synaptic plasticity. *PLoS biology*, 10(2), e1001259.

Neher, E., & Zuckert, R. S. (1993). Multiple calcium-dependent processes related to secretion in bovine chromaffin cells. *Neuron*, 10(1), 21-30.

Nett, W. J., Oloff, S. H., & Mccarthy, K. D. (2002). Hippocampal astrocytes in situ exhibit calcium oscillations that occur independent of neuronal activity. *Journal of Neurophysiology*, 87(1), 528–537.

Nez, A. I. J., Castro, E., Mirabet, M., Franco, R., Delicado, E. G., Mari´a, A., Mari´a, M., & Miras-Portugal, T. (1999). Potentiation of ATP calcium responses by A2B receptor stimulation and other signals coupled to Gs proteins in type-1 cerebellar astrocytes. Glia, 26(2), 119-128.

Nilsson, J., Gobom, J., Sjödin, S., Brinkmalm, G., Ashton, N. J., Svensson, J., Johansson, P., Portelius, E., Zetterberg, H., Blennow, K., & Brinkmalm, A. (2021). Cerebrospinal fluid biomarker panel for synaptic dysfunction in alzheimer's disease. *Alzheimer's and Dementia: Diagnosis, Assessment and Disease Monitoring,* 13(1), e12179.

Nishizaki, T., Nagai, K., Nomura, T., Tada, H., Kanno, T., Tozaki, H., Li, X. X., Kondoh, T., Kodama, N., Takahashi, E., Sakai, N., Tanaka, K., & Saito, N. (2002). A new neuromodulatory pathway with a glial contribution mediated via A2a adenosine receptors. *Glia*, 39(2), 133–147.

Nixon, R. A. (2013). The role of autophagy in neurodegenerative disease. Nature medicine, 19(8), 983-997.

Oakley, H., Cole, S. L., Logan, S., Maus, E., Shao, P., Craft, J., Guillozet-Bongaarts, A., Ohno, M., Disterhoft, J., van Eldik, L., Berry, R., & Vassar, R. (2006). Intraneuronal β-amyloid aggregates, neurodegeneration, and neuron loss in transgenic mice with five familial Alzheimer's disease mutations: potential factors in amyloid plaque formation. *Journal of Neuroscience*, 26(40), 10129–10140.

O'Callaghan, J. P., & Sriram, K. (2005). Glial fibrillary acidic protein and related glial proteins as biomarkers of neurotoxicity. *Expert opinion on drug safety*, 4(3), 433-442.

Octeau, J. C., Chai, H., Jiang, R., Bonanno, S. L., Martin, K. C., & Khakh, B. S. (2018). An optical neuron-astrocyte proximity assay at synaptic distance scales. *Neuron*, 98(1), 49-66.

Oddo, S., Caccamo, A., Kitazawa, M., Tseng, B. P., & LaFerla, F. M. (2003). Amyloid deposition precedes tangle formation in a triple transgenic model of Alzheimer's disease. *Neurobiology of Aging*, 24(8), 1063–1070.

Ormel, L., Stensrud, M. J., Chaudhry, F. A., & Gundersen, V. (2012). A distinct set of synaptic-like microvesicles in atroglial cells contain VGLUT3. *Glia*, 60(9), 1289–1300.

Paco, S., Margeli, M., Olkkonen, V., Imai, A., Blasi, J., Fischer-Colbrie, R., & Aguado, F. (2009). Regulation of exocytotic protein expression and Ca2+-dependent peptide secretion in astrocytes. *Journal of neurochemistry*, 110, 143–156.

Paco, S., Pozas, E., & Aguado, F. (2010). Secretogranin III is an astrocyte granin that is overexpressed in reactive glia. *Cerebral Cortex*, 20(6), 1386–1397.

Paco, S., Hummel, M., Plá, V., Sumoy, L., & Aguado, F. (2016). Cyclic AMP signaling restricts activation and promotes maturation and antioxidant defenses in astrocytes. BMC genomics, 17(1), 1-11.

Palade, G. E. (1956). Intracisternal granules in the exocrine cells of the pancreas. *The Journal of Cell Biology*, 2(4), 417–422.

Panatier, A., Theodosis, D. T., Mothet, J. P., Touquet, B., Pollegioni, L., Poulain, D. A., & Oliet, S. H. R. (2006). Glia-Derived d-Serine Controls NMDA Receptor Activity and Synaptic Memory. *Cell*, 125(4), 775–784.

Pangršič, T., Potokar, M., Stenovec, M., Kreft, M., Fabbretti, E., Nistri, A., Pryazhnikov, E., Khiroug, L., Giniatullin, R., & Zorec, R. (2007). Exocytotic release of ATP from cultured astrocytes. *Journal of Biological Chemistry*, 282(39), 28749–28758.

Parhizkar, S., & Holtzman, D. M. (2022). APOE mediated neuroinflammation and neurodegeneration in Alzheimer's disease. *Seminars in Immunology*. 101594.

Park, H., & Poo, M. M. (2013). Neurotrophin regulation of neural circuit development and function. *Nature Reviews Neuroscience*, 14(1), 7-23.

Park, J. J., Cawley, N. X., & Loh, Y. P. (2008). Carboxypeptidase E cytoplasmic tail-driven vesicle transport is key for activity-dependent secretion of peptide hormones. *Molecular Endocrinology*, 22(4), 989–1005.

Park, S. A., Jung, J. M., Park, J. S., Lee, J. H., Park, B., Kim, H. J., Park, J. H., Chae, W. S., Jeong, J. H., Choi, S. H., & Baek, J. H. (2020). SWATH-MS analysis of cerebrospinal fluid to generate a robust battery of biomarkers for Alzheimer's disease. *Scientific Reports*, 10(1), 1-10.

Parpura, V., Basarsky, T. A., Liu, F., Jeftinija, K., & Jeftinija, S. & H. P. G. (1994). Glutamate-mediated astrocyte–neuron signalling. *Nature*, 369(6483), 744–747.

Parpura, V., Fang, Y., Basarsky, T., Jahn, R., & Haydon, P. G. (1995). Expression of synaptobrevin II, cellubrevin and syntaxin but not SNAP-25 in cultured astrocytes. FEBS letters, 377(3), 489-492.

Parpura, V., Heneka, M. T., Montana, V., Oliet, S. H. R., Schousboe, A., Haydon, P. G., Stout, R. F., Spray, D. C., Reichenbach, A., Pannicke, T., Pekny, M., Pekna, M., Zorec, R., & Verkhratsky, A. (2012). Glial cells in (patho)physiology. *Journal of neurochemistry*, 121(1), 4-27.

Pedrero-Prieto, C. M., Frontiñán-Rubio, J., Alcaín, F. J., Durán-Prado, M., Peinado, J. R., & Rabanal-Ruiz, Y. (2021). Biological significance of the protein changes occurring in the cerebrospinal fluid of alzheimer's disease patients: Getting clues from proteomic studies. *Diagnostics*, 11(9), 1655.

Pedrero-Prieto, C. M., García-Carpintero, S., Frontiñán-Rubio, J., Llanos-González, E., Aguilera García, C., Alcaín, F. J., Lindberg, I., Durán-Prado, M., Peinado, J. R., & Rabanal-Ruiz, Y.

(2020). A comprehensive systematic review of CSF proteins and peptides that define Alzheimer's disease. *Clinical proteomics*, 17(1), 1-24.

Perea, G., & Araque, A. (2007). Astrocytes potentiate transmitter release at single hippocampal synapses. *Science*, 317, 1083–1086.

Perea, G., Navarrete, M., & Araque, A. (2009). Tripartite synapses: astrocytes process and control synaptic information. *Trends in Neurosciences*, 32(8), 421-431.

Pereda, A. E. (2014). Electrical synapses and their functional interactions with chemical synapses. *Nature Reviews Neuroscience*, 15(4), 250-263.

Perrin, R. J., Fagan, A. M., & Holtzman, D. M. (2009). Multimodal techniques for diagnosis and prognosis of Alzheimer's disease. *Nature*, 461(7266), 916-922.

Persoon, C., Moro, A., Nassal, J., Farina, M., Broeke, J., Arora, S., & Verhage, M. (2018). Pool size estimations for dense-core vesicles in mammalian CNS neurons. *The EMBO journal*, 37(20), e99672.

Piacentini, R., Li Puma, D. D., Mainardi, M., Lazzarino, G., Tavazzi, B., Arancio, O., & Grassi, C. (2017). Reduced gliotransmitter release from astrocytes mediates tau-induced synaptic dysfunction in cultured hippocampal neurons. *Glia*, 65(8), 1302–1316.

Pitas, R. E., Boyles, J. K., Lee, S. H., Foss, D., & Mahley, R. W. (1987). Astrocytes synthesize apolipoprotein E and metabolize apolipoprotein E-containing lipoproteins. *Biochimica et Biophysica Acta (BBA)-Lipids and Lipid Metabolism*, 917(1), 148–161.

Plá, V., Barranco, N., Pozas, E., & Aguado, F. (2017). Amyloid-β impairs vesicular secretion in neuronal and astrocyte peptidergic transmission. *Frontiers in Molecular Neuroscience*, 10, 202.

Plá, V., Paco, S., Ghezali, G., Ciria, V., Pozas, E., Ferrer, I., & Aguado, F. (2013). Secretory sorting receptors Carboxypeptidase E and Secretogranin III in amyloid β-associated neural degeneration in Alzheimer's Disease. *Brain Pathology*, 23(3), 274–284.

Platel, J. C., Dave, K. A., & Bordey, A. (2008). Control of neuroblast production and migration by converging GABA and glutamate signals in the postnatal forebrain. The Journal of physiology, 586(16), 3739-3743.

Porter, J. T., & McCarthy, K. D. (1995). Adenosine receptors modulate [Ca 2+]i in hippocampal astrocytes in situ. *Journal of Neurochemistry*, 65(4), 1515–1523.

Porter, J. T., & Mccarthy, K. D. (1996). Hippocampal astrocytes in situ respond to glutamate released from synaptic terminals. Journal of Neuroscience, 16(16), 5073-5081.

Potokar, M., Stenovec, M., Kreft, M., Kreft, M. E., & Zorec, R. (2008). Stimulation inhibits the mobility of recycling peptidergic vesicles in astrocytes. *Glia*, 56(2), 135–144.

Prasad, H., & Rao, R. (2018). Amyloid clearance defect in ApoE4 astrocytes is reversed by epigenetic correction of endosomal pH. *Proceedings of the National Academy of Sciences of the United States of America*, 115(28), E6640–E6649.

Proia, P., Schiera, G., Mineo, M., Ingrassia, A. M. R., Santoro, G., Savettieri, G., & di Liegro, I. (2008). Astrocytes shed extracellular vesicles that contain fibroblast growth factor-2 and vascular endothelial growth factor. *International journal of molecular medicine*, 21(1), 63–67.

Proskauer Pena, S. L., Mallouppas, K., Oliveira, A. M. G., Zitricky, F., Nataraj, A., & Jezek, K. (2021). Early spatial memory impairment in a double transgenic model of Alzheimer's Disease TgF344-AD. *Brain Sciences*, 11(10).

Puntman, D. C., Arora, S., Farina, M., Toonen, R. F., & Verhage, M. (2021). Munc18-1 is essential for neuropeptide secretion in neurons. *Journal of Neuroscience*, 41(28), 5980–5993.

Putcha, G. v, Deshmukh, M., & Johnson, E. M. (1999). BAX translocation is a critical event in neuronal apoptosis: regulation by neuroprotectants, BCL-2, and caspases. *Journal of Neuroscience*, 19(17), 7476-7485.

Quintanilla, R. A., Orellana, J. A., & von Bernhardi, R. (2012). Understanding risk factors for Alzheimer's disease: interplay of neuroinflammation, connexin-based communication and oxidative stress. *Archives of Medical Research*, 43(8), 632-644.

Raingo, J., Khvotchev, M., Liu, P., Darios, F., Li, Y. C., Ramirez, D. M. O., Adachi, M., Lemieux, P., Toth, K., Davletov, B., & Kavalali, E. T. (2012). VAMP4 directs synaptic vesicles to a pool that selectively maintains asynchronous neurotransmission. *Nature Neuroscience*, 15(5), 738–745.

Ramamoorthy, P., & Whim, M. D. (2008). Trafficking and fusion of neuropeptide Y-containing dense-core granules in astrocytes. *Journal of Neuroscience*, 28(51), 13815–13827.

Ramirez, D. M. O., Khvotchev, M., Trauterman, B., & Kavalali, E. T. (2012). Vti1a identifies a vesicle pool that preferentially recycles at rest and maintains spontaneous neurotransmission. Neuron, 73(1), 121-134.

Rao, S. K., Huynh, C., Proux-Gillardeaux, V., Galli, T., & Andrews, N. W. (2004). Identification of SNAREs Involved in Synaptotagmin VII-regulated Lysosomal Exocytosis. *Journal of Biological Chemistry*, 279(19), 20471–20479.

Reddy, P. H. (2011). Abnormal tau, mitochondrial dysfunction, impaired axonal transport of mitochondria, and synaptic deprivation in Alzheimer's disease. *Brain research*, 1415, 136-148.

Remnestål, J., Just, D., Mitsios, N., Fredolini, C., Mulder, J., Schwenk, J. M., Uhlén, M., Kultima, K., Ingelsson, M., Kilander, L., Lannfelt, L., Svenningsson, P., Nellgård, B., Zetterberg, H., Blennow, K., Nilsson, P., & Häggmark-Månberg, A. (2016). CSF profiling of the human brain enriched proteome reveals associations of neuromodulin and neurogranin to Alzheimer's disease. *PROTEOMICS - Clinical Applications*, 10(12), 1242–1253.

Renner, M., Lacor, P. N., Velasco, P. T., Xu, J., Contractor, A., Klein, W. L., & Triller, A. (2010). Deleterious Effects of Amyloid β Oligomers Acting as an Extracellular Scaffold for mGluR5. *Neuron*, 66(5), 739–754.

Reumiller, C. M., Schmidt, G. J., Dhrami, I., Umlauf, E., Rappold, E., & Zellner, M. (2018). Gender-related increase of tropomyosin-1 abundance in platelets of Alzheimer's disease and mild cognitive impairment patients. *Journal of Proteomics*, 178, 73–81.

Reyes, R. C., Verkhratsky, A., & Parpura, V. (2012). Plasmalemmal Na+/Ca2+ exchanger modulates Ca2+-dependent exocytotic release of glutamate from rat cortical astrocytes. *ASN Neuro*, 4(1), 33–45.

Rizzoli, S. O., & Betz, W. J. (2005). Synaptic vesicle pools. *Nature Reviews Neuroscience*, 6(1), 57-69.

Rorsman, P., Eliasson, L., Renstrom, E., Gromada, J., Barg, S., & Gopel, S. (2000). The cell physiology of biphasic insulin secretion. *Physiology*, 15(2), 72–77.

Ryder, J., Su, Y., Liu, F., Li, B., Zhou, Y., & Ni, B. (2003). Divergent roles of GSK3 and CDK5 in APP processing. *Biochemical and Biophysical Research Communications*, 312(4), 922–929.

Sandelius, Å., Portelius, E., Källén, Å., Zetterberg, H., Rot, U., Olsson, B., Toledo, J. B., Shaw, L. M., Lee, V. M. Y., Irwin, D. J., Grossman, M., Weintraub, D., Chen-Plotkin, A., Wolk, D. A., McCluskey, L., Elman, L., Kostanjevecki, V., Vandijck, M., McBride, J., … Blennow, K. (2019). Elevated CSF GAP-43 is Alzheimer's disease specific and associated with tau and amyloid pathology. *Alzheimer's and Dementia*, 15(1), 55–64.

Sanders, D. W., Kaufman, S. K., DeVos, S. L., Sharma, A. M., Mirbaha, H., Li, A., Barker, S. J., Foley, A. C., Thorpe, J. R., Serpell, L. C., Miller, T. M., Grinberg, L. T., Seeley, W. W., & Diamond, M. I. (2014). Distinct tau prion strains propagate in cells and mice and define different tauopathies. *Neuron*, 82(6), 1271–1288.

Santello, M., Bezzi, P., & Volterra, A. (2011). TNFα controls glutamatergic gliotransmission in the hippocampal dentate gyrus. *Neuron*, 69(5), 988–1001.

Sastre, M., Dewachter, I., Landreth, G. E., Willson, T. M., Klockgether, T., van Leuven, F., & Heneka, M. T. (2003). Nonsteroidal anti-inflammatory drugs and peroxisome proliferator-activated receptor-γ agonists modulate immunostimulated processing of amyloid precursor protein through regulation of β-secretase. *Journal of Neuroscience*, 23(30), 9796–9804.

Savtchouk, I., & Volterra, A. (2018). Gliotransmission: Beyond black-and-white. *Journal of Neuroscience*, 38(1), 14–25.

Sbai, O., Ould-Yahoui, A., Ferhat, L., Gueye, Y., Bernard, A., Charrat, E., Mehanna, A., Risso, J. J., Chauvin, J. P., Fenouillet, E., Rivera, S., & Khrestchatisky, M. (2010). Differential vesicular distribution and trafficking of MMP-2, MMP-9, and their inhibitors in astrocytes. *Glia*, 58(3), 344–366.

Scemes, E., & Giaume, C. (2006). Astrocyte calcium waves: what they are and what they do. *Glia*, 54(7), 716-725.

Scheff, S. W., DeKosky, S. T., & Price, D. A. (1990). Quantitative Assessment of Cortical Synaptic Density in Alzheimer's Disease. *Neurobiology of Aging*, 11(1), 29–37.

Scheuner, D., Eckman, C., Jensen, M., Song, X., Citron, M., Suzuki, N., & Younkin, S. (1996). Secreted amyloid β–protein similar to that in the senile plaques of Alzheimer's disease is increased in vivo by the presenilin 1 and 2 and APP mutations linked to familial Alzheimer's disease. *Nature Medicine*, 2(8), 864–870.

Schipke, C. G., Ohlemeyer, C., Matyash, M., Nolte, C., Kettenmann, H., & Kirchhoff, F. (2001). Astrocytes of the mouse neocortex express functional N-methyl-D-aspartate receptors. *The FASEB Journal*, 15(7), 1270–1272.

Seidah, N. G., & Chretien, M. (1999). Proprotein and prohormone convertases: a family of subtilases generating diverse bioactive polypeptides 1. *Brain research*, 848(1-2), 45-62.

Selkoe, D. J. (1991). The molecular pathology of Alzheimer's disease. *Neuron*, 6(4), 487-498.

Selkoe, D. J. (2002). Alzheimer's Disease Is a Synaptic Failure. *Science*, 298(5594), 789–791.

Selkoe, D. J., & Hardy, J. (2016). The amyloid hypothesis of Alzheimer's disease at 25 years. *EMBO Molecular Medicine*, 8(6), 595–608.

Serrano-Pozo, A., Frosch, M. P., Masliah, E., & Hyman, B. T. (2011). Neuropathological alterations in Alzheimer disease. *Cold Spring Harbor Perspectives in Medicine*, 1(1).

Shankar, G. M., Li, S., Mehta, T. H., Garcia-Munoz, A., Shepardson, N. E., Smith, I., Brett, F. M., Farrell, M. A., Rowan, M. J., Lemere, C. A., Regan, C. M., Walsh, D. M., Sabatini, B. L., & Selkoe, D. J. (2008). Amyloid-β protein dimers isolated directly from Alzheimer's brains impair synaptic plasticity and memory. *Nature Medicine*, 14(8), 837–842.

Sheng, M., Sabatini, B. L., & Südhof, T. C. (2012). Synapses and Alzheimer's disease. *Cold Spring Harbor Perspectives in Biology*, 4(5), 10.

Shimojo, M., Courchet, J., Pieraut, S., Torabi-Rander, N., Sando, R., Polleux, F., & Maximov, A. (2015). SNAREs Controlling Vesicular Release of BDNF and Development of Callosal Axons. *Cell Reports*, 11(7), 1054–1066.

Shuey, D. L., Sadler, T. W., Tamir, H., & Lauder, J. M. (1993). Serotonin and morphogenesis. *Anatomy and Embryology*, 187(1), 75–85.

Sjögren, M., Davidsson, P., Gottfries, J., Vanderstichele, H., Edman, Å., Vanmechelen, E., Wallin, A., & Blennow, K. (2001). The cerebrospinal fluid levels of tau, growth-associated protein-43 and soluble amyloid precursor protein correlate in Alzheimer's disease, reflecting a common pathophysiological process. Dementia and geriatric cognitive disorders, 12(4), 257-264.

Skowrońska, K., Obara-Michlewska, M., Zielińska, M., & Albrecht, J. (2019). NMDA receptors in astrocytes: In search for roles in neurotransmission and astrocytic homeostasis. *International journal of molecular sciences*, 20(2), 309.

Snyder, E. M., Nong, Y., Almeida, C. G., Paul, S., Moran, T., Choi, E. Y., Nairn, A. C., Salter, M. W., Lombroso, P. J., Gouras, G. K., & Greengard, P. (2005). Regulation of NMDA receptor trafficking by amyloid-β. *Nature Neuroscience*, 8(8), 1051–1058.

Söllner, T., Whiteheart, S. W., Brunner, M., Erdjument-Bromage, H., Geromanos, S., Tempst, P., & Rothman, J. E. (1993). SNAP receptors implicated in vesicle targeting and fusion. *Nature*, 362(6418), 318–324.

Song, L., & Fricker, L. D. (1995). Calcium- and pH-dependent aggregation of carboxypeptidase E. *Journal of Biological Chemistry*, 270(14), 7963–7967.

Sperlágh, B., Vizi, E. S., Wirkner, K., & Illes, P. (2006). P2X7 receptors in the nervous system. *Progress in neurobiology*, 78(6), 327-346.

Sperling, R. A., Aisen, P. S., Beckett, L. A., Bennett, D. A., Craft, S., Fagan, A. M., Iwatsubo, T., Jack, C. R., Kaye, J., Montine, T. J., Park, D. C., Reiman, E. M., Rowe, C. C., Siemers, E., Stern, Y., Yaffe, K., Carrillo, M. C., Thies, B., Morrison-Bogorad, M., … Phelps, C. H. (2011). Toward defining the preclinical stages of Alzheimer's disease: Recommendations from the National Institute on Aging-Alzheimer's Association workgroups on diagnostic guidelines for Alzheimer's disease. *Alzheimer's and Dementia*, 7(3), 280–292.

Spitzer, N. C., Gu, X., & Olson, E. (1994). Action potentials, calcium transients and the control of differentiation of excitable cells. Current opinion in neurobiology, 4(1), 70-77.

Spruce, B. A., Curtis, R., Wilkin, G. P., & Glover, D. M. (1990). A neuropeptide precursor in cerebellum: proenkephalin exists in subpopulations of both neurons and astrocytes. *The EMBO journal*, 9(6), 1787–1795.

Stadelmann, C., Deckwerth, T. L., Srinivasan, A., Bancher, C., Brü, W., Jellinger, K., & Lassmann, H. (1999). Activation of caspase-3 in single neurons and autophagic granules of granulovacuolar degeneration in Alzheimer's disease: evidence for apoptotic cell death. *The American Journal of Pathology*, 155(5), 1459–1466.

Steiner, D. F. (1998). The proprotein convertases. *Current Opinion in Chemical Biology*, 2(1), 31–39.

Stoiljkovic, M., Kelley, C., Stutz, B., Horvath, T. L., & Hajós, M. (2019). Altered Cortical and Hippocampal Excitability in TgF344-AD Rats Modeling Alzheimer's Disease Pathology. *Cerebral Cortex*, 29(6), 2716–2727.

Stokin, G. B., & Goldstein, L. S. B. (2006). Axonal transport and Alzheimer's disease. *Annual review of biochemistry*, 75(1), 607-627.

Stoothoff, W. H., & Johnson, G. V. W. (2005). Tau phosphorylation: physiological and pathological consequences. *Biochimica et Biophysica Acta (BBA)-Molecular Basis of Disease*, 1739(2-3), 280-297.

Strimbu, K., & Tavel, J. A. (2010). What are biomarkers?. *Current Opinion in HIV and AIDS*, 5(6), 463.

Strittmatter, W. J., Weisgraber, K. H., Huang, D. Y., Dong, L.-M., Salvesen1, G. S., Pericak-Vance, M., Schmechel, D., Saunders, A. M., Goldgaberii, D., & Roses, A. D. (1993). Binding of human apolipoprotein E to synthetic amyloid-β peptide: Isoform-specific effects and implications for late-onset Alzheimer disease. *Proceedings of the National Academy of Sciences*, 90(17), 8098-8102

Sturchler-Pierrat, C., Abramowski, D., Wiederhold, K.-H., Mistl, C., Rothacher, S., Ledermann, B., Bu¨rkibu¨rki, K., Frey, P., Paganetti, P. A., Waridel, C., Calhoun, M. E., Jucker, M., Probst, A., Staufenbiel, M., & Sommer, B. (1997). Two amyloid precursor protein transgenic mouse models with Alzheimer disease-like pathology. *Proceedings of the National Academy of Sciences*, 94(24), 13287-13292.

Suárez-Calvet, M., Kleinberger, G., Araque Caballero, M. Á., Brendel, M., Rominger, A., Alcolea, D., Fortea, J., Lleó, A., Blesa, R., Gispert, J. D., Sánchez-Valle, R., Antonell, A., Rami, L., Molinuevo, J. L., Brosseron, F., Traschütz, A., Heneka, M. T., Struyfs, H., Engelborghs, S., … Haass, C. (2016). sTREM 2 cerebrospinal fluid levels are a potential biomarker for microglia

activity in early-stage Alzheimer's disease and associate with neuronal injury markers. *EMBO Molecular Medicine*, 8(5), 466–476.

Südhof, T. C. (2004). The synaptic vesicle cycle. *Annual Review of Neuroscience*, 27, 509–547.

Südhof, T. C. (2012). The presynaptic active zone. *Neuron*, 75(1), 11-25.

Sumners, C., Tang, W., Paulding, W., & Raizada, M. K. (1994). Peptide receptors in astroglia: focus on angiotensin II and atrial natriuretic peptide. *Glia*, 11(2), 110-116.

Sun, W., Mcconnell, E., Pare, J.-F., Xu, Q., Chen, M., Peng, W., Lovatt, D., Han, X., Smith, Y., & Nedergaard, M. (2013). Glutamate-dependent neuroglial calcium signaling differs between young and adult brain. *Science*, 339(6116), 197–200.

Sun, Z., & Südhof, T. C. (2021). A simple Ca2+-imaging approach to neural network analyses in cultured neurons. *Journal of neuroscience methods*, 349, 109041.

Swerdlow, R. H., & Khan, S. M. (2004). A "mitochondrial cascade hypothesis" for sporadic Alzheimer's disease. *Medical Hypotheses*, 63(1), 8–20.

Szatkowski, M., Barbour, B., & Attwell, D. (1990). Non-vesicular release of glutamate from glial cells by reversed electrogenic glutamate uptake. *Nature*, 348(6300), 443–446.

Sze, C. I., Troncoso, J. C., Kawas, C., Mouton, P., Price, D. L., & Martin, L. J. (1997). Loss of the presynaptic vesicle protein synaptophysin in hippocampus correlates with cognitive decline in Alzheimer disease. *Journal of Neuropathology & Experimental Neurology*, 56(8), 933-944.

Takamori, S., Riedel, D., & Jahn, R. (2000). Immunoisolation of GABA-specific synaptic vesicles defines a functionally distinct subset of synaptic vesicles. *Journal of Neuroscience*, 20(13), 4904-4911.

Takeuchi, T., Duszkiewicz, A. J., & Morris, R. G. M. (2014). The synaptic plasticity and memory hypothesis: Encoding, storage and persistence. *Philosophical Transactions of the Royal Society B: Biological Sciences*, 369(1633), 20130288.

Tallent, M. K. (2007). Presynaptic inhibition of glutamate release by neuropeptides: use-dependent synaptic modification. *Inhibitory Regulation of Excitatory Neurotransmission*, 177-200.

Tamaoka, A., Fukushima, T., Sawamura, N., Ishikawa, ya, Oguni, E., Komatsuzaki, Y., & Shoji, ichi. (1996). Amyloid β protein in plasma from patients with sporadic Alzheimer's disease. *Journal of the Neurological Sciences*, 141(1-2), 65–68.

Tanemura, K., Murayama, M., Akagi, T., Hashikawa, T., Tominaga, T., Ichikawa, M., Yamaguchi, H., & Takashima, A. (2001). Neurodegeneration with tau accumulation in a transgenic mouse expressing V337M human tau. Journal of Neuroscience, 22(1), 133-141.

Tanzi, R. E. (2012). The genetics of Alzheimer disease. *Cold Spring Harbor Perspectives in Medicine*, 2(10), a006296.

Tatebayashi, Y., Miyasaka, T., Chui, D.-H., Akagi, T., Mishima, K.-I., Iwasaki, K., Fujiwara, M., Tanemura, K., Murayama, M., Koichi, I., Planel, E., Sato, S., Hashikawa, T., & Takashima, A. (2002). Tau filament formation and associative memory deficit in aged mice expressing mutant (R406W) human tau. *Proceedings of the National Academy of Sciences*, 99(21), 13896–13901.

Taupenot, L., Harper, K. L., Mahapatra, N. R., Parmer, R. J., Mahata, S. K., & O'Connor, D. T. (2002). Identification of a novel sorting determinant for the regulated pathway in the secretory protein chromogranin A. *Journal of Cell Science*, 115(24), 4827–4841.

Taupenot, L., Harper, K. L., & O'connor, D. T. (2003). The chromogranin–secretogranin family. *New England Journal of Medicine*, 348(12), 1134-1149.

Terry, R. D., Masliah, E., Salmon, D. P., Butters, N., Deteresa, R., Hill, R., Hansen, L. A., & Katzman, R. (1991). Physical basis of cognitive alterations in Alzheimer's disease: synapse loss is the major correlate of cognitive impairment. *Annals of Neurology: Official Journal of the American Neurological Association and the Child Neurology Society*, 30(4), 572-580

Thomas, P. D., Campbell, M. J., Kejariwal, A., Mi, H., Karlak, B., Daverman, R., Diemer, K., Muruganujan, A., & Narechania, A. (2003). PANTHER: a library of protein families and subfamilies indexed by function. *Genome Research*, 13(9), 2129–2141.

Thorsell, A., Bjerke, M., Gobom, J., Brunhage, E., Vanmechelen, E., Andreasen, N., Hansson, O., Minthon, L., Zetterberg, H., & Blennow, K. (2010). Neurogranin in cerebrospinal fluid as a marker of synaptic degeneration in Alzheimer's disease. *Brain Research*, 1362, 13–22.

Thureson-Klein, A. K., & Klein, R. L. (1990). Exocytosis from neuronal large dense-cored vesicles. *International review of cytology*, 121, 67-126.

Tible, M., Sandelius, Å., Höglund, K., Brinkmalm, A., Cognat, E., Dumurgier, J., Zetterberg, H., Hugon, J., Paquet, C., & Blennow, K. (2020). Dissection of synaptic pathways through the CSF biomarkers for predicting Alzheimer disease. *Neurology*, 95(8), e953–e961.

Tizon, B., Sahoo, S., Yu, H., Gauthier, S., Kumar, A. R., Mohan, P., Figliola, M., Pawlik, M., Grubb, A., Uchiyama, Y., Bandyopadhyay, U., Cuervo, A. M., Nixon, R. A., & Levy, E. (2010). Induction of autophagy by cystatin C: A mechanism that protects murine primary cortical neurons and neuronal cell lines. *PLoS one*, 5(3), e9819.

Tobin, V., Schwab, Y., Lelos, N., Onaka, T., Pittman, Q. J., & Ludwig, M. (2012). Expression of Exocytosis Proteins in Rat Supraoptic Nucleus Neurones. *Journal of Neuroendocrinology*, 24(4), 629–641.

Torrens, Y., Beaujouan, J. C., Saffroy, M., Daguet De Montety, M. C., Bergstrom, L., & Glowinski, J. (1986). Substance P receptors in primary cultures of cortical astrocytes from the mouse. *Proceedings of the National Academy of Sciences*, 83(23), 9216-9220.

Tsai, M.-S., Tangalos, E. G., Petersen, R. C., Smith, G. E., Schaid, D. J., Kokmen, E., Lvnik, R. J., & Thibodeau, S. N. (1994). Apolipoprotein E: risk factor for Alzheimer disease. *American journal of human genetics*, 54(4), 643.

Tulloch, J., Leong, L., Thomson, Z., Chen, S., Lee, E. G., Keene, C. D., Millard, S. P., & Yu, C. E. (2018). Glia-specific APOE epigenetic changes in the Alzheimer's disease brain. *Brain Research*, 1698, 179–186.

Ueda, K., Shinohara, S., Yagami, T., Asakura, K., & Kawasaki, K. (1997). Amyloid β protein potentiates Ca2+ influx through L-type voltage-sensitive Ca2+ channels: a possible involvement of free radicals. *Journal of neurochemistry*, 68(1), 265-271.

Ulgen, E., Ozisik, O., & Sezerman, O. U. (2019). PathfindR: An R package for comprehensive identification of enriched pathways in omics data through active subnetworks. *Frontiers in Genetics*, 10, 858.

Urbé, S., Dittie, A. S., & Tooze, S. A. (1997). pH-dependent processing of secretogranin II by the endopeptidase PC2 in isolated immature secretory granules. *Biochemical Journal*, 321(1), 65-74.

Urbé, S., Page, L. J., & Tooze, S. A. (1998). Homotypic fusion of immature secretory granules during maturation in a cell-free assay. *The Journal of cell biology*, 143(7), 1831-1844.

van den Pol, A. (2012). Neuropeptide transmission in brain circuits. *Neuron*, 76(1), 98–115.

van Hoesen, G. W., Hyman, B. T., & Damasio, A. R. (1991). Entorhinal Cortex Pathology in Alzheimer's Disease. *Hippocampus*, 1(1), 1-8.

Vázquez-Martínez, R., Díaz-Ruiz, A., Almabouada, F., Rabanal-Ruiz, Y., Gracia-Navarro, F., & Malagón, M. M. (2012). Revisiting the regulated secretory pathway: from frogs to human. *General and comparative endocrinology*, 175(1), 1-9.

Vazquez-Martinez, R., & Gasman, S. (2014). The regulated secretory pathway in neuroendocrine cells. *Frontiers in endocrinology*, 5, 48.

Verkhrasky, A., Krishtal, O. A., & Burnstock, G. (2009). Purinoceptors on neuroglia. *Molecular neurobiology*, 39(3), 190–208.

Verkhratsky, A. (2005). Physiology and pathophysiology of the calcium store in the endoplasmic reticulum of neurons. *Physiological reviews*, 85(1), 201-279.

Verkhratsky, A., Matteoli, M., Parpura, V., Mothet, J., & Zorec, R. (2016). Astrocytes as secretory cells of the central nervous system: idiosyncrasies of vesicular secretion. *The EMBO journal*, 35(3), 239–257.

Verkhratsky, A., & Nedergaard, M. (2018). Physiology of Astroglia. Physiological reviews, 98(1), 239-389.

Verkhratsky, A., Orkand, R. K., & Kettenmann, H. (1998). Glial calcium: homeostasis and signaling function. *Physiological reviews*, 78(1), 99-141.

Vilijn, M.-H., Das, B., Kessler, J. A., & Fricker, L. D. (1989). Cultured astrocytes and neurons synthesize and secrete carboxypeptidase E, a neuropeptide-processing enzyme. Journal of neurochemistry, 53(5), 1487-1493

Volknandt, W. (1995). The synaptic vesicle and its targets. *Neuroscience*, 64(2), 277–300.

Voorhees, J. R., Remy, M. T., Cintrón-Pérez, C. J., el Rassi, E., Khan, M. Z., Dutca, L. M., Yin, T. C., McDaniel, L. N., Williams, N. S., Brat, D. J., & Pieper, A. A. (2018). (−)-P7C3-S243 protects a rat model of Alzheimer's disease from neuropsychiatric deficits and neurodegeneration without altering amyloid deposition or reactive glia. *Biological psychiatry*, 84(7), 488-498.

Walsh, D. M., Klyubin, I., Fadeeva, J. v, Cullen, W. K., Anwyl, R., Wolfe, M. S., Rowan, M. J., & Selkoe, D. J. (2002). Naturally secreted oligomers of amyloid β protein potently inhibit hippocampal long-term potentiation in vivo. *Nature*, 416(6880), 535-539.

Wang, C., Najm, R., Xu, Q., Jeong, D. E., Walker, D., Balestra, M. E., Yoon, S. Y., Yuan, H., Li, G., Miller, Z. A., Miller, B. L., Malloy, M. J., & Huang, Y. (2018). Gain of toxic apolipoprotein E4 effects in human iPSC-derived neurons is ameliorated by a small-molecule structure corrector article. *Nature Medicine*, 24(5), 647–657.

Wang, C.-T., Grishanin, R., Earles, C. A., Chang, P. Y., J Martin, T. F., Chapman, E. R., & Jackson, M. B. (2001). Synaptotagmin modulation of fusion pore kinetics in regulated exocytosis of dense-core vesicles. *Science*, 294(5544), 1111–1115.

Wang, H. Y., Lee, D. H. S., D'Andrea, M. R., Peterson, P. A., Shank, R. P., & Reitz, A. B. (2000). β-Amyloid1-42 binds to α7 nicotinic acetylcholine receptor with high affinity: implications for Alzheimer's disease pathology. *Journal of Biological Chemistry*, 275(8), 5626–5632.

Wang, L. (2019). Association of cerebrospinal fluid Neurogranin with Alzheimer's disease. *Aging Clinical and Experimental Research*, 31(2), 185–191.

Warfel, A. H., Zucker-Franklin, D., Frangione, B., & Ghiso, J. (1987). Constitutive secretion of cystatin C (gamma-trace) by monocytes and macrophages and its downregulation after stimulation. *The Journal of Experimental Medicine*, 166(6), 1912–1917.

Watson, J. B., Szijan, I., & Coulter, P. M. (1994). Localization of RC3 (neurogranin) in rat brain subcellular fractions. *Molecular brain research*, 27(2), 323-328.

Weber, T., Zemelman, B. v, McNew, J. A., Westermann, B., Gmachl, M., Parlati, F., Sö llner, T. H., & Rothman, J. E. (1998). SNAREpins: Minimal Machinery for Membrane Fusion. Cell, 92(6), 759-772.

Wendler, F., Page, L., Urbé, S., & Tooze, S. A. (2001). Homotypic fusion of immature secretory granules during maturation requires syntaxin 6. *Molecular biology of the cell*, 12(6), 1699-1709

Wesenhagen, K. E. J., Teunissen, C. E., Visser, P. J., & Tijms, B. M. (2020). Cerebrospinal fluid proteomics and biological heterogeneity in Alzheimer's disease: a literature review. *Critical Reviews in Clinical Laboratory Sciences*, 57(2), 86-98.

Widmer, F., & Caroni, P. (1990). Identification, localization, and primary structure of CAP-23, a particle-bound cytosolic protein of early development. *The Journal of Cell Biology*, 111(6), 3035–3047.

Wilhelm, A., Volknandt, W., Langer, D., Nolte, C., Kettenmann, H., & Zimmermann, H. (2004). Localization of SNARE proteins and secretory organelle proteins in astrocytes in vitro and in situ. *Neuroscience Research*, 48(3), 249–257.

Wong, Y. H., Lee, C. M., Xie, W., Cui, B., & Poo, M. M. (2015). Activity-dependent BDNF release via endocytic pathways is regulated by synaptotagmin-6 and complexin. *Proceedings of the National Academy of Sciences of the United States of America*, 112(32), E4475–E4484.

Wyss-Coray, T., Loike, J. D., Brionne, T. C., Lu, E., Anankov, R., Yan, F., Silverstein, S. C., & Husemann, J. (2003). Adult mouse astrocytes degrade amyloid-β in vitro and in situ. *Nature Medicine*, 9(4), 453–457.

Xu, P.-T., Gilbert, J. R., Qiu, H.-L., Ervin, J., Rothrock-Christian, T. R., Hulette, C., Schmechel, D. E., & Bryan Alzheimer, K. (1999). Specific regional transcription of apolipoprotein E in human brain neurons. *The American journal of pathology*, 154(2), 601-611.

Yang, S., Smit, A. F., Schwartz, S., Chiaromonte, F., Roskin, K. M., Haussler, D., Miller, W., & Hardison, R. C. (2004). Patterns of insertions and their covariation with substitutions in the rat, mouse, and human genomes. *Genome Research*, 14(4), 517–527.

Ye, Z.-C., Wyeth, M. S., Baltan-Tekkok, S., & Ransom, B. R. (2003). Functional hemichannels in astrocytes: a novel mechanism of glutamate release. *Journal of Neuroscience*, 23(9), 3588-3596.

Yeh, F. L., Wang, Y., Tom, I., Gonzalez, L. C., & Sheng, M. (2016). TREM2 binds to apolipoproteins, including APOE and CLU/APOJ, and thereby facilitates uptake of amyloid-beta by microglia. *Neuron*, 91(2), 328-340.

Yoong, S. Q., Lu, J., Xing, H., Gyanwali, B., Tan, Y. Q., & Wu, X. V. (2021). The prognostic utility of CSF neurogranin in predicting future cognitive decline in the Alzheimer's disease continuum: A systematic review and meta-analysis with narrative synthesis. *Ageing Research Reviews*, 72, 101491.

Yu, Y., & Ye, R. D. (2015). Microglial Aβ receptors in Alzheimer's disease. *Cellular and molecular neurobiology*, 35(1), 71-83.

Yuan, A., & Nixon, R. A. (2021). Neurofilament proteins as biomarkers to monitor neurological diseases and the efficacy of therapies. *Frontiers in Neuroscience*, 1242.

Zaben, M. J., & Gray, W. P. (2013). Neuropeptides and hippocampal neurogenesis. *Neuropeptides*, 47(6), 431-438

Zafra, F., Lindholm, D., Cast&n, E., Hartikka, J., & Thoenen, H. (1992). Regulation of brain-derived neurotrophic factor and nerve growth factor mRNA in primary cultures of hippocampal neurons and astrocytes. *Journal of Neuroscience*, 12(12), 4793-4799.

Zamanian, J. L., Xu, L., Foo, L. C., Nouri, N., Zhou, L., Giffard, R. G., & Barres, B. A. (2012). Genomic analysis of reactive astrogliosis. *Journal of Neuroscience*, 32(18), 6391–6410.

Zhang, G., Bai, H., Zhang, H., Dean, C., Wu, Q., Li, J., Guariglia, S., Meng, Q., & Cai, D. (2011). Neuropeptide exocytosis involving synaptotagmin-4 and oxytocin in hypothalamic programming of body weight and energy balance. *Neuron*, 69(3), 523–535.

Zhang, H., Therriault, J., Kang, M. S., Ng, K. P., Pascoal, T. A., Rosa-Neto, P., & Gauthier, S. (2018). Cerebrospinal fluid synaptosomal-associated protein 25 is a key player in synaptic degeneration in mild cognitive impairment and Alzheimer's disease. *Alzheimer's research and therapy*, 10(1), 1-11.

Zhang, Z., Chen, G., Zhou, W., Song, A., Xu, T., Luo, Q., Wang, W., Gu, X. S., & Duan, S. (2007). Regulated ATP release from astrocytes through lysosome exocytosis. *Nature Cell Biology*, 9(8), 945–953.

Zhang, Z., Wu, Y., Wang, Z., Dunning, F. M., Rehfuss, J., Ramanan, D., Chapman, E. R., & Jackson, M. B. (2011). Release mode of large and small dense-core vesicles specified by different synaptotagmin isoforms in PC12 cells. *Molecular biology of the cell*, 22(13), 2324–2336.

Zhou, A., Martin, S., Lipkind, G., LaMendola, J., & Steiner, D. F. (1998). Regulatory roles of the P domain of the subtilisin-like prohormone convertases. *Journal of Biological Chemistry*, 273(18), 11107–11114.

Zotova, E., Nicoll, J. A., Kalaria, R., Holmes, C., & Boche, D. (2010). Inflammation in Alzheimer's disease: relevance to pathogenesis and therapy. *Alzheimers Res Ther*, 2(1), 1–9.